Investigating the role of CBFβ in breast cancer

Adiba Sanjana Khan
MSci Biomedical Science

Submitted in fulfilment of the requirements for the
Degree of Doctor of Philosophy

College of Medical, Veterinary and Life Sciences (MVLS)
Cancer Research UK Beatson Institute
University of Glasgow

September 2022

Abstract

Despite the advances in therapy and improved patient mortality rates, breast cancer remains one of the leading causes of cancer associated deaths in women across the globe. The transcription co-factor, Core Binding Factor-beta (CBFβ), which is the binding partner for the RUNX family of proteins, is a recurrently mutated gene in breast cancer. Up to 14% of breast cancer patients harbour genetic alterations in this gene, across both oestrogen receptor (ER) positive and ER negative subtypes of the disease. The majority of these alterations have been found to be loss of function mutations and homozygous deletions in *CBFβ,* indicating a potential tumour suppressive role of this protein. The functionality of *Cbfβ* loss in mammary tumorigenesis was studied here using genetically engineered mouse models of a luminal B breast cancer model (MMTV-PyMT) and a Wnt/β-catenin driven mammary cancer mouse model. Consistent with loss of function mutations/deletions in patient cohorts, a tumour suppressor role of *Cbfβ* was confirmed for the first time *in vivo* where homozygous loss of *Cbfβ* in mammary epithelial cells dramatically accelerated Wnt/β-catenin driven tumour initiation and progression. Transcriptomic analysis of tumour samples deficient in *Cbfβ* revealed significant upregulation of genes encoding various activators of the Wnt/β-catenin pathway and downregulation of its inhibitors indicating marked augmentation of this signalling cascade. Genes involved in activation of other oncogenic pathways, including the Notch pathway, also appeared enriched in samples where *Cbfβ* was absent. Strikingly, alterations in the immune regulatory pathways of the *Cbfβ*-deficient tumour microenvironment were particularly evident in the RNAseq analysis and *Cbfβ* deficient pre-neoplastic glands also displayed an increased infiltration of immune cell infiltrates. Combined deletion of CBFβ binding partners, *Runx1* and *Runx2* showed a similar acceleration of Wnt/β-catenin driven tumorigenesis although differences in the transcriptomic and immune landscape between *Runx1-Runx2* deficient and *Cbfβ* deficient tumours suggested that the mechanisms of action may not be entirely synonymous. Interestingly loss of *Cbfβ* from PyMT tumour cell lines showed that the tumour suppressor effect of CBFβ is not universal. This study provides the first *in vivo* evidence that *Cbfβ* loss might be associated with promotion of mammary tumorigenesis through hyperactivation of Wnt signalling and with an induction of a pro-tumorigenic immune response.

Author's declaration

I hereby declare that I am the sole author of this thesis and all work presented in this document is my own, unless stated otherwise.

I certify that no part of this thesis has been submitted for the award of any other degree at the University of Glasgow or any other institution.

Adiba Khan

September 2022

Acknowledgements

The research conducted throughout this project and the production of this thesis would not have been possible without the support provided by all the wonderful people at the CRUK Beatson Institute. I would like to express my deepest gratitude to my supervisor Prof. Karen Blyth, for giving me the opportunity to embark on this PhD journey and for her continuous support and invaluable guidance. Your scientific expertise and meticulous nature of analysis has shaped the way I approach research and your enthusiasm and passion has always been a constant source of encouragement and inspiration. I would also like to extend my sincere appreciation to my second supervisor Dr. Kirsteen Campbell for her mentorship. Your uplifting attitude has always helped me stay motivated at work and your guidance, advice and daily support has been invaluable to my progression as a scientist. I am also thankful to my two reviewers Dr. Seth Coffelt and Prof. Martin Bushell for their expert advice and helpful discussions on the project.

Thank you to all the past (Sandeep, Susan, Nick, Narisa and Kerri) and present Y35 lab members, Dimitris, Jay, Laura G, Laura ME, Dale and Matthew, for teaching me lab techniques, answering my numerous questions and for all their help, kindness and support. Special thanks to Sandeep Dhayade for being patient with me when I was first learning how to work with animals and to Narisa for all her encouraging words, advice and friendship. I would also like to thank Coffelt lab, particularly Rob for teaching me all flow cytometry techniques and Mark for all his technical help and guidance on data analysis.

Additionally, many thanks to Cancer Research UK for funding my studentship and all the research services and staff at the Beatson. Many thanks to Histology Services, BSU/BRU staff and Molecular technologies for their exceptional support. Thank you to Robin Shaw for all his help and advice with bioinformatics analysis.

My appreciation goes out to all my friends here at the Beatson, especially Rachel, Irene, Andy, Mikhalis and Andre who have made this city feel like home. Working with such amazing scientists and wonderful people has made my time here a very enjoyable experience. I would also like to thank my “forever friends” from home for all their support, even from a distance, during this journey. Special thanks to Elroy for all his help, moral support and encouragement during the last few months which helped me stay sane while writing this thesis.

Finally, I would like to thank my family: especially my parents whose unconditional love and support have allowed me to travel half-way across the world in pursuit of my passion for science. Their work ethic and perseverance has always inspired me to do my best and stay motivated even when things don't work out according to my plans. Ammu and Abbuji – I would not have been able to achieve any this without you!

Table of Contents

List of Tables

List of Figures

List of abbreviations and definitions

Abbreviations	Definitions
2D	Two-Dimensional
3D	Three-Dimensional
4OHT	4-Hydroxytamoxifen
aa	Amino Acids
AD	Activation Domain
ADC	Antibody-Drug Conjugates
AI	Aromatase Inhibitor
Akt	Ak Strain Transforming
ALY	Aly/Ref Export Factor
AML	Acute Myeloid Leukaemia
AP-1	Activator Protein 1
APC	Antigen Presenting Cells
APC	Adenomatous Polyposis Coli
aPES	Polyethersulfone
AWERB	Animal Welfare and Ethical Review Board
AXIN1	Axin-1
BCA	Bicinchoninic Acid
BCL9	B Cell Lymphoma 9
BLBC	Basal-Like Breast Cancers
BLG	Beta-Lactoglobulin
BMP-2	Bone Morphogenetic Protein 2
BRCA1	Breast Cancer Gene 1
BRCA2	Breast Cancer Gene 2
BSA	Bovine Serum Albumin
C/EBP	CCAAT-Enhancer-Binding Proteins
Cas9	Crispr-Associated Protein 9
CBF	Core Binding Factor
CBFβ	Core Binding Factor-Beta
CBP	CREB Binding Protein
CCL	Cytokine Ligand
CCND1	Ccnd1
ccRCC	Clear Cell Renal Cell Carcinoma
CD	Cluster Of Differentiation
CDK	Cyclin Dependent Kinases
CDX	Cell Line Derived Xenografts
Cela1	Chymotrypsin Like Elastase 1
CK	Cytokeratin

CK1α	Casein Kinase 1A
CML	Chronic Myeloid Leukaemia
c-*MYC*	Myc Proto-Oncogene
CRC	Colorectal Cancer
CRISPR	Clustered Regularly Interspaced Short Palindromic Repeats
CSC	Cancer Stem Cells
CSF-2	Colony Stimulating Factor 2
CT	Computed Tomography
CTNNB1	Catenin Beta 1
CXCL	Chemokine Ligand
CXCR4	Chemokine Receptor 4
DC	Dendritic Cells
DCIS	Ductal Carcinoma *In Situ*
DKK	Dickkopf
DMEM	Dulbecco'S Modified Eagle Medium
DNA	Deoxyribonucleic Acid
Dox	Doxycycline
Dsh	Dishevelled
Dxt1	Deltex1
ECM	Extracellular Matrix
EGF	Epidermal Growth Factor
EGFR	Epidermal Growth Factor Receptor
EMT	Epithelial To Mesenchymal Transition
Enz1	Epitope Retrieval Using Enzyme 1
ER	Oestrogen Receptor
ER2	Epitope Retrieval
ERBB2	Erb-B2 Receptor Tyrosine Kinase 2
ERK	Extracellular Signal-Regulated Kinases
ERα	Oestrogen Receptor Alpha
Erß	Oestrogen Receptor Beta
ESR1	Oestrogen Receptor Alpha Gene
Ets	Erythroblast Transformation Specific
ETs-1	ETS Proto-Oncogene 1
FACS	Fluorescence-Activated Cell Sorting
FBS	Foetal Bovine Serum
FCS	Foetal Calf Serum
FFPE	Formalin Fixed and Paraffin Embedded
FMO	Fluorescence Minus One
Fzd	Frizzled
G-CSF	Granulocytic Colony Stimulating Factor

GEM	Genetically Engineered Mouse
GEMM	Genetically Engineered Mouse Model
GM-CSF	Granulocyte-Macrophage Colony-Stimulating Factor
GRG	Groucho
GSK-3β	Glycogen Synthase Kinase 2B
γδ T cells	Gamma Delta T Cells
H&E	Haematoxylin And Eosin
HCC	Hepatocellular Carcinoma
HDACs	Histone De-Acetylases
HER2	Human Epidermal Growth Factor 2
HER3	Human Epidermal Growth Factor 3
HIER	Heat Induced Epitope Retrieval
HIF1a	Hypoxia-Inducible Factor 1-Alpha
HIPK2	Homeodomain Interacting Protein Kinase 2
HSC	Haematopoietic Stem Cells
ICAT	Inhibitor Of B-Catenin and Tcf-4
ID	Inhibitory Domain
IDC	Infiltrating Ductal Carcinoma
IFNγ	Interferon-Gamma
Ig	Immune Globulin
IgA	Immune Globulin A
IHC	Immunohistochemistry
IL	Interleukin
ILC	Innate Lymphoid Cell
IntClust	Integrative Clusters
ISH	In Situ Hybridisation
IVC	Individually Ventilated Cages
Jag1	Mouse Gene Encoding Jagged1
JNK2	Jun N-Terminal Kinase 2
kb	Kilo Bases
LCIS	Lobular Carcinoma In Situ
LDS	Lithium Dodecyl Sulfate
LEF	Lymphoid Enhancer Factor
LGB	Beta-Lactoglobulin
LGR5	Leucine-Rich G Protein Coupled Receptor
LINC01234	Long Intergenic Non-Protein Coding Rna 1234
LRP	Lipoprotein Receptor Related Protein
LSL	Lox-Stop-Lox
LTi	Lymphoid Tissue Inducer
LTR	Long Terminal Repeat

Maml2	Mouse Gene Encoding Mastermind Like Transcriptional Coactivator 2
M-CSF	Macrophage Colony Stimulating Factor
MDSC	Myeloid Derived Suppressor Cells
MECs	Mammary Epithelial Cells
METABRIC	Molecular Taxonomy of Breast Cancer International Consortium
MHC	Major Histocompatibility Complex
MIN	Mammary Intraepithelial Neoplasia
miR-204-5p	Microrna-204-5P
MMEC	Mouse Mammary Epithelial Cell
MMP	Matrix Metalloproteinase
MMTV	Mouse Mammary Tumour Virus
MORF	Homologue Of MOZ
MOZ	Monocytic Leukaemia Zinc Finger
MRI	Magnetic Resonance Imaging
mRNA	Messenger Ribonucleic Acid
mTOR	Mammalian Target of Rapamycin
MYH11	Gene Encoding Smooth Muscle Myosin Heavy Chain 11
N-CoR	Nuclear Hormone Co-Receptor
NF-kB	Nuclear Factor Kappa B
NICD	Notch Intracellular Domain
NK	Natural Killer
NMTS	Nuclear-Matrix Targeting Signal
OC	Osteocalcin
OPN	Osteopontin
PARP	Poly-ADP Ribose Polymerase
PBS	Phosphate-Buffered-Saline
pCR	Pathological Complete Response
PD-L1	Programmed Death-Ligand 1
PDX	Patient Derived Xenografts
PI3K	Phosphatidylinositol 3 Kinase
PIM-1	Pim-1 Oncogene Protein
PMA	Phorbol 12-Myristate-13-Acetate
PR	Progesterone Receptor
Prkaa2	Mouse Gene Encoding Protein Kinase Amp-Activated Catalytic Subunit Alpha 2
PRMT1	Protein Arginine Methyltransferase 1
PTEN	Phosphatase And Tensin Homolog
PTHRP	Parathyroid Hormone-Related Protein
PYGO	Pygopus

PyMT	Polyoma Middle Tumour-Antigen
QA	Alanine Rich Domain
qPCR	Quantitative Polymerase Chain Reaction
Rac-1	Rac Family Small GTPase 1
RBC	Red Blood Cells
RBD	RUNX Binding Domain
RFP	Red Fluorescent Protein
RHD	Runt-Homology Domain
RNA	Ribonucleic Acid
RNF43	Ring Finger Protein 43
ROR1	Receptor Tyrosine Kinase Like Orphan Receptor 1
Ror2	Mouse Gene Encoding Receptor Tyrosine Kinase Like Orphan Receptor 2
RSPO3	R-Spondin 3
RUNX	Runt-Related Transcription Factor
RUNX1	Runt-Related Transcription Factor 1
RUNX2	Runt-Related Transcription Factor 2
RUNX3	Runt-Related Transcription Factor3
SCID	Severe Combined Immunodeficiency
SDS	Sodium Dodecyl Sulphate
Ser	Serine
SERMs	Selective Er Modulators
sFRP	Secreted Frizzled-Related Proteins
shRNAs	Short Hairpin RNA
SMMHC	Smooth Muscle Myosin Heavy Chain
SMRT	Silencing Mediator of Retinoid and Thyroid Hormones
Snai2	Snail Family Transcriptional Repressor 2
SOST	Sclerostin
Sox1	SRY-Related HMG-Box
STAT3	Signal Transducer and Activator of Transcription 3
SWI/SNF	Switch/Sucrose Non-Fermentable
TAM	Tumour Associated Macrophages
TBST	Tris Buffered Saline with Tween
TCF	T-Cell Factor
TCR	T Cell Receptor
TDLU	Terminal Duct Lobular Unit
tdRFP	Tandem-Dimer Red Fluorescent Protein
TEB	Terminal End Bud
TFF1	Trefoil Factor 1
TGFβ	Transforming Growth Factor Beta
Thr	Threonine

TIL	Tumour Infiltrating Lymphocyte
TLE	Transducin-Like Enhancer of Split
TMA	Tissue Microarray
TME	Tumour Microenvironment
TMED	Transmembrane Emp24 Domain-Containing Protein
TN	Triple Negative
Tregs	T Regulatory Cells
TRS	High Ph Target Retrieval Solution
Wap	Whey Aciding Protein
WBC	White Blood Cells
Wnt-PCP	Wnt-Planar Cell Polarity
YAP	Yes-Associated Protein 1
ZNRF3	Zinc And Ring Finger 3
α-SMA	A-Smooth Muscle Actin

Chapter 1. Introduction

The birth of modern biology and our understanding of evolution can be primarily accredited to the 19th century biologist Charles Darwin and his concepts of natural selection. Just as survival of organisms, depends on their ability to adapt and change in order to attain the most advantageous characteristics for their sustenance: "survival of the fittest", every cell that makes up an organism goes through the same pressures of selection. Indeed, the approximately one trillion cells that make up the human body, undergo continuous forces of selection and genetic mutations from conception, through every stage of development until death (Cairns, 1975). For every cell division cycle, around 1-10 mutations are introduced into the genetic backbone of the cell (Martincorena and Campbell, 2015). While the majority of these mutations are phenotypically silent, owing to the numerous cellular repair and fail-safe mechanisms set in place, some of them provide a proliferative advantage (Nowell, 1976). Such mutations, resulting in the transformation of normal cells into malignant states are often the perpetrators of one the leading causes of death in humans today: cancer.

Nearly 1 in 6 people are predicted to succumb to cancer worldwide, with the highest incidence rates – around 2.26 million cases in 2020 – being in breast cancers (Sung et al., 2021; Siegel et al., 2022; World Health Organisation, 2022). Affecting both men and women, the incidence rate of this malignancy has increased by 20% over the last two decades and is predicted to rise further over the years (Ceruti et al., 2003). Although regular screening and advances in therapeutic interventions have dramatically improved survival rates of patients over the past decades, breast cancer remains the second most common cause of cancer related deaths in women (Cancer Research UK, 2016). Improving on our understanding of the natural biology of the mammary glands and the components involved in its transition towards a malignant state is therefore imperative.

1.1. Mammary gland biology

One of the key distinguishing features of mammals, compared to other animals is the development of mammary glands (Oftedal, 2002). Evolved more than 300 million years ago, from apocrine glands of the skin epidermis, the mammary gland is a unique tubuloalveolar branched structure (Hovey, Trott and Vonderhaar,

2002; Oftedal, 2002). The sole purpose of the mammary glands is lactation. Milk produced by this accessory reproductive organ acts as the main source of nutrition for survival of offspring after birth and therefore, sustenance of all young mammals (Peaker, 2002). Morphologically, the gland is divided into two distinct environments - a network of mammary ducts comprised of mammary epithelial cells, and the stroma - a layer of connective tissues containing extracellular matrix (ECM) proteins and a milieu of other cell types that work to support the ductal structures (Watson and Khaled, 2008; Muschler and Streuli, 2010; Biswas et al., 2022). A schematic representation of the cellular components making up the mammary gland is represented in Figure 1.1.

The mammary gland epithelium is comprised of luminal and basal epithelial cells. The luminal cells marked by their expression keratin 8, 18 and 19, generate the inner layer of the duct, facing the lumen with cells at the terminal end of the duct that differentiate into milk secreting cells, that form the lobulo-alveolar compartment (Visvader, 2009; Biswas et al., 2022). Once milk is secreted, it can pass through the hollow lumen during lactation to feed the offspring (Visvader, 2009; Biswas et al., 2022). On the other hand, the basal side of the epithelial layer, is made up of myoepithelial cells characterised by their expression of keratins 5 and 14 (Visvader, 2009; Biswas et al., 2022). These enclose around the luminal layer and aid in milk secretion using their contractile properties akin to smooth muscles (Visvader, 2009; Biswas et al., 2022). The basal layer also contains epithelial stem cells and progenitor cells that hold the capacity to differentiate into either of the two epithelial cell types (Visvader, 2009; Biswas et al., 2022). Traditionally, the mammary epithelial lineage has been explored through studies involving transplantation and lineage tracing (Blair and Deome, 1961; Daniel et al., 1968; Smith and Medina, 1988). These studies have revealed that differentiation of the mammary epithelium follows a hierarchical pattern stemming from multipotent foetal mammary epithelial stem cells (MaSCs) which give rise to a bipotent MaSC progenitor. Gene expression studies have identified that majority of MECs during embryogenesis express genes associated to both luminal and myoepithelial lineages (Lim *et al.*, 2010; Shi, Chakraborty and Chaudhuri, 2018; Anstine and Keri, 2019). Postnatal development of the mammary gland involves differentiation of such bi-potent progenitors capable of generating either luminal or myoepithelial cell types which become unipotent in nature and are restricted to their respective lineages. While the exact timing of this distinct

division between the two major lineages of epithelial cells remain uncertain, single-cell RNA sequencing studies have suggested that progenitor cells become increasingly lineage restricted in parallel with puberty (Anstine and Keri, 2019). Furthermore, advances in single-cell RNA sequencing have recently also allowed identification of multiple subpopulations within each major subtype that are transcriptionally distinct (4 basal and 11 luminal subpopulations) (Pal et al., 2017; Anstine and Keri, 2019; Bach et al., 2021). These are thought to represent a heterogenous assortment of cells that respond and differentiate further due to specific microenvironmental cues. For instance, independent progenitors of the luminal lineage generate cells of various intermediate states that differentiate into ER positive hormone responsive cells or alveolar cells of an ER negative lineage with secretory properties (Bach *et al.*, 2017; van Keymeulen *et al.*, 2017; Wang *et al.*, 2017; Giraddi *et al.*, 2018; Nguyen *et al.*, 2018).

While luminal and basal cells comprise the functional until of the mammary glands, extracellular matrix, known as the basement membrane, envelops the mammary epithelium and keeps it separated from cells in the stromal compartment (Streuli, 2003). The stroma contains a cocktail of various cell types with the most abundant variety being adipocytes which provide a base for the ductal network to be embedded (Sternlicht, 2005). Another major component of this stromal layer are fibroblasts. Stromal fibroblasts promote expansion of epithelial cells, elongation of normal mammary ducts and their invasion through the mammary tissue and are therefore fundamental in sustenance and development of the mammary gland (Avagliano et al., 2020). Working in conjunction with these two crucial cell types, are vascular endothelial cells which support the network of blood vessels within the mammary gland, cells forming the lymphatic and neuronal networks as well as immune cells - particularly dendritic cells and macrophages - that form the mammary glands' innate immunity (Polyak and Kalluri, 2010; Pellacani et al., 2019; Avagliano et al., 2020) (Figure 1.1).

This complex network of cells collaborates through direct cell-cell interactions, paracrine signals, mechanical signals, responses to growth hormones and growth factors to regulate the complex cellular pathways involved in the normal homeostasis of the mammary gland. Tight control of all these signalling pathways is essential in maintaining the dynamic stages of mammary gland development and remodelling throughout the lifetime of the mammal (Sternlicht, 2005; Biswas et al., 2022).

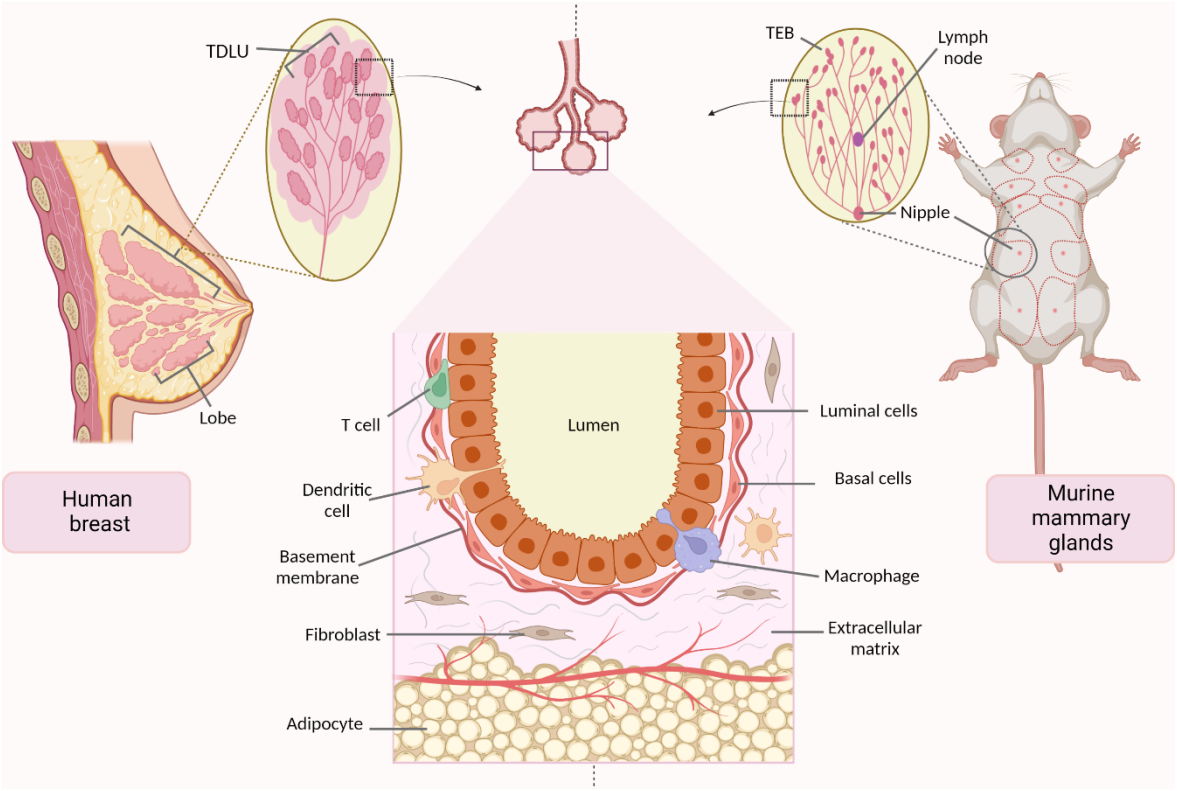

Figure 1.1: Schematic representation of the cellular components that make up the functional unit of the mammary gland.

Figure adapted from (Goff and Danforth, 2021). Organisation of the human breast TDLU into lobes is compared to the TEB of murine mammary glands. TDLU: Terminal ductal lobular unit. TEB: terminal end bud. The murine mammary glands come in 5 pairs as marked in red dotted lines. Within each mammary gland, the mammary ductal tree grows from the nipple and invades the whole of the mammary fat pad. Growth of the ductal tree is driven by the TEBs. The human breast on the other hand, is arranged in lobes, made up of a cluster of acinar lobules – TDLU. The epithelial layer of the mammary gland constitutes of luminal epithelial cells, facing the lumen followed by a layer of basal cells. The epithelial layer is separated from the mammary stroma by a basement membrane. The mammary ductal structures are supported by the ECM containing a cocktail of stromal cells and immune cells, blood vessels and adipose tissue. Figure created using Biorender.com

1.1.1. The developing mammary gland: insights from murine anatomy

Traditionally, the anatomy and physiology of the human breast was studied though the analysis of gross and/or histological samples from surgically resected breast tissues or cadavers donated to scientific research. While this approach provided us with invaluable information about the human breast morphology for several decades, it was not possible to study the dynamic developmental stages and the genetic and transcriptomic changes that give rise to fully functional mammary

glands through observational analysis. Consequently, mice have been one of the most widely used mammals in the research of normal breast biology as well in modelling diseases of this organ (Honvo-Houéto and Truchet, 2015). This is accredited to the fact that the murine genome is 99% similar to the human genome and the mouse mammary gland anatomy and physiology essentially mirrors that of the human. In addition to this, the short gestation period and lifespan means that developmental processes can be studied within short timeframes, ensuring research is time and cost-effective. Effects of genetically manipulating the murine germline to either overexpress or inactivate specific genes both temporally and spatially can be observed within relatively short spans. Furthermore, their small size allows for greater sample sizes and considering how mice have 5 pairs of mammary glands (Figure 1.1) as opposed to the one pair in humans, abundant tissue is available for research purposes (Honvo-Houéto and Truchet, 2015).

Development of the murine mammary gland closely resembles that of humans and therefore, serves as an important tool to study normal development, biology as well as disease. Both human and mouse mammary glands develop through multiple phases from the early embryonic and foetal stage though to puberty and adulthood, pregnancy to lactation and regressive involution. In mice, mammary glands first appear around embryonic day 10-11 (E10-E11) as “mammary buds” derived from placodes (Figure 1.2). Placodes are formed from mammary epithelium following the formation of bilateral milk-lines on either side of embryonic midventral line (Honvo-Houéto and Truchet, 2015). These mammary buds invade through the mesenchymal layer into 5 pairs of concentric stratums – 1st pair slightly below the neck, 2nd and 3rd pairs on either side of the thorax, 4th pair in the lower abdominal region and a 5th pair in the inguinal regions (Cardiff and Wellings, 1999; Richert et al., 2000). Around the 15th day of embryonic development (E15.5) the epithelial cells that make up the mammary buds begin to proliferate to form what is known as the primary sprout. The primary sprout elongates into the mammary fat pad through the mesenchymal layer and develops into a hollow duct that opens out on the skin. This opening marks the position of the nipples (Honvo-Houéto and Truchet, 2015). At E18.5, branches generated from the primary sprout give rise to a rudimentary ductal tree embedded within the mammary fat pad. Once this stage is reached, in female embryos, further development is paused until puberty. In males however, by E15.5 development of the embryonic mammary glands continue towards a degenerative state where

activation of androgen receptor signalling leads to regression of the buds until they disappear. Consequently, similar to their female counterpart, mammary development is maintained at a quiescent state until puberty is reached (Honvo-Houéto and Truchet, 2015).

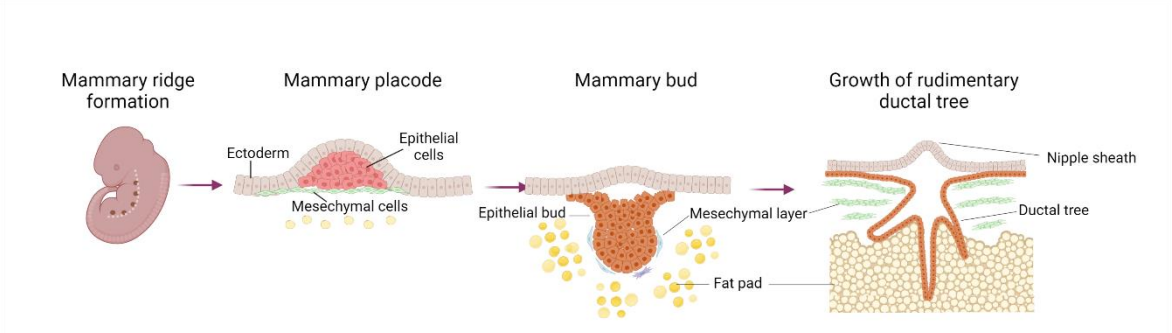

Figure 1.2: Schematic representation of the different stages of the murine mammary gland development within the womb.

Image adapted from (Mikkola and Millar, 2006). The early mammary gland develops from a mammary ridge in the developing foetus. Placodes arise from the mammary ridge as an aggregate of epithelial cells covered by the ectoderm. This develops into a mammary bud which ultimately invades into the mammary mesenchyme and fat pad giving rise to rudimentary mammary ducts. Simultaneously a nipple sheath develops from the ectodermal layer. Figure created using Biorender.com

While the ductal system undergoes some elongation and isometric development after birth, it isn't until puberty that noticeable morphological changes can be observed (Figure 1.3Figure 1.2). Particularly the tip of each duct, comprised of a multilayer of body cells enveloped by an outer layer of cap cells, develop into bulbous terminal end buds (TEBs). TEBs are highly responsive to hormonal signals and proliferate to invade through the surrounding stroma and therefore support further elongation and morphogenesis of the ductal branches. Within each TEB, the layer comprising of body cells are considered to contain luminal progenitor cells which can differentiate into mature luminal cells (Paine and Lewis, 2017). Apoptosis of cells within this layer produces a hollow lumen and ultimately gives rise to the ductal epithelial layer (Paine et al., 2016; Avagliano et al., 2020). With the onset of pregnancy, luminal progenitors can also differentiate into rapidly proliferating alveolar cells harbouring milk producing and secreting properties (Inman *et al.*, 2015). On the other hand, cap cells, which cover the end of the TEB, interact with the stromal cells though a thin layer of basal lamina and eventually differentiate into myoepithelial basal cells of the mammary duct (Williams and Daniel, 1983). Bifurcation of the duct at the TEBs lead to the

formation of new primary ducts with secondary and tertiary side-branches arising from the trailing ends of their trailing ends (Affolter et al., 2003; Sternlicht, 2005). Around 10-12 weeks from birth, the whole fat pad is infiltrated by this ductal tree originating from the nipple and the expansion of these branches only stop once the TEBs reach the edges of the fat pad. At this point, the mammary ducts undergo a succession of proliferative and regressive stages of remodelling dependent on the states of the estrous cycles.

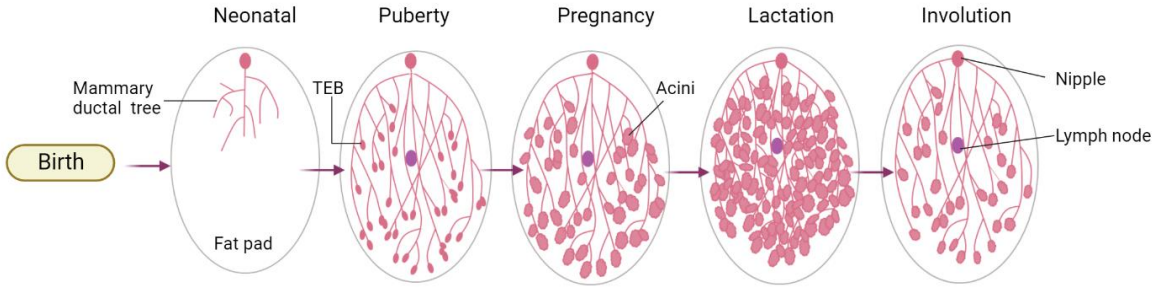

Figure 1.3: Development of the murine mammary gland and the changes associated with different stages of life.

Image adapted from (Paine and Lewis, 2017). The murine rudimentary mammary gland resumes development at puberty with the growth of the mammary tree stemming from the nipple. The ductal tree invades through the mammary fat pad driven by the TEB. During pregnancy, the mammary epithelium proliferates in response to hormonal cues resulting in the generation of lobulo-alveolar structures to prepare for lactation. Lactation involves a dense organisation of milk producing acinar lobules which are subsequently lost during involution following the weaning of offspring. Figure created using Biorender.com

The estrous or reproductive cycle in mice (spanning 4-5 days) is the equivalent of the menstrual cycle in humans (28-30 days) (Buffet et al., 1998; Fata, Chaudhary and Khokha, 2001). Throughout the 4 stages of this cycle namely, proestrus, estrus, metestrus and diestrus the mammary gland goes through phases of growth and differentiation in response to reproductive hormones to prepare for the potential onset of pregnancy (Chua et al., 2010; Byers et al., 2012). For instance, during diestrus, which resembles the end of luteal phase in humans, the mammary epithelial cells tend to undergo high levels of proliferation with an increase in the number of lateral branching and formation of alveoli, taking the mammary gland to its most differentiated state (Heape, 1900; Fata, Chaudhary and Khokha, 2001). In the female mouse, the next phase of major change within the mammary glands occurs during pregnancy. The primary objective of the following change in morphology is the production of milk for lactation. Extensive proliferation and

differentiation of the mammary epithelium occurs to give rise to a dense network of tubulo-alveolar branches (Figure 1.3). The alveolar structures or acini are comprised of mammary epithelial cells (MECs) encircled by myoepithelial cells and a stromal layer of connective tissues, nerve terminal and blood vessels (Honvo-Houéto and Truchet, 2015). The outer layer of the myoepithelial cells is also in contact with a basement membrane which in turn is in contact with a layer of fibroblasts, surrounded by adipose tissue. Within this environment, the MECs undergo priming and polarisation to produce and subsequently secrete milk in response to hormonal cues and paracrine signal between the MECs, ECM and the surrounding cells of the stroma. For instance, in response to progesterone and prolactin, alveologenesis and side branching are induced to maintain differentiation of the mammary alveoli. Near the end of pregnancy, the MECs produce and secrete colostrum into the lumen: a form of milk rich with proteins (Honvo-Houéto and Truchet, 2015).

Following birth or parturition, the mammary alveoli organise themselves into lobules which cluster together into lobes. These lobes all drain milk into a primary duct connected to the nipple. Once the offspring are weaned, lactation is ceased as the mammary tissues regresses back to its former pubertal state: a process termed involution.

1.1.2. Development of the human breast

Development of the human mammary gland follows a very similar trajectory as mentioned previously with one of the obvious differences being time. For instance, human embryos require around 4 weeks to develop the milk-line compared to 15 days in mice. The pubertal stage of human breast development is reached 12-14 years post birth while complete morphological and functional maturity is reached around 24 years of age in adult humans. Additionally, the formation of breast lobules is noted during puberty in humans, whereas in mice this process begins with pregnancy. Another difference lies in the human foetal stage wherein, the foetus and new-born hold a distinct capacity to produce and secrete colostrum, albeit to a limited capacity, in response to maternal hormones. The human breast also undergoes slightly different anatomical changes, known as the Tanner stages, such as elevation of the breast tissue, development and enlargement of the areola and nipple which are not seen in mice. Furthermore, at birth, while in mice, the ductal tree arises from a single primary duct connected

to the nipple, multiple minor networks of ducts feed into the nipple. This network then follows isomorphic growth until puberty is reached. As such, one functional unit of the human breast is constituted of a group of acini or lobules stemming from a single duct, known as a terminal duct lobular unit (TDLU), depicted in **Error! Reference source not found.**Figure 1.1. TDLUs have been proposed to be functionally equivalent to mouse TEBs, both being involved in milk production, although structurally they are different (Dontu and Ince, 2015). Of note, it is often the TDLU of the human breast that is found to be the origin point for breast tumour with increased proliferation of epithelial cells within this region leading to hyperplasia and carcinoma (Milanese et al., 2006; Cichon et al., 2010).

1.2. Breast Cancer

Although almost all primary breast tumours originate in the TDLU of mammary glands, the disease is highly heterogenous, exhibiting a diverse range of biological phenotypes and pathological features (Weigelt, Geyer and Reis-Filho, 2010). Classification systems for breast tumours have therefore been organised based on their morphological-histopathological characteristics (Elston and Ellis, 2002) or their genetic and transcriptomic features (molecular subtypes) (Ivshina et al., 2006; Pusztai et al., 2006; Weigelt, Geyer and Reis-Filho, 2010).

Traditional categorisation systems based on biological phenotypes such as size of tumour, involvement of lymph node, histological grade, tumour morphology, histological type, presence of oestrogen receptor (ER), progesterone receptor (PR) and human epidermal growth factor receptor 2 (HER2) fail to appreciate the biological incidents and complex genetic basis of this disease (Yersal and Barutca, 2014). For instance, while histological grade provides insight into the behaviour of these tumours (Elston et al., 1982), they fail to relate these phenotypes to biological and genetic events, making it difficult to accurately predict the nature of progression in these (Yersal and Barutca, 2014). Usually, analysis by a pathologist is incorporated into computer-based algorithms like the NPI (Nottingham Prognostic Index), Predict or Adjuvant! in order to accurately predict disease prognosis and assign the correct treatment regimens (Elston and Ellis, 2002; Wishart et al., 2012) Additionally, a genetic approach with the help of global gene expression profiling and microarray analysis has been devised to generate

molecular subtypes in breast cancer classification (Perou et al., 2000; Ciriello et al., 2015).

1.2.1. Histological Subtypes

Unlike other solid cancers such as pancreatic cancer or colon cancer, breast tumour progression has not been found to be driven by any single specific pathway or histological characteristic (Stingl and Caldas, 2007). Analysis of chromosomal abnormalities, germline and somatic mutations along with mRNA and gene expression profiles, has indicated a diverse spectrum of biological features among tumours (Stingl and Caldas, 2007). Oncogenesis and tumour progression in breast cancer do not seem to proceed linearly from a well differentiated state into tumours that are poorly differentiated (Stingl and Caldas, 2007). To date, approximately 18 distinct histological subtypes of human mammary tumours have been categorised based on the morphology of the breast tumour upon diagnosis (Tavassoli and Devilee, 2003; World Health Organisation, 2012). This is a more traditional method of classification based on tumour architecture and immunohistochemical features. Size of lesion (s), patterns of cellular arrangement, existence of necrosis, cell proliferative index (mitotic index) and nuclear grade are some of the features used for the classification of these subtypes (Stingl and Caldas, 2007).

According to this classification system, breast cancer can be broadly split into two main categories: in situ and invasive carcinoma (Malhotra et al., 2010). *In situ* carcinoma can be divided into lobular carcinoma in situ (LCIS) which resides within the breast lobules and the more common ductal carcinoma in situ (DCIS) which is contained within the mammary gland ducts and displays far more heterogenous characteristics (Nakhlis and Morrow, 2003; Inoue et al., 2017). At least 5 different histological types of DCIS tumours have been classified: Solid, Papillary, Micropapillary, Cribiform and Comedo (Malhotra et al., 2010). Invasive carcinomas encompass tumours with a wide variety of histological subtypes with infiltrating ductal carcinoma (IDC) making up 70-80% of all cases (Ivshina et al., 2006). Other major subtypes include invasive lobular, ductal-lobular, tubular, medullary, colloid and papillary invasive carcinomas. IDC is further sub-divided according to histological grade with Grade 1 comprising well differentiated IDCs and Grade 3 accounting for poorly differentiated tumours (Ivshina et al., 2006; Lester et al., 2009). This system of grading tumours originated by Greenough in 1925 and

subsequently improved by various other research groups (Elston and Ellis, 2002), is generally used for grading invasive breast carcinoma (Greenough, 1925; Patey and Scarff, 1928; Bloom and Richardson, 1957). The method looks at 3 specific histological features: proliferative potential of the tumour cells (mitotic rate), differentiation of tubules within the tumour and nuclear pleomorphisms (Elston and Ellis, 2002) (shape and size of the tumour cell nuclei) (Elston and Ellis, 2002). A score was then assigned within each of these 3 categories and added together to allocate a grade to the tumour such that Grade I represented well differentiated tumours, Grade II was assigned to the intermediate, moderately differentiated tumours and Grade III allocated to poorly differentiated tumours (Elston and Ellis, 2002).

In addition to these, the World Health Organisation classifies 25% of breast cancers into various different histological "special types" (Tavassoli and Devilee, 2003; Weigelt, Geyer and Reis-Filho, 2010; World Health Organisation, 2012).

While classification of breast tumours using histological features have been valuable for understanding the heterogeneity of breast cancers, it is less accurate in predicting patient prognosis. Therefore, newer markers based on transcriptomic and molecular features of tumours have been devised to accurately predict disease progression and stratify patients for tailored therapy.

1.2.2. Molecular Subtypes

In 2000 Perou *et al* were the first to analyse and compare 65 surgically removed human breast tumour tissues with normal mammary samples from 42 patients suffering from advanced stage breast cancer (Perou et al., 2000). 8102 genes were analysed with the help of complementary microarrays and the pervasive disparities in the expression patterns between the different tumour samples allowed the generation of distinguished molecular subtypes (Perou et al., 2000). Unbiased analysis of gene clusters uncovered two distinct branches marked by expression of the oestrogen receptor (ER positive and ER negative) (Perou et al., 2000). ER positive tumours could be characterised by a high expression of ER-responsive genes and cytokeratin associated markers for breast luminal epithelial cells (Perou et al., 2000). The luminal group could further be divided into luminal-A luminal-B subtypes which were correlated to discrete clinical outcomes. The latter subtype can also be characterised by HER2 expression (Gomes Do Nascimento and Otoni, 2020). On the other hand, the ER negative subtype was

divided into three categories: basal-like (resembling breast basal epithelial cells and characterised by the expression of basal cytokeratins), HER2 positive and normal-like breast tumours (Perou et al., 2000). Subsequently, microarray analysis was used for profiling mRNA expression signatures for specific sets of genes has allowed stratification of breast cancers into 4 major subtypes: Luminal-A, Luminal-B, HER2 positive and basal/triple negative (TN). (Perou et al., 2000; Sørlie et al., 2001, 2003; Ivshina et al., 2006; Mohammed, 2021).

Luminal-A tumours are characterised by high ER expression and low expression levels of genes involved in cell proliferation and low Ki67 index, a proliferating cell nuclear antigen. These tumours are recognised as ER positive and sometimes PR positive and negative for HER2 (Yersal and Barutca, 2014). Alongside expressing cytokeratins (CKs) associated with luminal epithelial cells such as CK8 and CK18, tumours classified as luminal-A also express the oestrogen receptor alpha gene (*ESR1*), and genes associated with ER pathway and activity (Yersal and Barutca, 2014). Luminal-A constitutes the majority of all breast cancers, representing approximately 50-60% of cases and generally have low histological grade, good prognosis and also include histological special types (lobular, tubular, mucinous and invasive cribriform). The rate of relapse in patients under this subtype is significantly low compared to the remaining subtypes and recurrence is mainly noted in bone (Yersal and Barutca, 2014). Less than 10% patients suffer from metastatic dissemination to lung, liver and the central nervous system (Yersal and Barutca, 2014). Due to its dependence on ER signalling, hormone therapy is usually the first line of therapy for these patients (Freedman et al., 2015).

Similar to luminal-A, tumours of the luminal-B subtype are positive for ER (Wirapati et al., 2008) and luminal markers but differ in their significantly higher expression of genes involved with cellular proliferation (Cheang et al., 2009). This is correlated to higher proportion of tumours in this category being of histological grade III and poorer prognosis of patients compared to the luminal-A subtype (Sotiriou and Pusztai, 2009). A proportion of luminal-B tumours is also classified by HER2 positivity and higher ki67 expression (Gomes Do Nascimento and Otoni, 2020). Untreated patients with luminal-B cancers are similar to their basal-like and HER2-positive high-risk counterparts in terms of overall survival (Hu et al., 2006). Relapse rate is also significantly higher in this subtype (Hu et al., 2006). This increased rate of relapse is usually limited to the first 5 years, which could be correlated to the high proliferative potential of tumours in this subtype

(Ignatiadis et al., 2009). Known as the most aggressive form of ER positive cancers, breast cancers of the luminal-B subgroup are known to respond poorly to hormone therapy and chemotherapy compared to luminal-A and basal like or HER2-enriched cancers respectively (Gomes Do Nascimento and Otoni, 2020). The pathological complete response (pCR) rate was found to be consistently lower in luminal-B samples compared to basal-like and HER2 cancers in 5 separate studies (Rouzier et al., 2005; Carey et al., 2007; Esserman et al., 2009; Bhargava et al., 2010; De Ronde et al., 2010).

HER2 tumours generally fall under the ER negative category and characteristically have HER2 overexpression and amplification of genes related to the HER2 pathway, particularly *ERBB2* which encodes HER2 (Perou et al., 2000; Sørlie et al., 2001, 2003). While more than 80% of tumours of this subtype have amplified *ERBB2*, some tumours positive for HER2 and ER are classified as luminal-B subtype depending on microarray expression clusters (Perou et al., 2000; Brenton et al., 2005; Rouzier et al., 2005). HER2 cancers are known to be highly aggressive but respond to tailored treatments with anti-HER2 monoclonal antibodies or inhibitors of HER2 tyrosine kinase (Slamon et al., 2001; Geyer et al., 2006; Figueroa-Magalhães et al., 2014).

Characterised by an aggressive disease progression, the neoplastic cells in TN or basal-like breast cancers (BLBC) are characterised by the expression of basal and myoepithelial cell markers such as CK5/6, CK14, CK17 along with Caveolin1, Caveolin2, α-Smooth muscle actin (α-SMA), P-cadherin and Epidermal growth factor receptor (EGFR) (Van de Rijn et al., 2002; Abd El-Rehim et al., 2004; Fulford et al., 2006; Savage et al., 2007, 2008). This subtype of breast cancer is usually negative for ER, PR and HER2 (triple-negative) although a small proportion of basal-like tumours are found to be positive for HER2 and sometimes the hormone receptors (Perou et al., 2000; Hu et al., 2006). The aggressive nature of this subtype is linked to high proliferation rate of the tumour cells, development of necrotic centres within the tumour mass, invasive borders, prominent infiltration of stromal lymphocytes and a high metastatic rate to the brain and lungs (Livasy et al., 2006; Badowska-Kozakiewicz and Budzik, 2016). Due to these characteristics, BLBC patients generally have a high relapse rate and poor prognosis (Toft and Cryns, 2011; Badowska-Kozakiewicz and Budzik, 2016). Germline mutations of *BRCA1* or dysfunctional BRCA1 pathway is often correlated to this subtype (Livasy et al., 2006; Turner et al., 2007; Badowska-Kozakiewicz

and Budzik, 2016). BLBC patients do not respond well to targeted hormone therapy; only about 5-10% of patients show evidence of tamoxifen sensitivity – a selective ER modulator (Manna and Holz, 2016). This is due to the lack of hormone receptors in most of these tumours and therefore more TN patients are generally treated with pre-operative chemotherapy followed by surgery and conventional chemotherapy or radiotherapy.

It is important to note that molecular stratification of tumours is not fixed to these 4 groups and is constantly evolving based on the generation of new and improved molecular methods, next generation sequencing and bioinformatics analysis techniques. The METABRIC study for instance, through combined analysis of copy number alterations and gene expression data, stratified breast cancer subtypes into 10 different integrative clusters (IntClust). These 10 subtypes are associated with distinct aberrations in gene copy number, patterns of survival and response to therapy (Pereira et al., 2016). Furthermore, through integration of clinical variables such as recurrence and survival with gene expression data, a 2019 paper revealed 3 luminal-A and 2 luminal-B subtypes distinguished by differences in the expression of genes related to distinct biological pathways, tumour-immune microenvironment modulation, and relevancy to disease prognosis (He et al., 2019). Through gene expression profile analysis, TN cancers have also been subdivided into basal-like 1, basal-like 2, luminal androgen receptor type, immunomodulatory type, claudin-low types and two mesenchymal types and based on differences in immune responses, expression of genes involved in androgen metabolism, immune signalling pathways, cell-junction proteins (such as claudins and E-cadherin), epithelial to mesenchymal transition (EMT), angiogenesis and cancer cell stemness (Gomes Do Nascimento and Otoni, 2020). A small proportion of breast tumours have also been grouped into the category of normal-breast like breast cancer (Perou et al., 2000). Characteristically, these tumour cells display gene expression patterns typical of adipose and basal epithelial cells with low expression of genes associated with luminal cells (Perou et al., 2000; Peppercorn, Perou and Carey, 2008). Gene expression signatures in these tumours tend to cluster with normal breast samples -hence the name – and also fibroadenomas (Peppercorn, Perou and Carey, 2008). However, this subtype and its clinical significance is poorly characterised and recently classification of this subtype has been challenged (Pusztai et al., 2006; Correa Geyer and Reis-

Filho, 2009). Proponents have suggested that it may have originated due to artefacts in sample representation (Weigelt, Geyer and Reis-Filho, 2010).
Integration of tradition methods of classification and modern molecular stratification of breast tumours have proven to be considerably accurate in predicting overall survival of patients, response to therapy as well as the risks of relapse and recurrence. This has greatly improved clinical management of the disease over the years and overall quality of patient life especially when patient tumours are treated as distinct biological entities that require personalised therapy.

1.2.3. Clinical Management of Breast Cancer

In the United Kingdom (UK), clinical management of breast cancer depends on the stage of the cancer - its size, location, metastasis status and health of the patient. Screening by physical examination of the breast either by oneself or a clinician, mammography, ultrasound, and magnetic resonance imaging (MRI) are used in the detection of breast cancer (Kolak et al., 2017). Once diagnosed, breast cancers may be staged according to chest radiograms or computed tomography (CT) scans, blood tests and tumour biopsies (McDonald et al., 2016). Integrated classification methods then allow patient stratification and the determination of appropriate treatment regimes. Primary methods of treatment include surgery, chemotherapy, radiotherapy, targeted endocrine therapy and immunotherapy (McDonald et al., 2016; Akram et al., 2017; Emens, 2018).

1.2.3.1. Surgery

Usually considered the primary method of management in breast cancer, patients generally have a choice of undergoing a breast conserving approach -lumpectomy or a non-breast conserving approach – mastectomy (McDonald et al., 2016; Akram et al., 2017). Lumpectomy is a form of partial mastectomy where only the tumour bearing part of the breast along with surrounding tissue is removed. While a small section of healthy tissue around the periphery of the tumour may need to be resected, most of the breast is kept intact. Generally, patients in earlier stages of breast cancer, when the primary tumour is relatively small are eligible for this procedure. Lumpectomy is generally paired with neo-adjuvant therapy prior to

surgery or adjuvant therapy such as chemotherapy, hormone replacement therapy and/or radiation therapy post-surgery (McDonald et al., 2016; Akram et al., 2017). Women diagnosed with large primary tumours or multicentric tumours may be treated with neo-adjuvant therapy followed by lumpectomy to require a mastectomy - complete removal of breast tissue - for tumour removal and to reduce the risk of recurrence. Prophylactic bilateral mastectomy is also beneficial, especially in patients with hereditary predispositions (Rebbeck et al., 2004; McDonald et al., 2016; Akram et al., 2017). Although it does not completely eliminate risk of developing the disease, this method reduces the risk of breast cancer by approximately 90% in women with BRCA1/2 mutations (Rebbeck et al., 2004). Reconstructive surgery is often an option for women undergoing lumpectomies or mastectomies to relieve them of the potential negative psychosocial effects of surgery (McDonald et al., 2016; Akram et al., 2017).

1.2.3.2. Radiation therapy

Post mastectomy or lumpectomy, most patients and especially those with a higher risk of regional recurrence are recommended radiation therapy as an adjuvant therapy (Kim et al., 2019). It is also used to eliminate any residual tumour cells in the area after surgery or dispersed tumour cells in other organs (Darby et al., 2011; Kim et al., 2019). High energy radiation is used to eradicate cancer cells and the exact dose, duration and type of radiotherapy depends on the stage of cancer at diagnosis as well as patient health (Kim et al., 2019). Patients can undergo whole breast radiation, accelerated partial breast irradiation, chest wall irradiation or specifically lymph node radiation depending on the spread of the tumour (Valachis et al., 2010; Ajkay et al., 2015; Kim et al., 2019).

1.2.3.3. Chemotherapy

Chemotherapy employs the administration of chemical compounds that induce cytotoxic or cytostatic events in neoplastic cells thereby reducing proliferation and survival of tumour cells. Neo-adjuvant chemotherapy prior to primary surgical treatment or adjuvant chemotherapy prescribed post-surgery in patients with high predicted recurrence rates such as those with triple negative disease, sizeable primary tumour at diagnosis and affected lymph nodes (McDonald et al., 2016; Akram et al., 2017). Neoadjuvant chemotherapy is often prescribed in patients

with a large primary tumour with the aim of reducing tumour size prior to surgery. Chemotherapy is also used to manage metastatic disease and delay tumour growth at secondary tumour sites (Gradishar, 2012; McDonald et al., 2016; Akram et al., 2017). Chemotherapeutic drugs fall under the following categories based on how they induce cytotoxic effects : (1) alkylating agents which form covalent bonds with cellular DNA, RNA or proteins thereby impairing cellular function, (2) anti-metabolites which mimic and compete with natural metabolites involved in synthesis of DNA or RNA or catalytic activation of enzymes, (3) anti-tumour antibiotics which induce breakage of specific DNA sequences, (4) topoisomerase inhibitors which inhibit the function of enzymes involved in the uncoiling of DNA prior to replication, and (5) tubulin-binding drugs which interfere with microtubule formation and their normal function leading mitotic-inhibition (Caley and Jones, 2012; Gradishar, 2012; Johnstone, Park and Lippard, 2014; McGowan et al., 2017; Willson et al., 2019). Most therapeutic regimes employ a combination of several agent from the different classes of chemotherapeutics to achieve effective treatment response (Caley and Jones, 2012). Although chemotherapeutics has been used as standard therapy for more than 50 years, there are various side effects ranging from hair loss, loss of appetite and fatigue to infertility, neuropathy, heart damage and in rare cases, increased risk of leukaemia (American cancer society, 2019). The recent rise of alternate targeted therapies such as endocrine therapy or immunotherapy has improved clinical management and patient quality of life to a considerable extent (Akram et al., 2017; Burstein et al., 2019; Cynthia X Ma and PhDJoseph A Sparano, 2020).

1.2.3.4. Hormone therapy

Hormone therapy is often used as first line adjuvant therapy in patients with ER positive disease and similar to chemotherapy, has served as standard therapy for decades. Nearly 70% of all breast cancers cases are positive for hormone receptors (mainly ER) where proliferation and spread of tumour cells are driven by activation of the oestrogen-ER pathway (Pereira et al., 2016). ER positive patients are generally treated with selective ER modulators (SERMs) such as Tamoxifen or selective ER degraders such as Fulvestrant (Cynthia X Ma and PhDJoseph A Sparano, 2020). Both of these compete with endogenous oestrogen and inhibit its interaction with ER. Fulvestrant goes a step further by inducing ER degradation and therefore is generally only prescribed to post-menopausal women and patients

with acquired resistance to tamoxifen (Vergote and Robertson, 2004). Tamoxifen treatment in patients with previously untreated metastatic disease has been found to have positive impact on response rate and disease stabilisation in 50% of ER positive cases (Ring and Dowsett, 2004). Another study has demonstrated 49% reduced risk of developing breast cancer in the previously unaffected breast due to hormone therapy (Akram et al., 2017). Tamoxifen treatment for 10 years post-surgery has also been shown to halve recurrence rates even after 20 years post-diagnosis (Davies et al., 2013).

Aromatase, the enzyme responsible for the last stage of oestrogen formation - usually in post-menopausal women, is also targeted in therapy (Goss and Strasser, 2001). Aromatase inhibitors (AIs) such as letrozole, Anastrozole and Exemestane have shown considerable effectiveness in patients with advanced ER positive disease and has shown to have a synergistic effect with tamoxifen (Goss and Strasser, 2001; Freedman et al., 2015). Current standard of care for ER positive patients generally includes the use of AIs either with or after a round of tamoxifen treatment (Freedman et al., 2015; Burstein et al., 2019).

Albeit the advantages, endocrine therapy is known to induce adverse side effects in 94% of patients such as hot flashes, increased risk of carpal tunnel, arthralgias, thickening of tendons and increased bone resorption resulting in fractures (Amir et al., 2011; Aiello Bowles et al., 2012; Awan and Esfahani, 2018). AI therapy is additionally known to induce vaginal dryness in women leading to vaginal atrophy, vaginitis, cystitis and overall physical and mental distress owing to sexual disfunction. Tamoxifen is associated with increased risk of venous thromboembolism as well as ocular pathologies such as cataract development (Awan and Esfahani, 2018). However, the most concerning issue with endocrine therapy lies in the development of resistance to therapy and the subsequent recurrence of disease (Lei et al., 2019). Indeed, intrinsic resistance is noted in up to 20% tumours while 30-40% of tumours acquire resistance over several years of treatment (Ring and Dowsett, 2004; Anurag, Ellis and Haricharan, 2018).

1.2.3.5. Targeted therapy

In recent years the use of therapeutics targeting specific molecular components of tumour cells such as cell surface receptors, cell cycle regulators, or tumour-immune micro-environmental factors have generated promising results. Treatment with cell cycle checkpoint inhibitors targeting cyclin dependent kinases

(CDK) that take advantage of the CDK4/6 dependence in tumour cells, are rapidly improving treatment of patients with hormone receptor positive, HER2 negative and TN disease (Shah, Nunes and Stearns, 2018). Exploiting components of the host immune system to target tumour cells have also considerably improved treatment of certain breast cancer subtypes (McDonald et al., 2016; Akram et al., 2017). In this regard, use of immune checkpoint inhibitors has emerged as a useful treatment strategy for immunogenic subsets of breast cancer (Swoboda and Nanda, 2018). Treatment with the monoclonal antibodies such as Trastuzumab or Pertuzumab which targets the HER2/HER3 receptors (as an antigen) on breast cancer cells has significantly increased overall survival of patients (Figueroa-Magalhães et al., 2014) (Ishii, Morii and Yamashiro, 2019). Antibody-drug conjugates (ADCs) such as Ado-trastuzumab and Fam-trastuzumab deruxtecan, where HER2 targeting antibodies are linked to chemotherapeutic agents is often recommended for patients with HER2 positive metastatic disease (von Minckwitz et al., 2019; Modi et al., 2020). Useful in TN disease, the recently-FDA-approved ADC, Sacituzumab Govitecan, attaches to the Trop-2 protein expressed on the surface of breast cancer cells and allows the chemotherapeutic compound to specifically target the malignant cells (FDA,2021; Bardia et al., 2019). Another protein often targeted in TN disease is programmed death-ligand 1 (PD-L1) and monoclonal antibodies are often used to block this protein from allowing interaction of cancer cells with the host immune system. This can stimulate an immune response against the breast cancer cells thereby reducing tumour growth and size (Schmid et al., 2018). Manipulation of the tumour immune niche to promote anti-tumorigenic responses would provide a critical avenue in therapy especially for patients experiencing resistance chemotherapy or hormonal therapy.

On the other hand, taking advantage of tumour intrinsic vulnerabilities unlocks new possibilities for breast cancer treatment. Overexpression of oncogenes and loss of function mutations in tumour suppressor genes have been recognised as drivers of numerous cases of breast cancer. These provide alternative targets for breast cancer patients who have developed some sort of resistance to the standard therapies discussed above. Inhibitors of oncogenic proteins such as Phosphatidylinositol 3 kinase (PI3K) and mammalian target of rapamycin (mTOR) have been shown to successfully inhibit or limit tumour growth, prevent angiogenesis and thereby reduce tumour size, especially when taken

concomitantly with other forms of neoadjuvant and adjuvant therapy (Royce and Osman, 2015; Patienten and Therapie, 2020). Additionally, vulnerabilities in tumour cells harbouring mutations in tumour suppressor genes can be targeted for inducing synthetic lethality. For instance, tumour cells with mutations in the *BRCA1* tumour suppressor gene, critically involved in homologous recombination and DNA damage repair mechanisms, can be targeted for DNA damage induced cytotoxicity by inhibitors of poly-ADP ribose polymerase (PARP), which further prevent the cells from sensing DNA damage and inducing repair through the activity of PARP enzymes (McCann and Hurvitz, 2018).

However, as increasing numbers of patients are developing resistance to current treatment regimes, there is an ever-growing need to find new targets. Oncogenesis is modulated by multiple drivers and identification and investigation of such drivers and the role they play in normal breast as well as tumour biology and tumour microenvironmental interactions, is crucial in developing the next generation of therapeutics.

1.3. The CBFβ-RUNX complex: regulators of development and disease

The Runt-related transcription factor (RUNX) family comprises three members: RUNX1, RUNX2 and RUNX3, which operate as part of a heterodimeric core binding factor (CBF) complex with their obligate partner – core binding factor-beta (CBFβ) (Blyth, Ewan R Cameron and Neil, 2005; Chimge and Frenkel, 2013). RUNX1, historically found to undergo frequent chromosomal translocations in acute myeloid leukaemia (AML) patients, is critical in the development, differentiation, and homeostasis of haematopoietic stem cells (HSC) (Voon, Hor and Ito, 2015). RUNX2 is known as the master regulator in bone development, particularly in the differentiation of osteoblasts (Ducy et al., 1997; Komori et al., 1997; Otto et al., 1997). RUNX3, expressed in a range of epithelial tissues, has overlapping distribution and functions with the two other RUNX family members (Voon, Hor and Ito, 2015). In the differentiation of dorsal root ganglion neurons, RUNX3 is essential (Inoue et al., 2002). Regulating the activity of these three key players of normal development, is their obligate binding partner and transcription co-factor: CBFβ (Voon, Hor and Ito, 2015; Malik et al., 2019). Together the CBFβ/RUNX complex regulate transcription of numerous genes involved in cell proliferation,

differentiation and survival (Blyth, Ewan R. Cameron and Neil, 2005; Chimge and Frenkel, 2013).

1.3.1. Functional relevance of CBFβ and RUNX

During a screen conducted to identify genes involved in segmentation pattens in Drosophila, (Nusslein-Volhard and Wieschaus, 1980) discovered a gene which, when mutated, resulted in the generation of runted embryos – the *runt* gene. Subsequently, the protein encoding the human *RUNX1* gene, cloned in 1991 by Okhi *et al*. while analysing chromosomal translocations in AML patients (Miyoshi et al., 1991; Shimizu and Ohki, 1991), was found to have a region of amino acid sequences that was highly homologous to the Drosophila runt (Kagoshima et al., 1993).

In a paper published in 2002, (Strippoli et al., 2002) reported identifying triplication of a 500kb segment of the human chromosome (21q22, 1p35 and 6p12-21) encoding the trinity of mammalian RUNX genes. Notably, a key feature common to all three members is the presence of a highly conserved domain comprised of 128 amino acids – the Runt-homology domain (RHD) (aa 58-178), named after the Drosophila *runt* (Kagoshima et al., 1993; Blyth, Ewan R Cameron and Neil, 2005). This region was found to support two functions: allowing the RUNX proteins to bind to DNA and enabling heterodimerisation to CBFβ (Bravo et al., 2001).

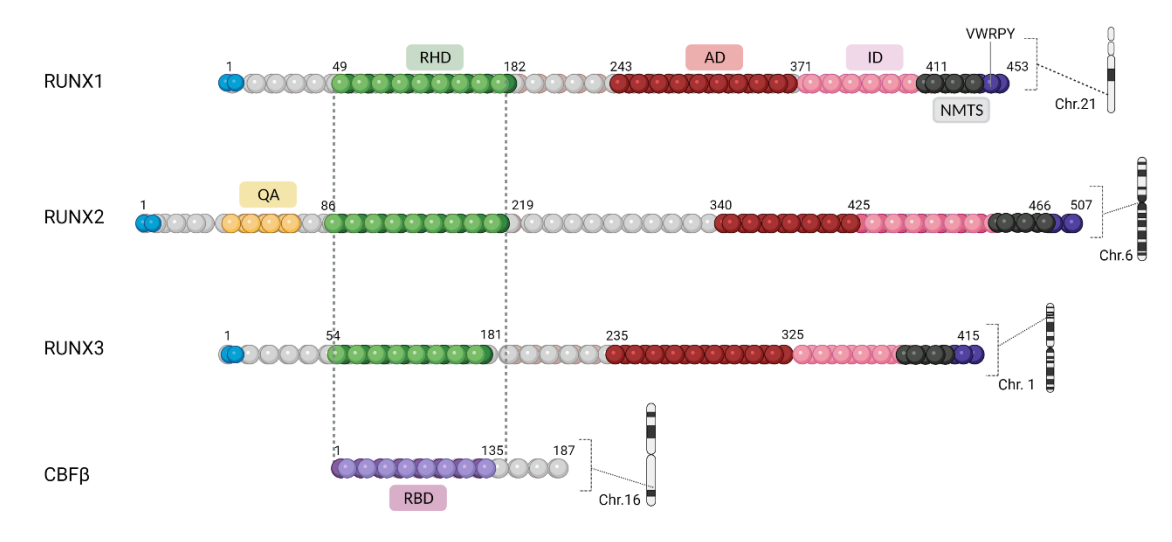

Figure 1.4: Schematic representation of the domains of CBFβ and RUNX proteins.
The human RUNX proteins are encoded by the 3 RUNX genes, RUNX1 (in chromosome 21), RUNX2 (in chromosome 6) and RUNX3 (in chromosome 1) while CBFβ is encoded by the CBFβ gene in chromosome 16. The Runt-homology domain (RHD) on RUNX proteins binds to the Runx binding domain (RBD) on CBFβ to allow formation of the CBF complex. The activation domain (AD) and inhibitory domain (ID) and nuclear matrix targeting signal (NMTS) are indicated. The QA region on RUNX2 is an extended region of glutamine-alanine repeats that differentiate it from the two other RUNX family members. The carboxy-terminal VWRPY motif is used in the interaction with co-factors. Figure created using Biorender.com

The transcriptional co-factor CBFβ, is a ubiquitously expressed protein, encoded in mammals by the 50 kb *CBFβ* gene, located on chromosome 16q22 (Kent et al., 2002) (Figure 1.4). With 6 exons generating three isoforms (with polypeptides comprised of 155, 182 and 187 amino acids) achieved through alternative splicing (Tahirov et al., 2001a), CBFβ is a non-DNA binding protein that lacks a nuclear localisation signal (Hajra and Collins, 1995; Qing Wang et al., 1996; Tahirov et al., 2001b; Rooney et al., 2017) and resides in the cytoplasm. Excluding the 155aa one, the two bigger isoforms use residues 1-141 (the CBFβ heterodimerisation domain) to bind RHD on RUNX proteins (Ogawa et al., 1993; Bushweller et al., 1999). While binding to RUNX proteins allows CBFβ to be shuttled into the nucleus, it repays the favour by allosterically stabilising the point of contact between RHD and DNA (Bravo et al., 2001) thereby improving the DNA-binding affinity of RUNX proteins by 40-fold (Gu et al., 2000; Yan et al., 2004). The co-factor plays an additional role in aiding RUNX-DNA interaction by blocking oxidation of cystine residues on RUNX proteins: a process which has been shown to reduce their DNA binding affinity (Bushweller et al., 1999). Furthermore, binding to CBFβ protects RUNX proteins, as shown in the case of RUNX1 where heterodimerisation with CBFβ

prevents its degradation. This highlights another important role of CBFβ in RUNX regulation (Huang et al., 2001; Riggio and Blyth, 2017). Indeed, RUNX1 levels are barely detected in *Cbfβ* $^{-/-}$ mice (Riggio and Blyth, 2017) and in mammals, CBFβ has been shown to increase the half-life of this protein by preventing proteolysis of RUNX1 via ubiquitination (Huang et al., 2001).

Inside the nucleus, RHD on RUNX is used to modulate transcription of their target genes through interactions with specific promoter and enhancer elements (Otto, Lübbert and Stock, 2003). RHD recognises and binds the 5'-TG (T/C)GGT-3' consensus sequence – or what seems more frequently bound in putative RUNX target promoters, the 5'-R/TAACCRCA-3' sequence (Otto, Lübbert and Stock, 2003; Blyth, Ewan R Cameron and Neil, 2005). Together the CBFβ/RUNX complex then recruits additional cofactors to target genes and regulates transcription of numerous genes involved in cell proliferation, differentiation, and survival (Westendorf and Hiebert, 1999; Blyth, Ewan R Cameron and Neil, 2005) Figure 1.5.

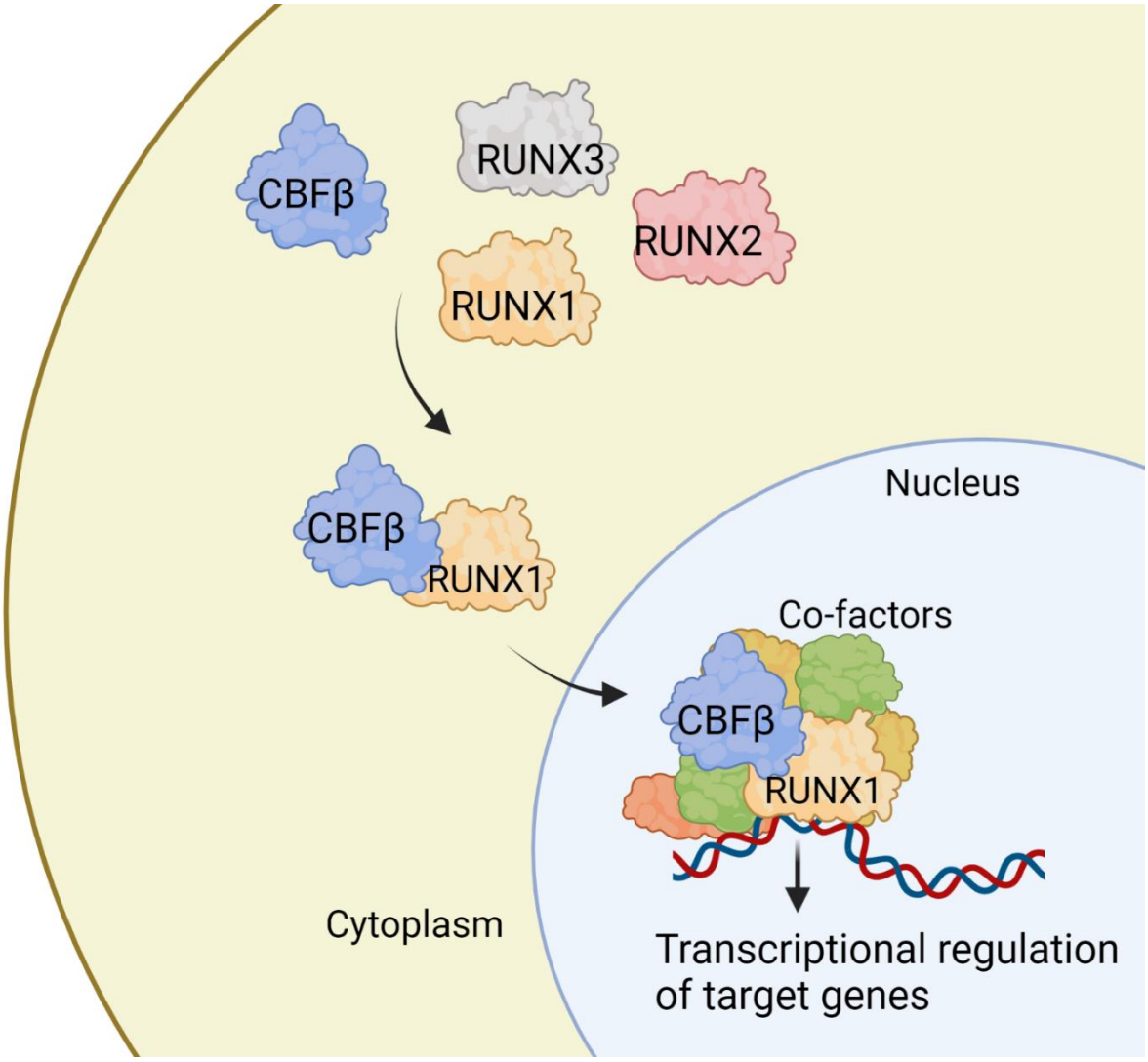

Figure 1.5: The RUNX-CBFβ complex. CBFβ interacts with members of the RUNX family of proteins within the cytoplasm.

Once bound to any of the three RUNX proteins, in this case RUNX1 is depicted, the complex is then translocated into the nucleus where it can bind to DNA and regulate transcription. Recruitment of various co-factors determine the fate of transcription regulation of RUNX/CBFβ target genes. Figure created using Biorender.com

While some of these cofactors such as C/EBP, Myb, AP-1, and Ets, have promoter sites in close proximity to the RHD binding elements and therefore help regulate transcription through direct interaction with DNA; other coactivators including ALY, YAP and p300/CBP, directed to the appropriate location through their interaction with CBF, activate transcription initiation through histone acetylation, direct acetylation of RUNX proteins, or recruiting the transcription initiation complex (Westendorf and Hiebert, 1999; Jin et al., 2004; Yamaguchi et al., 2004). Direct or indirect interactions with co-repressors such as the Transducin-Like Enhancer of Split (TLE) proteins, members of the Groucho family, mSin3A, histone

de-acetylases (HDACs), nuclear hormone co-receptor (N-CoR) and silencing mediator of retinoid and thyroid hormones (SMRT) are also used by CBF to negatively regulate transcription (Westendorf and Hiebert, 1999; Blyth, Ewan R Cameron and Neil, 2005).

The impact of this collaborative approach of CBF on gene transcription is powerful. For instance, RUNX/CBFβ synergistically activates C/EBP mediated regulation of the promoter for macrophage colony stimulating factor (M-CSF) receptor (Petrovick et al., 1998). Without the presence of CBF, activation of the M-CSF receptor promoter by C/EBP is weak (Petrovick et al., 1998). The CBF complex alone, improves the activation of the promoter by five-fold. However, the combined effect of RUNX/CBFβ and C/EBP is an increase in promoter activation of over 100-fold (Petrovick et al., 1998). An alternative example is of RUNX/CBFβ on T cell receptor (TCR) regulation in conjunction with ETs-1 (Kim et al., 1999). RUNX has been shown to use an auto-inhibitory domain to prevent the function of its transactivation domain and potentially block its interaction with DNA (Kim et al., 1999). At the enhancer for TCR, RUNX/CBFβ recruit Ets-1 which binds to the adjacent sites of the enhancer (Wotton et al., 1994; Kim et al., 1999). Ets-1 interacts with RUNX and induces a conformational change in the protein which allows its DNA binding domain and transactivation domain to be exposed (Kim et al., 1999). The trio together can then regulate TCR expression (Kim et al., 1999).

Transcription regulation by RUNX/CBFβ is additionally impacted by post-translational modifications of the CBF members (Chuang, Ito and Ito, 2013). Activity of RUNX proteins is dynamically controlled by phosphorylation (via kinases such as CDKs, ERK, HIPK2 and PIM-1), acetylation (by p300 and BMP-2), methylation (through the PRMT1 methyltransferase) and ubiquitin mediated proteolysis (Chuang, Ito and Ito, 2013). Further regulation of RUNX/CBFβ is achieved through chromatin modifications by HDACs. MOZ and MORF are two acetyltransferases that directly interact and stimulate RUNX function while an active chromatin status has been associated to the collaboration of the chromatin modelling complex SWI/SNF with RUNX/CBFβ (Chuang, Ito and Ito, 2013).

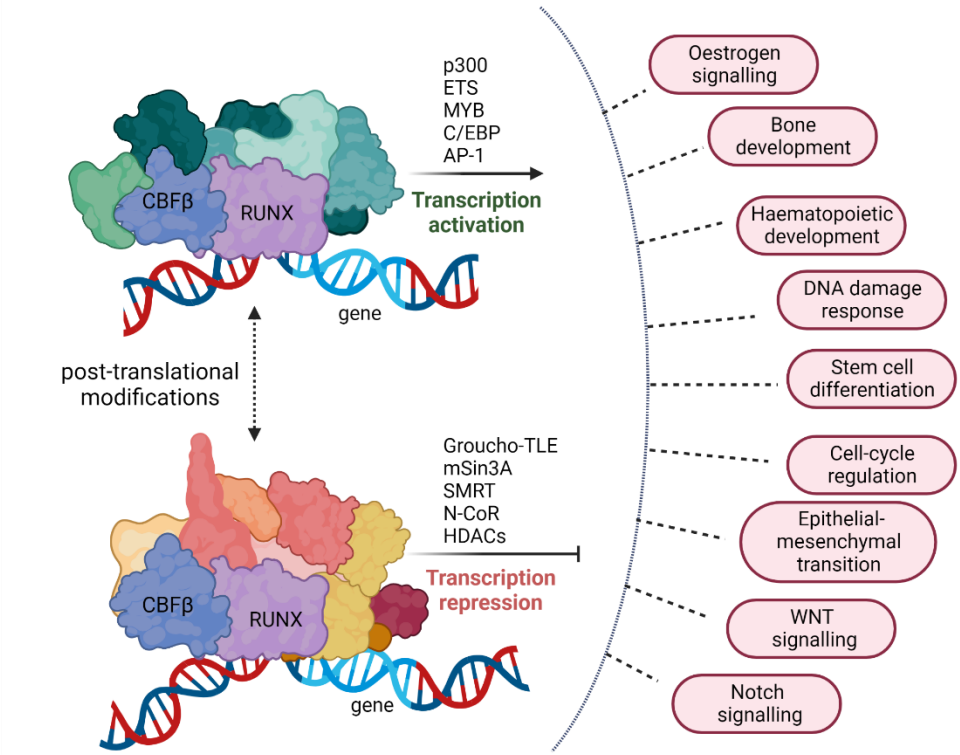

Figure 1.6: The core binding factor complex works in conjunction with an array of transcription co-activators and co-repressors to regulate crucial cellular pathways.
Schematic adapted from (Blyth, Ewan R Cameron and Neil, 2005). Figure created using Biorender.com

This comprehensive regulation of and by RUNX/CBFβ is imperative in controlling cellular pathways in both development and disease (Figure 1.6). Indeed, loss of either component of the CBF complex – CBFβ or RUNX – has lethal effects on normal development. Homozygous deletions of RUNX proteins or CBFβ *in vivo* prevent hematopoietic development, induce central nervous system haemorrhaging, respiratory issues and ultimately lead to death of embryos within 12-14 days post conception (Okuda et al., 1996; Qing Wang et al., 1996; Q Wang et al., 1996). Mice with full body deletion of RUNX2 succumb to death from malformations in bone development with a distinct phenotype of concaved rib cages which leads to severe respiratory defects (Komori et al., 1997). CBFβ is also known to be an important player in osteogenesis although loss of CBFβ still allows for some differentiation of osteoblasts unlike RUNX2 knockdown (Kundu, Javed, et al., 2002; Yoshida et al., 2002). Additionally, CBFβ is required for RUNX3 activity as a critical regulator of neuronal development alongside mediating the development and function of bone, blood, and immune cells (Lutterbach and Hiebert, 2000; Lallemend et al., 2012; Wang et al., 2013). Noting how critical

RUNX and CBFβ are in normal homeostasis and development, it is not surprising that these genes are frequent targets of various alterations and mutations in a multitude of cancers including various subtypes of breast cancer (Niini et al., 2000; Kundu and Liu, 2001; Blyth, Ewan R Cameron and Neil, 2005; Sakakura et al., 2005; Miyagawa et al., 2006; Mallo et al., 2007; Davis et al., 2010; Rooney et al., 2017; Carlton et al., 2018). Notably in breast cancer, mutations in the RUNX genes and CBFβ have been credited to play context dependent roles (Chimge and Frenkel, 2013; Rooney et al., 2017).

1.3.2. CBFβ in cancer: oncogene or tumour suppressor?

As a master regulator of RUNX, it is evident that involvement of CBFβ is key to overall RUNX function. However, independent of RUNX, CBFβ also plays important roles in the regulation of various other pathways and cellular systems (Malik et al., 2019). In fact, a recent paper by (Malik et al., 2019) presented a novel role of CBFβ in the translation of hundreds of mRNA including that of RUNX1. Noting how critical CBFβ is in normal homeostasis and development it is not surprising that this gene is frequently a target of various alterations and mutations in a multitude of cancers (Kundu and Liu, 2001; Blyth, Ewan R Cameron and Neil, 2005; Sakakura et al., 2005; Miyagawa et al., 2006; Mallo et al., 2007; Davis et al., 2010; Rooney et al., 2017; Carlton et al., 2018) (Figure 1.7).

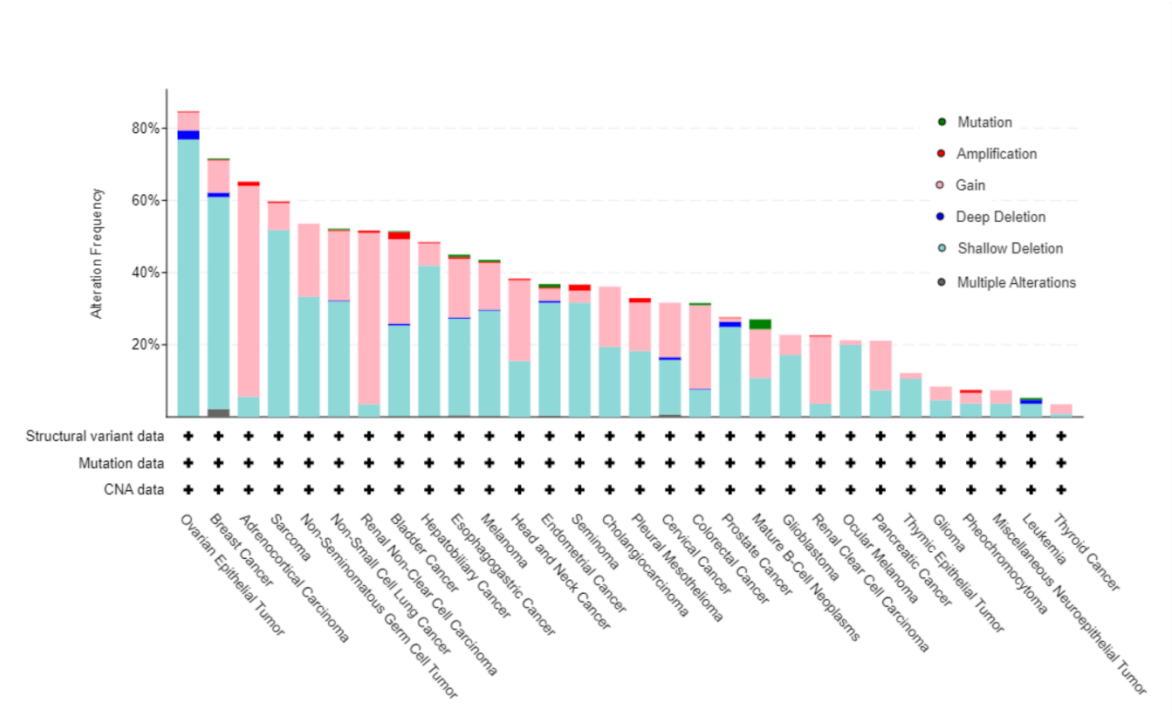

Figure 1.7: Alteration frequencies in *CBFβ* noted in a multitude of human cancers.
Data acquired from the METABRIC dataset and presented using cBioportal (Cerami et al., 2012; Gao et al., 2013; Pereira et al., 2016).

1.3.2.1. CBFβ in cancers of the blood

Originally discovered as the gene on chromosome 16 that undergoes inversion inv (16) (p13;q22) leading to approximately 10% of AML cases (AML M4Eo), CBFβ has been most widely researched in leukaemia (Liu et al., 1993; Kundu and Liu, 2001). One of the very first alterations in the CBF complex was reported in AML and since then RUNX1 and CBFβ have been implicated as crucial players in leukemogenesis (Look, 1997; Davis et al., 2010). The CBFβ Inv (16) (p13:q22) translocation or its equivalent t (16:16) (p13:q22), where the fusion gene *CBFβMYH11* is generated after the break-and-join inversion of chromosome 16, is found in almost all cases of the M4Eo subtype of AML (Liu et al., 1993). This translocation results in the fusion between the coding region of *CBFβ* and the *MYH11* gene encoding a smooth muscle myosin heavy chain (SMMHC) (Liu et al., 1993). *In vitro* studies have shown that the fusion protein, CBFβ-SMMHC, resides mostly in the cytoplasm via its SMMHC C-terminal which is involved in dimerization and multimerization of myosin (Cao et al., 1998). Compared to wild-type CBFβ, the oncogenic CBFβ-SMMHC protein binds to RUNX proteins with a higher affinity and stabilises them to a considerable extent. This has been shown to sequester RUNX, retain it within the cytoplasm and inhibit function of the CBF complex (Kanno et al., 1998). This in

turn can slow down progression of the cell cycle and apoptotic responses to DNA damage and ultimately lead to uncontrolled expansion of HSCs classically noted in AML (Speck et al., 1999; Kundu and Liu, 2001; Castilla et al., 2004).

Mouse embryos with a heterozygous knock-in of *CBFβ-MYH11* phenocopy *Cbfβ*$^{-/-}$ embryos such that they fail to undergo definitive haematopoiesis (Kundu, Chen, et al., 2002). *In vivo* studies have shown that the resulting fusion protein, CBF*β*-SMMHC acts as a dominant repressor and inhibits normal role of the RUNX1-CBFβ complex in regulating transcription (Castilla et al., 1996). CBFβ-SMMHC has been shown to block not only definitive haematopoiesis in early embryonic development but also differentiation of hematopoietic stem cells in adults (Castilla et al., 1996). While translocations and somatic mutations involving the RUNX1 gene is also observed in AML patients, most of these affect the RHD and therefore the association of RUNX1 with CBFβ (Davis et al., 2010).

Interestingly, depletion of RUNX1 in leukemic cells have been shown to result in a compensatory increase in CBFβ. Indeed, compared to normal cells, malignant cells expressed elevated levels of this protein and cells derived from patients who went through relapse, exhibited even higher expression of CBFβ (Morita, Suzuki, et al., 2017). Following this, a recent paper revealed an autonomous feedback loop where any loss of RUNX1 was compensated by p53 induced upregulation of CBFβ transcription and translation (Morita, Noura, et al., 2017). Increased levels of CBFβ in the cytoplasm in turn enabled stabilisation of RUNX1 and RUNX1 mediated transcription. This autonomous loop has been deemed crucial in the maintenance of AML cell tumorigenicity and linked to acquired chemo-resistance (Morita, Noura, et al., 2017).

Apart from AML, rearrangements of CBFβ – such as *CBFβMYH11*- can also be noted in chronic myeloid leukaemia (CML) patients with a t (9;22) (q34;q11.2)/BCR-ABL1 mutation. Although co-occurrence of both these mutations in one patient is rare, it is associated with adverse prognosis and clinical outcome similar to the more aggressive blast phase of CML (Salem et al., 2017). On the other hand, in granulocytic sarcomas and human B-cell acute lymphoblastic leukaemia, amplification of the CBFβ gene indicative of its oncogenic role, is more common (Niini et al., 2000; Mallo et al., 2007).

All these studies highlight crucial role of CBFβ in disorders of haematopoietic system and how deregulation of its normal expression levels and protein function

or even mutations in its RUNX counterparts that interfere with their interactions with CBFβ may play a crucial role in cancers of the blood.

1.3.2.2. CBFβ in solid tumours

While CBFβ has been put under a spotlight for its role in leukemogenesis, the past few decades have alluded to its contribution in the oncogenesis of various other organs and epithelial cancers (Figure 1.7). Association of CBFβ with a malignant phenotype has also been noted in a wide variety of solid tumours, with the highest alteration frequencies being in ovarian and breast cancers. In healthy ovarian tissue expression of RUNX proteins are generally low (Davis et al., 2010). In a subset of ovarian cancers however, all three RUNX proteins are overexpressed (Davis et al., 2010; Carlton et al., 2018). Inhibition of CBFβ, which as we know affects potency of RUNX function, *in vitro* led to significant reduction in cell proliferation, anchorage independent growth and migration of ovarian cancer cells (Davis et al., 2010).

In support of this, CBFβ function was also manipulated using a small molecule inhibitor (AI-10-104) in ovarian cancer cell lines (Carlton et al., 2018). This inhibitor is known to bind to CBFβ and allosterically inhibit its interaction with RUNX proteins, thereby compromising RUNX mediated transcription (Illendula et al., 2016). Proliferation and migration of the ovarian cancer cells were significantly decreased upon inhibition of the cofactor (Carlton et al., 2018). CBFβ inhibition also led to a decrease in the expression of EMT-related genes, delayed the S-phase cell cycle and reduced anchorage-dependent growth in ovarian cancer cells (Carlton et al., 2018). These results strengthen the association of CBFβ in the oncogenesis of ovarian cancer.

In prostate cancer cells, CBFβ has also been linked to oncogenesis as knockdown of the gene led to reduced growth of tumour cells both *in vitro* and in a subcutaneous transplantation mouse model (Davis et al., 2010). Davis *et al*, knocked down *CBFβ* in the PPC1 prostate cancer cell line using shRNA and analysed the 200 differentially expressed genes in PPC1 cells identified using whole genome array. RUNX binding sites were discovered in the promoter regions of over 20% of these genes suggesting that their expression may have been under direct control of CBF (Davis et al., 2010). The remaining 80% of the genes were known to be associated in key biological processes known to be regulated by the CBF such as osteoblast differentiation, odontogenesis, hormone metabolism and secretion,

along with other genes associated with cancer cell growth, proliferation and epithelial to mesenchymal transition (Davis et al., 2010). Various proteases involved in tumour progression and their invasive phenotype such as matrix metalloproteinase-3 (MMP3) were significantly downregulated in CBFβ knockout cells in vitro (Davis et al., 2010).

Curiously, deletion of *CBFβ* is the major aberration noted in prostate and ovarian cancer cases according to TCGA and METABRIC datasets as shown in Figure 1.7. Therefore, although the studies discussed above suggest an oncogenic function of this protein, there is clearly more complexity in the relationship between CBFβ and these cancers.

In gastric cancer, the dualistic role of CBFβ is presented through two different studies. CBFβ (as well as RUNX3) has been shown to play a tumour suppressive role in gastric cancers (Sakakura et al., 2005). Downregulation of CBFβ has been noted in a significant proportion of gastric cancer samples, the degree of downregulation being directly proportional to disease progression, indicating that loss of CBFβ might be facilitating RUNX1 and RUNX3 dysregulation in this instance (Sakakura et al., 2005). More recently, however, sequencing data from the TCGA dataset in combination with staining of human gastric cancer samples by immunohistochemistry (IHC) revealed increased expression of CBFβ in gastric tumours, compared to normal tissue samples (X. Chen et al., 2018). An increase in CBFβ expression was also correlated to poor prognosis in patients and a shorter overall survival time (X. Chen et al., 2018). Further *in vitro* analysis revealed a previously undiscovered LINC01234-miR-204-5p-CBFβ axis whereby the long noncoding RNA LINC01234 acts as an oncogene in gastric cancer and suppresses miR-204-5p mediated negative regulation of CBFB (X. Chen et al., 2018). An oncogenic role for CBFβ in gastric cancer was unveiled for the first time when knockdown of the cofactor significantly reduced gastric cancer cell growth and proliferation, induced a G1-G0 phase arrest, increased apoptosis *in vitro* and inhibited tumour growth *in vivo* (X. Chen et al., 2018).

Among other solid cancers, a role for members of the CBF complex in clear cell renal cell carcinoma (ccRCC) has been uncovered recently (Rooney et al., 2020). Rooney *et al*. demonstrated that RUNX1 acts as a driver of RCC and deletion of *Runx1* reduced tumour cell proliferation and improved disease-free survival *in vivo* (Rooney et al., 2020). Although *Runx2* deletion in the genetically engineered mouse model (GEMM) used was unattainable due to embryonic lethality, high

RUNX2 expression was shown to be correlated to poor prognosis in human ccRCC patients. (Rooney et al., 2020). Following these results, *in silico* analysis of the PanCancer genome Atlas (TCGA) dataset of ccRCC patients has revealed gene amplification and gain of *CBFβ* in a small proportion of samples. Amplification of *CBFβ* was also associated with poor prognosis in these patients although a greater sample size would be required to confirm a significant correlation. Although thorough experimental evidence is required to determine the exact role of CBFβ in human ccRCC, preliminary *in silico* data, together with the evidence showing contribution of RUNX1 and RUNX2 in the oncogenesis of ccRCC, seems supportive of the hypothesis that CBFβ may be acting as an oncogene in ccRCC.

Conversely, an indication of tumour suppressive role of CBFβ has been exhibited in hepatocellular carcinoma and colorectal cancer (Miyagawa et al., 2006; Andersen et al., 2009). Reduction in CBFβ and all three RUNX protein levels is observed in samples from liver cirrhosis patients. In 2006, Miyagawa *et al* revealed that loss of this complex may be involved in the early stages of tumorigenesis in hepatocellular carcinoma (HCC) (Miyagawa et al., 2006). While components of the CBF complex is known to be strongly expressed in normal liver, analysis by qRT-PCR as well as in situ hybridisation of patient samples revealed that in HCC, this is significantly reduced (Miyagawa et al., 2006). Therefore, CBFβ alongside its RUNX counterparts, maybe be playing a tumour suppressive role in liver cancer with a potential role in HCC tumorigenesis in the early stages (Miyagawa et al., 2006).

In colorectal cancer (CRC), (Andersen et al., 2009) suggested a potential tumour suppressive role of CBFβ with higher levels of CBFβ correlated to better patient prognosis, and low expression or the absence of CBFβ associated to poor survival and increased metastasis in CRC patients. Intriguingly, analysis of 424 colorectal cancer (CRC) patient samples when compared to 20 samples of normal mucosa led to the identification of CBFβ as one of the top 51 upregulated transcription factors in CRC (Andersen et al., 2009). While CBFβ protein expression was absent in normal epithelium, IHC staining of tissue microarrays (TMAs) was positive for the protein in neoplastic cells as well as in infiltrating stromal lymphocytes in both normal mucosa and tumours (Andersen et al., 2009). CBFβ expression was seen to progressively increase from normal to adenoma to adenocarcinoma but diminish in liver metastases (Andersen et al., 2009). Andersen and colleagues hypothesised that this increase in CBFβ gene expression might be a defence response of

colorectal cells approaching neoplasia to suppress growth of the tumour although further evidence is required to confirm this notion.

Ultimately, these complex patterns of CBFβ suggest that while this transcription factor could be acting as a tumour suppressor or an oncogene, it is difficult to draw a straightforward conclusion owing to the context dependent roles exhibited by this protein.

1.4. CBFβ as an emerging player in breast cancer

In a comprehensive targeted sequencing-based study analysing almost a thousand primary breast cancer samples, *CBFβ* was shown to be one of the top 17 recurrently mutated genes (Griffith et al., 2018). This data was complimented by results from the METABRIC study (Pereira et al., 2016) where *CBFβ* was shown to be altered in 14% of the 2433 breast cancer cases investigated (Figure 1.8). Additionally, alterations in this transcription co-factor were also noted in 13% of primary breast cancer cases in the TCGA Firehose legacy dataset and in 5% of metastatic breast cancer samples as reported in the study by Li *et al* (Cerami et al., 2012; Gao et al., 2013; Li et al., 2022).

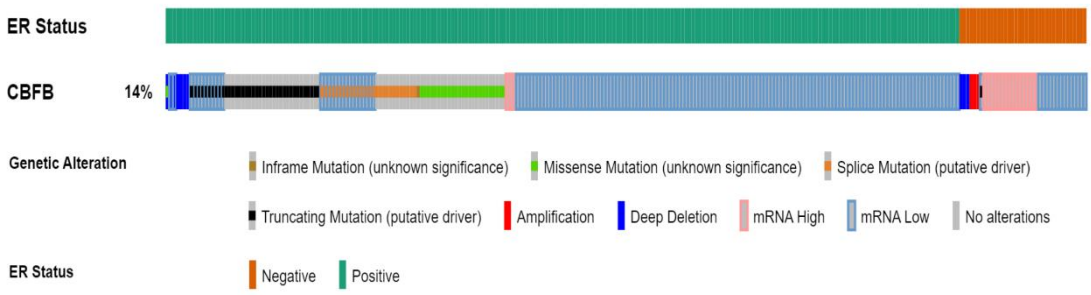

Figure 1.8: Genetic alternations in CBFβ in ER-positive and ER-negative breast cancer.
Figure represents data acquired in the METABRIC (Pereira et al., 2016) dataset presented via cBioportal (Cerami et al., 2012; Gao et al., 2013). ER status presented in the top oncoprint showing cases with ER positive breast cancer in green and those with ER negative tumours in orange. Patient samples with genetic alterations in *Cbfβ* presented in the second oncoprint labelled CBFB. Data acquired in August 2022.

These results also highlighted that this one gene undergoes varying alterations depending on the subtype of breast tumour. For instance, in ER positive tumours, truncating or missense mutations and gene deletions are the predominant type of genetic alteration. Conversely, these mutations are rare in ER negative tumours

where a proportion of cases show amplification and high expression of CBFβ mRNA (Ciriello et al., 2015; Nik-Zainal et al., 2016; Pereira et al., 2016; Rooney et al., 2017).

1.4.1. CBFβ as a tumour suppressor in breast cancer

In ER positive breast cancer, the presence of mostly loss-of-function mutations and deletions of *CBFβ* suggests that it may be acting as a tumour suppressor gene in this context (Griffith et al., 2018; Malik et al., 2019). The missense mutations noted in *CBFβ* are focussed around the RUNT-binding domain and therefore would abrogate the interaction between CBFβ and RUNX proteins (Griffith et al., 2018; Pegg et al., 2019). Emerging evidence has shown that removing *CBFβ* in ER positive MCF7 cells via CRISPR-Cas9 mediated gene deletion increases ER dependent migration of these cells. The activated CBFβ-RUNX1 complex suppresses ER mediated activation of the mitogen, TFF1, and thus inhibits migration (Pegg et al., 2019). In the absence of CBFβ, ER drives expression of TFF1 which leads to the migratory phenotype (Pegg et al., 2019). In a similar manner CBFβ is crucial for the inhibitory function of RUNX1 in the ER mediated repression of AXIN1 (Chimge et al., 2016). AXIN1 is known to repress the Wnt signalling pathway and when *CBFβ* is deleted in ER positive cells, this repression of the cell proliferative Wnt pathway is removed (Chimge et al., 2016; Pegg et al., 2019).

The role of *CBFβ* as a tumour suppressor was also supported by a recent study where transfecting *CBFβ*-knockout MCF10A cells with plasmids encoding tumour-derived mutated variants of *CBFβ* led to transformation of the MCF10A cells (Malik et al., 2019). This malignant phenotype was rescued upon overexpression of wildtype *CBFβ* in these cells as well as deletion of NOTCH3 thereby suggesting that *CBFβ* complexes with RUNX1 in the nucleus and acts as a tumour suppressor by repressing NOTCH3 transcription. This study also demonstrated that subcutaneous transplantation of *CBFβ*-knockout ER positive MCF7 cells into immunocompromised mice led to the generation of mammary tumours and overexpression of this co-factor reversed transformation of cells *in vitro,* a characteristic tumour suppressive trait (Malik et al., 2019). Interestingly, this paper also revealed a novel role of *CBFβ* in translation initiation revealing how versatile the role of *CBFβ* can be and how important it is to investigate this multifaceted protein in cancer.

1.4.2. CBFβ as an oncogene in breast cancer

Over the past few years, an oncogenic role of *CBFβ* has been discovered in the field of breast cancer. Indeed, elevated mRNA expression and amplification in *CBFβ* has been observed in 3% breast cancer patients, according to the Metastatic Breast Cancer study (Li et al., 2022). Among the various *CBFβ* copy number alterations observed in breast cancer patients, amplification of this gene was noted particularly in ER negative samples, alongside high expression of *CBFβ* mRNA, although the latter was also observed in some ER positive samples (Cerami et al., 2012; Gao et al., 2013; Li et al., 2022). High CBFβ expression has been positively correlated with increased metastasis and poor prognosis of patients (Hsu et al., 2022). Supportive of the clinical data, Mendoza-Villanueva *et al*. associated CBFβ and RUNX2 to the metastatic phenotype of the TN breast cancer cell line MDA-MB-231 (Mendoza-Villanueva et al., 2010). Indicative for their cooperative function, CBFβ bound to RUNX2 was noted in the nucleus of metastatic cells and the transcription co-factor was deemed essential for the expression of various genes associated with invasive phenotypes such as osteoclast promoting *OPN, OC, MMP9, MMP13*, *CSF-2* and *IL-11* and osteoblast inhibiting *SOST* which encodes sclerostin. MMP-9 and MMP-13 are matrix metalloproteinases involved in degradation of the ECM around breast tumours which facilitates metastasis to bone (Mendoza-Villanueva et al., 2010). Osteopontin (OPN), IL-11 and GM-CSF in metastatic breast cancer cells induce destruction of bone tissue by promoting differentiation of osteoclasts thereby allowing breast tumour cells to invade the bone microenvironment (Kang et al., 2003; Bonewald and Johnson, 2008; Mendoza-Villanueva, Zeef and Shore, 2011). Additionally, secretion of sclerostin by MDA-MB-231 cells antagonises the Wnt signalling pathway in osteoblasts and interferes with bone development; this could contribute to growth of secondary tumours in the bone (Mendoza-Villanueva, Zeef and Shore, 2011; Rutkovskiy, Stensløkken and Vaage, 2016). Invasion assays with knockdown of *CBFβ* in the TN cell line MDA-MB-231 showed a 90% reduction in the migratory ability of these cells, a characteristic subsequently rescued upon re-introduction of CBFβ (Mendoza-Villanueva et al., 2010).

More recently, high expression of CBFβ, and a consequent increase in tumour cell invasiveness and migratory potential has been demonstrated in two further metastatic breast cancer cell lines (Hsu et al., 2022). In an *in vivo* xenograft model, knockdown of CBFβ in the metastatic MDA-MB-436 cells resulted in reduced

tumour growth and improved overall survival of mice. Migration, invasion, expression of EMT and bone modulating markers such as Vimentin, Snail, chemokine receptor 4 (CXCR4), OPN as well as RUNX2 were also reduced in response to loss of CBFβ (Hsu et al., 2022). As mentioned earlier, these properties allow breast cancer cells to invade the bone microenvironment and modulate bone cells to allow development of secondary tumours. Interestingly, circulating exosomes derived from the serum of breast cancer patients with bone metastasis demonstrated significantly higher levels of CBFβ compared to those derived from healthy patients or patients with no observable metastasis (Hsu et al., 2022). These CBFβ mediated phenotypes seemed transferrable through the exosomes. For instance, breast cancer cells with low metastatic potential (T47D and MCF12A), when treated with media containing high CBFβ expressing exosomes, mimicked their metastatic counterparts, exhibiting elevated levels of CBFβ and RUNX2 alongside EMT and bone regulatory markers, increased migratory and invasive properties. Overexpression of CBFβ in the same cell lines, recapitulated the effect noted with exosome treatment, confirming the oncogenic role played by CBFβ in these cells (Hsu et al., 2022). Collectively, these data implicate CBFβ in metastasis of TN breast cancer cells. 70% of metastatic breast cancer (mostly from ER positive but also ER negative and TN subtypes) patients develop incurable bone metastases (Pulido et al., 2017). If RUNX2/CBFβ could be targeted to inhibit or delay this process, it could potentially improve disease prognosis and survival of such patients.

1.5. Modelling breast cancer

Breast cancer is a heterogenous disease with diverse genetic and histopathological variations and clinical outcomes. In order to get the best therapeutic responses, it is important to customise treatment according to the genetic makeup of the disease as much as possible. The first step to achieving this would be though advancement of our understanding of the complex biology of this disease and the mechanisms underpinning transformation of normal mammary cells and progression of tumour development. In view of that, various experimental systems can be used to model and recapitulate the different versions of breast cancers. The current milieu of breast cancer modelling systems includes (1) *in vitro* models using breast cancer cell lines, (2) *ex vivo* models whereby human or animal derived

tumour cells can be studied in two-dimensional (2D) and three-dimensional (3D) cultures outside of the host and (3) *in vivo* models, typically using mice, in the form of xenografts, virally/chemically/radiation induced models and genetically engineered mice (GEM), transgenic or knockout models.

1.5.1. In vitro models of breast cancer

In 1951, cervical cancer cells from a patient named Henrietta Lacks were used to culture and establish the first cancer cell line (Scherer, Syverton and Gey, 1953). Soon after, in 1958, BT-20 was established as the first breast cancer cell line (Lasfargues and Ozzello, 1958). From this revolutionary point, a vast proportion of the knowledge on cancer biology and efficacy of cancer therapeutics have been acquired from *in vitro* studies using cell lines. With the advancement of gene expression profiling technology, a plethora of breast cancer cell lines have been characterised based on the status of hormone receptors and classified into the specific breast cancer subtypes they resemble, both genetically and in terms of their morphological characteristics (Dai et al., 2017). For instance, one of the most widely used breast cancer cell lines, MCF-7, used over the past several decades to uncover crucial information on breast cancer biology is considered a model for ER positive, luminal-A breast cancer with low invasive and metastatic capacity (Kao et al., 2009; Hollestelle et al., 2010; H. et al., 2011; Gest et al., 2013; Comsa, Cimpean and Raica, 2015; Liu et al., 2019). MDA-MB-231 cells on the other hand, are considered triple negative and used in the study of metastatic disease (Kao et al., 2009; Hollestelle et al., 2010; Dai et al., 2017). Several mouse derived cell lines are also included in modelling breast cancer: such as E0771 which are considered to model luminal-B breast cancers lacking ERα but expressing ERβ, PR and ErbB2 (le Naour et al., 2020). Additionally, various cell lines are used to study normal mammary biology and allow us to understand the factors that tip the balance into transforming healthy cells into malignancy. As such the mouse derived HC11 cells have been widely used to study differentiation of mammary epithelial cells, whilst the human nontumorigenic MCF10A cells have greatly facilitated research on the changes involved in the regulatory mechanisms in normal breast epithelial cells that drive them into malignancy in disease states (Soule et al., 1990; Merlo et al., 1996; Sornapudi et al., 2018; Puleo and Polyak, 2021).

Cancer cell lines derived from breast carcinomas are often used as a first-line tool to model the heterogenous panel of breast cancer subtypes each associated with distinct phenotypes (Neve et al., 2006). This is because, not only do cell lines provide an unlimited, homogenous source of biological material for research, but they are easy to cultivate and maintain in culture, require low-cost compared to animal models, need easy to prepare media as their nutritional source and allow direct and repeated comparison of results generated through experiments (Lacroix et al., 2004; Greshock et al., 2007; Edmondson et al., 2014; Duval et al., 2017). One of the main advantages of using *in vitro* models, especially 2D models using a simple monolayer of cells, is the relatively quicker experimental time compared to more complicated animal models (Bahcecioglu et al., 2020). Cell lines can be manipulated chemically, mechanically, or electrically and the resulting specific changes can be measured within hours depending on the type of experimental assay (Hulkower and Herber, 2011; Wirtz, Konstantopoulos and Searson, 2011; A. Longo et al., 2013; Infanger et al., 2013). Mechanistic information regarding tumour cell proliferation, differentiation, invasion, migration, dormancy, intra and extravasation, angiogenesis, response to drugs or irradiation and interactions with ECM have been modelled *in vitro* for decades (Prabhakaran et al., 2013; Shologu et al., 2016; Amann et al., 2017; Gao et al., 2019; Bahcecioglu et al., 2020; Fulghieri, Stivala and Sottile, 2021). With cell lines modelling specific tumour types, such as the highly proliferative TN tumour cells or hormone therapy responsive ER positive tumour cells, various forms and stages of a disease and the molecular pathways or tumorigenic systems involved can be exclusively studied (Dai et al., 2017). Additionally, heterotypic cultures, such as co-culture systems involving tumour cells with immune cells or stromal cells can provide valuable insight into the signalling pathways involved in mediating the crosstalk between these two cell types in promoting invasion and metastasis of tumour cells (Müller-Quernheim et al., 2012; Estrada et al., 2016).

It is important to note, however, that in physiological environments, cells exist in a dynamic 3D ecosystem, bound to and influence by multiple neighbouring cells and the ECM. To mimic this, 3D *in vitro* models such as tumour cell derived spheroids, tumourspheres and mammospheres among others, are becoming increasingly popular (Weiswald, Bellet and Dangles-Marie, 2015; Duval et al., 2017). For instance, spheroid models, comprised of an aggregate of cancer cells (either homotypic or in combination with other cell types) in either a liquid media

suspension or basement matrix extract (such as Matrigel) can reflect how cells within a tumour mass behave when they are exposed to non-uniform levels of oxygen, nutrients, signalling molecules and metabolites and the impact of necrosis within the central core, spatial arrangement and also matrix stiffness on growth and invasion of tumour cells (Durand and Raleigh, 1998; Pampaloni, Reynaud and Stelzer, 2007; Katt et al., 2016). Mammospheres and tumourspheres, seeded as low density, single cell suspensions of normal mammary or tumour cells have been widely used to study and characterise tumour initiating cancer stem cells and the mechanisms involved in their propagation. These model circulating tumour cells in breast cancer patients which proliferate in a non-adherent environment dependent on their self-renewal capacity (Ponti et al., 2005; Grimshaw et al., 2008; Smart et al., 2013; Weiswald, Bellet and Dangles-Marie, 2015). Moreover, genetically, compared to 2D models, expression profiles of such 3D tumour models also show closer resemblance to patient or animal tumours (Imamura et al., 2015; Breslin et al., 2016; Bahcecioglu et al., 2020).

It is clear that advances in *in vitro* technology are progressively improving the capacity to accurately replicate physiological tumour micro-environments. Nevertheless, use of cell lines come with a series of disadvantages. Firstly, the source of the cell lines must be considered when deciding how representative the cell line model is of a certain subtype of breast cancer. For instance, owing to the difficulties in extracting tumours cells within the mammary stomal environment, most of the cancer cell lines popular amongst researchers originate from advanced-stage invasive carcinomas and pleural effusions (Vargo-Gogola and Rosen, 2007; Dai et al., 2017). This means the cell lines circulating throughout the research community are mostly representative of malignant subtypes of breast cancer. In some cases, the cell lines may not even be from the cancer type in question at all, as seen with MDA-MB-435 cells which previously marked to originate from a breast tumour was later suggested to have been derived from an unusual melanoma (Ellison et al., 2002). Secondly, multiple studies have warned against the tendency of cell lines to accumulate mutations and evolve in culture. Compared to the primary tumours, significant alterations in the genetic and epigenetic make-up of cells have been noted during initial establishment and following sub-culturing of cell lines (Neve et al., 2006; Kao et al., 2009; Cope et al., 2014). In support of this, analysis by Gray *et al* registered key differences between cell lines from their primary tumour of origin indicating that *in vitro*

culture selected for certain genomic alterations (Neve et al., 2006). The same cell line when cultured under different conditions across different labs may therefore evolve into very distinct cell types (Thompson et al., 1993; Dai et al., 2017). This poses a dangerous issue when they are used to model one particular breast cancer type across various groups. Thirdly, *in vitro* methods fall short in simulating how microenvironmental cell signalling significantly impacts tumour cell molecular biology and therefore any experimental results derived from them. A good example of this selective pressure selecting for certain tumour cell types, was noted when ER positive cells were observed to become ER negative when grown in environments with high EGFR signalling (Briand and Lykkesfeldt, 2001). The heterogenous tumour naturally holds cells with various survival strategies to ensure propagation of the tumour through multiple pathological stages of the disease. While some cells would possess tumour initiating stem cell potential or hyperproliferative properties, others would enter dormancy or quiescence to survive through unfavourable conditions. This heterogenous population is lost when establishing cell lines as the initial culture process, especially in plastic dishes or in the absence of particular growth factors, might be too harsh for their sustenance and certain cell types may therefore be eliminated from the population. In this case, the reliability of the cell line to represent the intra-tumoral heterogeneity becomes questionable (Gerlinger et al., 2012; Martelotto et al., 2014; Dai et al., 2017).

It is, therefore, important to determine whether the cell lines being used to draw conclusions regarding certain tumour types are indeed reliable. Additionally, an expansive panel of cell lines should be used in addition to 2D homotypic cultures and where possible co-cultures and 3D models (Bruna et al., 2016). Limiting sub-culturing of cells to ensure their integrity and regular authentication checks of frozen stocks to ensure the cell lines used are indeed genetically representative of the tumour type being modelled is advisable.

Nevertheless, while *in vitro* technology is advancing rapidly to overcome caveats of the system, *ex vivo* methods are gaining recognition as better models that closely resemble the original tumour *in vivo*.

1.5.2. Ex vivo models of breast cancer

Primary tumour slices resected during surgery, tumour biopsy samples from breast cancer patients or tumour cells harvested from animal models can be maintained

ex vivo for a few days to several months either in culture medium or embedded within a matrix (Katt et al., 2016; Pinto, Estrada and Brito, 2020). One of the key benefits of using such freshly isolated samples in the study of tumorigenesis include preservation of the primary tumour heterogeneity, architecture and microenvironmental factors. For instance, compared to homotypic *in vitro* models, *ex vivo* organotypic 3D cultures or culturing tissue explants would ensure more accurate evaluation of treatment efficacy in a heterotypic mixture of cells, mimicking the original intra-tumoral heterogeneity of the primary tumour (Tanos et al., 2013). This can act as an important tool for assessing therapies personalised to specific patients. Additionally, while the shorter culture time of *ex vivo* models prevents monitoring of disease progression or long-term effects of treatments, it helps to avoid any radical genetic and morphological alterations acquired through prolonged sub-culturing of cell lines *in vitro* (van der Kuip et al., 2006; Katt et al., 2016).

Albeit the advantages over *in vitro* cell lines, acquiring primary material for experimental purposes is challenging and interpretation of results become complicated when heterogeneity within and between patients and tumour samples are taken into consideration (Nath and Devi, 2016). Moreover, thorough understanding of the carcinogenic process requires experimental analysis at all stages of the disease – a task which is difficult to accomplish and model accurately outside of the physiological environment.

1.5.3. In vivo models of breast cancer

In vivo animal models, particularly mouse models of breast cancer have added a whole new dimension in the modelling and evaluation of the complex intra-tumoral interactions and crosstalk between cancer cells and the microenvironment along with disease initiation and progression. Two of the most popular classes of mouse models used to emulate human breast cancers are generated through (1) transplantation of murine cancer cells, human cancer cell lines or tumour cells/fragments into mice; (2) genetic manipulation of the mouse genome (Matulka and Wagner, 2005).

1.5.3.1. Transplantable models

Transplantable mouse models of breast cancer come in the form of xenografts, which can be derived from human cell lines or tumours, and allografts using cell-lines or tumours from syngeneic mice (Rygaard and Povlsen, 1969; Kim, O'Hare and Stein, 2004; Manning, Buck and Cook, 2016). These models can be used to acquire valuable information on assessing efficacy of therapeutics, evaluate drug toxicity, study disease progression and metastasis, and the pro- and anti-tumour immune responses implicated in breast cancer.

Allotopic cell line derived xenografts (CDX), where tumour cells are transplanted under the subcutaneous layer of the skin, or orthotopic CDX models with tumour cells injected into the mammary fat pad are useful for tracking growth of primary tumours as well as metastasis and the subsequent malignant phenotypes (Hoffman, 1999; Kim and Baek, 2010; Zhang et al., 2018). Multiple cancer cell lines such as T47D and MCF7 (luminal-A subtype) alongside MDA-MB-231 (TN subtype) have been used in the generation of such models (Cerliani et al., 2011; Cochrane et al., 2014; Ran et al., 2020). Metastatic cell lines are also often injected into the tail veins of mice to monitor their migratory and invasive potentials (Zhang et al., 2014). CDX models therefore improve on the widely used *in vitro* models of breast cancer to generate more physiologically relevant results. However, as cell lines generally used in CDX models are homogenous in nature, these models fail to recapitulate tumour heterogeneity (Kopetz, Lemos and Powis, 2012). As cell lines go through several passages outside of the recipient mouse, genetic drift and selective pressures associated with *in vitro* culturing can lead to irreversible changes where daughter clones no longer resemble the original primary tumours (Daniel et al., 2009). This may lead to unreliable or misleading perceptions regarding the patient/cancer type specific tumour biology.

On the other hand, patient derived xenografts (PDX) can be generated by allotopic or orthotopic transplantation of primary human tumour cells or tumour fragments into immune-deficient mice. This leads to the development of tumours that show strong similarities, in terms of tissue histology, heterogeneity and gene expression profiles, to the patient derived tumour of origin (Kopetz, Lemos and Powis, 2012; Pillai et al., 2018). Several PDX models have been shown to successfully recapitulate the distinct subtypes of breast cancer with respect to hormone receptor status and gene expression patterns (DeRose et al., 2011). Importantly,

PDXs are deemed as valuable models for clinical trials due to their ability to retain the clinically observed responses to various therapeutics (Gao et al., 2015).

A key drawback of xenograft models, however, is the lack of association between the tumour and the immune system due to the requirement for immunocompromised hosts when using human cells (DeRose et al., 2013). To avoid rejection of transplanted cells or tumours from the human donors, transplanted mice need to be immune-deficient such as *nude* mice with an incompetent immune system or mice with severe combined immunodeficiency (SCID), among others (Flanagan, 1966; Bosma and Carroll, 1991; Morton and Houghton, 2007). Considering how intricately tied the immune system is to carcinogenesis, cancer progression and response to therapeutics, a gaping hole is left in the cancer story if it is studied outside the context of the immune system. Therefore, allografts can be used with mouse tumours or murine cell lines transplanted into syngeneic mice with fully competent immune systems (Tao et al., 2008). Allografts, however, possess their own host of disadvantages. For one, cell lines of murine origin are limited in supply and fail to cover the panel of different breast cancer subtypes adequately. Secondly, while various drug compounds may be extensively tested in allograft models, their effects may be specific to murine hosts and not as potent in human cancers (Manning, Buck and Cook, 2016).

Therefore, albeit the numerous advantages of transplantation models which make them vital in preclinical research, *in vivo* technology required further improvement in modelling breast cancer.

1.5.3.2. Genetically engineered models

Over the past several decades, GEMMs have been put under the spotlight for recapitulating both the genetic and histopathological characteristics of human breast cancers within an appropriate physiological microenvironment.

Manipulation of the mouse genome can be used to either drive expression of oncogenes (transgenic GEMMs) or knockout endogenous genes encoding tumour suppressors (knockout-GEMMs) (C. Liu et al., 2021). The former, more traditional approach involves microinjection of genetic material into a single mouse oocyte or zygote resulting in random insertion of the desired transgenic construct into the mouse genome or over-expression of genes endogenous to the mouse (Gordon et al., 1980; Thomas and Capecchi, 1987; Haruyama, Cho and Kulkarni, 2009). The latter technique, used in more recent times employs targeted gene deletion to

generate a loss of function mutations or targeted homologous recombination to disrupt or replace an endogenous gene with a transgene in the mouse genome. Cells, usually mouse embryonic stem cells, which have undergone successful recombination are selected for injection into a blastocyst and subsequently implanted into mice to generate progeny (Thomas and Capecchi, 1987; Hall, Limaye and Kulkarni, 2009). These first and second generation of GEMMs have granted the field of cancer research with invaluable novel information regarding gain-of-function of oncogenic products or loss of tumour suppressors in the initiation of carcinogenesis (Matulka and Wagner, 2005; Sakamoto, Schmidt and Wagner, 2015).

Reports of the first breast cancer GEMM date back to 1984, where a strong promoter – the mouse mammary tumour virus long terminal repeat (MMTV-LTR) – was fused with the c-*MYC* oncogene (Stewart, Pattengale and Leder, 1984). The consequent expression of human c-*MYC* in the mouse mammary epithelial cells led to the induction of spontaneous mammary adenocarcinomas. This system enforces a progressive transformation of cells from hyperplasia to DCIS and ultimately IDC thereby allowing researchers the opportunity to study every stage of the disease from tumour initiation through progression until endpoint (Stewart, Pattengale and Leder, 1984). A second GEMM subsequently displayed synergistically accelerated tumorigenesis following co-expression of MMTV/c-*MYC* and MMTV/v-Ha-*RAS* while the first transgenic GEMM to model HER2-positive disease was established in 1988 (Sinn et al., 1987). Whole body knockout of tumour suppressor genes was achieved in the second generation of GEMMs to generate mammary tumours in mice (Donehower et al., 1992; Jacks et al., 1994). Thereafter, a wide variety of transgenic and knockout GEMMs have facilitated the modelling of specific clinical subtypes of breast cancer as validated by comparative analyses of tumour samples from mouse and humans (Pfefferle et al., 2013).

One of the main caveats of such conventional GEMMs is the lack of tissue specificity for oncogene expression or gene deletion (Kim, O'Hare and Stein, 2004). When transgenic mice have multiple tissue types experiencing over expression of an oncogene of interest or loss of a tumour suppressor gene throughout the body, they fail to mimic the key trait of human sporadic cancers: the transformation of a single tumour initiating cell within a microenvironment that is otherwise normal (Kim, O'Hare and Stein, 2004; Holen et al., 2017a). On top of this, since a good proportion of tumour suppressors are critical in

development and normal cell homeostasis, whole body knockouts lead to embryonic lethality or death promptly after birth in about 30% cases (Sakamoto, Schmidt and Wagner, 2015). For instance, loss of the tumour suppressors BRCA1, BRCA2 or PTEN lead to loss of embryos between 7.5-9.5 days from the start of gestation (Sakamoto, Schmidt and Wagner, 2015). Furthermore, conventional GEMMs fail to address the effect of pro-oncogenic alterations and mutations arising in adult mice and developing neoplasms (Matulka and Wagner, 2005). In adult human cancers for instance, mutations are accumulated gradually over time to ultimately trigger tumorigenesis. If such mutations are introduced into an animal model at birth, they do not accurately mimic adult cancers, but are rather modelling for the human equivalent of familial cancer syndromes (Kim, O'Hare and Stein, 2004).

Thus, improving on these models, third generation GEMMs have been developed to add an element of temporal and spatial control to the expression of oncogenes or somatic deletion of tumour suppressor genes. The *Cre/loxP* system is employed to conditionally knockout or alter the expression of genes with the help of promoters specific to the tissue of interest, in this case mammary glands. The Cre recombinase enzyme is site-specific, meaning it recognises specific *loxP* sites which can be inserted into the mouse genome on either side of the gene/genes of interest (Sternberg and Hamilton, 1981; Sauer and Du, 1987; Lakso et al., 1992; Orban, Chui and Marth, 1992; Kühn et al., 1995; St-Onge, Furth and Gruss, 1996; Wagner et al., 1997) Expressed under the control of mammary specific promoters, this enzyme can therefore, activate transgenes of interest or remove endogenous genes via homologous recombination exclusively in mammary cells. Pioneering the use of this system in generating the first mouse strains of transgenic Wap-Cre and MMTV-Cre GEMMs was the Lothar Hennighausen lab (NIH) (Wagner et al., 1997, 2001). These transgenic lines, where deletion of genes was achieved specifically in mammary epithelial cells during multiple stages of mammary gland development, were used in the generation of a mammary specific *Brca1* knockout mice (Xu et al., 1999). While promoters and enhancers could be used to regulate the specificity and to some extent the timing of Cre expression and therefore, expression of target genes, further sophistication of this technology has allowed enhancement of this spatial and temporal control. Cre-expression under a specific promoter can now be induced by exogenous compounds such as tamoxifen, 4-hydroxytamoxifen (4OHT), tetracycline or doxycycline (Dox). Further

developments in the Cre/loxP system are continually generating GEMMs that allow more accurate and precise control of gene expression to enable better understanding of the function of specific genes (Kim et al., 2018).

Conditional GEMMs have thus far been invaluable in cancer research. However, it is important to acknowledge the time, cost, and labour-intensive nature of generating and maintaining such models. Achieving the right combination of alleles within a strain may require multiple rounds of breeding and certain models may take several months to develop tumours. Additionally, albeit the various improvements in technology, breast cancer GEMMs do not always recreate the pathology and heterogeneity of the human tumours. Even though various promoters specific to the various mammary cell lineages are available, off-target effects or unforeseen expression patterns of Cre-recombinase enzymes may confound experimental findings (Holen et al., 2017b; Kersten et al., 2017). However, despite the caveats, it is undeniable that GEMMs models are instrumental in the study of tumour initiation and the multistage progression of breast cancer within an immune enriched, physiological microenvironment that make them indispensable in preclinical research (Kersten et al., 2017).

1.6. The tumour immune microenvironment

The immune system, comprised of a complex and dynamic network of immune cells, cytokines and chemokines, acts as an organism's natural defence towards external pathogens and diseases. Tight control of this system ensures accurate recognition and clearance of threats such as foreign organisms or toxins, as well as transformed, malignant cells of the body, without affecting healthy tissues or the natural healthy microbiome of the body. Broadly divided into two types of defence mechanisms: innate and adaptive, the immune system is not only capable of providing acute and immediate protection against threating pathogens or cells but also ensures long-term immunity in case of re-encounter with the same threats based on immunological memory (Janeway et al., 2001; Cruse, Lewis and Wang, 2004; Sharpe and Mount, 2015).

All immune cells are derived from a common pluripotent hematopoietic precursor stem cell population within the bone marrow (Figure 1.9). These stem cells differentiate into two lines of intermediate progenitor cells called the myeloid and lymphoid progenitors. The myeloid progenitor gives rise to a host of blood

leukocytes (white blood cells- WBCs) including neutrophils, eosinophils, basophils, monocytes, macrophages, dendritic cells (DCs), mast cells along with blood erythrocytes (red blood cells- RBC) and platelets. The WBCs circulate between blood vessels, tissue interstitial spaces and the lymphatic system, a network of vessels where fluid from tissue extracellular spaces, originally filtered from blood, is collected and returned to the blood (Janeway et al., 2001; Cruse, Lewis and Wang, 2004).

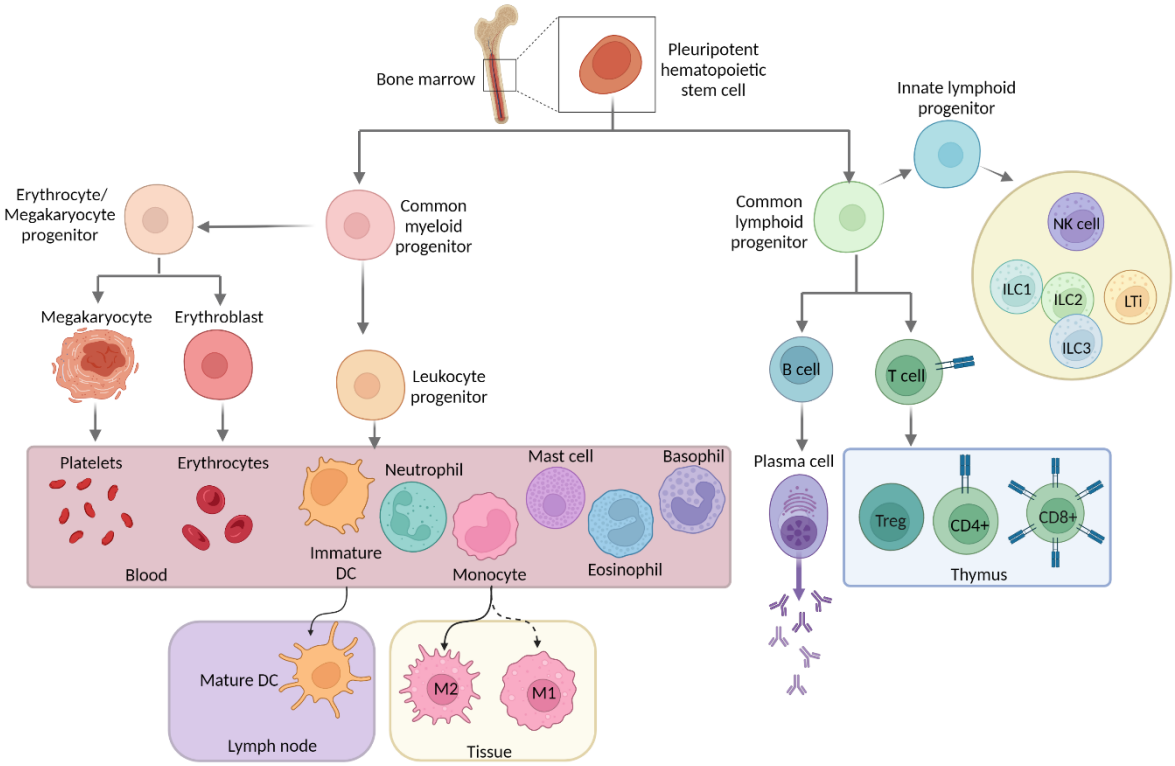

Figure 1.9: Development and differentiation of the immune system.
Figure created using Biorender.com

The lymphoid progenitors generate two major lymphocyte subtypes: B cells (which reside and mature within the bone marrow) and T cells (which migrate to the thymus for maturation). Mature lymphocytes circulate between the blood and peripheral secondary lymphoid organs such as lymph nodes, tonsils, spleen, and mucosal associated lymphoid tissues, where they can be activated upon antigen exposure. B cells, when activated by antigens or other immune cells in response to a threat, can further differentiate into antibody producing plasma cells (Janeway et al., 2001). T cells differentiate into 3 main lineages of effector lymphocytes: CD8+ cytotoxic T cells, CD4+ helper cells and γδ T cells (Janeway et al., 2001; Nanno et al., 2007). Additionally, a subpopulation of CD4+ T cells with immunosuppressive properties, the T regulatory cells (Tregs), help regulate the

immune system via downregulating activation and proliferation of the other effector T cells. This is useful in preventing autoimmune diseases and maintaining tolerance against self-antigens while also dampening down aggressive immune responses to prevent tissue damage (Thornton and Shevach, 1998; Fehérvari and Sakaguchi, 2004; Harrington et al., 2005). Once effector cells have undergone activation, differentiation and proliferation, the circulatory system is then used to circulate lymphoid cells via the blood to the source of the antigen, for example a wounded site or a tissue harbouring malignant cells (Cruse, Lewis and Wang, 2004). A third, more recently discovered subtype emerging from the common lymphoid progenitor is the innate lymphoid cell (ILC) which can further differentiate into ILC1s, ILC2, ILC3, natural killer (NK) cells and LTi cells (lymphoid tissue inducer cells). ILCs are generally localised to tissues, especially in mucosal layers, and react to tissue damage by secreting signalling molecules such as interleukins and participate in regulating responses from both arms of the immune system (Spits and di Santo, 2010; Vivier et al., 2012; Panda and Colonna, 2019).

The WBCs of myeloid progeny generally form the innate immunity whereas lymphocytes, except ILCs, from the lymphoid progenitor are involved in the adaptive immune system (Janeway et al., 2001). NK cells and γδ T cells use their cytotoxic functions and are involved in both innate and adaptive immunity (Holtmeier and Kabelitz, 2005; Sharpe and Mount, 2015). DCs, known as antigen presenting cells (APC), function as a link between the two arms of the immune system. Immature DCs tend to reside in tissue spaces, scanning for pathogens or neoantigens in their surroundings. Once a threatening antigen is identified, DCs mature rapidly and migrate to present the antigen to lymphocytes within lymph nodes to activate an adaptive immune response (Janeway et al., 2001).

The immune population present within the breast microenvironment make up one of the key elements involved in the maintenance of the normal breast phenotype through immunosurveillance. However, they are often influenced by the tumour to become pro-tumorigenic and aid cancer development and progression. Indeed, carcinogenesis of the breast tissue is often associated with changes –quantitative as well as qualitative – in the location and composition of the mammary immune infiltrate (Denton, Roberts and Fearon, 2018; Goff and Danforth, 2021).

1.6.1. Immune microenvironment of the normal mammary gland

In normal mammary gland development from mammogenesis through lactation and involution, the immune system is known to be key in influencing healthy growth and maintaining defence within the mammary microenvironment. For instance, mucosal immunosurveillance in the mammary glands are known to provide protection against infection (mastitis) while production of secretory IgA in breast milk during lactation is critical in protection during infancy. Post lactation, macrophages and mast cells are vital in mediating regression of the glandular structure and mediate involution (Goldman, 1993; Jeanne, 2008; O'Brien et al., 2012; Ramirez et al., 2012; Degnim et al., 2014).

Immune cell populations within the breast are primarily located within the lobules (TDLU in humans) in closer proximity to epithelial cells than stromal cells or adipocytes. Cells of both myeloid and lymphoid lineages such as, monocytes, dendritic cells, macrophages, B cells, NK cells, CD8+ T cells and CD4+ T cells among others, reside in these compartments and work to eliminate pathogenic threats and transformed mammary cells (Degnim et al., 2014; Zumwalde et al., 2016; Azizi et al., 2018). Characterisation of the immune population of healthy breast tissues have shown that leukocytes (CD45+) were found predominantly in the intraepithelial layer of the mammary ducts (Lwin et al., 1985; Degnim et al., 2014). CD3+ T lymphocytes (CD8+ and CD4+) were most abundant, followed by myeloid cells including macrophages, neutrophils, and DCs (Ruffell et al., 2012). These immune cells were found in almost all lobules studied by (Degnim et al., 2014). CD8+ T cells and DCs were notably found in close association with the epithelial cells of the lobular acini, mainly at the basal end of the epithelium. A deeper look into these cell types, by (Zumwalde et al., 2016) showed that most of the CD8+ T cells were of the effector memory subtype, potentially activated by antigens. The source of these antigens could be endogenous, i.e., cellular proteins, extracellular proteins, or exogenous, such as viruses or bacteria, and neoantigens. Neoantigens, expressed in response to oestrogen or carcinogen induced mutations arising within the ductal epithelial cells, can be targeted for elimination of cancerous cells by immune cells within the mammary epithelium (Roy and Liehr, 1999; Goff and Danforth, 2021). In fact, CD8+ T cells are one of the main eliminators of malignant cells identified via the neoantigens expressed on major histocompatibility (MHC) Class I molecules on tumour cell surfaces (Peng et al., 2019). CD20+ B cells, CD68+ macrophages and CD11c+ DCs have also been

associated with effector functions, mediating response to stress, antigen presentation and overall maintenance of tissue integrity within the epithelial layer (Degnim et al., 2017). Experimental analysis of organoids derived from normal breast tissue additionally revealed the presence of the cytotoxic CD3+ γδ T cells (Zumwalde et al., 2016).

Altogether the cocktail of immune cells within the breast, work to protect the mammary epithelial layer through innate and adaptive immunity. Elimination of transformed cells using such immune responses within the mammary environment is one of the most crucial defence mechanisms used by the body against cancer. Therefore, knowledge of this immune landscape and understanding the functional roles played by the breast immune infiltrate in both healthy and diseased states is imperative for uncovering new methods of breast cancer prevention and treatment.

1.6.2. Immune microenvironment in breast cancer

With lymph nodes of the mediastinum and ipsilateral axilla in close proximity, all the fundamental components – both cellular and lymphatic – required for an adaptive immune response are available to the ductal mammary epithelium (Goff and Danforth, 2021). Having immune cells within the TDLU, usually the origin point for breast cancers, enables intimate interactions between the two cell populations wherein they can influence the behaviour each other (Yang et al., 2016). In a study conducted by Degnim *et al.*, looking at the density of immune cells in breast samples, elevated proportions of CD8+ T cells, macrophages, CD20+ B cells and DCs were found, suggestive of an immunogenic environment, in breast lobules from patients with benign disease versus healthy breast tissues (Degnim et al., 2017). This is supported by an older study showing 10-30% of lymphocytes in sections from human breast carcinomas presented activation markers, a characteristic absent in lymphocytes of the normal breast (Lwin et al., 1985). Increased infiltration of such immune cells can affect growth of tumour cells either through the direct cytotoxic effects of CD8+ T cells and CD4+ T cells, or the indirect impact from cytokines and growth factors released to suppress or stimulate the immune system as required (Goff and Danforth, 2021). The immune population may also change depending on the specific subtype of breast cancer, oestrogen sensitivity of the tumour cells and their mutational landscapes (Bense et al., 2017; Tower, Ruppert and Britt, 2019). This crosstalk between the tumour

cells and the immune infiltrate induces the dynamic process of immunoediting. Tumour immunoediting transpires in three phases: Elimination, Equilibrium and Escape (Salemme et al., 2021). This is summarised in Figure 1.10.

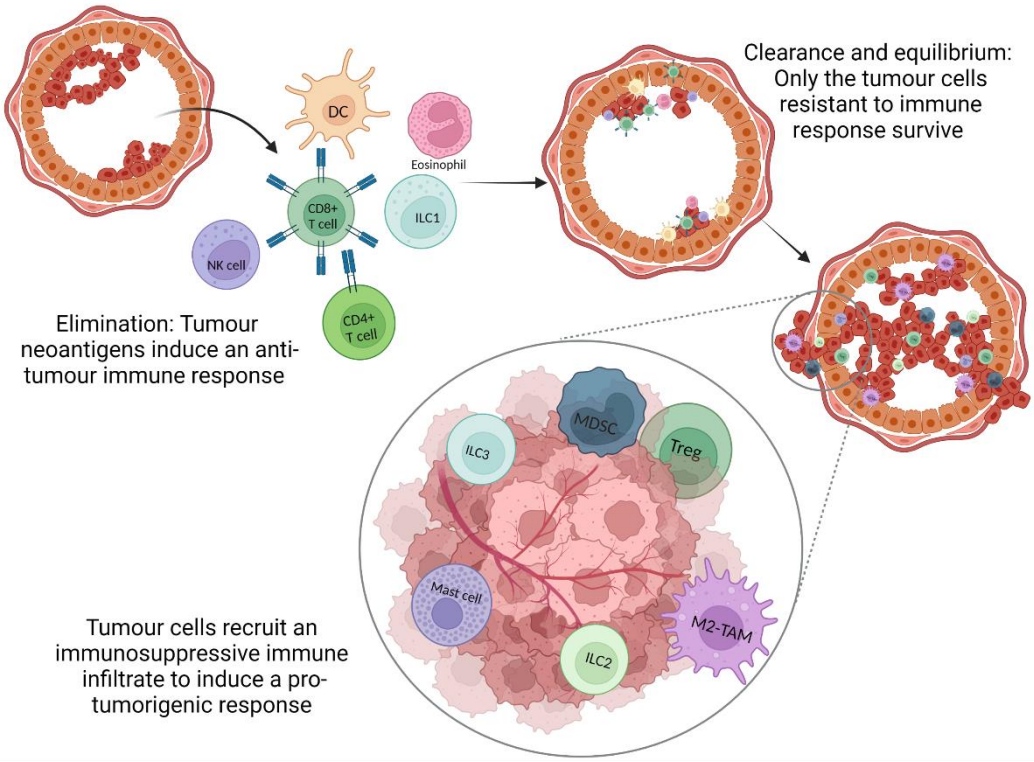

Figure 1.10: Immune response to a developing mammary tumour.
During the first stage of tumour development, the immune system is induced to launch an anti-tumorigenic attack. CD8+ T cells, Dendritic cells (DC), NK cells, innate lymphoid cells (ILC1), CD4+ T cells and Eosinophils drive the elimination of tumour cells. An equilibrium state is reached subsequently as the immune system works to re-establish the normal mammary tumour microenvironment. Tumour cells that escape the immune attack, manipulate the immune system to induce a pro-tumorigenic response that facilitates the growth and dissemination of tumour cells. Figure created using Biorender.com.

The first response of the immune system to the presence of cancerous cells is to trigger immunosurveillance, whereby a strong immune response is elicited against transformed mammary cells to eliminate them (Salemme et al., 2021). At this stage, infiltration of immunostimulatory cells such as innate lymphoid cells, tumour infiltrating lymphocytes (TILs), macrophages, NK cells, DCs and eosinophils, into the tumour microenvironment is critical for limiting tumour growth (Gatti-Mays et al., 2019). TILs, particularly CD8+ T cells are one of the crucial players in cancer cell elimination. Tumour associated antigens or neoantigens presented by MHC class I molecules on tumour cell surfaces are identified and targeted by CD8+ T cells which then elicit a cytotoxic response.

CD4+ T cells act to support the activation of CD8+ T cells through the secretion of immunostimulatory cytokines. Generally, tissue infiltrating lymphocyte (TIL) infiltration is key to driving the anti-tumour immune response (Pruneri, Vingiani and Denkert, 2018; Peng et al., 2019; Salemme et al., 2021). NK cells, as part of the innate immune system, are involved in immunosurveillance and secrete cytolytic granzymes and perforins to kill abnormal or primary tumour cells. A classic evasion method used by tumour cells is the downregulation of MHC Class I molecules from their plasma membranes that would otherwise display tumour neoantigens. An added advantage of NK cells over TILs, is their ability to recognise and target tumour cells even without MHC class I antigen presentation. Therefore, breast cancer cells and cancer stem cells (CSCs) which often evade T-cell surveillance, fail to escape from NK cells (Tallerico et al., 2017; Melaiu et al., 2020). Other members of the ILC family, as part of the innate immune system, are also responsible for triggering adaptive immunity once threats have been detected through receptor interactions or cytokines, although in some cases they may become pro-tumorigenic (Bruchard and Ghiringhelli, 2019). Evidence of ILC1s exerting a strong cytotoxic phenotype against mammary tumour cells have been noted in a pre-clinical model (Dadi, Chhangawala, Benjamin M. Whitlock, et al., 2016). However, another study suggested a role of ILC3s in the promotion of breast cancer metastasis into the lymphatic system though alteration of the local chemokine profile. An enriched population of ILC2s was noted in breast tumour samples compared to healthy samples while an increase in intratumoral ILCs along with myeloid derived suppressor cells (MDSCs) and Tregs was associated with accelerated growth and metastasis of breast tumour cells (Jovanovic et al., 2014; Dadi, Chhangawala, Benjamin M. Whitlock, et al., 2016; Irshad et al., 2017; Salimi et al., 2018; Bruchard and Ghiringhelli, 2019). DCs hold the capacity to present tumour antigens on MHC class I and MHC class II molecules to T cells. This, together with the release of immunostimulatory factors and direct cell-cell contact, serves as activation signals to T cells which can then stimulate an anti-tumour response to eliminate cancer cells (Binnewies *et al.*, 2018; Wculek *et al.*, 2020). Macrophages, known to be fully differentiated myeloid cells are highly plastic cells, prone to adapt and change in function and morphology according to different tissue specific and microenvironmental cues (Mowat, Scott and Bain, 2017). Tumour associated macrophages (TAMs) are characterised either as anti-tumour M1-like TAMs or pro-tumorigenic M2-like TAMs (Coffelt, Hughes and Lewis,

2009; Jayasingam et al., 2020). M1-like TAMs, once activated, generally induce an interferon-gamma (IFNγ) mediate cytotoxic response against tumour cells through the release of toxic intermediates and pro-inflammatory chemokines such as CXCL9 and CXCL10 (van Dalen et al., 2018; Hachim et al., 2020). However, their exact benefit on overall patient survival and breast cancer prognosis needs further investigation. Eosinophils, within the TME, are able to secrete cytokines and interleukins such as CCL5, CXCL9, CXCL10, IL-6 and IL-12 to attract and activate T cells, NK cells and induce polarisation of macrophages to the M1-like (anti-tumour) subtype. As such, eosinophils improve the anti-tumour immune response in breast cancer patients and are linked to favourable disease outcome (Varricchi et al., 2018).

Once the majority of the malignant cells have been removed, an Equilibrium phase of intimate crosstalk between the tumour and immune cells is reached where the immune system continues to select against rapidly mutating, genetically unstable tumour cells, and the tumour cells try to bring about an immunosuppressive environment in favour of their survival (Salemme et al., 2021). Release of cytokines and growth factors by the tumour cells to attract pro-tumorigenic immune cells such as MDSCs, Tregs cells and type 2 tumour associated macrophages (M2-like TAMs) begin to combat the initial anti-cancer immune response (Lorenzo-Sanz and Muñoz, 2019; Salemme et al., 2021). Macrophages, especially M2-TAMs have been implicated in the promotion of tumorigenesis as well as metastasis (Coffelt, Hughes and Lewis, 2009). In addition to supporting an immunosuppressive microenvironment through suppression of CD8+ T cells and depletion of amino acids within the TME which are crucial for NK and T cell survival and proliferation, M2-TAMs also secrete angiogenic growth factors and various signalling molecules involved in the stimulation of tumour cell EMT (Chanmee et al., 2014; Anfray et al., 2019; Salemme et al., 2021). M2-TAMs work to promote invasion and migration of tumour cells to distant secondary sites and are generally correlated to poor disease prognosis (Coffelt, Hughes and Lewis, 2009; van Dalen et al., 2018; Anfray et al., 2019). Furthermore, tumour cells secreting various chemokines and cytokines such as CCL5, CXCL2, CXCL5, CXCL12 and granulocytic colony stimulating factor (G-CSF) is thought to induce the generation of MDSCs from immature myeloid cells. MDSCs in turn, express the CD40 receptor to recruit Tregs while also inhibiting proliferation of T cells through binding the CD40L ligand expressed on T cell surfaces (Salemme et al., 2021). T regulator cells (Tregs) arise

from a subpopulation of CD4+CD25+ T cells with immunosuppressive properties. They are critically involved in suppressing the host immune system via direct cell to cell mechanisms as well as through the secretion of immunosuppressive metabolites and cytokines. Recruited to the tumour microenvironment (TME), mainly through CXCL12 secreted by breast tumour cells, other immunosuppressive cells or cancer associated fibroblasts, Tregs help disrupt the anti-tumour control of the immune system and promote growth, progression, and an overall aggressive phenotype of tumour cells (Yan et al., 2011; Paluskievicz et al., 2019; Salemme et al., 2021). Tregs have been implicated in poor prognosis of breast cancer patients across various subtypes, and depletion of Tregs in advanced stage primary tumours has been shown to induce a strong anti-tumour immune response mediated by CD4+ T cells and IFNγ (Martinez et al., 2019).

Ultimately, malignant cells that manage to acquire resistance to elimination, proliferate and grow into a clinically apparent tumour. They have reached the final Escape phase where an immunosuppressive tumour microenvironment has been established (Salemme et al., 2021).

Historically breast cancer was thought to be an “immune cold” cancer with low immunogenicity, however, increasing amounts of emerging research is now contesting this notion and unveiling the complex interplay between the immune system and breast tumour cells (Azizi et al., 2018). Understanding the mechanisms employed by tumours cells to evade anti-tumour immune responses while taking advantage of the plastic nature of immune cells to orchestrate a pro-tumorigenic microenvironment is imperative in the improvement of current, and development of new immunotherapies that can be used in conjunction with current treatment regimes.

1.7. Hypothesis and Aims

Based on evidence from patient data, published literature and previous results generated in the Blyth lab, it was hypothesised that CBFβ would act as a tumour suppressor in breast cancer. To explore this notion, three aims were proposed.

(1) To investigate the role of *Cbfβ* in breast cancer through *in vivo* mouse models of breast cancer with conditional deletion of *Cbfβ* targeted to mammary epithelial cells. This would allow determination of the impact of *Cbfβ* loss on mammary tumorigenesis within a physiologically relevant environment.

(2) Transcriptional regulation by the RUNX/CBFβ complex is known to influence various cell signalling pathways involved in critical cellular functions. Therefore, to understand the functionality of *Cbfβ* loss in mammary tumours and probe the mechanism behind the role of *Cbfβ* on breast tumorigenesis, the aim was to conduct transcriptomic analysis of *Cbfβ* deficient tumours.

(3) Emerging evidence has highlighted the importance of the breast immune micro-environment in the regulation of tumorigenesis. Recent studies have associated increased infiltration of immune cells in breast cancer tumours where RUNX/CBFβ is altered. Therefore, the third aim of the project was to determine whether *Cbfβ* expression in mammary tumours impacted the composition and pro- or anti-tumour functions of immune microenvironment in mammary glands.

Chapter 2. Materials and Methods

2.1. Animal work

2.1.1. Breeding and Maintenance of animals

All experimental work involving mice was conducted under license and regulations issued by the UK Home Office, in accordance with the Animals (Scientific Procedures) Act, 1986 and the European Directive 2010/63/EU and authorised by Animal Welfare and Ethical Review Board (AWERB). For breeding and maintenance of all animals, individually ventilated cages (IVC) were used with *ad libitum* access to standard diet, water and regular monitoring of general health. For genotyping purposes, tissue biopsies of ear notches routinely acquired from mice by the Biological Services Unit at the CRUK Beatson Institute were submitted to Transnetyx, Inc. (Cordova, TN, USA). Animals were humanely euthanised using Schedule 1 protocols and sampled in accordance with project license (70-8645; PP6345023).

2.1.2. Sources of mouse lines and the generation of mouse models

The *MMTV-Cre* and *MMTV-PyMT* lines were kindly provided by the WJ Muller lab (Guy, Cardiff and Muller, 1992; Andrechek et al., 2000). The LGB-Cre allele, *Tg (LGB-cre)74Acl*, hereafter referred to as *BLG-Cre,* and *Catnb*$^{wt/lox(ex3)}$ lines were acquired from AR Clarke (Selbert et al., 1998) and OJ Sansom (Harada et al., 1999) respectively. The *Cbfβ*$^{fl/fl}$ line generated at the Taniuchi lab were bought from The Jackson Laboratory (USA) (Naoe et al., 2007). The *Runx1*$^{fl/fl}$ line was kindly provided by Marella De Bruijn, Oxford, originally generated at the lab of Professor Nancy Speck (Growney et al., 2005). Mice carrying *Runx2*$^{fl/fl}$ alleles were produced by Theresa Higgins and Ian Rosewell in Professor Mike Owen's lab (ICRF lab, London) and characterised at the Blyth lab (Ferrari et al., 2015). The *Gt (ROSA)26Sor*^{tm1Hjf} line encoding for tandem dimer red fluorescent protein (tdRFP), as previously described by (Luche et al., 2007) and *Gt (ROSA)26Sor*$^{tm2\ (cre/ERT2)Brn}$ (encoding ROSA-Cre-ER^{T2}) described in (Hameyer *et al.*, 2007) was sourced from the EMMA archive.

MMTV-PyMT, MMTV-Cre and *Cbfβ*$^{fl/fl}$ alleles on a C57BL/6J, backcrossed for up to 10 generations (N10) were inter-crossed in order to generate the *MMTV-PyMT;MMTV-Cre;Cbfβ*$^{fl/fl}$ mouse model and relevant controls. The tdRFP mice (C57BL/6J) were also crossed onto this model to introduce a reporter gene that could be used as a surrogate for tracking expression of *MMTV-Cre* and recombination of *Cbfβ*. For generation of the MMTV-PyMT model with an inducible Cre; the *ROSA-CreER*^{T2} line was crossed onto *MMTV-PyMT;Cbfβ*$^{fl/fl}$ mice. These were derived from and maintained on an FVB/N background where the *MMTV-Cre* and *MMTV-PyMT* mice were backcrossed for up to 20 generations and *Cbfβ*$^{fl/fl}$ mice had been backcrossed for more than 10 generations onto commercially bought FVB/N (Charles River, UK). These were inter-crossed as above to generate the *MMTV-PyMT;ROSA-CreER*^{T2}*;Cbfβ*$^{fl/fl}$ model.

In order to study the effect of *Cbfβ* loss in Wnt/β-catenin activated mammary cancer, *BLG-Cre;Catnb*$^{wt/lox(ex3)}$ FVB/N mice (N10) were bred with FVB (N10) mice carrying the *Cbfβ*$^{fl/fl}$ allele created through generational mating with commercially bought FVB/N mice (Charles River, UK). *BLG-Cre;Catnb*$^{wt/lox(ex3)}$ (FVB/N, N10) mice were crossed onto *Runx1*^{flfl} FVB/N mice (N10) and subsequently crossed with mice carrying *Runx2*^{flfl} to generate two separate cohorts of *BLG-Cre;Catnb*$^{wt/lox(ex3)}$*Runx1*$^{fl/fl}$ and *BLG-Cre;Catnb*$^{wt/lox(ex3)}$*Runx1*$^{fl/fl}$*;Runx2*$^{fl/fl}$ experimental mice on an FVB/N background (N10). Analysis of disease progression, sample collection and processing

Experimental cohorts of mice used for tracking tumour growth and development were maintained under enhanced monitoring of at least twice a week. Formation of mammary tumours were identified through palpation and the size of the lesion recorded using calliper measurements. Clinical endpoint was considered when the length or width of a tumour reached 15mm. Additionally ulcerations of the tumour or deterioration of general health of the animal were also considered clinical endpoints. At this stage, the mouse was sacrificed humanely using increasing concentrations of CO_2 in a chamber with a secondary technique of cervical dislocation used for confirmation of death. Cardiac blood was drawn for further analysis through cardiac puncture with a needle and syringe. Mouse body weight, cumulative mammary gland weight (tumour bearing and non-bearing) and lung weight was recorded. These were used to calculate mammary tumour burden and lung burden (where mammary gland weights and lung weights were expressed a

percentage of total body weight). Post-dissection, mammary glands (normal or tumour bearing) were processed for wholemounts, fixed in 10% neutral buffered formalin [100ml 37-40% formalin, 4g/l NaH2PO4 (monobasic), 6.5g/l NaH2PO4 (dibasic/anhydrous), 900 ml distilled water (for 1 litre solution)] for use in histological analysis or snap-frozen in dry ice and stored in -80°C for future use in molecular analysis. Lung tissues were also fixed in formalin. All formalin fixed samples were transferred into 70% ethanol after 24-48h and subsequently sent to Beatson Histology for paraffin embedding.

2.1.3. Survival Analysis

To generate Kaplan-Meier curves for survival analysis, overall survival data were plotted using Graphpad Prism and the appropriate statistical tests conducted. Clinical onset was calculated as the time between birth and development of the first palpable tumour (under 5mm in size). Tumour progression was tracked through calculating the difference between clinical onset and clinical endpoint. Mice culled due to pathologies unrelated to genotype or due to the development of cystic tumours or lipomas were treated as censored observations.

2.1.4. Imaging of RFP positive tumours

For *ex vivo* analysis of red fluorescent protein (RFP) expression, all 10 mammary glands and lungs from experimental mice were harvested and promptly imaged using the in vivo imaging system (IVIS Spectrum, PerkinElmer). Samples placed on 100mmx20mm petri dishes (Corning®) were illuminated using the 554nm excitation filter and fluorescence detected through the 581nm emission filter.

2.2. Preparation of mammary gland wholemounts

Inguinal mammary glands were harvested from female mice, mounted onto glass slides (631-0880, VWR) and air dried for 10-20 minutes. Slides were submerged into Carnoy's fixative in 50ml conical tubes (Cellstar® Tubes, Greiner Bio-One) and incubated overnight. For preparation of Carnoy's fixative, 30% chloroform (C2432-25ML, Sigma-Aldrich) and 10% glacial acetic acid (A/0400/PB17, Fisher Chemical) was added to absolute ethanol (BP2818-500, Fisher Scientific). Fixed glands were put through successive ethanol washes lasting 15 minutes in 70%, 50% and 25%

concentrations. A final wash in distilled H_2O was performed after which slides were stained overnight in Carmine Alum. This was prepared by adding 1g Carmine (C1022, Sigma), 2.5g aluminium potassium sulphate dodecahydrate (237086, Sigma) to 500ml distilled water and boiling for 20 minutes. The resulting solution was then filtered through a 0.2µm aPES membrane in a sterile 500ml Filter unit (FB12566504, Fisherbrand) and refrigerated for use. Post staining, mammary glands were dehydrated by 15-minute washes in 70%, 90% and 100% ethanol sequentially and then submerged in Xylene (534056-4L, Sigma-Aldrich) overnight. Finally, glands were mounted using Pertex Mounting Medium (SEA-0100-00A, CellPath). Slides were imaged using a Zeiss stereomicroscope and analysed though ImageJ software.

2.3. Histology

All histological procedures up to section 1.3.3 were conducted by the Core Histology Service at the CRUK Beatson Institute. Animal tissues were formalin fixed and paraffin embedded (FFPE), prior to processing for haematoxylin and eosin (H&E) staining, immunohistochemical staining and *in situ* hybridisation (ISH). 4µm sections were cut from FFPE tissue blocks, mounted on slides (VWR) and incubated for 2 hours in a 60°C oven prior to H&E, IHC and RNAscope (ISH) staining. Post staining, all sections were rinsed with tap water, dehydrated through graded ethanol solutions and placed in xylene. Coverslips were placed over stained sections in xylene using DPX mountant (SEA-1300-00A, CellPath).

2.3.1. H&E staining

For H&E staining, the Leica autostainer (ST5020) was used. Tissue sections were dewaxed in xylene, taken through graded ethanol solutions and stained with Haem Z (RBA-4201-00A, CellPath) for 13 minutes. Subsequently, tissue sections were washed in water, differentiated in 1% acid alcohol, washed and nuclei blued in Scotts tap water substitute (in-house). After washing with tap water, sections were placed in Putt's Eosin (in-house) for 3 minutes.

2.3.2. Immunohistochemistry

For IHC staining, either the Agilent Autostainer Link48 or Leica Bond Rx Autostainer was used. For antigen retrieval, one of the three following methods were utilised: (1) heat induced epitope retrieval (HIER) with high pH target retrieval solution (TRS high) (K8004, Agilent), (2) epitope retrieval using enzyme 1 (Enz1) solution (AR9551, Leica) and (3) epitope retrieval with ER2 solution (AR9640, Leica). A list of all antibodies used, including their details along with the type of autostainer, antigen retrieval methods and secondary antibodies utilised are provided in Table 2.1.

Table 2.1: List of antibodies, autostainers and antigen retrieval methods used for IHC staining.

Antibody	Dilution	Clone	Company	Code	Autostainer	Antigen retrieval method; time	Secondary Antibody
CD4	1:500	4SM 95	eBioscience	14-9766-82	Leica Bond Rx	ER2; 20 mins	Rat ImmPRESS
CD8	1:500	4SM 15	eBioscience	14-0808-82	Leica Bond Rx	ER2; 20 mins	Rat ImmPRESS
Estrogen Receptor	1:400	E115	Abcam	ab32063	Agilent autostainer link48	TRS High	Rabbit Envision
F4/80	1:100	CI:A3-1	Abcam	ab6640	Leica Bond Rx	Enz1; 10 mins	Rat ImmPRESS
Keratin 14	1:300	LL002	Abcam	ab7800	Agilent autostainer link48	TRS High	Mouse Envision
Keratin 18	1:1000		Abcam	ab181597	Leica Bond Rx	ER2; 30 mins	Rabbit Envision
Ki67	1:1000	D3B5	Cell Signaling	12202	Leica Bond Rx	ER2; 20 mins	Rabbit Envision
Ly6G	1:60000	IA8	BioXcell	BE0075-1	Leica Bond Rx	ER2; 20 mins	Rat ImmPRESS
NIMP	1:600	NIMP-R14	Abcam	ab2557	Leica Bond Rx	Enz1; 10 mins	Rat ImmPRESS

For all antibodies stained on the Agilent Autostainer Link48, FFPE sections were dewaxed in Agilent pre-treatment module. HIER-TRS high antigen retrieval method was used, and sections heated for 20 minutes to 97°C. Subsequently, prior to being loaded onto the autostainer, sections were rinsed with flex wash buffer (K8007, Agilent), followed by peroxidase blocking (S2023, Agilent) for 5 minutes and rinsed again in flex wash buffer. Additional blocking steps with mouse Ig block (MKB-2213, Vector Labs) applied for 20 minutes was required for Keratin 14 stained sections. Flex wash buffer was applied before primary antibody application and sections were washed again with flex wash buffer before application of rabbit envision (ER) (K4003) or mouse envision (K40) (K4001) secondary antibody (Agilent) for 30 minutes. A final wash with flex buffer followed application of Liquid DAB (K3468, Agilent) for 10 minutes. Sections were then washed in water and counterstained with haematoxylin z (RBA-4201-001 CellPath).

For antibodies stained on the Leica Bond Rx autostainer, FFPE sections were dewaxed on-board (AR9222, Leica) and appropriate retrieval solutions (Enz1 or ER2) were used to retrieve epitopes. Next, sections were washed with Leica wash buffer (AR9590, Leica) before peroxidase block was performed using an Intense R kit (DS9263, Leica). Blocking solution was applied from the Rat ImmPRESS kit (MP-7404, Vector Labs) for 20 minutes after which, sections were washed with wash buffer and primary antibodies applied at optimal dilutions (Table 2.1). The sections were then rinsed with wash buffer and incubated for 30 minutes with appropriate secondary antibodies. Finally, Sections were washed with flex wash buffer, visualised using DAB and counterstained with haematoxylin in the Intense R kit.

2.3.3. RNAscope

ISH detection was performed using RNAScope 2.5 LSx (Brown) detection kit (322700; Bio-Techne) on a Leica Bond Rx autostainer strictly according to the manufacturer's instructions. Probes included Cxcl1 (407728, Bio-Techne), Cxcl2 (437588, Bio-Techne) and Cxcl5 (467448, Bio-Techne).

2.3.4. Histological Analysis

Scanned images of IHC and ISH tissue stains were analysed using HALO™ v3.4.2986. The algorithms used for analysis were as follows: Area Quantification, CytoNuclear and ISH v3.4.7. For quantification of immune cell staining, the CytoNuclear module was applied for the entire tissue image. The H-score generated was used to show both the stain intensity and proportion of positively stained cells within the whole tissue. For cytokine staining, the ISH module was applied for the entire tissue scan. Positively stained areas were presented as a percentage of the total tissue are. Total RNAcopies as calculated by the algorithm was also provided. Qualitative analysis of scanned H&E, IHC and ISH images were conducted on Aperio ImageScope (Leica).

2.4. Tissue culture

2.4.1. Generation of mouse cell lines

The largest mammary tumour from *MMTV-PyMT;ROSA-CreER^{T2}* mice with either *Cbfβ$^{fl/fl}$* or *Cbfβ$^{wt/wt}$* alleles at clinical endpoint were harvested after euthanization of the animal. Extracted tumour was washed twice in phosphate-buffered-saline (PBS), comprised of 70mM NaCl, 3.3mM KCl, 1.8mM Na2HPO4 and 10.6mM H2PO4, and manually dissociated using sterile scalpels (0510, Swann-Morton®) in a containment level II tissue culture hood under sterile conditions. Dissociated tumour cells were suspended in Tumour cell culture media. This was prepared by adding 10% Foetal Bovine Serum (FBS) (10270, Thermo Scientific), 1% penicillin/streptomycin (15140-122, Gibco), 1% L-glutamine (25030-032, Thermo Fisher Scientific), 10 ng/ml epidermal growth factor (EGF) (78016.1, Stemcell Technologies), and 5 µg/ml Insulin (I9278-5ML, Merck) and 10ng/ml cholera toxin (C8052-.5MG, Merck) into 500ml Dulbecco's Modified Eagle Medium (DMEM) (Thermo Fisher Scientific). Tumour cells in suspension were collected into a 50ml conical tube for centrifugation at 1200rpm for 5 minutes. Supernatant containing any dead cells and debris was discarded and tumour cells resuspended in culture media. Primary tumour cells were subsequently transferred into a Falcon® 150mm culture dish (353025, Corning®) and incubated at 37°C, 5% CO_2. Mycoplasma tests were conducted routinely through Beatson Molecular Technologies using culture media from near confluent cells. Cells that survived past 5 consecutive rounds of passaging were considered stable subcultures and deemed as one established cell line suitable for experimental use.

2.4.2. Cell culture

Tumour cells used in experimental procedures were cultured in tumour cell culture media supplemented with growth factors as described above. To maintain integrity of cultures, cells were passaged upon reaching 70-80% confluency. For this purpose, cells were washed with PBS once the culture media was removed via aspiration. To induce detachment of the monolayer, cells were incubated in 0.25% trypsin (Gibco, USA) for 5 minutes at 37°C. Tumour cell culture media containing FBS was added to neutralise trypsin following which the cell suspension was collected into a 50ml conical tube for centrifugation at 1200rpm for 5 minutes.

Supernatant was discarded and the cell pellet resuspended in fresh culture media. For freezing of cells, the cell pellet acquired at this point was washed with PBS and resuspended into Freezing medium – 50% FBS, 40% tumour cell culture medium and 10% DMSO (D2650, Sigma Aldrich) and stored into 1ml conical bottom cryovials (123263, Greiner Bio-one) in a CoolCell® FTS 30 cryostorage container (Biocision®) at -80˚C. Otherwise, the cell suspension was then transferred into sterile culture dishes and incubated in 37˚C under 5% CO_2 for subculturing. Regular mycoplasma tests on culture media from near confluent cell cultures were conducted to confirm absence of any contamination.

2.4.3. 4OHT treatment

MMTV-PyMT;MMTV-ROSA-CreER^{T2} mouse tumour derived cell lines were treated with 4-hydroxytamoxifen (4OHT) (H7904-5MG, Sigma) diluted in 95% sterile ethanol for a final concentration of 100nM in culture media. For vehicle treated control groups, 95% ethanol was used at the same volume as 4OHT. $3x10^5$ cells from each cell line treated with 100nM 4OHT or vehicle control once every 24 hours for 2 consecutive days. At the end of 48 hours, treatment was stopped, cells washed twice with PBS, detached using trypsin as described above and centrifuged for 5 minutes at 1200rpm. The supernatant was discarded, and the pellet resuspended in fresh tumour cell culture media. Cells were counted using the trypan blue exclusion method where cell suspensions were diluted 1:10 in 0.4% Trypan blue (T10282, Thermo Scientific). 10µl of stained cell suspensions were pipetted into the cell counting chamber of the CellDrop™ Automated Cell Counter (Denovix) and the Trypan Blue programme chosen to record the number of cells. Appropriate cell numbers were subsequently used for biological assays or protein quantification. For all biological assays cells were cultured in fresh tumour cell culture media free of 4OHT or vehicle.

2.5. MTS cell viability assay

All cells were treated with either vehicle control or 100nM 4OHT every 24h for two consecutive days prior to use in MTS assay– this point is considered as day 0 of the MTS assay. MTS assays were set up for 6 timepoints of day 0, 1, 2, 3, 5, and 7. Cells were plated into 96 well plates (Falcon® 96-well Polystyrene Microplates 353072, Corning®) at an optimal seeding density of 500 cells per well, determined

through previously conducted pilot experiments. Tumour cell culture media was added to each well to encourage optimal growth of experimental cells. At each timepoint, the CellTiter 96 AQueous One Solution Cell Proliferation Assay (MTS) (G3581, Promega) was used to conduct viability assays. 20µl MTS reagent was added to 100µl media in each well as per manufacturer's protocol. Subsequently, cells were incubated in the absence of light at 37°C in 5% CO_2 for 2 hours. The SpectraMax® ABS Plus spectrophotometer and SoftMax Pro software was used to measure and record the absorbance at 490nm. Absorbance readings from 4OHT treated cells were normalised to the mean of the respective vehicle treated controls for each cell line.

2.6. Colony formation assay

Two tumour derived *MMTV-PyMT;ROSA-CreER^{T2};Cbfβ$^{fl/fl}$* cell lines (labelled *Cbfβ$^{fl/fl}$* cell line 1 and *Cbfβ$^{fl/fl}$* cell line 2) and one *MMTV-PyMT;ROSA-CreER^{T2};Cbfβ$^{wt/wt}$* cell line (labelled *Cbfβ$^{wt/wt}$* cell line) pre-treated with 4OHT or vehicle (as described in section 2.4.3) were seeded at 2500 cells per well for *Cbfβ$^{wt/wt}$* cell line and *Cbfβ$^{fl/fl}$* cell line 1, and 1000 cells per well for *Cbfβ$^{fl/fl}$* cell line 2 onto 6 well plates with 2ml tumour cell culture media. Assay plates were incubated at 37°C in 5% CO_2. At day 4, the culture media was aspirated and replaced with fresh pre-warmed media. Assay endpoint was considered to be 8 days after plating for the two *Cbfβ$^{fl/fl}$* cell lines and 12 days after plating for the *Cbfβ$^{fl/fl}$* cell line based on colony growth rates. At this stage, colonies were washed with PBS and fixed by incubation in 100% methanol (67-56-1, Fisher Scientific) for 30 minutes. Fixed colonies were subsequently washed in PBS and stained with 1ml 0.1% Crystal Violet Solution (V5265-250ML, Sigma) for 30 minutes. Finally, the solution was removed, and stained plates washed in distilled H_2O to remove excess dye. For quantification of colonies, plates were scanned using the LI-COR Odessy Clx plate scanner and the stain intensity recorded at 800nm for each well. Mean fluorescence intensity for 4OHT pre-treated samples from technical repeats per experiment were normalised to their respective vehicle pre-treated samples for each cell line.

2.7. Tumoursphere assay

Tumoursphere media was prepared by adding 10% FBS (10270, Thermo Scientific), 1% penicillin/streptomycin (15140-122, Gibco), 1% L-glutamine (25030-032, Thermo Fisher Scientific), 20ng/ml EGF (78016.1, Stemcell Technologies), 20ng/ml Fibroblast Growth Factor-basic (SRP4038-50UG, Merck), 4µg/ml Heparin (H3149-50KU, Merck) and 1ml 50x B-27™ Supplement (17504044, Thermo Fisher Scientific) to 50ml Advanced-DMEM/F12 (12634010, Thermo Fisher Scientific). Single cell suspensions of tumour cells pre-treated with either 4OHT or vehicle vehicle (as described in section 2.4.3) were seeded at 2000 cells per well for *Cbfβ*$^{wt/wt}$ cell line and *Cbfβ*$^{fl/fl}$ cell line 1, and 1000 cells per well for *Cbfβ*$^{fl/fl}$ cell line 2 in ultra-low attachment 24 well plates (734-1584, VWR). 2ml of tumoursphere media was added to each well to encourage growth of tumourspheres. Assay plates were incubated at 37°C in 5% CO_2. At day 3, 10µl of EGF and B-27 was added to the culture media. At day 7 the number of primary tumourspheres per well were manually counted using Olympus CKX41 microscope under 4x objective lens. Tumourspheres were also counted separately according to size. A semi-quantitative method using the grid embedded on the microscope lens was used to classify tumourspheres into small, medium and large groups. Representative images were captured using the Olympus CKX41 microscope and the Q-Capture Pro 7 software.

2.8. Flow Cytometry

2.8.1. List of flow cytometry antibodies

Table 2.2: List of antibodies used in flow cytometric analysis of myeloid cells.

Antigen	Fluorochrome	Dulution	Stock Concentration	Clone	Catalogue #	Source
CD103	BV421	1:100	0.2 mg/ml	2E7	121422	Biolegend
CD11b	BV785	1:200	0.2 mg/ml	M1/70	101243	Biolegend
CD11c	PE	1:200	0.2 mg/ml	N418	15-0114-82	Biolegend
CD19	FITC (DUMP)	1:400	0.5 mg/ml	eBio1D3	11019386	eBioscience
CD317	PE-Cy7	1:200	0.2 mg/ml	eBio927	25-3172-82	eBioscience
CD3e	FITC (DUMP)	1:50	0.5 mg/ml	145-2C11	11003186	eBioscience
CD45	BV605	1:200	0.2 mg/ml	30-F11	130140	Biolegend
CD80	APC	1:25	0.2 mg/ml	16-10A1	17-0801-82	eBioscience
EpCAM/CD326	APC-eFluor780	1:50	0.2 mg/ml	G8.8	47-5791-82	eBioscience
F4/80	BV650	1:25	0.2 mg/ml	BM8	123149	Biolegend
Ly6C	PeDazzle	1:100	0.2 mg/ml	HK1.4	128044	Biolegend
Ly6G	BUV395	1:25	0.2 mg/ml	1A8	563978	BD Biosciences
MHCII	PerCP-eFluor 710	1:50	0.2 mg/ml	M5/114.15.2	46-5321-82	eBioscience
Ter119	FITC (DUMP)	1:50	0.5 mg/ml	TER-119	115921	eBioscience

Table 2.3: List of antibodies used in flow cytometric analysis of T cells and their cytokines

Extracellular antibodies						
Antigen	**Fluorochrome**	**Dulution**	**Stock Concentration**	**Clone**	**Catalogue #**	**Source**
CD11b	Brilliant Violet 785	1:400	0.2 mg/ml	M1/70	47-0112-82	eBioscience
CD19	APC-eFluor780	1:200	0.2 mg/ml	1D3	47-0193-82	eBioscience
CD27	PE/Dazzle 594	1:200	0.2 mg/ml	LG.3A10	124228	Biolegend
CD3	BV650	1:50	0.1 mg/ml	17A2	100229	Biolegend
CD4	BV605	1:50	0.2 mg/ml	RM4-5	100429	Biolegend
CD44	PerCP-Cy5.5	1:50	0.2 mg/ml	IM7	103032	Biolegend
CD69	BV510	1:25	0.1 mg/ml	BV510	104532	Biolegend
CD8	BUV395	1:50	0.2 mg/ml	53-6.7	563786	BD Bioscience
EpCAM	APC-eFluor780	1:50	0.2 mg/ml	G8.8	47-5791-82	eBioscience
γδTCR	FITC	1:100	0.5 mg/ml	GL3	11-5711-85	eBioscience
NKp46	BV421	1:50	0.2 mg/ml	29A1.4	137612	Biolegend
Intracellular antibodies						
Antigen	**Fluorochrome**	**Dulution**	**Stock Concentration**	**Clone**	**Catalogue #**	**Source**
IFNγ	PE-Cy7	200	0.2 mg/ml	XMG1.2	25-7311-82	eBioscience
IL-17A	PE	100	0.2 mg/ml	eBio17B7	12-7177-81	eBioscience
Granzyme B	AlexaFluor-647	50	0.2 mg/ml	GB11	515406	Biologend

2.8.2. Isolation of immune cells from mammary glands

Mammary glands (10 per mouse) were extracted from female mice. Lymph nodes from inguinal and thoracic glands were removed and tissues subsequently collected into PBS on ice. For homogenisation of tissues, mammary glands were chopped on 100mmx20mm petri dishes (430167, Corning®) using a sterile scalpel and transferred into a gentleMACs C-tube (130-096-334, Miltenyi) with 2.35ml RPMI Medium 1640 (31870-025, Gibco) and 12.5µl Enzyme A, 100µl Enzyme D and 50µl Enzyme R from the Miltenyi Tumour Dissociation Kit (130-096-730, Miltenyi Biotec). GentleMACs C-tubes containing the sample suspensions were then placed into a gentleMACs Octodissociator (Miltenyi) and the "37_m_TKD1" program was chosen for enzymatic dissociation of soft tissues at 37°C according to manufacturer's instructions. After 40 mins of enzymatic dissociation, the mammary cell suspensions were strained using 70µm cell filters (542070, Greiner Bio-one) and transferred into 50ml conical tubes. 2ml foetal calf serum (FCS, Gibco) was added to each sample in order to neutralise activity of enzymes. Subsequently, the samples were centrifuged in 4°C for 5 minutes at 1500rpm. The supernatant was discarded, and 1x RBC lysis buffer (prepared by diluting 10x RBC Lysis buffer, Invitrogen with distilled water) was used to resuspend cell pellets which were then vortexed and incubated at room temperature for 5 minutes. The

supernatant was discarded to remove lysed erythrocytes and the pellet was resuspended in 1ml FACS buffer prepared by adding 0.5% bovine serum albumin (BSA) (A7906-100A, Sigma Aldrich) into PBS which was filter sterilised and stored at 4°C.

For enrichment of lymphocytes, Percoll gradient centrifugation was performed as follows: 15ml conical tubes (Cellstar Tubes, Greiner Bio-One) were coated with 10%FCS in DMEM to aid the formation of density phases. This FCS-DMEM mixture was removed prior to adding samples into the tube. 100% Percoll stock was made by adding 45ml of Percoll (17089101, SigmaAldrich) to 5ml 10xPBS. Percoll concentrations of 20%, 40% and 80% were prepared by diluting 100% Percoll with PBS. 3ml of 80% Percoll was added to each of the FCS coated,15ml conical tubes. Mammary gland suspensions in FACS buffer were centrifuged in 4°C for 5 minutes at 1500rpm and the pellet resuspended in 3ml of 40% Percoll after discarding the supernatant. Using a P1000 pipette, this was gently added into the conical tube containing 80% Percoll at a near 90° angle. On top of this 40% phase, 1ml of 20% Percoll was added in the same manner and the samples subsequently centrifuged in 21°C, for 30 minutes at 1800rpm with no/lowest brake setting. Next, the 20% Percoll layer was removed, followed by aspiration of half of the 40% phase. Approximately 2ml of the 40/80% interphase was then collected to be transferred into a fresh conical tube (50ml). 8ml of FACS buffer was added to this before centrifugation for 5 minutes at 1800rpm. The supernatant was discarded and 1ml FACS buffer was used to resuspend the pellets.

Immune cells were then counted using the trypan blue exclusion method where cell suspensions were diluted 1:10 in 0.4% Trypan blue (T10282, Thermo Scientific). 10µl of stained cell suspensions were pipetted into the cell counting chamber of the CellDrop™ Automated Cell Counter (Denovix) and the Trypan Blue programme chosen to record the number of cells. Cells per sample were counted in triplicate and $2x10^6$ cells from each sample were plated onto 2 x V bottom 96 well plates (Thermo) for each antibody panel to prepare for staining.

2.8.3. Cytokine Stimulation

In order to investigate cytokine production, T cells within the samples were induced using a T cell Stimulation Medium. This consisted of a pre-made Cell

Activation Cocktail (Biolegend) with PMA (phorbol 12-myristate-13-acetate) and Brefeldin A diluted 1:500 in stimulation medium made up of 8% FCS (Gibco), 1% penicillin/streptomycin (Sigma) and 0.5% β-mercaptoethanol (Gibco) in IMDM medium (Gibco). PMA is known to activate T cells and stimulate production of cytokines while Brefeldin A is involved in the inhibition of cytokine secretion. This allows retention of cytokines within the cells which can be detected through intracellular fluorescent antibodies. Immune cell samples in the V bottom 96 well plates to be stained for the T cell panel of antibodies were centrifuged in 4°C for 2 minutes at 2000rpm. After discarding the supernatant, cell pellets were resuspended in 200µl T cell Stimulation Medium, and samples were incubated for 3 hours at 37°C.

2.8.4. Extracellular and Intracellular staining

Samples in 96 well plates to be stained with the T cell panel of antibodies following cytokine stimulation were centrifuged in 4°C for 2 minutes at 2000rpm. The cytokine stimulation cocktail was removed, and the cells washed in 100µl FACS buffer. These samples after centrifugation in 4°C for 2 minutes at 2000rpm and removal of the supernatant containing FACS buffer, together with those to be stained with the myeloid panel of antibodies, were resuspended in 50µl Fc Blocking Buffer. Cells were then incubated at 4°C for 20 minutes. Fc Blocking Buffer was prepared by diluting TruStain FcX™ anti-mouse CD16/32 (101320, Biolegend) 1:50 in FACS buffer. Next, 50µl of myeloid panel antibody mix (Table 2.2) or T cell extracellular antibody mix (Table 2.3) was added to the samples according to the experimental plan. All antibodies were diluted in Brilliant Stain Buffer (BD). Samples were incubated at 4°C for 30 minutes. Subsequently, cells were centrifuged at 4°C for 2 minutes at 2000rpm and washed in 100µl FACS buffer. The centrifugation step was repeated, and the pellets washed in cold PBS before a second round of centrifugation. To distinguish between live and dead cells, sample pellets to be stained for myeloid antibodies were then resuspended in 100µl Zombie Green viability dye (423112, Biolegend) and those to be stained for lymphoid antibodies were resuspended in 100µl Zombie NIR viability dye (423106, Biolegend). Both dyes were diluted 1:400 in cold PBS. Samples were refrigerated in the appropriate viability dyes for 20 minutes. Finally, cells were centrifuged, washed in FACS buffer, and centrifuged again at 4°C for 2 minutes at 2000rpm before being resuspended in 100µl of IC Fixation Buffer (00-8222-49,

Invitrogen). Incubation time was 20 minutes at 4°C. Following incubation, samples for the myeloid panel analysis were centrifuged to remove the fixation buffer and resuspended in 100µl FACS buffer.

Samples stained with the T cell panel of extracellular antibodies were also incubated in a cocktail of intracellular antibodies for detection of cytokines. Fixed cells were centrifuged and resuspended in 100µl of 1X permeabilization buffer – prepared by diluting 10X stock Permeabilization Buffer (00-8333-56, Invitrogen) in distilled water. Following subsequent centrifugation, cell pellets were resuspended in 100µl of intracellular antibody mixture (Table 2.3) (all antibodies diluted in 1X permeabilization buffer) and incubated at 4°C for 30 minutes. Fluorescence Minus One (FMO) controls prepared were also stained with intracellular antibodies. Following incubation, FACS buffer was used to wash all samples twice after which samples were centrifuged and resuspended in 100µl FACS buffer.

Finally, all samples were filtered into 5ml Corning™ Falcon® Round-Bottom Tubes with cell strainer caps (10585801, Fisher Scientific) for acquisition.

2.8.5. Compensation and analysis

For preparation of compensation, 1.4ml U-bottom FACS tubes (Micronic) were set up for each antibody utilised in the experiment. To each tube, 50µl FACS buffer and 1µl of antibody was added to generate a single stain control. UltraComp eBeads™ Compensation Beads (Invitrogen) were vortexed for a minimum of 40 seconds and 25µl of these were added to each tube. A separate tube with only FACS buffer and compensation beads was prepared as an unstained control. Following compensation, sample acquisition was carried out on LSRFortessa™ (BD Bioscience) using the DIVA software. Data analysis was performed using Flowjo software v10.8.1 (Flowjo, LLC).

2.9. RNA Sequencing of tumours

2.9.1. RNA extraction from frozen murine mammary tumours

Tumour fragments were recovered from -80°C and defrosted on ice. For tissue homogenisation, fragments were transferred into Precellys Hard Tissue Tubes (CK28R, P000916-LYSK0-A) consisting of ceramic beads to assist dissociation of hard tissue. 1ml of TRIzol® Reagent (15596026, Ambion® by Life Technologies) was added to each tube which were then placed into a pre-cooled Precellys Evolution Homogenizer (Bertin Technologies) at 4°C. Tumour fragments were homogenized through at 5500rpm for 4 x 20-second cycles with 30 second pauses in between each run cycle. Subsequently, tubes were pulsed for 10 seconds to remove any residual tissue lysate from the lid. Tissue lysates were then transferred into clean, RNase free 2ml tubes and centrifuged for 5 minutes at 13,000rpm. 200µl chloroform (C2432-25ML, Sigma-Aldrich) was added to each sample, vortexed for 30 seconds to achieve a milky suspension after which they were centrifuged at 13,000rpm for 10 minutes at 4°C. The aqueous layer generated was transferred into an RNase free tube for each sample and an equal volume of isopropanol (I9516-500ML, Sigma-Aldrich) along with 5µl of Glycol blue (D-α-Tocopherol polyethylene glycol 1000 succinate, 57668-5G, Sigma-Aldrich) was added. The mixture was vortexed for 10 seconds and incubated on dry ice for 20 minutes to allow precipitation of RNA. Next, sample tubes were centrifuged at 13,000rpm for 15 minutes at 4°C. The supernatant was discarded, and the pellet washed with 700µl of 70% ethanol. Following a second centrifugation step for 5 minutes at 13,000rpm, the supernatant was discarded, and the pellet containing RNA resuspended in 20µl of 60°C Nuclease-free water (129115, Qiagen). RNA concentration was measured using the NanoDrop 2000c Spectrophotometer (Thermo Fisher Scientific) at 260nm absorbance (A_{260}) and data recorded through NanoDrop 2000 software. For removal of any residual genomic DNA contamination, the TURBO DNA-free™ Kit (AM1907, Thermo Fisher Scientific) was used to treat extracted RNA according to the standard manufacturer's protocol. Final concentration and RNA quality was measured, and purified RNA was stored at -80°C until further use.

2.9.2. RNA sequencing

RNA sequencing was conducted by William Clark from the Molecular Technology Services at the CRUK Beatson Institute. Agilent 2200 Tapestation with RNA Screentape (Agilent, Thermofisher) was used for checking RNA quality and RNAseq libraries were created using the TruSeq Stranded mRNA Library Prep Kit (20020594, Illumina) in accordance with manufacturer's instructions. For library preparation, 100ng of RNA from samples was used to extract mRNA though PolyA selection with OligodT coated beads. Heat fragmentation was used to generate transcripts of 120-200 base pairs in size. For cDNA synthesis, SuperScript III Reverse Transcriptase kit (18080-044, Invitrogen) with random primers was used and subsequently 13 cycles of PCR conducted. Quantification of RNAseq libraries used the Qubit v2.0 HS DNA assay (Q32854, Invitrogen). NextSeq500 sequencer (Illumina) was used in 2 x 36 cycle pair-end sequencing of the libraries.

2.9.3. Bioinformatics Analysis

Processing of raw RNAseq data and bioinformatic analysis was performed by Robin Shaw of the Bioinformatics Core Facility at the CRUK Beatson Institute. FastQC v0.11.9 FastP v0.20.1 and FastQ Screen v0.14 were used to conduct quality checks and trimming of raw fastq RNA-Seq data files. RNA-Seq paired-end reads were aligned to the GRCm39.104 version of the mouse genome and annotation, using HiSat2 v2.2.1 and sorted using Samtools v1.7. Aligned genes were identified using Feature Counts from the SubRead package version 2.0.1. Expression levels were determined and statistically analysed using the R environment version 4.1 and utilizing packages from the Bioconductor data analysis suite. Differential gene expression was analysed based on the negative binomial distribution using the DESeq2 package version 1.32 and adaptive shrinkage using Ashr. Identification of enriched biological functions was achieved using g:Profiler, GESA version 7.5.1 from the Broad Institute, and MetaCore from Clarivate Analytics (https://portal.genego.com/). Computational analysis was documented at each stage using MultiQC, Jupyter Notebooks and R Notebooks.

For generation of bar graphs comparing gene expression between CBFB_HOM, WT and R1R2_HOM samples, Graphpad prism was used. Genes considered to be significantly altered in CBFB_HOM samples compared to WT as presented in the

differential gene expression table generated by Robin Shaw were selected according to an absolute fold-change threshold of 1.5 and a p-adjusted (padj) value of less than 0.05. The same filtering process was used to select genes significantly altered in R1R2_HOM samples compared to WT. For generation of heatmaps, z-scores of differential gene expression values were calculated, and GraphPad Prism v9 used to plot heatmaps. List of genes for Wnt heatmap generation (section 4.2.7) were manually curated based on available literature. Significance and absolute fold change for expression of all cytokine and cytokine receptors within the differential gene expression table was analysed. Only genes with padj<0.05 and absolute foldchange=1.5 were selected for heatmap generation.

2.10. Protein extraction and gel electrophoresis

2.10.1. Extracting protein from cells

For extraction of protein, 1X lysis buffer was prepared by diluting 100X HALT™ Protease Inhibitor Cocktail (78429, Thermo Scientific) and PhosSTOP™ Phosphatase Inhibitor Cocktail Tablets (4906837001, Roche, Merck) into RIPA Lysis and Extraction buffer (89900, Thermo Scientific). Tumour cells in culture were collected into 50ml conical tubes, centrifuged at 1200rpm for 5 minutes to generate a cell pellet. The supernatant was discarded, and the pellet resuspended in 30-150µl 1X lysis buffer and incubated on ice for 15 minutes. Subsequently, the lysate was centrifuged in 4°C for 10 minutes at 13000rpm. The supernatant containing protein extracts was transferred into fresh Eppendorfs and stored on ice until required for determining protein concentration, gel electrophoresis and western blotting. For long term storage, lysates were transferred into a -80 °C freezer.

2.10.2. Extracting protein from frozen tumours

Frozen tumour fragments were removed from -80°C freezer and defrosted on ice before they were transferred into Precellys Hard Tissue tubes (CK28R, P000916-LYSK0-A) containing ceramic beads for dissociation of hard tissues. 200µl protein lysis buffer, prepared as described above, was added to samples and the tubes were transferred into a pre-cooled Precellys Evolution Homogenizer

(BertinTechnologies) for homogenisation at 4°C. Samples were processed under at 5500rpm for 3x20 second cycles with 30 second pauses. Next, samples were centrifuged in 4°C at 4000rpm for 5 minutes and supernatants were transferred into pre-cooled Eppendorf tubes. For removal of debris, samples were centrifuged again in 4°C for 15 minutes at 13000rpm and supernatants containing protein extracts were collected into pre-cooled Eppendorfs. Lysates were stored as described in the previous section.

2.10.3. Determination of protein concentration

Protein concentration was measured using the Pierce™ BCA Protein Assay Kit (23227, ThermoFisher) according to manufactors instructions. Standard protein solutions of 1000µg/ml, 400µg/ml, 200µg/ml, 100µg/ml and 80µg/ml were generated through serial dilution of a 2000µg/ml stock of BSA (Pierce Bovine Serum Albumin Standard Ampules, 23209, Thermo Scientific) in protein lysis buffer. For the blank control, protein lysis buffer was used. 10µl of each standard solution including the blank control was loaded onto a flat bottom 96 well plate (655101, Greiner Bio-One). Samples were diluted 1:2 in protein lysis buffer and loaded onto the assay plate. To each well, 190µl of developing solution was added. This comprised of a 50:1 mixture of Solution A (BCA) and Solution B (Cu (II) Sulphate Pentahydrate 4%w/v from the BCA assay kit. Assay plates were then incubated at 37°C for 45 minutes. Finally, to determine protein concentration, plates were inserted into the SpectraMax® ABS Plus (Molecular Devices) spectrophotometer and absorbance readings representing concentration of protein were recorded at 562nm using the SoftMax Pro software.

2.10.4. Gel electrophoresis

Protein samples were subjected to Polyacrylamide gel electrophoresis (PAGE) to separate proteins according to their molecular weight. 10x NuPAGE™ SDS Sample Reducing Agent (NP0004, Invitrogen™) and 4x NuPage™ LDS sample buffer (NP0007, Invitrogen™) diluted in RIPA buffer to achieve a 1x final concentration was added to 25-30µg protein to create a reaction mixture. This was boiled for 10 minutes at 95°C on a heat block and subsequently centrifuged for 5 minutes at 13000rpm. For the gel electrophoresis process, 25µl of reaction mixture was added to each well of a pre-cast NuPAGE 10% 10 well Bis-Tris Gel (Invitrogen™). 7µl of

Full Rainbow Protein Marker (Cytiva) was used as a protein reference ladder. Gels were run at 150V, 400mA for 1.5 hours in Running Buffer (1% MES SDS Running Buffer, NP0002, Invitrogen™). Finally, gels were removed and used in western blotting.

2.11. Western blotting

Each gel containing separated protein extracts was sandwiched between layers of sponges and filter papers (3030-917, GE LifeSciences) with a nitrocellulose membrane (10600002, GE Healthcare Amersham) placed over the gel. All contents, pre-soaked in transfer buffer, comprised of 5% Transfer Buffer (NuPAGE™ Transfer Buffer x20, NP0006, Invitrogen™), 20% methanol and 75% distilled water, were stacked into a XCell™ II Blot/Module (EI9051 Novex® by Life Technologies™) with transfer buffer. The transfer process was run for 1 hours at 100V. Nitrocellulose membrane containing the transferred protein extracts were submerged in blocking buffer – 5% (w/v) semi-skimmed milk powder (3025308, Marvel) in 1xTBST (20mM Tris – HCl pH 7.5, 136mM NaCl, 0.1% Tween 20 diluted 1:10 in distilled H_2O) – for 1 hour at room temperature. Membranes were then incubated overnight at 4°C in anti-Cbfβ (ab33516, Abcam) or anti-GAPDH-HRP-Conjugate (3683S, Cell Signalling Technology) primary antibodies diluted 1:500 and 1:5000 respectively in blocking buffer. Post-incubation, membranes were washed for 10 minutes thrice in 1xTBST and incubated for 1 hour at room temperature in secondary antibody (Anti rabbit IgG-HRP-linked antibody, 7074S, Cell Signalling Technology) diluted 1:7500 in blocking buffer. Subsequently, blots were washed in 1xTBST as described above and incubated in Pierce™ SuperSignal™ West Pico PLUS Chemiluminescent Substrate (34577, Thermo Scientific) for 5 minutes at room temperature in a lightproof container. Protein bands were visualised through ChemiDoc Imager (Bio-Rad). For editing and densitometry analysis of western blot images, ImageJ (Fiji) was used.

2.12. Statistics

All statistical tests except those used in bioinformatics analysis of RNAseq data was performed using GraphPad Prism (v9.2.0). For analysis of Kaplan Meier survival curves, the Log-rank (Mantel-Cox) test was employed. For statistical analysis of all data generated from *in vivo* experiments, such mouse weights,

tumour burden, clinical onset, tumour burden etc. and all those generated from *in vitro* biological assays, comparison between two groups with non-paired data was conducted using non-parametric, Mann Whitney test. For statistical analysis comparing more than two groups, ANOVA and/or Tukey's multiple comparisons was performed. Statistical tests are mentioned in each figure legend. P values are shown as *$p<0.05$, **$p<0.01$, ***$p<0.001$ and ****$p<0.0001$.

Chapter 3. Investigating the role of *Cbfβ* in breast cancer using the *MMTV-PyMT* mouse model.

3.1. Introduction

In 1936, Jackson Lab's John J. Brittner presented a ground-breaking discovery to the world of breast cancer: the "milk factor". While exploring the possibility that breast cancer could be transmitted from nursing mice to previously heathy offspring, Brittner shed light on the existence of this factor in milk, later realised to be the MMTV retrovirus (Bittner, 1936). The mammary hormonal milieu induces a corticosteroid hormone responsive element within the MMTV long terminal repeat (*MMTV-LTR*). As a result, increase in transcription from this LTR leads to the production of large numbers of infectious viral particles which can ultimately lead to transformation of mammary epithelial cells (Dudley, 2008). Additionally in certain mouse strains, endogenous MMTV proviruses, integrated into the mouse genome can also be transmitted down the germline. Insertion of the proviral sequence into the mouse genome can induce expression of neighbouring genes, some of which could be oncogenes (Hennighausen, 2000). These characteristics of MMTV, especially its natural mammary tropism has been crucially employed in the generation of transgenic breast cancer mouse models. Within the past several decades, *MMTV-LTR* driven expression of various oncogenes such as *MMTV-neu/ErBb2*, *Ras*, *Myc*, *int-1*, *Cyclin-D*, *Cyclin-E* and *C-rel* have been used to model the wide array of breast cancer subtypes and study critical oncogenic pathways involved in this disease (Taneja et al., 2009). One such oncogene, the polyoma middle T antigen (PyMT) acquired from the murine polyoma virus, specifically expressed within the mammary gland under the control of the *MMTV-LTR*, lead to the development of the widely used *MMTV-PyMT* model (Guy, Cardiff and Muller, 1992).

The oncoprotein PyMT, acts as a membrane bound scaffold protein involved in the modulation of numerous cell signalling pathways frequently altered in breast cancer patients such as the Src, PI3K/Akt and Ras-MAP kinase pathways (Rodriguez-Viciana, Collins and Fried, 2006). Expression of PyMT in mammary cells, therefore, induces transformation of the healthy mammary epithelium and

gives rise to poorly differentiated, multifocal adenocarcinomas with a high propensity for distant metastases especially to the lungs (Guy, Cardiff and Muller, 1992). Although the PyMT antigen is not found in the human disease, this oncogene mimics the aberrant signalling of receptor tyrosine kinases frequently involved in various diseases including human breast cancer (Attalla et al., 2020).

The primary advantage of the *MMTV-PyMT* model is the histopathological similarity with human breast cancer. Spontaneous development of mammary tumours and the multi-stage progression from benign hyperplasia to advanced stage ductal carcinoma resemble the stereotypical stages of human breast cancer. Hyperplastic regions of densely packed clusters of lobular structures where the mammary acini are filled with epithelial cells, mimic the TDLU hyperplasia in humans (Guy, Cardiff and Muller, 1992; Lin et al., 2003). These gradually transform into mammary adenomas or mammary intraepithelial neoplasia (MIN) characterised by an aggregation of florid epithelial cells within the mammary acini, akin to the morphology seen in human ductal hyperplasia, early, and finally late carcinoma with highly invasive tumours. The mammary gland subsequently transitions into the early-stage carcinoma, similar to human DCIS where acini adopt a distended morphology with more pleomorphic tumour cells, stromal invasion and increased infiltration of leukocytes (Lin et al., 2003). This is followed by progression into late carcinoma – resembling human invasive ductal carcinoma where the normal mammary morphology of *MMTV-PyMT* mice is completely lost as the original acinar structures become replaced with sheets of highly proliferative malignant tumour cells (Lin et al., 2003).

Early stage *MMTV-PyMT* tumours have been noted to resemble luminal breast cancer, proficient for ER, PR and HER-2 whereas progression into the later stages of disease lead to loss of hormone receptors and the adoption of a more TN breast cancer phenotype (Maglione et al., 2001; Lim et al., 2010; Pfefferle et al., 2013; Hollern and Andrechek, 2014; C. Liu et al., 2021). This allows the exploration of tumorigenesis relative to the molecular profiles of different breast cancer subtypes. Additionally, although the *MMTV-LTR* is responsive to endogenous steroid hormones, combined with high potency and penetrance of the PyMT oncogene, this model achieves induction of tumorigenesis independent of pregnancy and lactation (Fantozzi and Christofori, 2006). This combined with the short latency for tumour development (Fantozzi and Christofori, 2006), makes the

MMTV-PyMT GEMM a highly attractive, time-effective model in the study of breast cancer.

Lastly, while PyMT acts as the initial driver for mammary tumorigenesis, additional synergistic genetic events are required for the progression of disease – a valuable characteristic of this model to study the multi-hit process of human tumour development and metastasis. Indeed, expression of *MMTV-PyMT* paired with conditional deletion of tumour suppressors or transgenic expression of oncogenes, has provided an indispensable platform for investigating several genes involved in the onset and progression of mammary tumours such as *HIF1a*, *STAT3*, *SNAIL1*, *MMP8, IL15*, *PTHRP* and *RHEB1* among others (Attalla et al., 2020).

CBFβ, deemed as one of the frequently altered genes in human breast cancer, was therefore investigated for the first time *in vivo* using the *MMTV-PyMT* mouse model. Governing both translation and transcription of hundreds of genes involved in critical cell regulatory pathways such as Wnt, Notch and TGFβ (Malik et al., 2019), emerging evidence through *in silico* and *in vitro* analysis has implicated *CBFβ* in breast cancer. Several studies utilising whole genome sequencing and transcriptomic analysis of thousands of patient-derived primary tumour samples as well as metastasized lesions revealed varying degrees of copy number alterations and mutations in this gene (Banerji et al., 2012; Nik-Zainal et al., 2016; Pereira et al., 2016; Rajendran and Deng, 2017; Griffith et al., 2018; Pegg et al., 2019; Li et al., 2022).

In both METABRIC and TCGA breast cancer datasets, analysed through cbioportal (Cerami et al., 2012; Gao et al., 2013; Pereira et al., 2016), majority of breast cancer cases with alterations in *CBFβ* displayed downregulation of CBFβ in the form of low *mRNA* expression, deletion of the gene or loss-of-function mutations. Additionally, a small proportion also contained amplifications and elevated mRNA levels of *CBFβ (*Figure 3.1A). This is supported by (Banerji *et al.*, 2012) and subsequently by (Griffith *et al.*, 2018) in their whole genome and whole-exome sequencing analyses of breast cancer patient samples. These revealed recurrent mutations in CBFβ, especially loss-of-function truncating mutations and missense mutations. (Pereira *et al.*, 2016)as well as (Griffith *et al.*, 2018) highlighted that the missense mutations frequently resided within the coding regions of CBFβ and were likely to affect its protein sequence. Further investigation by Pegg and

colleagues revealed that most of these mutations were found near the RBD, especially around a specific region between amino acid residues 100 and 120 (Pegg et al., 2019). Proteins encoded from the mutant CBFβ constructs could often still bind to their RUNX counterparts, however the assembly of the RUNX-CBFβ complex with DNA was hampered, suggesting loss of CBFβ function (Pegg et al., 2019).

Interestingly, deletion, reduced expression, and such loss of function mutations of CBFβ are particularly observed in luminal, ER positive disease (Figure 3.1B-C). Indeed, among the 14% of breast tumour samples in the METABRIC dataset with alterations in CBFβ, approximately 70% fell under the luminal category (49.5% luminal A and 20.8% luminal B) with loss of CBFβ recorded in most of these cases (Pereira et al., 2016) (Figure 3.1C). This suggests CBFβ may potentially play the role of a tumour suppressor in this disease setting and deletion of this gene or abrogation of its function may be advantageous to growth and progression of tumours. On the contrary, amplifications and elevated mRNA expression of this gene, indicative of its oncogenic potential, seems to be more common in the ER negative subtypes of breast cancer (Pereira et al., 2016). In fact, amplified levels of *CBFβ* was noted only in ER negative patient samples in the METABRIC dataset. Elevated *CBFβ* mRNA levels were noted in both ER positive and ER negative patients, but a higher frequency was noted in the latter subgroup (Figure 3.1B).

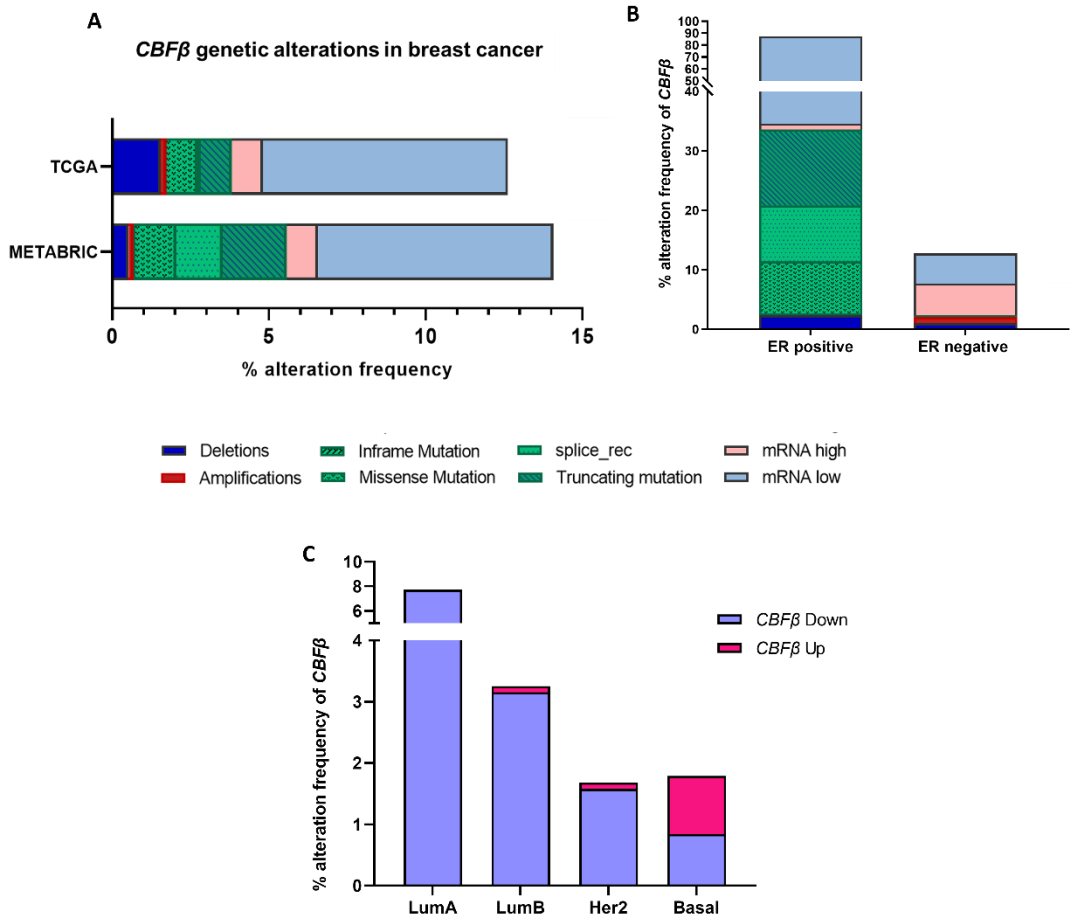

Figure 3.1: Loss of *CBFβ* associated with ER positive breast cancer in patient datasets.
(A) Stacked bar chart showing CBFβ alteration frequencies in primary tumour samples from the METABRIC and TCGA datasets (Cerami et al., 2012; Gao et al., 2013; Pereira et al., 2016). (B) *CBFβ* alteration frequencies in ER positive and ER negative breast cancer patients in the METABRIC (Pereira et al., 2016) dataset. (C) Stacked bar chart showing alterations of *CBFβ* across different subtypes of breast cancer in the METABRIC (Pereira et al., 2016) dataset. All data acquired from cbioportal (Cerami et al., 2012; Gao et al., 2013) and graphs prepared using GraphPad Prism. Alteration frequency for each type of alteration determined by calculating the number of *CBFβ* altered samples as a percentage of the total number of samples with copy number alteration and mRNA level information in each of the datasets explored. For alterations leading to downregulation in *CBFβ* (*CBFβ* down), samples with deletions, loss-of-function mutations and low *CBFβ* mRNA levels were collated. For alterations leading to upregulation in *CBFβ* (*CBFβ* up), samples with amplified copy number alterations and high *CBFβ* mRNA levels were collated.

So far, studies involving *CBFβ* expression and its role in breast cancer (discussed in Chapter 1) have mostly used *in vitro* and *ex vivo* techniques. *In vivo* investigations using biologically relevant models are crucial in determining whether CBFβ acts as a tumour suppressor, an oncogene or has a dualistic context dependent effect – similar to the RUNX proteins (Chimge and Frenkel, 2013; Riggio and Blyth, 2017) – within the natural mammary microenvironment. For this

purpose, a conditional knockout mouse model was used to assess the effect of both homozygous and heterozygous *Cbfβ* loss in mammary tumorigenesis.

3.1.1. Hypothesis and Aims

So far, studies involving CBFβ expression and its role in breast cancer have mostly used *in vitro* and *ex vivo* techniques. *In vivo* investigations using the appropriate models are crucial in determining whether CBFβ exerts growth promoting or growth suppressing effects in mammary tumour cells. Based on patient data as well as experimental results from the available literature, it was hypothesised that CBFβ plays a tumour suppressive role in breast cancer. In order to investigate this notion, the aim was to use a conditional knockout mouse model was to assess the effect of both homozygous and heterozygous Cbfβ loss in mammary tumorigenesis.

3.2. Results

3.2.1. Generation of the *Cbfβ* knockout MMTV-PyMT breast cancer mouse model.

Whole body homozygous loss of *Cbfβ* is known to cause embryonic lethality due to disrupted foetal haematopoiesis, neuronal and skeletal development (Okuda et al., 1996; Qing Wang et al., 1996; Q Wang et al., 1996). Therefore, in order to achieve loss of *Cbfβ* in the mouse mammary glands for the purpose of assessing its role in mammary tumorigenesis, the Cre/lox system was employed (Farley et al., 2000; Nagy, 2000; Jo et al., 2001). The $Cbf\beta^{fl/fl}$ construct used to generate $Cbf\beta^{fl/fl}$ mice was achieved by (Naoe et al., 2007) through insertion of *loxP* sites across exon 5 of the *Cbfβ* gene. Mating of mice possessing either heterozygous or homozygous $Cbf\beta^{fl/fl}$ with mice expressing Cre-recombinase under tissue specific promoters such as *MMTV* allows targeted heterozygous or homozygous loss of *Cbfβ* in mammary cells. Thus, breeding of *MMTV-PyMT* mice, with mice possessing the *MMTV-Cre* and $Cbf\beta^{fl/fl}$ allele was used to achieve a *Cbfβ* conditional knockout breast cancer model. This model was established on a pure C57BL/6 background, backcrossed for more than 10 generations to avoid any inter-strain variability. The selection of C57BL/6J, over other strains such as FVB was made with the strain associated rate of tumorigenesis in mind. The relatively longer tumour latency

attributed to the C57BL/6J strain compared to FVB for instance, has been shown to allow a more comprehensive analysis of tumour incidence and progression, an important characteristic when looking at potential tumour suppressors, the loss of which could dramatically accelerate tumorigenesis (Davie et al., 2007).

3.2.2. Genetic deletion of *Cbfβ* does not have an overt effect on the *MMTV-PyMT* breast cancer model

To assess the effect of *Cbfβ* loss on mammary tumorigenesis, three cohorts of *MMTV-PyMT;MMTV-Cre* mice consisting of wildtype *Cbfβ* ($Cbf\beta^{wt/wt}$); one floxed copy of the gene ($Cbf\beta^{fl/wt}$) for heterozygous expression or two homozygous floxed alleles of $Cbf\beta^{fl/fl}$ were generated (Figure 3.2).

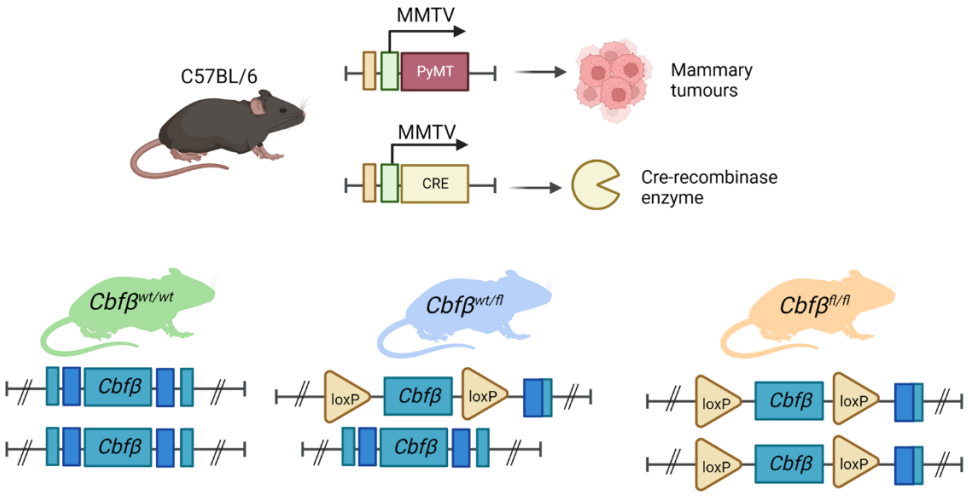

Figure 3.2: Schematic representation of the *MMTV-PyMT;MMTV-Cre* mouse model with three different allelic combinations of *Cbfβ*.

The mouse model was established in a C57BL/6J (>N10) strain with mammary specific oncogenesis accelerated by *MMTV-PyMT*. Mammary specific MMTV-Cre is used for targeted gene deletion. Three cohorts of mice are generated. Control *MMTV-PyMT;MMTV-Cre;*$Cbf\beta^{wt/wt}$ and two test cohorts *MMTV-PyMT;MMTV-Cre;*$Cbf\beta^{wt/fl}$ and *MMTV-PyMT;MMTV-Cre;*$Cbf\beta^{fl/fl}$. Figure created using Biorender.com

All three cohorts were monitored for palpable tumours post weaning with regular tumour measurements used to track disease progression. A pre-determined limit on tumour size where either tumour height or width reached 15mm by calliper measurements, was used to mark clinical endpoint. Alternatively, ulceration of the skin around the tumour or deterioration of the animal's general health was also considered as clinical endpoint. At this stage the mice were euthanised and sampled for tissues. Gross analysis of the disease phenotype was comparable

across all three cohorts with multifocal tumours observed in multiple glands per mouse. As depicted in Figure 3.3, compared to healthy mammary glands in wildtype controls (Figure 3.3A), *MMTV-PyMT;MMTV-Cre* mice across the three experimental cohorts (Figure 3.3B) displayed gross pathological transformations with majority of the mammary glands affected.

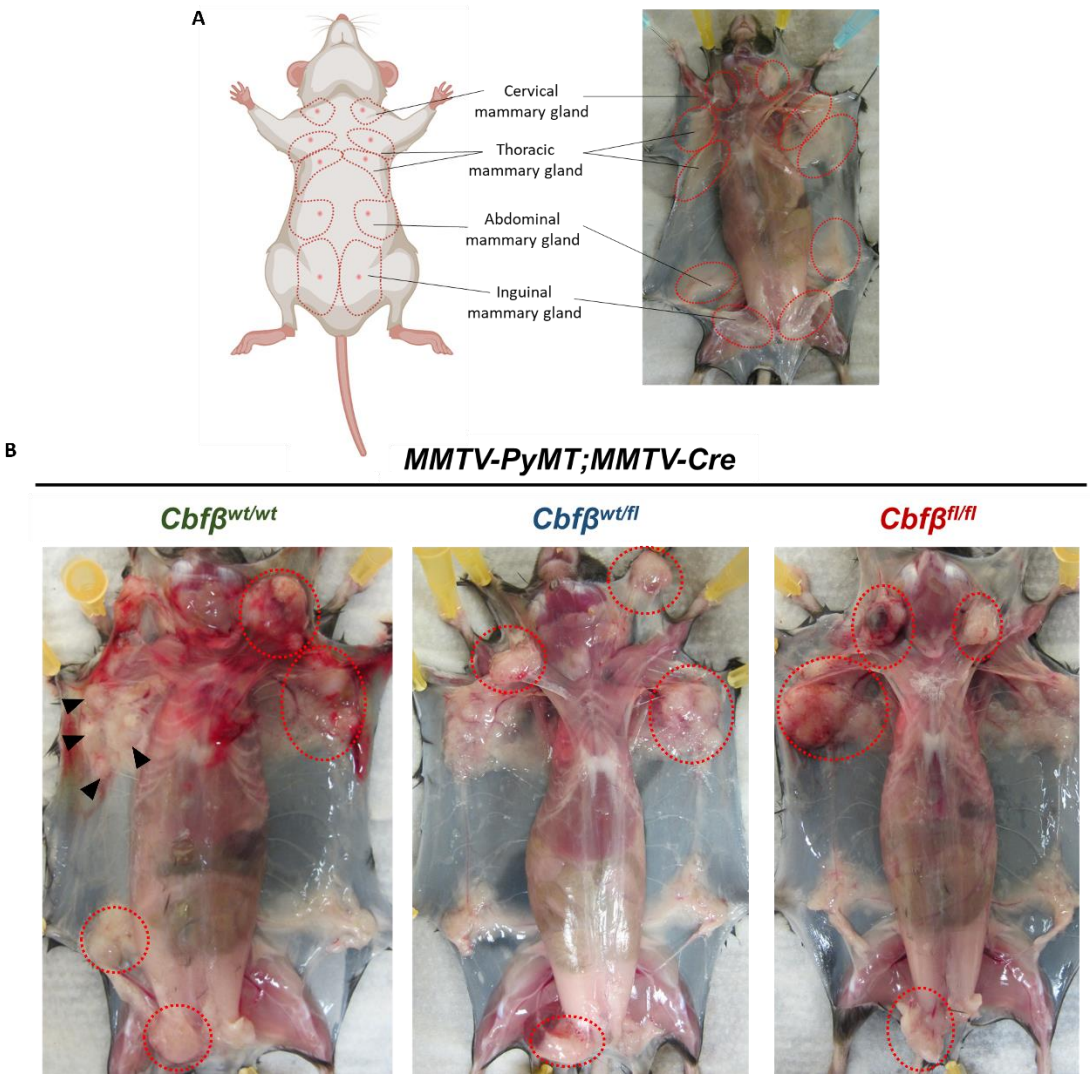

Figure 3.3: Mammary tumour induction under *MMTV-PyMT;MMTV-Cre*.

(A) The 5 pairs of murine mammary glands and their anatomical locations are schematically represented (left) and image of a dissected one year old, wildtype, C57BL/6J mouse is shown to demonstrate the gross morphology of normal mammary glands (right). All glands are highlighted in red dotted circles. Figure created using Biorender.com (B) Representative gross pathology images of mammary glands from the two experimental cohorts: *MMTV-PyMT;MMTV-Cre;Cbfβ*$^{wt/fl}$ and *MMTV-PyMT;MMTV-Cre;Cbfβ*$^{fl/fl}$ and one control cohort: *MMTV-PyMT;MMTV-Cre;Cbfβ*$^{wt/w}$. Glands affected with palpable tumours are highlighted in red dotted circles. Multifocal phenotype of lesions in a gland are indicated in black arrow heads. Note the morphological change between the normal mammary glands in A compared to tumour affected glands in the *MMTV-PyMT;MMTV-Cre* mice in B.

Once mice reached clinical endpoint, total body weight was recorded along with number of palpable tumours and total mammary gland weight to determine whether loss of *Cbfβ* impacted tumour burden. To this end, no significant differences were observed in body weight across the three cohorts of mice (Figure 3.4A). The number of palpable tumours at clinical endpoint was determined with fusion of multifocal tumours within an individual gland recorded as one palpable

mass. No obvious differences were noted between the cohorts, with all specimens averaging at approximately 3 tumours per mouse at endpoint (Figure 3.4B). Finally, mammary burden, calculated by taking the cumulative weight of all 10 mammary glands (with and without lesions) as a percentage of the total body weight, was also comparable between *Cbfβ*$^{wt/wt}$, *Cbfβ*$^{wt/fl}$ and *Cbfβ*$^{fl/fl}$ mice (Figure 3.4C).

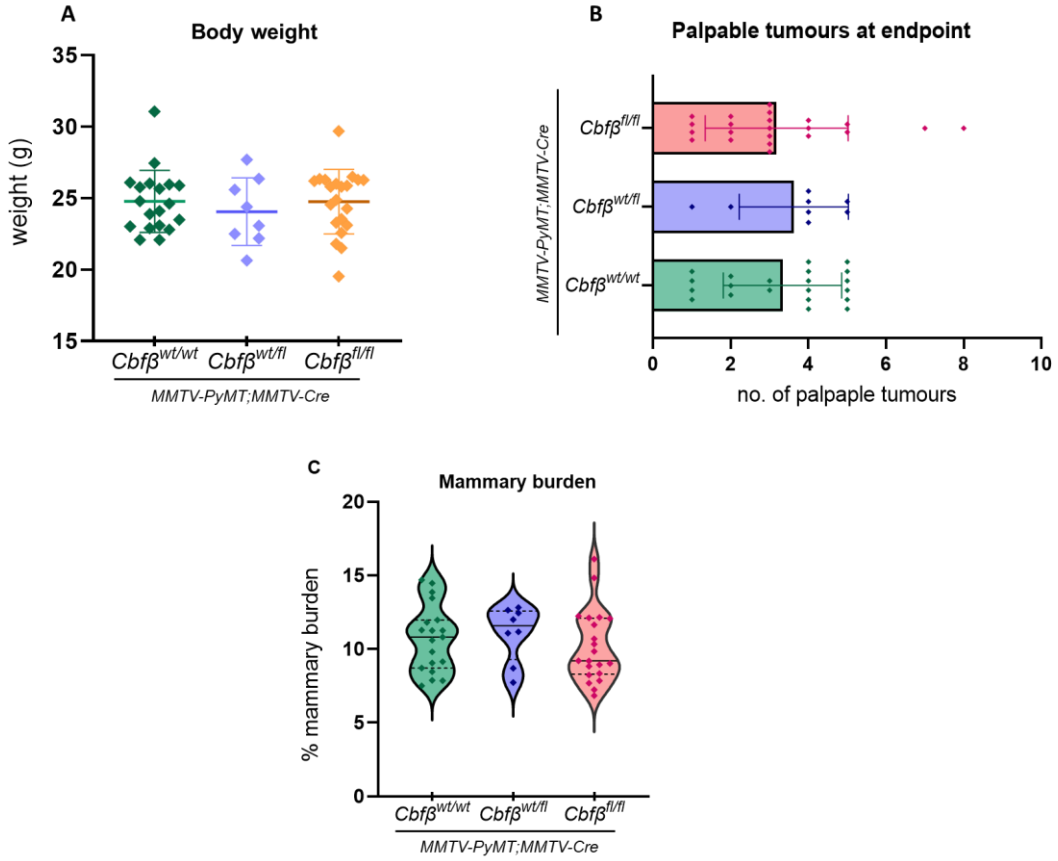

Figure 3.4: Mammary tumour burden is not altered by loss of *Cbfβ* in an *MMTV-PyMT* model. Dot plot of total body weight (A), bar graph depicting number of palpable tumours (B) and violin plots for mammary burden (C) are presented. Each data point represents individual mice from *MMTV-PyMT;MMTV-Cre;Cbfβ*$^{wt/wt}$ (n=19), *MMTV-PyMT;MMTV-Cre;Cbfβ*$^{wt/fl}$ *(n=8)* and *MMTV-PyMT;MMTV-Cre;Cbfβ*$^{fl/fl}$ (n=21) cohorts. Error bars in (A) and (B) are generated from mean ±SD. Median in (C) is represented by the solid line and quartiles are denoted by the dotted lines. Statistical analysis using ordinary one-way ANOVA in GraphPad Prism indicated non-significant difference in the results across the three cohorts for each of the graphs presented.

Compared to *MMTV-PyMT;MMTV-Cre;Cbfβ*$^{wt/wt}$ mice with an median overall survival of 166 days, no significant difference was noted in the overall disease free survival of mice in the *MMTV-PyMT;MMTV-Cre;Cbfβ*$^{wt/fl}$ (156 days) *or MMTV-PyMT;MMTV-Cre;Cbfβ*$^{fl/fl}$ (160 days) cohorts (Figure 3.5A). Through regular tumour measurements, clinical onset and tumour progression was tracked to determine

the effect of losing *Cbfβ* at different stages of mammary tumorigenesis. As depicted in the schematic in Figure 3.5B, clinical onset was measured as the time between birth of animals to detection of physically palpable tumours while tumour progression was calculated as the time taken for the palpated masses to reach the pre-determined endpoint tumour size. Mean time to clinical onset was 135 days for $Cbf\beta^{wt/wt}$, 134 days for $Cbf\beta^{wt/fl}$ and 133 days for $Cbf\beta^{fl/fl}$ mice, showing no difference between the cohorts. Time for tumour progression was 32, 23 and 27 days for $Cbf\beta^{wt/wt}$, $Cbf\beta^{wt/fl}$ and $Cbf\beta^{fl/fl}$ mice respectively (Figure 3.5C and D). These results indicated, MMTV-Cre targeted deletion of *Cbfβ* did not seem to have an overt effect on primary tumour development or progression in this model.

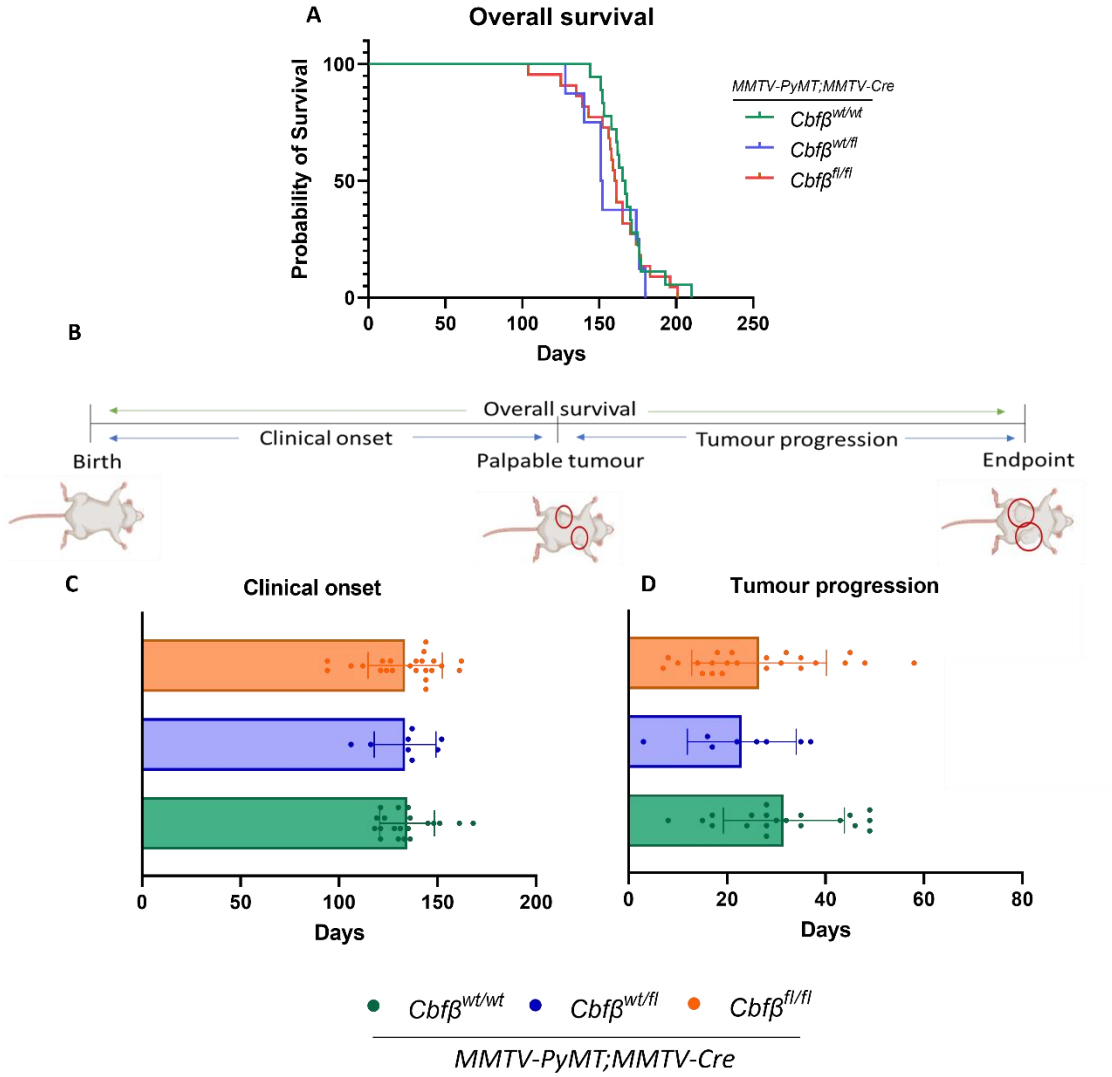

Figure 3.5: Loss of *Cbfβ* does not have an overt effect on mammary tumorigenesis in *MMTV-PyMT* model.

(A) Kaplan Meier curves comparing overall disease-free survival between *MMTV-PyMT;MMTV-Cre;Cbfβ*$^{wt/wt}$ (n=18), *MMTV-PyMT;MMTV-Cre;Cbfβ*$^{wt/fl}$ *(n=8)* and *MMTV-PyMT;MMTV-Cre;Cbfβ*$^{fl/fl}$ (n=22) cohorts. (B) Schematic representation of model showing overall survival (time between birth and clinical endpoint), clinical onset (time between birth and the detection of palpable tumours) and tumour progression (time between detection of the first palpable tumour to clinical endpoint). Bar graphs with dot plots comparing clinical onset (C) and (D) tumour progression across *MMTV-PyMT;MMTV-Cre;Cbfβ*$^{wt/wt}$ (N=20), *MMTV-PyMT;MMTV-Cre;Cbfβ*$^{wt/fl}$ *(N=8)* and *MMTV-PyMT;MMTV-Cre;Cbfβ*$^{fl/fl}$ (N=22) cohorts. Statistical analysis using Log-rank (Mantel-Cox) for the Kaplan Meier curves and Tukey's multiple comparison test performed for the bar graphs in GraphPad Prism indicated non-significant difference in the results across the three cohorts.

3.2.3. MMTV-Cre targeted deletion of *Cbfβ* does not affect mammary tumour cell metastasis to lungs

CBFβ has been implicated in facilitating metastatic dissemination and growth of secondary tumours (Ran et al., 2020) and as *MMTV-PyMT* mice are known to form metastatic lesions in the lung (Fantozzi and Christofori, 2006), tissue samples were acquired from cohort mice to explore the relationship between loss of *Cbfβ* and metastatic spread. Whole-lung samples from cohort mice, once examined for macro-metastatic lesions (macromets) by eye, were formalin fixed, paraffin embedded, and tissue sections stained with H&E. Macromets were not evident in any of the cohort mice. Figure 3.6A shows the comparison between a normal lung section and micro-metastatic lesions noted in samples from cohort mice. Microscopic analysis of lung H&E samples failed to show any significant difference in the number of lung metastases in the three different cohorts of mice (Figure 3.6B). However, a greater percentage of $Cbf\beta^{fl/fl}$ mice developed lung metastases when compared to $Cbf\beta^{wt/fl}$ and $Cbf\beta^{wt/wt}$ mice. 66% (8/12) of the $Cbf\beta^{fl/fl}$ mice developed lung metastases whereas lung metastases were observable in 50% (4/8) of $Cbf\beta^{wt/wt}$ and only around 16% (1/6) of $Cbf\beta^{wt/fl}$ mice (Figure 3.6C). While it might be tempting to speculate that loss of *Cbfβ* may facilitate an increased propensity for metastatic spread, these numbers did not reach significance. .

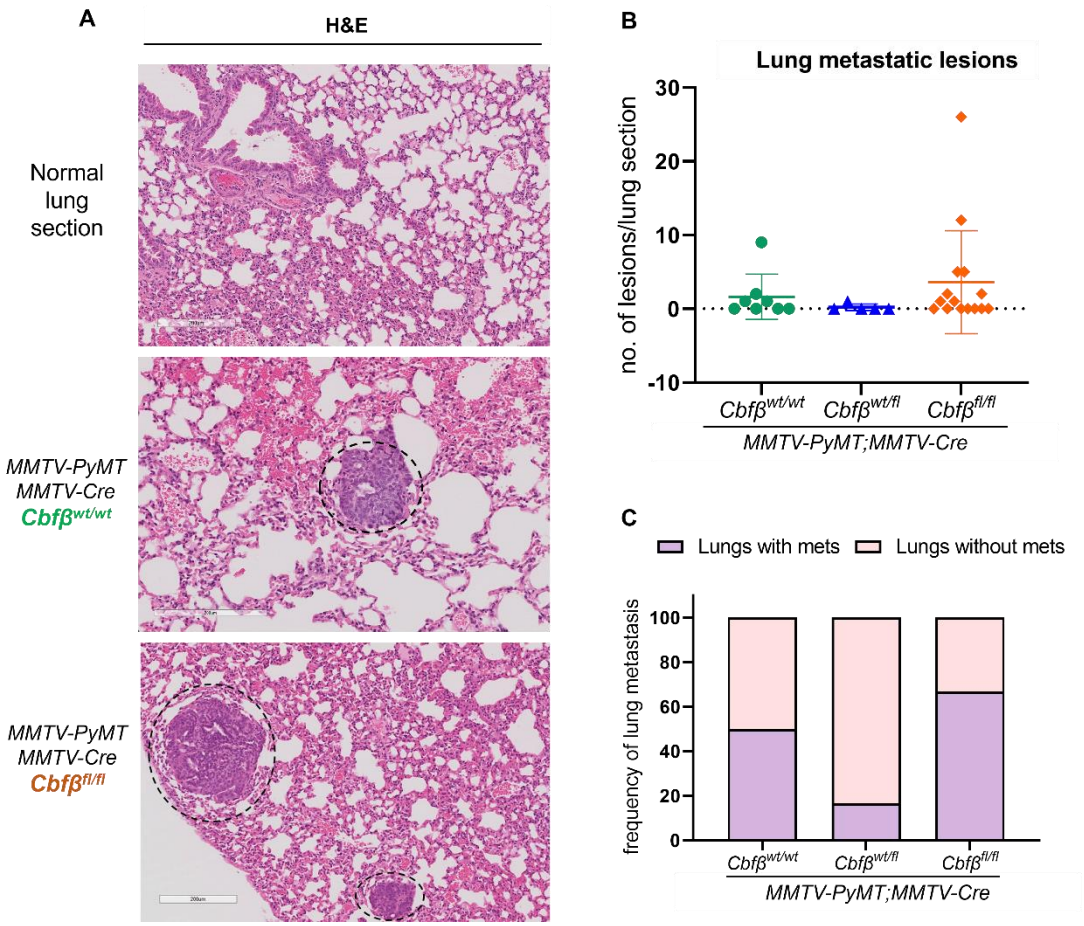

Figure 3.6: Genetic deletion of *Cbfβ* in mammary tumours does not significantly alter lung metastasis.

(A) Representative H&E sections showing histopathology of normal lung from a C57BL/6J mouse (top), metastatic lesion in lung tissue of a *MMTV-PyMT;MMTV-Cre;Cbfβ*$^{wt/wt}$ mouse (middle) and *MMTV-PyMT;MMTV-Cre;Cbfβ*$^{fl/fl}$ mouse (bottom). Tumour lesions are highlighted by dotted circles. Scale bar, 200µm. (B) Dot plot showing quantification of number of metastatic lesions counted per lung sample from *MMTV-PyMT;MMTV-Cre;Cbfβ*$^{wt/wt}$ (n=8), *MMTV-PyMT;MMTV-Cre;Cbfβ*$^{wt/fl}$ (n=6) and *MMTV-PyMT;MMTV-Cre;Cbfβ*$^{fl/fl}$ (n= 12) mice. Each dot represents whole lung sample from one mouse. Error bars represent mean ± SD. Statistical analysis using ordinary one-way ANOVA in GraphPad Prism indicated non-significant difference between the three cohorts. (C) Stacked bar graph representing the frequency of lung metastasis observed in primary tumour bearing *MMTV-PyMT;MMTV-Cre;Cbfβ*$^{wt/wt}$ (n=8), *MMTV-PyMT;MMTV-Cre;Cbfβ*$^{wt/fl}$ (n=6) and *MMTV-PyMT;MMTV-Cre;Cbfβ*$^{fl/fl}$ (n= 12) mice. Mets = metastatic lesions.

3.2.4. Cbfβ is inefficiently deleted in *MMTV-PyMT; MMTV-Cre* tumours

Considering the available *in vivo* and *ex vivo* evidence, addressed in Chapter 1, associating deletion of *Cbfβ* with significant changes in mammary cell tumorigenicity, it was surprising to see a lack of overt effects upon deletion of this gene in the *MMTV-PyMT* model. To this end it was important to confirm

efficient deletion of *Cbfβ* in this model. Lysates from end-stage tumours were used compare CBFβ protein levels in *MMTV-PyMT;MMTV-Cre;Cbfβ*$^{fl/fl}$ mice and control *MMTV-PyMT;MMTV-Cre;Cbfβ*$^{wt/wt}$ mice. Results from western blots presented in (Figure 3.7A) and the corresponding densitometry analysis (Figure 3.7B), indicated a presence of CBFβ protein in tumour samples from *Cbfβ*$^{fl/fl}$ mice. Albeit reduced compared to CBFβ protein expression in tumours from *Cbfβ* wildtype mice, these results indicated incomplete deletion of *Cbfβ* in *Cbfβ*$^{fl/fl}$ mice. This suggested that mammary cells in the *MMTV-PyMT;MMTV-Cre;Cbfβ*$^{fl/fl}$ mice retain some expression of the gene, which may explain the lack of difference noted in tumorigenesis across the cohorts.

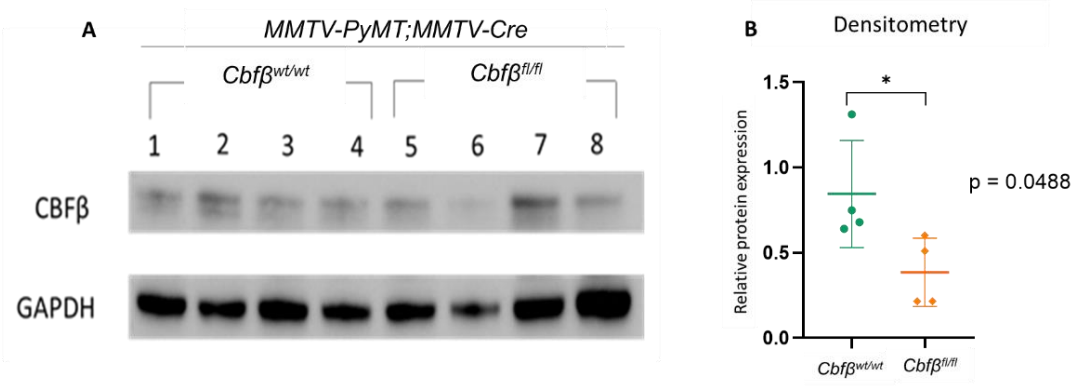

Figure 3.7: Incomplete deletion of *Cbfβ* in the *MMTV-PyMT;MMTV-Cre model*.
(A) Western blot comparing CBFβ protein expression in tumour lysates from *MMTV-PyMT;MMTV-Cre;Cbfβ*$^{wt/wt}$ (n=4) and *MMTV-PyMT;MMTV-Cre;Cbfβ*$^{fl/fl}$ (n=4) cohorts. GAPDH expression was used as a loading control. (B) Dot plot represents densitometry analysis conducted through ImageJ Fiji, quantifying CBFβ protein expression from western blot analysis in A. Error bars represent mean ± SD. Unpaired two-tailed t-test performed in GraphPad Prism was used to determine a statistically significant difference (p=0.0488) between the two groups.

Essentially, these results revealed a caveat in the mouse model whereby consistent loss of *Cbfβ* was not achieved through the Cre/lox system as expected. One possible reason for this could be that in *MMTV-PyMT;MMTV-Cre* mice, expression of the PyMT transgene, driving oncogenesis, is uncoupled from expression of the MMTV-Cre recombinase which exists as a separate transgene. As a result, it is possible that cells in which MMTV-PyMT is expressed, may not also co-express the MMTV-Cre transgene and hence have Cre mediated deletion of *Cbfβ*. Consequently, mammary cells that undergo transformation through PyMT, may still be proficient for *Cbfβ* despite possessing *Cbfβ*$^{fl/fl}$ alleles due to the absence of Cre recombinase.

3.2.5. Introduction of a fluorescent reporter to track MMTV-Cre efficiency and *Cbfβ* deletion.

Genes encoding fluorescent proteins such as green fluorescent protein (GFP) and red fluorescent protein (RFP) have been used as an invaluable tool in the imaging of biological systems including in the reporting of Cre recombinase activity (Luche et al., 2007; Li et al., 2018). Expression of a transgenic knock-in "reporter" gene can be placed under the control of a Cre recombinase so that any resulting fluorescence can be attributed to the activation of and successful recombination by the enzyme. In view of this, an exceptionally bright version of genetically modified RFP called tandem-dimer2 (12) or tdRFP, was used in the tracking to Cre induction (Luche et al., 2007; Li et al., 2018).

To detect Cre-mediated recombination (and hence *Cbfβ* deletion) in the mammary tumours in the *MMTV-PyMT* model, *MMTV-PyMT;MMTV-Cre;Cbfβ*$^{fl/fl}$ and *MMTV-PyMT;MMTV-Cre;Cbfβ*$^{wt/wt}$ mice were crossed with mice possessing a *tdRFP* reporter construct expressed under a ubiquitous promoter of the *ROSA26* locus (Zambrowicz et al., 1997) (Figure 3.8*A*). The reporter construct is positioned downstream of a transcriptional stopper that is flanked by two *loxP* sites (*loxP-STOP-loxP* or LSL). Presence of Cre recombinase results in excision of the stopper guided by the *loxP* sites and hence expression of the tdRFP reporter (Luche et al., 2007). Cohort mice were aged as above. From each cohort mouse taken at end point, all 10 mammary glands were placed on a petri dish with lungs marking the centre of the dish (Figure 3.8B). tdRFP expression to track Cre-activation and therefore *Cbfβ* deletion *in vivo* was detected by using the In Vivo Imaging System (IVIS) (Figure 3.8C). Within a single mouse, varying levels of red fluorescence irrespective of the stage of tumorigenesis were noted across all 10 mammary glands. In some mice, the biggest tumour (endpoint tumour) was positive for RFP while in others, RFP expression was observed in one or more of the smaller tumours. These results were supported by IHC staining of tumours to evaluate RFP expression. As depicted in Figure 3.9, small regions of positivity exist in otherwise RFP negative tumour samples. Altogether these data confirm a mosaic pattern of MMTV driven Cre expression and thus *Cbfβ* recombination in murine mammary glands.

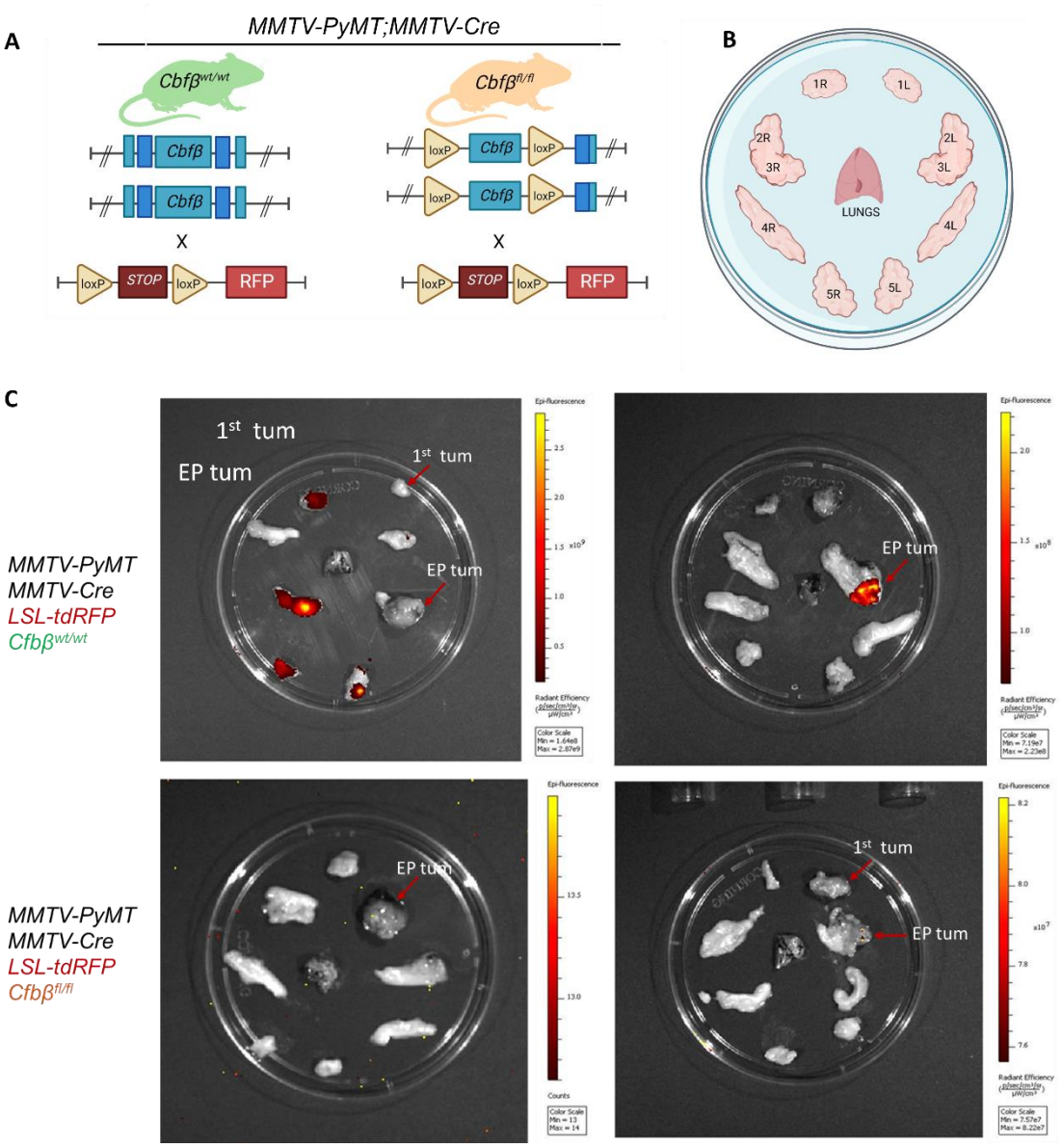

Figure 3.8: Detecting Cre-recombinase activation via RFP expression.

(A) Schematic representation of the *MMTV-PyMT;MMTV-Cre,tdRFP* mouse model. Crossing *MMTV-PyMT;MMTV-Cre;Cbfβ*$^{wt/wt}$ and *MMTV-PyMT;MMTV-Cre;Cbfβ*$^{fl/fl}$; cohort mice onto an *LSL-tdRFP* reporter allele allowed tracking of Cre-activation. (B) Arrangement of mouse mammary gland and lung samples from cohort mice. Glands marked 1 are the cervical mammary glands, 2 and 3 are the thoracic glands, 4 denotes the abdominal mammary glands and 5 represents inguinal mammary glands. R denotes right side of the mouse; L indicates left side. (C) IVIS imaging used to detect red fluorescence in mammary glands of tumour-bearing mice. Red fluorescence of tumours in *MMTV-PyMT;MMTV-Cre;Cbfβ*$^{wt/wt}$*;tdRFP* mice (upper panel) compared to *MMTV-PyMT;MMTV-Cre;Cbfβ*$^{fl/fl}$*;tdRFP* mice (bottom panel). Endpoint tumours marked (EP tum) and first tumours palpated are indicated (1st tum).

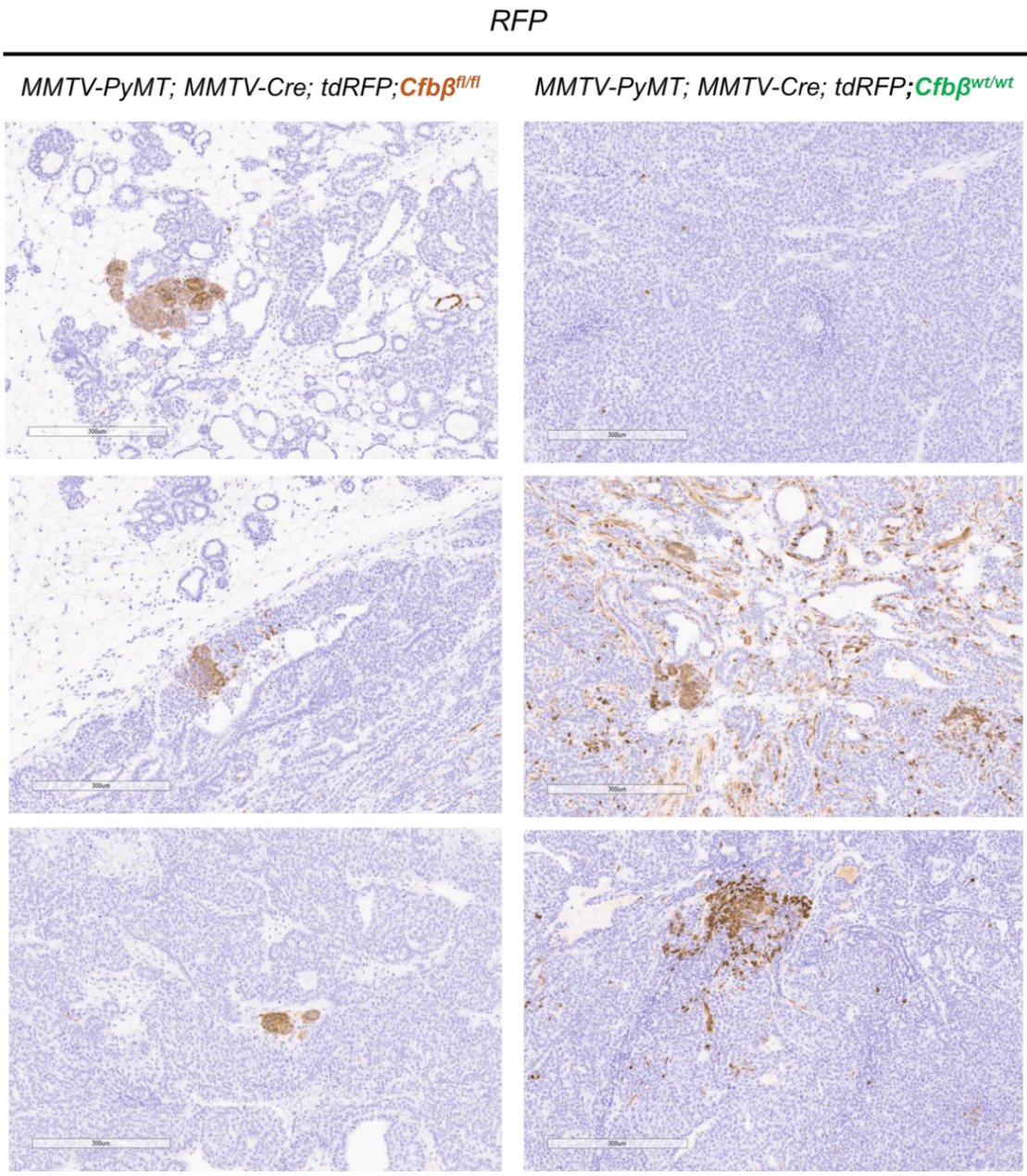

Figure 3.9: Immunohistochemistry for RFP in *MMTV-PyMT* tumours demonstrates mosaic expression of *MMTV-Cre*.

Representative images of tumours from n=3 mice per cohort shows patches of RFP positive cells in an otherwise negatively stained tumour. Scale bar, 300μm.

3.2.6. Generating models from efficient deletion of *Cbfβ* using a ubiquitous ROSA-CreER^{T2} driver

To overcome caveats of the *MMTV-Cre* model where it is difficult to control Cre-activation or achieve uniform gene deletion, an alternative mouse model employing the ubiquitous ROSA26-CreER^{T2} recombinase was used. Here, Cre recombinase is fused to a mutated version of the ligand binding domain (LBD) of ER which can only be induced for translocation into the nucleus by tamoxifen or

its active metabolite 4-hydroxytamoxifen (4OHT) (Jordan, 1993) and not endogenous estrogen (Indra et al., 1999). Being a second generation inducible Cre, CreER^{T2} consists of three mutations in its ER LBD making it highly sensitive to induction by 4-OHT (Indra et al., 1999). In this manner, efficient activation of Cre and therefore deletion of any floxed alleles present *(*in this case *Cbfβ*) can be controlled both spatially and temporally. Additionally, since the CreER^{T2} construct is inserted into the *ROSA26* locus, ubiquitous expression of the enzyme is ensured, thereby circumventing the mosaicism and unpredictable expression pattern experienced with MMTV-Cre. As previously, oncogenesis was induced by *MMTV-PyMT* with resulting cohorts of mice having wildtype *Cbfβ (MMTV-PyMT; Rosa-CreER^{T2}; Cbfβ$^{wt/wt}$*) *or* homozygous floxed alleles of *Cbfβ (MMTV-PyMT; Rosa-CreER^{T2}; Cbfβ$^{fl/fl}$*) (Figure 3.10).

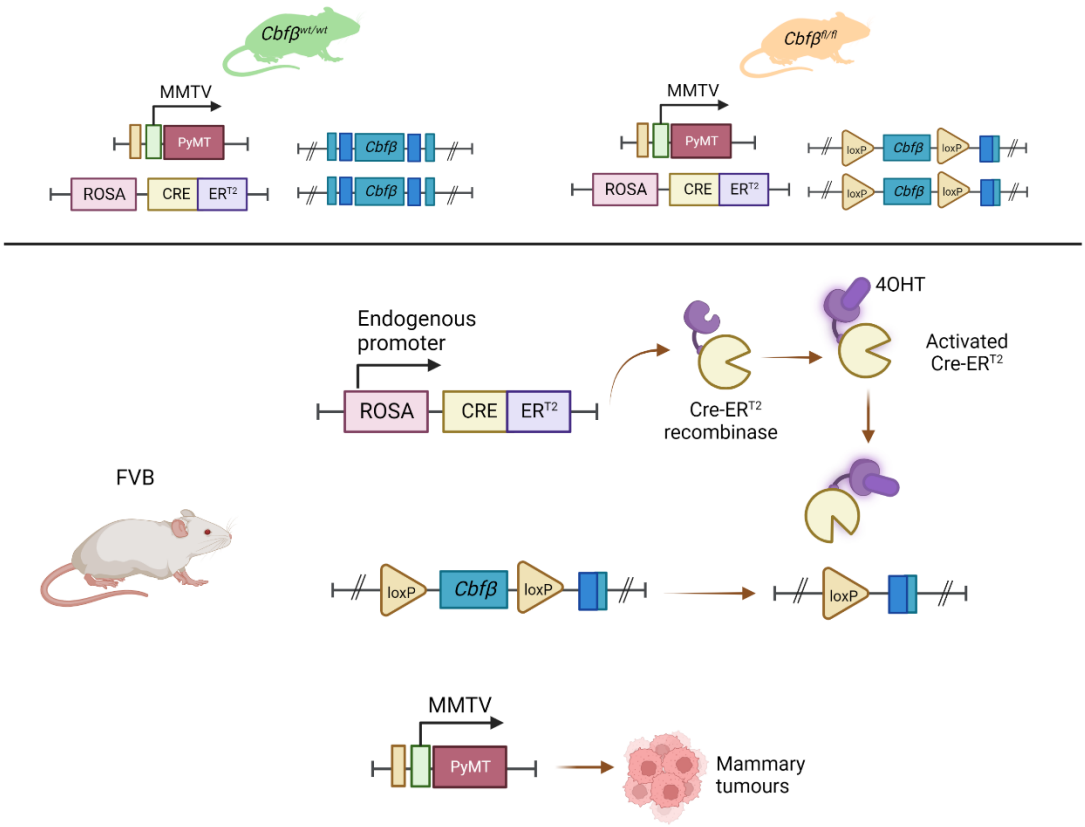

Figure 3.10: Generation of the *MMTV-PyMT;ROSA-CreER^{T2};Cbfβ$^{fl/fl}$* model.
Two cohorts of mice with the genotypes *MMTV-PyMT;ROSA-CreER^{T2};Cbfβ$^{wt/wt}$* and *MMTV-PyMT;ROSA-CreER^{T2};Cbfβ$^{fl/fl}$* were generated (top) on an FVB (N10) background. Schematic shows mechanism of 4OHT mediated activation of CreER^{T2} and the subsequent deletion of floxed *Cbfβ* alleles. The genetic construct encoding CreER^{T2} expression is inserted into the ROSA26 locus which drives ubiquitous expression of the enzyme. Mammary tumorigenesis is driven by *MMTV-PyMT*. Figure created through BioRender.com.

This model was used to determine the impact of deleting *Cbfβ* in the context of *MMTV-PyMT* breast cancer. A schematic of the experimental plan is presented in Figure 3.11A. Since CreER^{T2} allows temporal control over genetic manipulation, acute deletion of *Cbfβ* in *ex vivo* tumours was explored to determine whether *Cbfβ* loss in late-stage carcinoma provides a growth advantage (or otherwise). Accordingly, treatment naïve female mice, proficient for CBFβ, were monitored until the development of end-stage mammary tumours. Upon reaching clinical endpoint, as determined by tumour size, tumour derived cell lines were generated. Established tumour cell lines – considered once cells survived past a minimum of 5 passages in monolayer culture – from two different *Cbfβ$^{fl/fl}$* mice and one *Cbfβ$^{wt/wt}$* mouse were used. These were treated with 4OHT at varying time points to determine the minimum duration of 4OHT exposure required to induce sufficient CreER^{T2} activation and achieve loss of CBFβ. Prior to this, the optimal

dose of 4OHT was also determined to avoid any cytotoxicity induced by the drug itself. The purpose of the *Cbfβ*$^{wt/wt}$ cell line was to account for the existence of any treatment related side effects as well as to validate that induction of CreER^{T2} in non floxed cells had no impact on the protein levels of CBFβ. A concentration of 100nM 4OHT was found to be enough to activate Cre-recombinase without considerably affecting cell viability.

Treatment with vehicle or 4OHT, as expected, had no effect on CBFβ protein expression in *Cbfβ*$^{wt/wt}$ cells (Figure 3.11B). In *Cbfβ*$^{fl/fl}$ cells, a single dose with 100nM 4OHT was not enough to induce complete loss of CBFβ within 24h as shown by the highlighted band in Figure 3.11B. However, two consecutive doses of 100nM 4OHT every 24h was enough to significantly reduce CBFβ protein expression in the *Cbfβ*$^{fl/fl}$ cell line. By the 72h timepoint, the lack of a band for CBFβ indicated successful and sustained deletion of *Cbfβ* which was confirmed again at the 96h timepoint (Figure 3.11B). These results confirmed successful loss of CBFβ via deletion of *Cbfβ* $^{fl/fl}$ using 4OHT inducible CreER^{T2} *in vitro*.

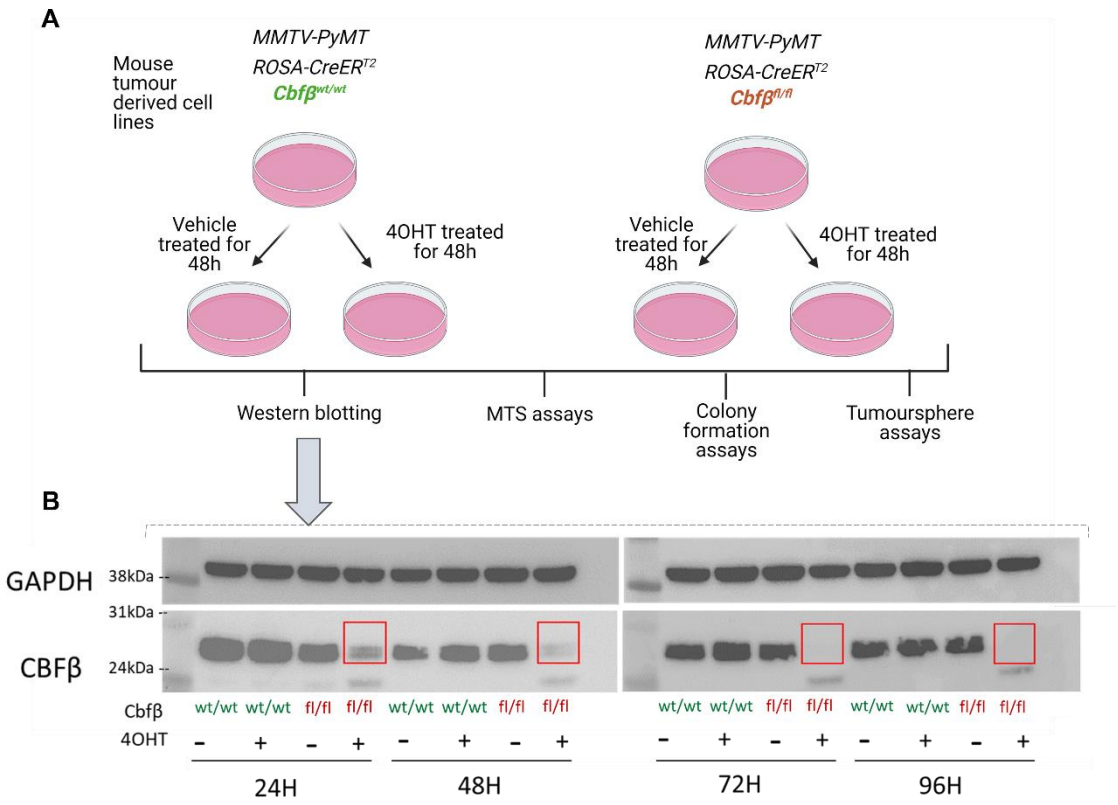

Figure 3.11: *Ex vivo* deletion of *Cbfβ* in tumour derived *MMTV-PyMT;ROSA-CreER^{T2};Cbfβ$^{fl/fl}$* cells.

(A) Schematic representation of the experimental plan designed to determine the impact *Cbfβ* deletion on isogenic MMTV-PyMT driven mammary tumour cells. Tumour cell lines derived from end-stage tumours of *MMTV-PyMT;ROSA-CreER^{T2};Cbfβ$^{fl/fl}$* and *MMTV-PyMT;ROSA-CreER^{T2};Cbfβ$^{wt/wt}$*, were treated with either 4OHT to delete *Cbfβ* or vehicle. (B) Immunoblot of CBFβ showing gradual loss of the protein in *MMTV-PyMT;ROSA-CreER^{T2};Cbfβ$^{fl/fl}$* cells. *MMTV-PyMT;ROSA-CreER^{T2};Cbfβ$^{fl/fl}$* tumour cells (fl/fl) and *MMTV-PyMT;ROSA-CreER^{T2};Cbfβ$^{wt/wt}$* cells (wt/wt) treated with 100nM of 4OHT (+) for two consecutive days every 24h. After the second dose, 4OHT or vehicle treatment was stopped, and the cells were subsequently cultured in fresh media. Protein lysates were taken every 24h for 4 days. 24h treatment with 4OHT showed reduction in CBFβ levels in *MMTV-PyMT;ROSA-CreER^{T2};Cbfβ$^{fl/fl}$* cells (first red box from the left). After 48h of treatment this was further reduced (second red box). At 72h and 96h, the reduction noted at the 48h timepoint was sustained (third and fourth red box). Western blot image is representative of at least N=4 experimental repeats. Figure created using Biorender.com

3.2.6.1. MMTV-PyMT tumour cell proliferation reduced upon loss of CBFβ *in vitro*

The loss of an oncogene or tumour suppressor tends to induce direct phenotypic changes in tumour cells, usually in the form of altered proliferation rates (Hanahan and Weinberg, 2000, 2011). Thus, tumour cells were monitored through qualitative microscopic analysis to assess the gross impact of *Cbfβ* loss. In this

regard, once treated with either vehicle or 100 nM 4OHT equal numbers of cells from one *Cbfβ*$^{fl/fl}$ and one *Cbfβ*$^{wt/wt}$ cell line were cultured in fresh, treatment free tumour cell growth media. Interestingly, within 3 days, a noticeable decrease in the number of 4OHT treated *Cbfβ*$^{fl/fl}$ cells was observed compared to vehicle treated and *Cbfβ*$^{wt/wt}$ controls (Figure 3.12). While the *Cbfβ*$^{wt/wt}$ cells continued to proliferate and expand across the cell culture plate despite being pre-treated with 4OHT, the drug treated *Cbfβ*$^{fl/fl}$ cells struggled to maintain a population. Additionally, the few *Cbfβ*$^{fl/fl}$ cells in the 4OHT treated group that did manage to survive until day 3, seemed to have transformed into more elongated spindly structures compared to the vehicle treated population. This hinted towards a potential induction of epithelial to mesenchymal transition associated with loss of *Cbfβ*. Overall, these results did not support a tumour suppressive role for *Cbfβ* in these *MMTV-PyMT* cells which demanded further investigation.

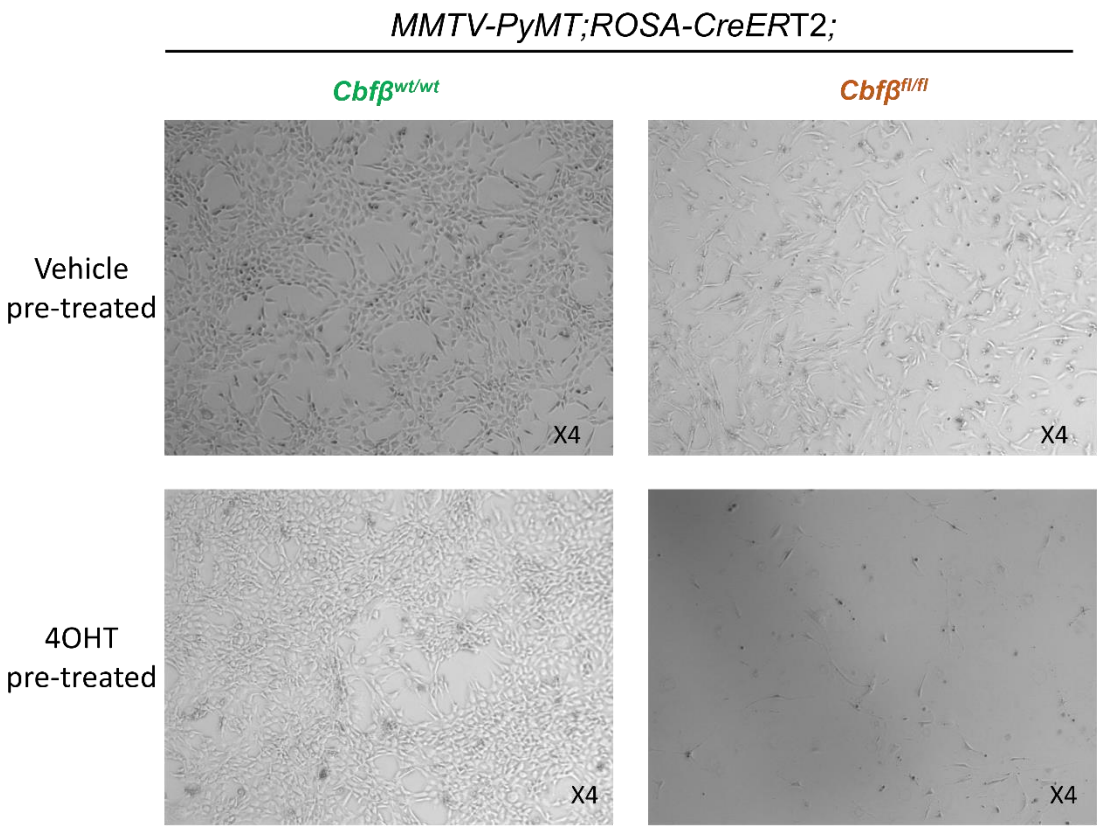

Figure 3.12: Loss of *Cbfβ* reduces tumour cell proliferation and induces changes in epithelial cell morphology in *MMTV-PyMT*cells.

Representative images of tumour cells from tumour derived *MMTV-PyMT;ROSA-CreERT2;Cbfβ*$^{wt/wt}$ (left panels) and *MMTV-PyMT;ROSA-CreERT2;Cbfβ*$^{fl/fl}$ (right panels) cell lines at day 3 of growth in fresh, treatment free media. Prior to this, cells were treated with vehicle (top panels) or 100nM 4OHT (bottom panels) according to the predetermined treatment regime. Images were taken at x4 objective with the Olympus CKX41 microscope. Images are representative of at least N=4 experimental repeats.

3.2.6.2. Loss of CBFβ reduces viability and clonogenic potential of MMTV-PyMT tumour cells *in vitro*

To determine how acute deletion of *Cbfβ* affects growth of established tumour cell lines, MTS assays (Riss et al., 2016) were conducted to measure cell viability. Tumour derived cell lines from two different *Cbfβ*$^{fl/fl}$ mice and one *Cbfβ*$^{wt/wt}$ mouse were treated with 4OHT according to the optimised treatment regime of 100nM 4OHT or vehicle added every 24hrs for two consecutive days (Figure 3.11A). Loss of CBFβ in 4OHT treated *Cbfβ*$^{fl/fl}$ cells was confirmed using western blotting for every experimental repeat (data not shown) to ensure cells used in biological assays were indeed lacking the protein of interest. Treated cells were plated onto 96 well plates in fresh, drug free cell culture media at optimised seeding densities and subjected to MTS assay-based measurement of cell viability at 6 different time

points over the course of 7 days (Figure 3.13). Considering how each cell line was derived from independent murine tumours with heterogenous growth rates, to accurately determine any changes in viability, absorbance readings from MTS assays for each cell line was compared to their respective vehicle treated controls rather than directly to the control *Cbfβ*$^{wt/wt}$ cell line. Between vehicle versus 4OHT treatment of *Cbfβ*$^{wt/wt}$ cells, no difference in cell viability was noted over 7 days (Figure 3.13A), confirming that 4OHT or vehicle treatment had no intrinsic impact on the growth of tumour cells. Interestingly, viability of both *Cbfβ*$^{fl/fl}$ cell lines that had undergone 4OHT treatment and lost *Cbfβ*, was significantly reduced compared to vehicle treated isogenic *Cbfβ*$^{fl/fl}$ cells. (Figure 3.13B and C). The MTS assay results highlight how a change in cell viability and proliferation is noticed during the later timepoints in the assay. These results are emphasised further in the bar graphs depicted in Figure 3.13D. While 4OHT pre-treated cells from the *Cbfβ*$^{wt/wt}$ cell line (top two bar graphs) did not show any significant change in cell viability at day 5 and day 7 of growth compared to their vehicle treated counterparts, 4OHT pre-treated cells from both *Cbfβ*$^{fl/fl}$ cell lines showed marked decrease in cell viability at day 5 and day 7 of the assay compared to the vehicle control groups. This indicated that loss of *Cbfβ* in established PyMT breast tumour cells negatively impacted cell viability over time *in vitro*.

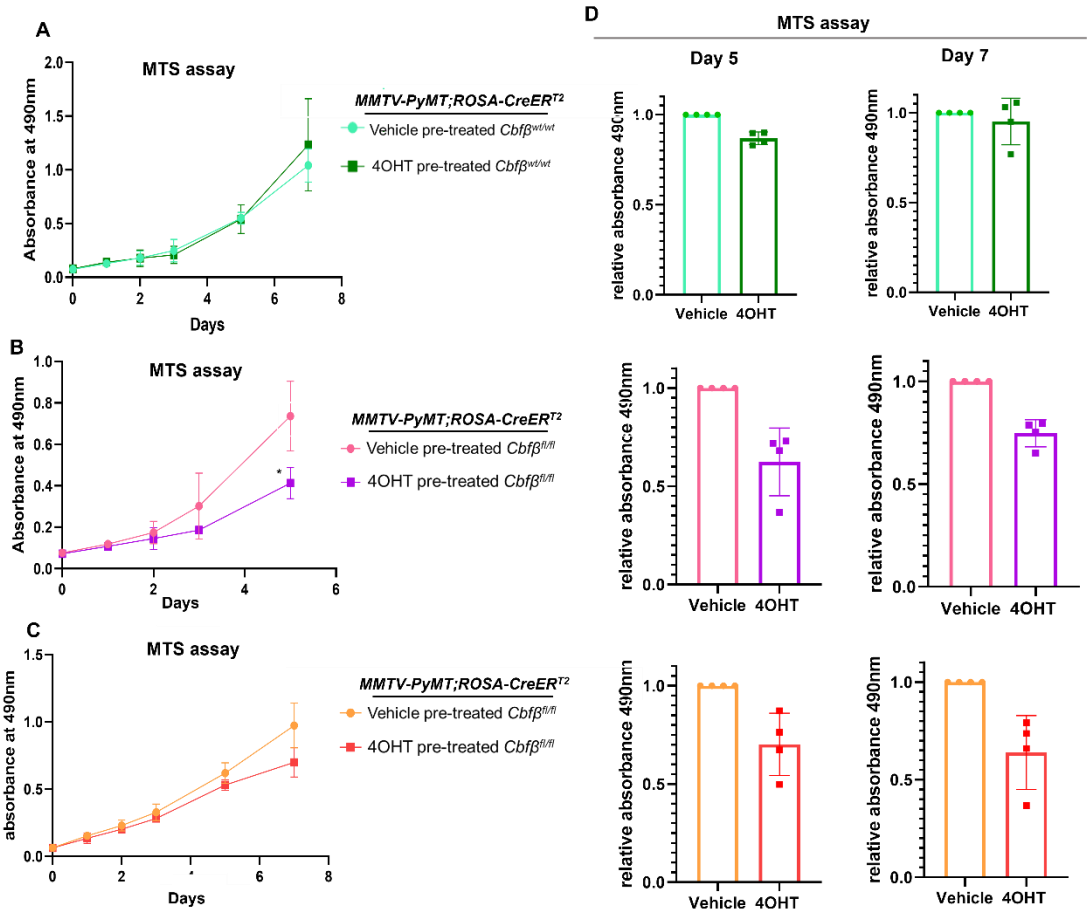

Figure 3.13: Loss of *Cbfβ* results in reduced tumour cell viability and proliferation.
MTS assay results depicting viability of tumour cells from the control *MMTV-PyMT;ROSA-CreER^{T2};Cbfβ$^{wt/wt}$* cell line (A) and two *MMTV-PyMT;ROSA-CreER^{T2};Cbfβ$^{fl/fl}$* cell lines (B – C). Error bars represent mean ± SD from n=3 experimental repeats, each with 6 technical repeats. * p<0.05. (D) Bar graphs represent MTS assay results at day 5 (graphs on the left) and day 7 (graphs on the right) to highlight the difference in cell viability between 4OHT and vehicle treated tumour cells in the control *MMTV-PyMT;ROSA-CreER^{T2};Cbfβ$^{wt/wt}$* cell line (top graphs in green) and two *MMTV-PyMT;ROSA-CreER^{T2};Cbfβ$^{fl/fl}$* cell lines (middle and bottom graphs in pink and orange). Error bars represent mean ± SD from n=4 experimental repeats, each with 6 technical replicates.

A key trait of tumour cells that enables their survival and propagation, especially after dissemination from the primary tumour into distal secondary sites, is their ability to form colonies from a single cell of origin. Genetic alterations, such as amplifications of oncogenes, that provide an intrinsic advantage for this form of unrestrained cell proliferation are naturally selected for supporting growth of tumours (Hanahan and Weinberg, 2000, 2011; Franken et al., 2006). Thus, to investigate whether loss of *Cbfβ* affected the ability of tumour cells to colonise an environment from a single parental source, clonogenic assays (Franken et al., 2006) were performed.

As previously described, cells from each of the *Cbfβ*$^{fl/fl}$ and *Cbfβ*$^{wt/wt}$ cell lines post 4OHT/vehicle treatment, were plated onto 6 well plates in triplicates at a pre-determined optimum seeding density. Colonies were allowed to grow for 8 days for both *Cbfβ*$^{fl/fl}$ cell lines and 12 days for the *Cbfβ*$^{wt/wt}$ cell line. The duration was decided on after several optimisation experiments with each cell line to determine the time required to achieve distinct colonies (data not shown). Crystal violet staining followed by fluorescence intensity measurement using LICOR Odyssey® CLx was used for accurate quantification of the colony formation (Figure 3.14A and B). Evident from the crystal violet staining (Figure 3.14A) as well as the LICOR images (Figure 3.14B), colony formation remained fairly unaffected across the two treatment arms for *Cbfβ*$^{wt/wt}$ cells. For both *Cbfβ*$^{fl/fl}$ cell lines, however, cells pre-treated with 4OHT formed fewer colonies compared to their respective vehicle controls (Figure 3.14B). Closer microscopic inspection revealed that the size of colonies was also smaller in the population of cells lacking CBFβ. These qualitative observations were validated post quantification where the graphs showed a bigger difference in stain intensity for both *Cbfβ*$^{fl/fl}$ cell lines between the two treatment arms (Figure 3.14D and E), compared to the *Cbfβ*$^{wt/wt}$ cell line (Figure 3.14C). It is therefore implied that loss of CBFβ in PyMT murine breast cancer cells leads to a reduction in cell viability and their colony forming potential – two key traits characteristic of oncogenes.

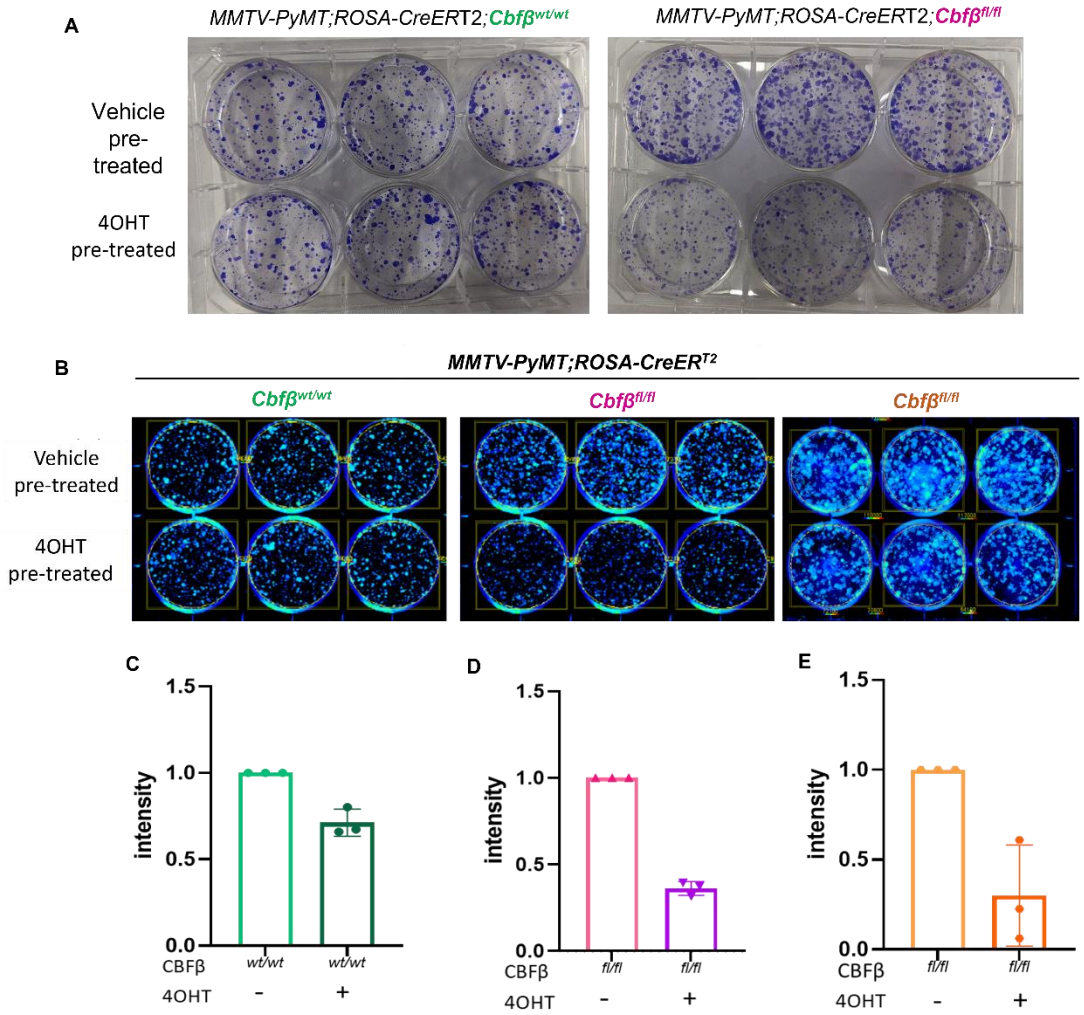

Figure 3.14: Loss of *Cbfβ* results in reduced tumour cell clonogenicity.

(A) Image depicts colony formation assay of cells from the control *MMTV-PyMT;ROSA-CreER^{T2};Cbfβ$^{wt/wt}$* cell line (left) and *MMTV-PyMT;ROSA-CreER^{T2};Cbfβfl/fl* cell line (right). Images are representative of at least n=3 experimental repeats, each with 3 technical repeats per cell line. (B) Fluorescent images of colony formation assay plates on the LI-COR Odessy Clx plate scanner at 800nm. Assays were conducted using tumour derived cell lines from one *Cbfβ* wildtype control *MMTV-PyMT;ROSA-CreER^{T2};Cbfβ$^{wt/wt}$* mouse (left) and two *MMTV-PyMT;ROSA-CreER^{T2};Cbfβ$^{fl/fl}$* mice (middle and right panel). (C-E) Quantification of colony formation assay from B. *MMTV-PyMT;ROSA-CreER^{T2};Cbfβ$^{fl/fl}$* tumour cells denoted by "fl/fl" and *MMTV-PyMT;ROSA-CreER^{T2};Cbfβ$^{wt/wt}$* cells denoted by "wt/wt". "+" indicates 4OHT pre-treatment and "-" indicates vehicle -pre-treatment. Error bars represent mean ± SD from n=3 experimental repeats, each with 3 technical repeats.

3.2.6.3. *Cbfβ* loss does not alter tumoursphere forming ability of *MMTV-PyMT* tumour cells *in vitro*

The impact of CBFβ loss on tumour cell growth, proliferation and clonogenicity was tested further in the 3D culture of tumourspheres. While *in vitro* experiments provide a valuable platform for interrogating tumour cell characteristics and the

relationships between genetic alterations and the resulting phenotypic changes, 3D cultures better recapitulate the *in vivo* physiological environment where tumour cells interact with each other in three dimensional planes (Katt et al., 2016; Pinto, Estrada and Brito, 2020). Malignant tumours often possess a population of tumour initiating cells with inherent stem cell like properties and the ability to survive and proliferate extensively under the influence of mitogens in anchorage-independent settings (Dontu et al., 2003; Ponti et al., 2005). Tumoursphere assays select for such cells and can provide insight into the impact of certain genetic alterations on cancer cell stemness. Arising from self-propagation of a single cell, morphologically tumourspheres resemble solid aggregates of cells fused together into one sphere akin to the avascular tumour masses or micro-metastases noted in patients (Katt et al., 2016). Since results from the 2D assays indicated that loss of CBFβ attenuates PyMT tumour cell growth, loss of this protein might be hypothesised to be disadvantageous to anchorage-independent growth and tumoursphere formation.

To this end, single cell suspensions of tumour cells from each cell line, pre-treated with either 4OHT or vehicle, were plated in ultra-low adherence 24 well plates. Growth factors were added to the culture media periodically to encourage formation of primary tumourspheres over 7 days. Tumourspheres, at the end of 7 days were counted manually under the microscope.

Across the 3 cell lines, there were no apparent differences in the total number of primary tumourspheres formed by cells with and without CBFβ (Figure 3.15A). Tumourspheres were also counted separately according to size. A semi-quantitative method using the grid embedded on the microscope lens was used to classify tumourspheres into small, medium and large groups. Representative images of these have been presented in Figure 3.15B While a slight increase in the number of small tumourspheres compared to medium and large spheres were noted in the 4OHT treated cells across all 3 cell lines, the results were not significant. Furthermore, the number of tumourspheres of either size remained comparable in cells with and without CBFβ with no difference noted upon loss of CBFβ (Figure 3.15C). These results suggest that loss of CBFβ does not impact anchorage independent-growth or tumour cell stemness in this assay. However, these cell lines are from established endpoint tumours and perhaps a more accurate cell population to analyse for mammary stemness would be mammary

epithelial cells (MMECs) from murine mammary glands at the brink of transformation or tumorigenesis.

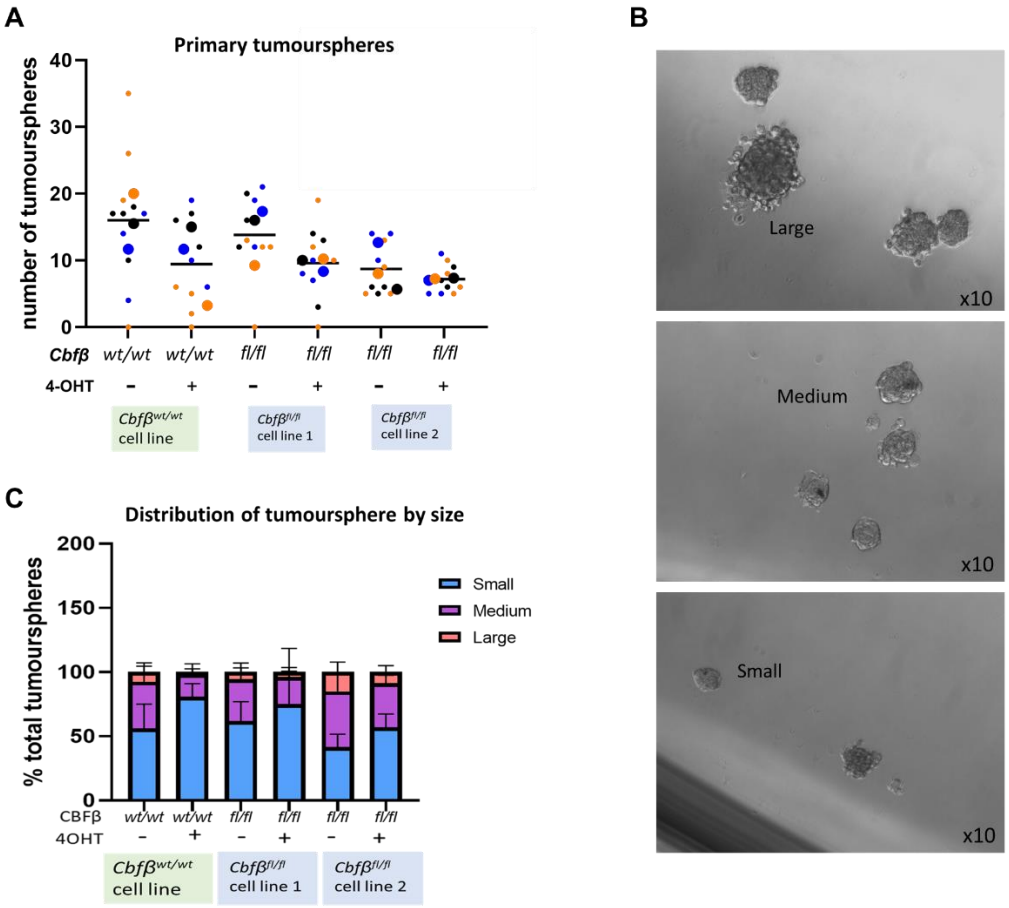

Figure 3.15: Loss of *Cbfβ* does not affect anchorage-independent growth of tumourspheres in tumour derived cell lines.

(A) Superplot representing the total number of tumourspheres produced by one *MMTV-PyMT;ROSA-CreER^{T2};Cbfβ$^{wt/wt}$* cell line and two *MMTV-PyMT;ROSA-CreER^{T2};Cbfβ$^{fl/fl}$* cell lines (cell line 1 and cell line 2). Smaller dots represent number of primary tumourspheres counted in each technical replicate (n=4) and bigger dots represent the mean of the technical replicates. The different colours of the dots represent the n=3 different experimental replicates. Bar represents mean of all experimental replicates. (B) Snapshot of large (top), medium (middle) and small (bottom) tumourspheres. (C) Stacked bar graph showing the distribution of small, medium and large tumourspheres in 4OHT or vehicle pre-treated samples for each of the three cell lines. Error bars represent mean ± SD from n=3 experimental repeats, each with 4 technical repeats. *MMTV-PyMT;ROSA-CreER^{T2};Cbfβ$^{fl/fl}$* tumour cells denoted by "fl/fl" and *MMTV-PyMT;ROSA-CreER^{T2};Cbfβ$^{wt/wt}$* cells denoted by "wt/wt". "+" indicates 4OHT treatment and "-" indicates vehicle treatment. Statistical analysis using ordinary one-way ANOVA conducted in GraphPad Prism indicated non-significant difference between 4OHT and vehicle treated groups for each cell line.

3.3. Discussion

With the surge in high throughput whole genome sequencing studies in the recent decades, an increasing number of previously undiscovered genetic alterations have been identified in breast tumour biopsies and associated to the transformation of healthy mammary cells into malignant states. On that account, a growing body of evidence has attributed tumour growth promoting as well as growth suppressive characteristics to the RUNX co-transcription factor CBFβ. Multiple studies (referred in Chapter 1.4) have suggested that the dichotomy of CBFβ may be linked to ER status in breast carcinogenesis with a protective role played in ER positive disease and an oncogenic role adopted in the absence of ER. As such, this arm of the project first focussed on inducing loss of endogenous *Cbfβ* in murine mammary glands *in vivo* to assess its impact on both tumour initiation and progression alongside investigating the metastatic potential of *Cbfβ* deficient breast tumours. As a widely used GEMM for mammary specific induction of carcinogenesis, the *MMTV-PyMT;MMTV-Cre* GEMM (Attalla et al., 2020) was used to investigate the role of *Cbfβ*. While in the first instance, loss of *Cbfβ* did not seem to yield any overt effects on tumour burden, carcinogenesis or metastasis, a closer look revealed technical caveats of the system in inducing uniform deletion of *Cbfβ* mediated by MMTV-Cre. The C57BL/6J strain of mice used for generation of this model is known for its reduced latency of MMTV-PyMT induced tumours compared to other strains such as FVB/N (Davie et al., 2007). It is possible that this may be associated with lower levels of MMTV mediated expression resulting in reduced levels of MMTV-Cre expression. Additionally, the mosaic nature of MMTV-Cre and the inability to achieve consistent expression across the mammary gland due to its sensitivity to mammary hormones made it an unreliable means of genetic manipulation in this context. Because of this, the majority of the mammary tumours remained proficient for *Cbfβ in vivo,* even in $Cbf\beta^{fl/fl}$ mice, and thus it was difficult to accurately ascertain the effect of *Cbfβ* loss in this system. It should be noted however, that RFP mediated reporting of Cre-activation revealed small areas of the tumours where Cre expression was indeed actuated, indicating loss of *Cbfβ* (a notion supported by the slightly reduced protein expression of CBFβ noted in $Cbf\beta^{fl/fl}$ tumours).

The fact that growth of these small groups of *Cbfβ* deficient tumour cells seemed overpowered by those in which *Cbfβ* was present, proposes an interesting phenomenon: loss of *Cbfβ* did not induce enough of a growth advantage in the tumour cells to encourage their accelerated propagation and invasion over the mammary gland. This might be one reason why majority of any end-stage tumour consisted of *Cbfβ* proficient cells capable of unrestrained growth to invade through the mammary infrastructure. *MMTV-PyMT* tumours are known to progressively lose expression of ER as the disease advances (Blyth lab, unpublished), recapitulating some of the more aggressive subtypes of human breast cancer with unfavourable prognosis. In the late-carcinoma phases of *MMTV-PyMT* disease, ER negative cells have been shown to make up over 90% of a tumour section (Lin et al., 2003). As discussed earlier in this chapter, amplifications of *Cbfβ* coincided primarily with ER negative breast cancer in patient samples, and *in vitro* studies with ER negative breast cancer cells lines have been supportive of this association (Mendoza-Villanueva et al., 2010; Mendoza-Villanueva, Zeef and Shore, 2011; Hsu et al., 2022). Observations from the *MMTV-PyMT;MMTV-Cre;Cbfβ*$^{fl/fl}$ mouse model may therefore fit the narrative of *Cbfβ* potentially playing an oncogenic role in ER negative tumours. However, further characterisation of the ER status of PyMT tumours at both early and late stage of disease would be required to confirm that this model is indeed mimicking ER negative breast cancer. Additionally, a more refined model with improved control over Cre expression would be required to ensure efficient deletion of *Cbfβ* within PyMT driven tumour cells *in vivo*.

The *MMTV-PyMT;ROSA-CreER*^{T2}*;Cbfβ*$^{fl/fl}$ model was utilised to have better control over Cre-activation and attain consistent deletion of *Cbfβ* in tumour cells. Here, instead of having Cre expression linked to the *MMTV-LTR*, the CreER^{T2} expressing construct is in the *ROSA26* locus (Zambrowicz et al., 1997; Ventura et al., 2007). The benefit of this system is twofold: 1) In mice, transcriptional activity from the *ROSA26* locus is ubiquitous and unaffected by changes in the epigenetic states of chromatin which hold the potential to repress expression of transgenes. Furthermore, loss or replacement of this gene throughout the body is not lethal to the animal (Zambrowicz et al., 1997). This makes it an ideal locus for transgene insertion. Thus, linking expression of a Cre-recombinase to this region would allow constitutive expression of the enzyme throughout the body – avoiding the

mosaicism issue experienced with *MMTV-Cre*. 2) The use of an inducible version of Cre, such as CreER^{T2} introduces spatial and temporal control over Cre activity and hence deletion of any floxed alleles of interest. This is critical when Cre expression is being driven by a ubiquitous promoter throughout the body and the gene targeted for deletion is essential in normal development (Qing Wang et al., 1996).

As mentioned previously, homozygous deletion of *Cbfβ* results in embryonic lethality and therefore, *MMTV-PyMT;ROSA-CreER^{T2};Cbfβ$^{fl/fl}$* mice were allowed grow in the absence of 4OHT or tamoxifen stimulation to avoid any impact on development. The result was generation of *Cbfβ* proficient mammary tumours reaching late-carcinoma. *Ex vivo* deletion of *Cbfβ* in tumour derived cell lines supported the results that *Cbfβ* loss indeed appeared disadvantageous to tumour growth and viability as well as negatively impacting tumour cell clonogenicity. Future experiments involving invasion and migration assays would help explore this relationship further. Interestingly, tumoursphere forming ability of these cells, indicative of the presence of any cancer stem cells within the populations, in a 3D setting did not seem to be affected by *Cbfβ* deletion. This indicated that while PyMT carcinoma cells had the capacity to self-renew and expand in an anchorage independent manner, as demonstrated by their ability to form primary tumourspheres in culture, loss of *Cbfβ,* at least in this instance, did not induce any changes to this characteristic. These results were unexpected considering how previous investigations in the Blyth lab demonstrated that loss of *Runx1* was shown to augment stemness in mammary stem cells (Kerri Sweeny, unpublished). Hong *et al.*, also implicated interruption of the CBFβ/RUNX complex and particularly loss of *RUNX1* in driving EMT of breast cancer cells (Fritz et al., 2020). Of course, further experiments are required to validate the results from the tumoursphere assays. Analysis of tumourspheres for stem markers and continual subculturing of spheres over multiple passages to test the extent of their self-renewing capacity with and without *Cbfβ* for instance, could provide additional insight into the relationship between *Cbfβ* and mammary cell tumorigenicity.

Following *in vitro* investigation, in order to test our hypothesis in the physiological context of the murine mammary gland, orthotopic transplantation experiments were attempted. The CBFβ proficient *MMTV-PyMT;ROSA-CreER^{T2};Cbfβ$^{wt/wt}$* or *MMTV-PyMT;ROSA-CreER^{T2};Cbfβ$^{fl/fl}$* mammary tumour derived cells were used for

orthotopic allograft experiments in syngeneic recipient mice. These were then monitored for growth of palpable tumours with plans of introducing tamoxifen or vehicle treatment intraperitoneally in order to delete *Cbfβ* specifically in the tumour cells. Unfortunately, due to poor take-rate of the tumour cells, almost none of the experimental mice developed mammary tumours. However, only two pairs of the established cells lines from *MMTV-PyMT;ROSA-CreER*^{T2} were trialled for this experiment and it is possible that more stable cell lines of the same genotype and optimisation of experimental techniques such as using a mix of basement membrane extract and tumour cells to encourage better settlement of the tumour cells into the mammary fat-pads could aid in achieving success with this method.

The ultimate objective of the *MMTV-PyMT;ROSA-CreER*^{T2}*;Cbfβ*$^{fl/fl}$ model, taking advantage of the temporal control over gene expression attainable though CreER^{T2}, lies in the *in vivo* deletion of *Cbfβ* at different timepoints along the carcinogenic stages of pre-neoplasia, hyperplasia, adenoma, early and late carcinoma. This could help dissect whether *Cbfβ* expression is critical in driving a particular phase of the carcinogenesis process such as tumour initiation or required later during tumour progression. Additionally, acute deletion of *Cbfβ* in this manner could also help capture the transcriptional and translational targets under immediate control of this protein and involved in mammary oncogenesis. This would help reveal the convergence points between this transcription co-factor and other pathways that can be targeted specifically for therapy. It is important to note that given the ubiquitous expression of CreER^{T2} under the *ROSA26* locus, and the lethal consequence of germline deletion of *Cbfβ* noted in mice, systemic exposure to Cre-activation would need to be approached with caution. For mammary specific activation of CreER^{T2} and thus removal of *Cbfβ*$^{fl/fl}$ alleles, one approach could be intraductal delivery (ID) of tamoxifen through the nipple. This method has been used in a number of preclinical studies to successfully administer chemotherapeutics into the nipples of experimental animals where significant drug exposure was localised to mammary tissue with limited leakage into systemic circulation (Okugawa et al., 2005; Murata et al., 2006; Stearns et al., 2011; Groot et al., 2017). An added benefit of this system is that within the same mouse it is possible to treat only a select few glands and use

other glands as an internal control to validate local phenotypic changes induced upon gene deletion.

It is worth bearing in mind however, that ID would mainly work in mice with healthy glands or early-stage mammary cancer where the mammary architecture is still somewhat preserved. In the later stages of carcinogenesis, the mammary gland structure including the nipple and ductal tree becomes completely obliterated by the uncontrolled expansion of invasive tumour cells and therefore it would be difficult to achieve uniform delivery of any drug into the tumour mass. In order to study the effects of tamoxifen activated $CreER^{T2}$ mediated acute deletion of *Cbfβ* in more advanced mammary cancer cells, orthotopic transplantation models involving *MMTV-PyMT;ROSA-CreER*^{T2}*;Cbfβ*$^{fl/fl}$ tumour cells derived from latestage invasive tumours could prove useful.

In summary, *in vivo* results using the PyMT mammary tumour model with genetic deletion of *Cbfβ*, shows no evidence of potent tumour suppressor activity. Similarly, *in vitro* results did not support a tumour suppressive role for CBFβ in established tumour derived cell lines. In fact, a growth inhibitory effect of *Cbfβ* loss in PyMT cell lines was indicated. In order to investigate whether this is a generalised phenomenon, the impact of *Cbfβ* loss was explored further.

Chapter 4. CBFβ as a tumour suppressor in a mouse model of Wnt/β-catenin driven mammary cancer

4.1. Introduction

Experimental evidence discussed in the previous chapter revealed some of the key caveats of the *MMTV-PyMT;MMTV-Cre* mouse model, especially in achieving deletion of *Cbfβ* efficiently throughout the mammary epithelium. In view of this, the need for an alternate mouse model with more stringent control over oncogene expression and Cre mediated deletion of *Cbfβ* within the mammary cells was imperative in investigating the role of CBFβ in breast cancer. Previously in the Blyth lab, a *BLG-Cre;Catnb*$^{wt/lox(ex3)}$ GEMM was used to successfully knock out *Runx1* and *Runx2* in mouse mammary tumours (Riggio, 2017). Modelling Wnt/β-catenin deregulation noted in human breast cancers (Hatsell et al., 2003; Wang et al., 2015), tumorigenesis in the *BLG-Cre;Catnb*$^{wt/lox(ex3)}$ mice was dramatically accelerated upon simultaneous loss of these two RUNX proteins. Considering the close relationship between RUNX proteins and CBFβ, the *BLG-Cre;Catnb*$^{wt/lox(ex3)}$ model was therefore chosen to explore the phenotypic consequence of deleting *Cbfβ* in the context Wnt/β-catenin driven breast cancer.

4.1.1. Wnt signalling and its implications on breast cancer

In 1982, while MMTV-LTR induced mammary tumours were being screened for provirus integration sites, a novel oncogene termed as *MMTV int-1* was discovered and associated to mammary tumorigenesis. Integration of the MMTV proviral genome within *int-1* and the subsequent upregulation of the *int-1* expression mediated by the enhancer activity of *MMTV-LTR* was hypothesised to be advantageous to the survival and growth of mammary cells and ultimately their transformation (Nusse and Varmus, 1982). Following further characterisation of this pro-oncogene, in 1997, the murine *int-1* was identified as a homologue for the Drosophila, *Dint-1* or *wingless* gene involved in segment polarity (van Ooyen and Nusse, 1984; Rijsewijk et al., 1987). In this regard, the term Wnt as a portmanteau generated from “wingless” and “Int-1” was adopted to define all

subsequently discovered members of the Wnt family of genes in order to dissociate *int-1* and related genes from other MMTV provirus integration sites such as *int-2* and *int-3* (Nusse et al., 1991). Since the discovery of these Wnt proteins and their association to mammary tumorigenesis, genome wide sequencing and analysis of gene expression pattens have implicated the Wnt signalling pathway in breast cancer proliferation, metastasis, maintenance of cancer cell stemness, regulation of the breast tumour-immune microenvironment as well as the development of therapeutic resistance (Xu et al., 2020).

Encoded by any of the 19 Wnt genes discovered in the human genome thus far, binding of Wnt ligands to Frizzled (Fzd) receptors found on the surfaces of target cells activates the evolutionarily conserved Wnt signalling pathway. Conventionally, the Wnt pathway is divided into three signalling systems: the canonical pathway mediated by Wnt and β-catenin, the non-canonical Wnt-planar cell polarity (Wnt-PCP) and Wnt-Ca^{2+} pathways (Xu et al., 2020). The canonical pathway and to some extent the non-canonical signalling pathways work to mediate the activity of a key protein: β-catenin. In this regard, a two-fold approach is taken to control activity of this protein: (1) by ensuring induction and maintenance of the activated state of β-catenin and (2) by inhibiting its clearance from the cytoplasm and the repression of β-catenin mediated transcription in the nucleus.

Addressing the former, Wnt ligands of the canonical pathway are activated to their lipid-associated form by the process of palmitoylation via Porcupine, in the endoplasmic reticulum and subsequently trafficked to the Golgi apparatus by members of the p24 family of proteins (such as TMED2, TMED4 and TMED5) (Xu et al., 2020). From this point, the activated Wnt ligands are transported out of the organelle and across the cytoplasm within endosomes by Wntless (alternative names include Evenness, Sprinter, Interrupted, GPR177) to the plasma membrane, from where they are secreted into the ECM and carried to target cells in exosomes (Xu et al., 2020). On the surface of target cells, the 7-pass transmembrane Frizzled receptors form heterodimers with a single pass transmembrane low-density lipoprotein receptor related protein (LRP) which acts as a co-receptor. Additionally, synergising with Wnt mediated activation, R-spondin, by binding to the leucine-rich G protein coupled receptor (LGR5) helps remove Fzd ubiquitinating E3 ligases RNF43 and ZNRF3, thus increasing the number of Fzd

receptors available for Wnt ligand binding on LGR5. Binding of Wnt ligands to these Frizzled receptors, activated upon interaction with a protein called Norrin, leads to initiation of canonical Wnt signalling (Xu et al., 2020). Subsequently, activation of Rac-1 and Jun N-terminal kinase 2 (JNK2) mediates phosphorylation of cytoplasmic β-catenin at specific serine residues (Ser191 and Ser605) and expedites its translocation into the nuclear compartment of the cell. Here, β-catenin forms a scaffolding complex on DNA with lymphoid enhancer factor (LEF) and T-cell factor (TCF) proteins to recruit various transcription coactivators such as CBP/p300, B cell lymphoma 9 (BCL9) and Pygopus (PYGO). Essentially, Wnt activated β-catenin replaces the repressor complex interacting with TCF and converts it into a transcription activation complex (Xu et al., 2020). This ultimately allows transcription regulation of various target genes involved in mammary cell biology and tumorigenesis including *Myc* and *Cyclin D1* (Xu et al., 2020).

Considering the critical role played by β-catenin in the regulation of gene transcription, cytoplasmic β-catenin and its translocation to the nucleus is maintained under stringent regulation primarily by the β-catenin destruction complex (Xu et al., 2020). Serving as scaffolds for the complex, adenomatous polyposis coli (APC) and AXIN provide a platform for the phosphorylation of β-catenin, first by casein kinase 1α (CK1α) at the Ser45 residue and subsequently by glycogen synthase kinase 2β (GSK-3β) at residues Thr41, Ser37 and Ser33 (Xu et al., 2020). The phosphorylated Ser33 and Ser37 residues are recognised by various ubiquitination apparatuses which mediate proteolytic degradation of β-catenin (Liu et al., 2001; Wu et al., 2003; Xu et al., 2020). Additionally, β-catenin activity in the nucleus is also inhibited to regulate β-catenin mediated transcription. This occurs in a two-fold process. On one hand, β-catenin and TCF/LEF association is interrupted by the β-catenin antagonist Chibby and the inhibitor of β-catenin and TCF (ICAT) (Daniels and Weis, 2002; Takemaru et al., 2003). Conversely, repressor complexes including HDACs and Transducing-like enhancer/Groucho (TLE/GRG) which interact with TCF and LEF1 can also block TCF/LEF association with β-catenin thereby suppressing transcription of Wnt target genes (Xu et al., 2020). Outside of the canonical pathway, Wnt/β-catenin signalling is also negatively regulated by the non-canonical Wnt-Ca^{2+} pathway. The successive cascade of

events following activation of this non-canonical pathway leads to phosphorylation of TCF which inhibits TCF–β-catenin mediated transcription (Xu et al., 2020).

The second consequence of Wnt signalling activation is in the inhibition of β-catenin clearance from the cytoplasm. Binding of Wnt ligands to the Fzd-LRP6 receptor complex induces recruitment of several members of the destruction complex such as AXIN, Dishevelled (Dsh), GSK-3β and APC and stimulates phosphorylation of amino acid residues present at the cytoplasmic tail of LRP6 (Xu et al., 2020). These phosphorylated residues act as a docking site for AXIN thus retaining the protein along with AXIN bound Dsh and other members of the destruction complex (Logan and Nusse, 2004; Xu et al., 2020). Therefore, Wnt activation disrupts assembly of the destruction complex by restraining its members to the cell membrane. This prevents destruction of β-catenin and supports its accumulation in the cytoplasm, encouraging its normal functioning.

β-catenin is crucial in the control of intercellular interactions via E-cadherin which help maintain tissue architecture, protection against apoptosis and transcriptional regulation of various target genes involved in cell proliferation, differentiation, and stem-cell phenotypes (Hülsken, Birchmeier and Behrens, 1994; Orford, Orford and Byers, 1999; Zeng and Nusse, 2010). These characteristics are also applied in mammary development and disease. For instance, by facilitating the interaction between the actin cytoskeleton and cadherins, β-catenin helps stabilise the mammary luminal infrastructure. The protein is also implicated in embryonic mammary gland development as well as in the initiation of alveologenesis and propagation of lobuloalveolar progenitor cells. Predictably, aberrant activation of the Wnt pathway, the related activation of β-catenin and its accumulation in the nucleus has been associated with promotion of breast cancer in humans with increased expression noted in tumours with high histological grade and poorer prognosis (Hatsell et al., 2003; Wang et al., 2015). Approximately 25% of tumour samples from patients with metaplastic breast cancers were shown to possess mutations which result in stabilisation of β-catenin of which 92% samples displayed accumulation of β-catenin protein (Hayes et al., 2008). Additionally, upregulated expression of Frizzled receptors and Wnt ligands, loss of the non-canonical antagonism of β-catenin, inactivation of Wnt pathway inhibitors such as sFRPs and DKK and downregulation or loss of heterozygosity of components of the destruction complex such as AXIN and APC have all been implicated in numerous

breast tumours and tumour derived cell lines (Incassati et al., 2010). Elevated levels of *CCND1* and *C-MYC*: two of the main target genes under the control of Wnt signalling, are found in 40% of breast tumours (Incassati et al., 2010). Wnt-independent β-catenin stabilisation mediated by the NF-κB pathway or via loss of tumour suppressors such as p53, and PTEN have also been evident in various cases of mammary tumorigenesis (Incassati et al., 2010).

4.1.2. Association between Wnt signalling and CBFβ/RUNX members

Concurrent changes in Wnt signalling activation and alterations in the *RUNX* genes have been frequently detected in a multitude of cancers (Sweeney, Cameron and Blyth, 2020). Converging with Wnt/β-catenin pathway in the context of the mammary gland, the RUNX family of proteins and their transcription co-factor CBFβ have been shown to play important roles in both development and disease (Sweeney, Cameron and Blyth, 2020). RUNX1 in cooperation with oestrogen for instance, has been shown to inhibit AXIN1 suppression thereby preventing activation of β-catenin in ER positive breast cancer cells (Chimge et al., 2016). The Blyth lab has previously established the existence of a putative relationship between Wnt/β-catenin activation and Runx2 in regenerative potential of mammary stem cells and transformation of mammary epithelial cells (Ferrari et al., 2013, 2015; McDonald et al., 2014). RUNX3 has been deemed critical for normal functioning and maintenance of Wnt signalling with inactivation of the gene associated to carcinogenesis of the breast (Chen, 2012). Less is known about the direct interplay between CBFβ and Wnt signalling in mammary development. However, in conjunction with RUNX1, CBFβ has been shown to induce transcription of the Wnt activator RSPO3 in breast cancer cells (Recouvreux et al., 2016). Furthermore, CBFβ was associated to suppression of mammary tumours in cooperation with p53 (Malik et al., 2021) and through inhibition of NOTCH3. Considering the various nodes of connection between Wnt signalling and the p53 and NOTCH pathways, this leaves room to speculate on a potential relationship of the RUNX co-factor with the Wnt/β-catenin pathway (Braune, Seshire and Lendahl, 2018; Wellenstein et al., 2019; Xiao et al., 2022).

4.1.3. Hypothesis and Aims

Based on the findings discussed above and data acquired previously in the lab implicating *Runx1* and *Runx2* in suppression of Wnt/β-catenin driven mammary tumorigenesis, it was hypothesised that *Cbfβ* would act as a tumour suppressor in Wnt/β-catenin driven breast cancer.

As such, loss of CBFβ and its effect on Wnt/β-catenin was investigated using the *BLG-Cre;Catnb*$^{wt/lox(ex3)}$ GEMM (Riggio, 2017). In the first instance, the aim was to determine the relationship between *Cbfβ* and Wnt/β-catenin induced mammary carcinogenesis *in vivo*. Subsequently, whether loss of *Cbfβ* phenocopies loss of its two RUNX counterparts (*Runx1 and Runx2*) under the context of Wnt/β-catenin activation was interrogated to better understand the interplay between *Runx* and *Cbfβ*. Finally, the biological mechanisms underpinning the impacts of *Cbfβ* or *Runx1 and Runx2* on mammary tumorigenesis was to be explored.

4.2. Results

4.2.1. Generation of a new *Cbfβ* knockout GEMM modelling Wnt/β-catenin driven breast cancer

In an effort to achieve efficient deletion of *Cbfβ* throughout the mammary epithelium, the *β-lactoglobulin* (*BLG*) promoter was chosen to mediate expression of Cre-recombinase. Found in the milk of almost every mammalian species, BLG is a whey protein expressed under the control of lactogenic hormones such as prolactin and oestrogen among others. As lactogenesis occurs specifically in luminal epithelial cells, expression of any transgene under the BLG-promoter is preferentially restricted to the lobuloalveolar cells of the mammary glands and can be increased with the onset of lactation and pregnancy owing to the increase in hormonal signalling (Webster et al., 1995; Selbert et al., 1998; Hennighausen, 2000; Borowsky, 2011). Indeed, comparison between *MMTV-EGFR* and *BLG-EGFR* mice demonstrated exclusive expression of EGFR in the mammary glands of both virgin and postpartum female *BLG-EGFR* animals while transgenic expression in the former model was noted in additional organs such as ovaries, testis, and salivary glands (Brandt et al., 2000). With these advantages in mind, *BLG-Cre;Catnb*$^{wt/lox(ex3)}$ mice were used to model Wnt/β-catenin driven mammary

cancer *in vivo*. The *Catnb*$^{wt/lox(ex3)}$ allele consisted of *loxP* sites situated across exon 3 of the *Catnb* gene. Deletion of this exon removes critical amino acid residues from the protein structure involved in the degradation of β-catenin (Harada et al., 1999). Thus, BLG-Cre activity on *Catnb*$^{wt/lox(ex3)}$ in the mammary epithelial cells generates a stabilised form of β-catenin mimicking the unrestricted activation of the canonical Wnt pathway observed in various cases of breast cancers. Considering the heavy influence of β-catenin on the pre and post pubertal mammary gland development, the use of homozygous *Catnb*$^{wt/lox(ex3)}$ mice were avoided. Owing to the potency of constitutive β-catenin activity in stimulating Wnt signalling, heterozygous expression of the *Catnb*$^{wt/lox(ex3)}$ allele has been shown to be enough for mammary tumorigenesis (Harada et al., 1999; Miyoshi et al., 2002; Riggio, 2017). As such, only *Catnb*$^{wt/lox(ex3)}$ heterozygous female mice were used in the generation of all experimental cohorts.

Subsequently, mice with *Cbfβ*$^{fl/fl}$ alleles (described previously in Chapter 3) were crossed with those carrying *BLG-Cre;Catnb*$^{wt/lox(ex3)}$ on an FVB background to investigate the impact of *Cbfβ* deletion in Wnt/β-catenin driven mammary cancer. Cohorts of mice were generated to achieve either homozygous (*BLG-Cre;Catnb*$^{wt/lox(ex3)}$*;Cbfβ*$^{fl/fl}$) or heterozygous loss of *Cbfβ* (*BLG-Cre;Catnb*$^{wt/lox(ex3)}$*;Cbfβ*$^{wt/fl}$); both of which were compared to a control cohort of mice expressing wildtype copies of the gene of interest (*BLG-Cre;Catnb*$^{wt/lox(ex3)}$*;Cbfβ*$^{wt/wt}$). A schematic of this model is presented in Figure 4.1. The added benefit of this arrangement, especially over the *MMTV-PyMT;MMTV-Cre* model, was the fact that expression of the neoplasm-inducing oncogene (β-catenin) and loss of *Cbfβ* was placed under the control of a singular system: the BLG-Cre. This meant, the event of tumorigenic transformation and loss of the target gene (*Cbfβ)* should coincide within the same mammary cell.

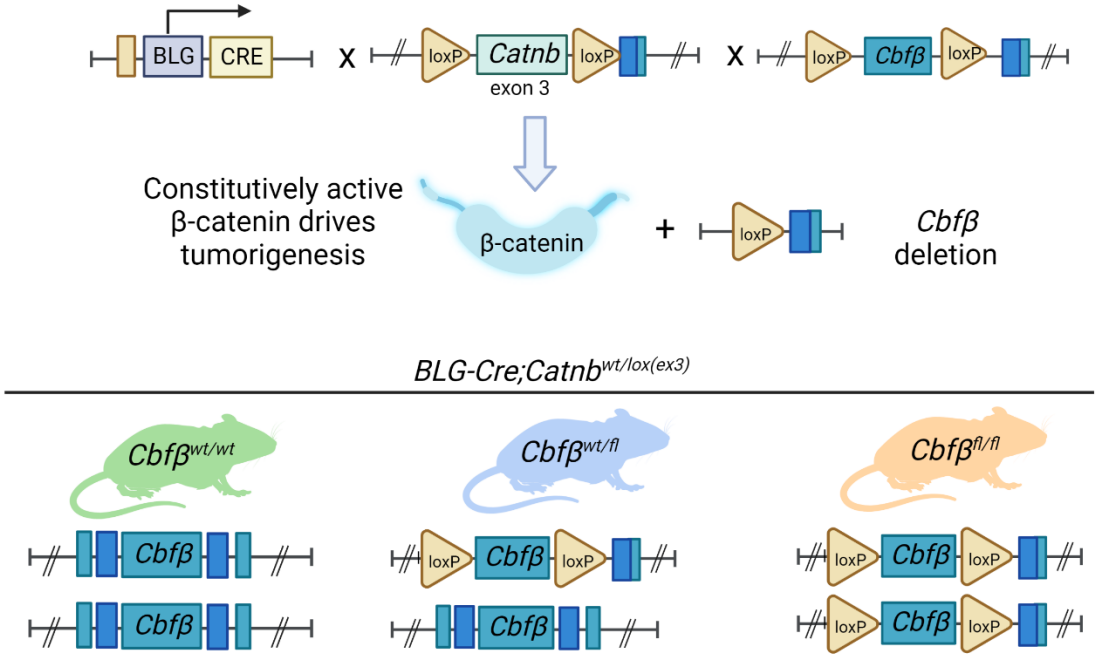

Figure 4.1: Schematic representation of the *BLG-Cre;Catnb*$^{wt/lox(ex3)}$*;Cbfβ*$^{fl/fl}$ mouse model. Mice carrying the *BLG-Cre;Catnb*$^{wt/lox(ex3)}$ construct were crossed with those carrying either *Cbfβ*$^{wt/wt}$, *Cbfβ*$^{wt/fl}$ or *Cbfβ*$^{fl/fl}$ alleles. This resulted in the generation of the three experimental cohorts: *BLG-Cre;Catnb*$^{wt/lox(ex3)}$*;Cbfβ*$^{fl/fl}$, *BLG-Cre;Catnb*$^{wt/lox(ex3)}$*;Cbfβ*$^{fl/fl}$ and *BLG-Cre;Catnb*$^{wt/lox(ex3)}$*;Cbfβ*$^{fl/fl}$. Figure created using Biorender.com

A small cohort of *BLG-Cre;Catnb*$^{wt/lox(ex3)}$*;Cbfβ*$^{fl/fl}$ and *BLG-Cre;Catnb*$^{wt/lox(ex3)}$*;Cbfβ*$^{wt/wt}$ mice were also crossed with the LSL-tdRFP reporter line (Luche et al., 2007), described in chapter 3, to validate Cre activity within the mammary glands. Fluorescence imaging of end-stage tumours (Figure 4.2A) from cohort mice revealed red fluorescence indicative of tdRFP expression and therefore reported BLG-Cre activity in all overt tumours. IHC of formalin fixed tumours also supported these results in showing RFP expression across the whole tumour (Figure 4.2B). This suggested that all tumours consisted of mammary epithelial cells where Cre was activated and any floxed alleles subsequently deleted. Thus, alterations in β-catenin driven tumorigenesis in these mice could be reliably accredited to *Cbfβ* status in this model.

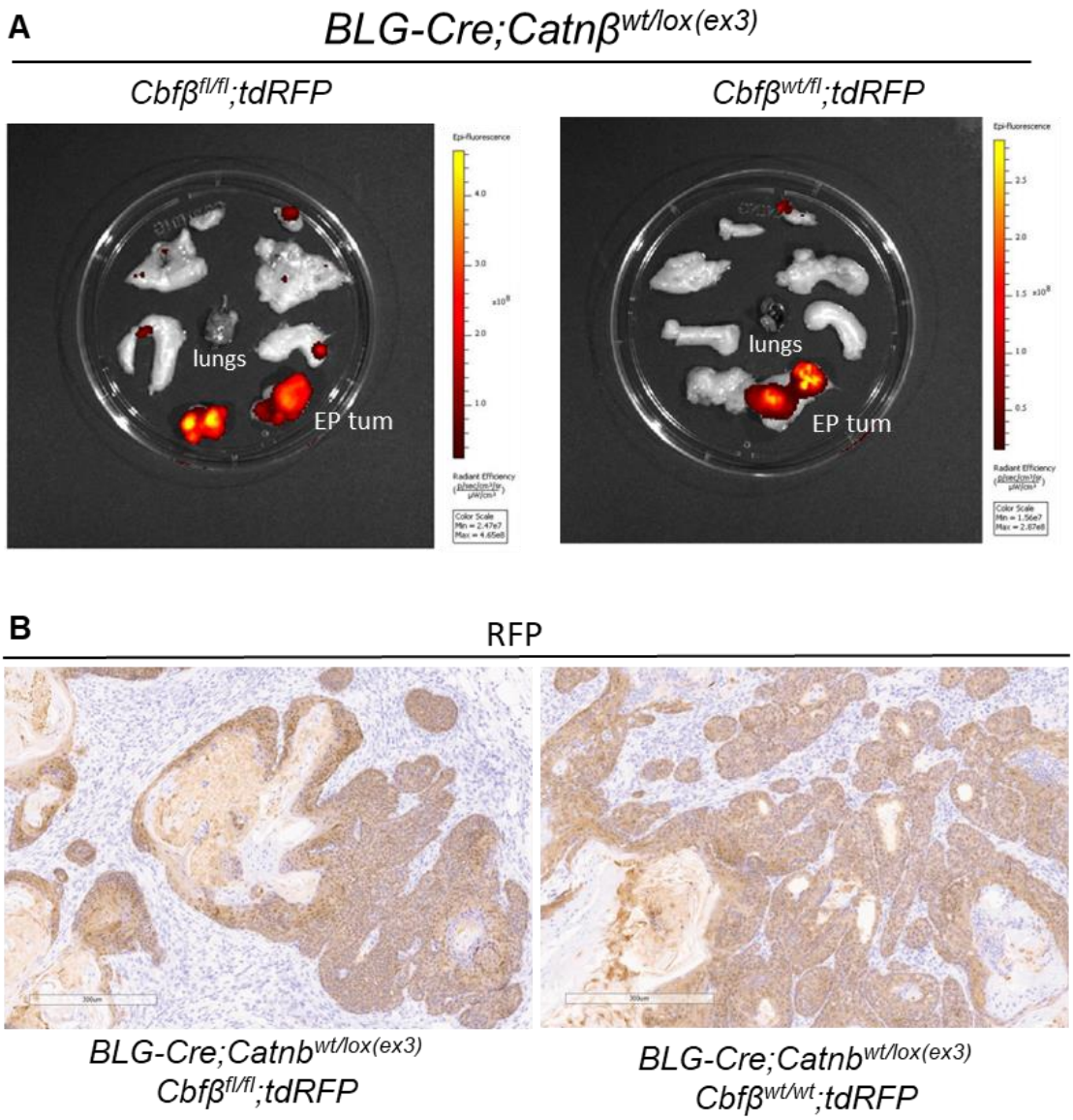

Figure 4.2: Activation of BLG-Cre detected through RFP expression.

(A) Representative mages acquired *ex vivo* on an IVIS Specturm showing red RFP fluorescence in tumours harvested at clinical endpoint. All 10 mammary glands and lungs were dissected, endpoint tumour (EP tum) is indicated. (B) Representative IHC images confirming RFP expression in mammary epithelial cells in end-stage mammary tumours. Scale bar: 300μm.

4.2.2. Loss of *Cbfβ* accelerates Wnt/β-catenin driven mammary tumorigenesis

The impact of heterozygous or homozygous loss of *Cbfβ* in the context of Wnt/β-catenin driven mammary cancer was studied through regular monitoring of *BLG-Cre;Catnb*$^{wt/lox(ex3)}$*;Cbfβ*$^{wt/fl}$ and *BLG-Cre;Catnb*$^{wt/lox(ex3)}$*;Cbfβ*$^{fl/fl}$ mice respectively. Mice with *BLG-Cre;Catnb*$^{wt/lox(ex3)}$*;Cbfβ*$^{wt/wt}$ alleles were used as *Cbfβ* wildtype controls. In *BLG-Cre;Catnb*$^{wt/lox(ex3)}$*;Cbfβ*$^{fl/fl}$ mice, the development of palpable tumours (size>5mm in any dimension, “clinical onset”) indicative of

disease onset was noticed as early 83 days from birth of the animal (Figure 4.3A). In comparison, time to clinical onset was significantly delayed in mice expressing at least one wildtype copy of *Cbfβ* (*Cbfβ*$^{wt/fl}$) while *Cbfβ* wildtype mice reached an average of 250 days in age without having developed any overt mammary tumours (Figure 4.3A). These results proved that loss of *Cbfβ* dramatically accelerates tumour initiation. As the disease progressed, a similar trend was observed in the rate of tumour progression from the point of initiation (Figure 4.3B). While time to reach disease endpoint was extended up to 65 days on average in *BLG-Cre;Catnb*$^{wt/lox(ex3)}$*;Cbfβ*$^{wt/wt}$ mice, this duration was significantly reduced in the *Cbfβ*$^{wt/fl}$ cohort (38 days) and even more so in *Cbfβ*$^{fl/fl}$ mice, which succumbed to disease within approximately 30 days from clinical onset. As depicted in Figure 4.3D, following the accelerated disease phenotype associated with loss of *Cbfβ,* overall survival was significantly reduced in *Cbfβ*$^{wt/fl}$ mice (222 days) compared to *Cbfβ*$^{wt/wt}$ mice (325 days), a pattern further exacerbated in *Cbfβ*$^{fl/fl}$ animals with a remarkably short median overall survival of only 120 days. Considering the marked difference in time to clinical onset across the cohorts compared to the more subtle differences noted in their tumour progression, it seems likely that the difference in overall survival can be attributed primarily to the significantly accelerated clinical onset in *Cbfβ*$^{fl/fl}$ mice. In this regard, these results indicate for the first time *in vivo* that loss of *Cbfβ* dramatically accelerates tumorigenesis and plays an important role in the initiation of Wnt driven mammary cancer.

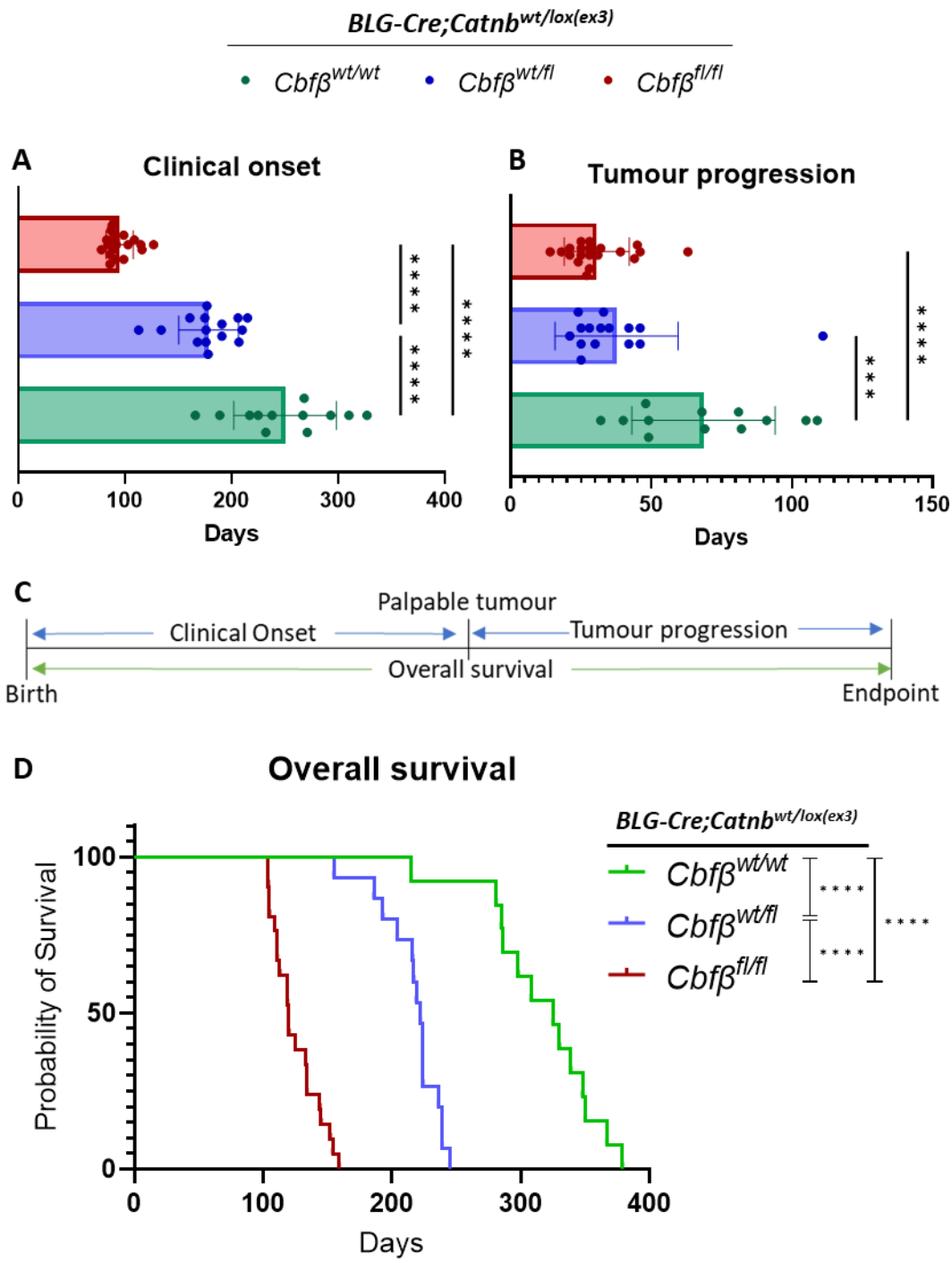

Figure 4.3: Loss of *Cbfβ* dramatically accelerates Wnt/B-catenin driven breast cancer.
Bar graph with dot plots comparing clinical onset (A) and tumour progression (B) in mice with wildtype (N=12), heterozygous (N=15) and homozygous (N=20) loss of *Cbfβ*. Each datapoint represents one individual mouse. (C) Schematic representation of the three parameters used to determine the impact of *Cbfβ* loss on mammary tumorigenesis. (D) Kaplan Meier curves comparing overall survival of *BLG-Cre;Catnb*$^{wt/lox(ex3)}$ mice carrying *Cbfβ*$^{wt/wt}$ (N=13), *Cbfβ*$^{wt/fl}$ (N=15) and *Cbfβ*$^{fl/fl}$ (N=21) alleles. GraphPad prism was used to perform ordinary one-way ANOVA and Tukey's multiple comparisons test for statistical analysis of dot plots and the Log-rank (Mantel-Cox) test for the Kaplan Meier curves. ***p<0.001, ****p<0.0001.

4.2.3. *Cbfβ* loss exacerbates Wnt/β-catenin driven mammary tumour pathology

Analysis of body weights (Figure 4.4A) supported the survival analysis data in showing that $Cbf\beta^{fl/fl}$ mice had significantly lower body weights at clinical endpoint as they succumbed to disease at a much younger age compared to $Cbf\beta^{wt/fl}$ and $Cbf\beta^{wt/wt}$ mice. For each mouse, the cumulative weight of all 10 mammary glands was also calculated (including non-tumour-burdened glands) (Figure 4.4B). Again, similar to the differences noted in body weight, potentially due to the age-related higher fat content in the older $Cbf\beta^{wt/wt}$ mice, a significantly lower total mammary weight was apparent in $Cbf\beta^{fl/fl}$ mice compared the former group. Subsequently, tumour burden was calculated as a ratio of the total mammary gland weight to the total body weight (Figure 4.4C). While tumour burden did not significantly differ between the three cohorts, the total number of affected mammary glands (Figure 4.4D) were significantly higher in $Cbf\beta^{fl/fl}$ mice compared to $Cbf\beta^{wt/fl}$ mice. This indicated that homozygous loss of *Cbfβ* in mammary epithelial cells increased their propensity to undergo Wnt/β-catenin induced transformation which elicited a greater number of neoplastic lesions across multiple glands. Perhaps having one wildtype copy of this gene, provides some compensation to this effect. Although, not significant, similar to the $Cbf\beta^{wt/fl}$ cohort, $Cbf\beta^{wt/wt}$ mice seemed to develop slightly fewer number of lesions compared to those in the $Cbf\beta^{fl/fl}$ cohort.

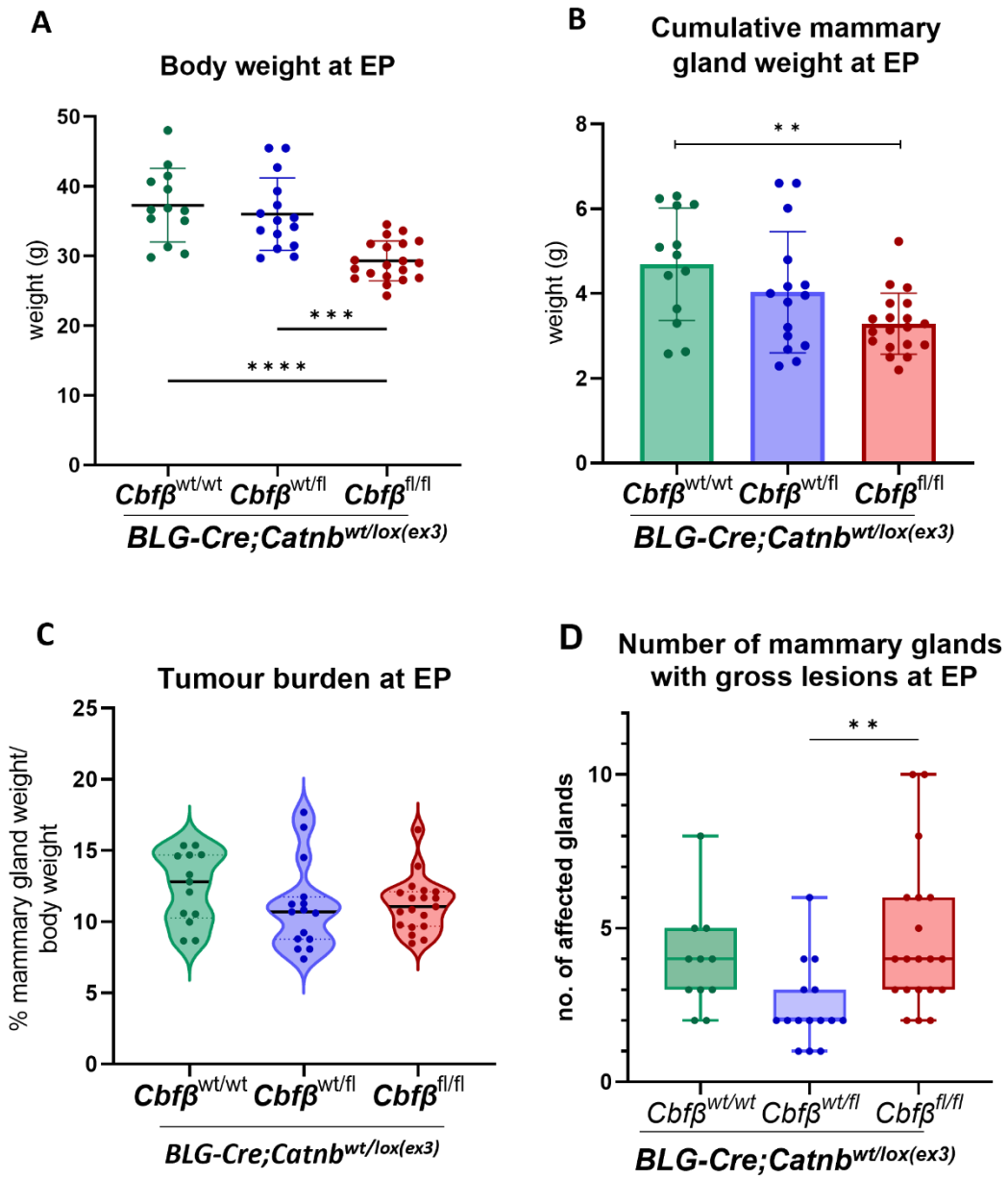

Figure 4.4: Interrogating the impact of *Cbfβ* loss on body weight, tumour burden and gross lesions in *BLG-Cre;Catnb*$^{wt/lox(ex3)}$ cohorts.

Body weights (A) and cumulative mammary gland weights (B) were recorded at clinical end point. (C) Violin plots showing changes in tumour burden across the three experimental cohorts. (D) Box and whiskers plot depicting changes in the number of mammary glands bearing gross lesions at clinical endpoint (EP). Data points represent individual mice. *Cbfβ*$^{wt/wt}$ N=13; *Cbfβ*$^{wt/fl}$ N=15; *Cbfβ*$^{fl/fl}$ N=19. Statistical test: One-way ANOVA and Tukey's multiple comparisons test. **p<0.01, ***p<0.001, ****p<0.0001.

The trends discussed above are highlighted in the representative gross pathology images of cohort mice bearing end-stage tumours (Figure 4.5). *Cbfβ*$^{wt/wt}$ mice showed a greater degree of heterogeneity in the number of glands affected by neoplastic lesions with some mice developing only one mammary tumour and others bearing multiple tumour-affected glands at clinical endpoint. *Cbfβ*$^{wt/fl}$ mice

displayed a slightly more consistent phenotype with tumours evident in roughly 2-3 glands per mouse on average. Comparatively, the disease phenotype appeared considerably exacerbated in *Cbfβ*$^{fl/fl}$ mice. As depicted in Figure 4.5, *Cbfβ*$^{fl/fl}$ mice exhibited multifocal tumours across multiple glands, with at least 3-4 glands displaying overt tumours at clinical endpoint. Almost all remaining glands in these mice presented smaller neoplastic lesions (black dotted circles) noticeable upon dissection, unlike their *Cbfβ*$^{wt/wt}$ and *Cbfβ*$^{wt/fl}$ counterparts which consisted of some seemingly unaffected glands alongside the tumour bearing ones. Curiously, tumour development in *BLG-Cre;Catnb*$^{wt/lox(ex3)}$ mice with *Cbfβ*$^{wt/wt}$ and *Cbfβ*$^{wt/fl}$ seemed to primarily affect the cervical and thoracic mammary glands while end-stage tumours in *Cbfβ*$^{fl/fl}$ mice displayed tropism towards the abdominal and inguinal mammary glands.

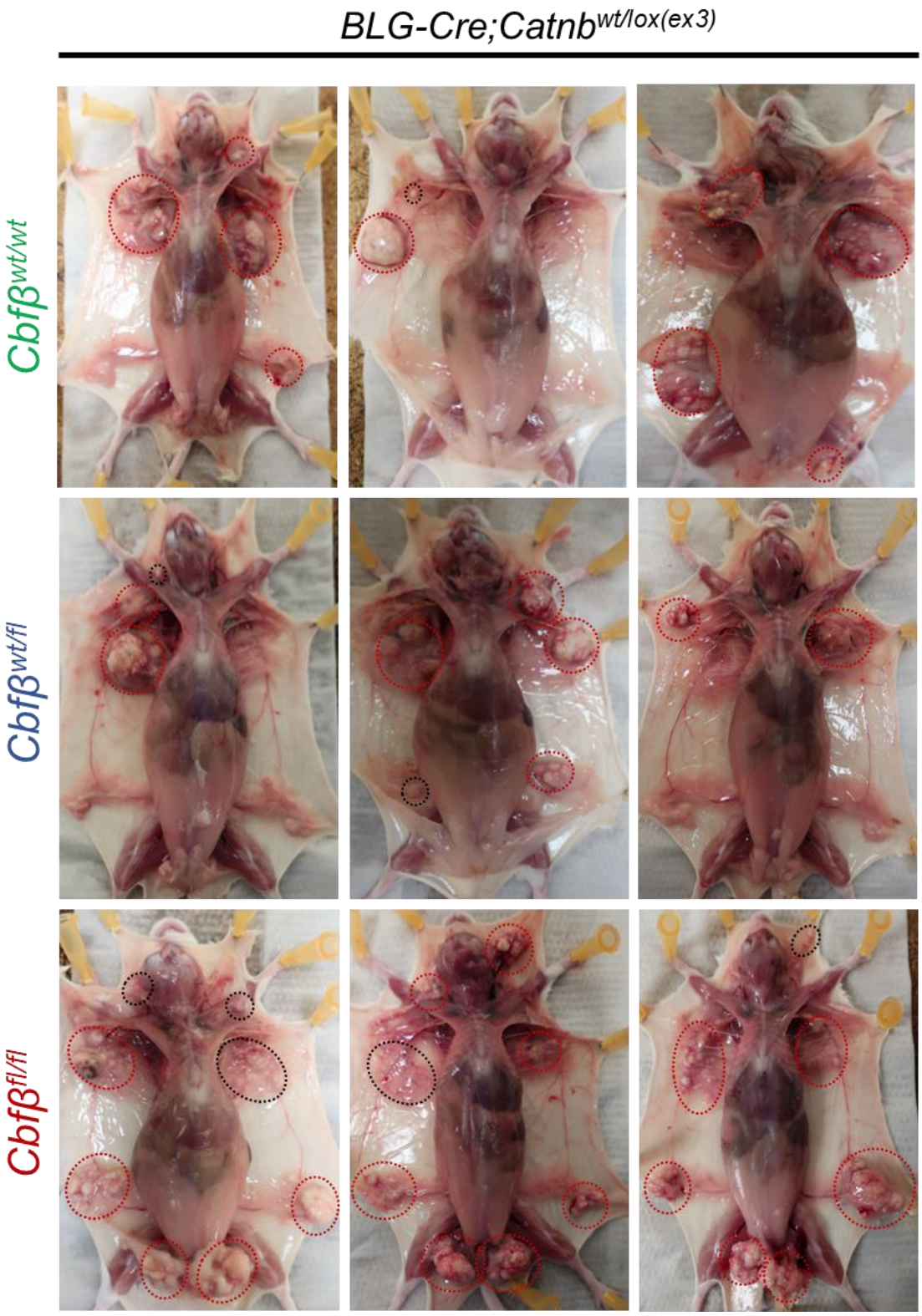

Figure 4.5: Loss of *Cbfβ* exacerbates mammary pathology at clinical endpoint in the *BLG-Cre;Catnb*$^{wt/lox(ex3)}$ model.

Representative images from N=3 mice per cohort display changes in the gross pathology. Red circles highlight overt mammary tumours palpable prior to dissection. Black circles denote small neoplastic lesions only noticed post-mortem.

4.2.4. Wnt/β-catenin activation in the murine mammary gland yields a highly keratinous, adeno-squamous phenotype

Post-mortem analysis of experimental cohorts revealed that Wnt/β-catenin activation in the mammary epithelium resulted in the formation of overtly keratinous tumours. In order to characterise Wnt/β-catenin tumours deficient of *Cbfβ,* mammary tumours at clinical endpoint were fixed in formalin, embedded in paraffin and the subsequent tissue sections used for histopathological analysis. H&E staining of tumour sections from both *BLG-Cre;Catnb*$^{wt/lox(ex3)}$*;Cbfβ*$^{wt/wt}$ and *BLG-Cre;Catnb*$^{wt/lox(ex3)}$*;Cbfβ*$^{fl/fl}$ mice displayed obliteration of normal mammary infrastructure due to the development of highly differentiated lesions resembling the adeno-squamous phenotype observed in human metaplastic breast cancers (Figure 4.6). The normal mammary ductal structure was replaced by layers of epithelial cells around keratinous centres surrounded by extensive connective tissue. This resembled the trans-differentiated mammary epithelial-to-epidermal phenotype characteristic of mammary tumours driven through constitutive β-catenin (Miyoshi et al., 2002).

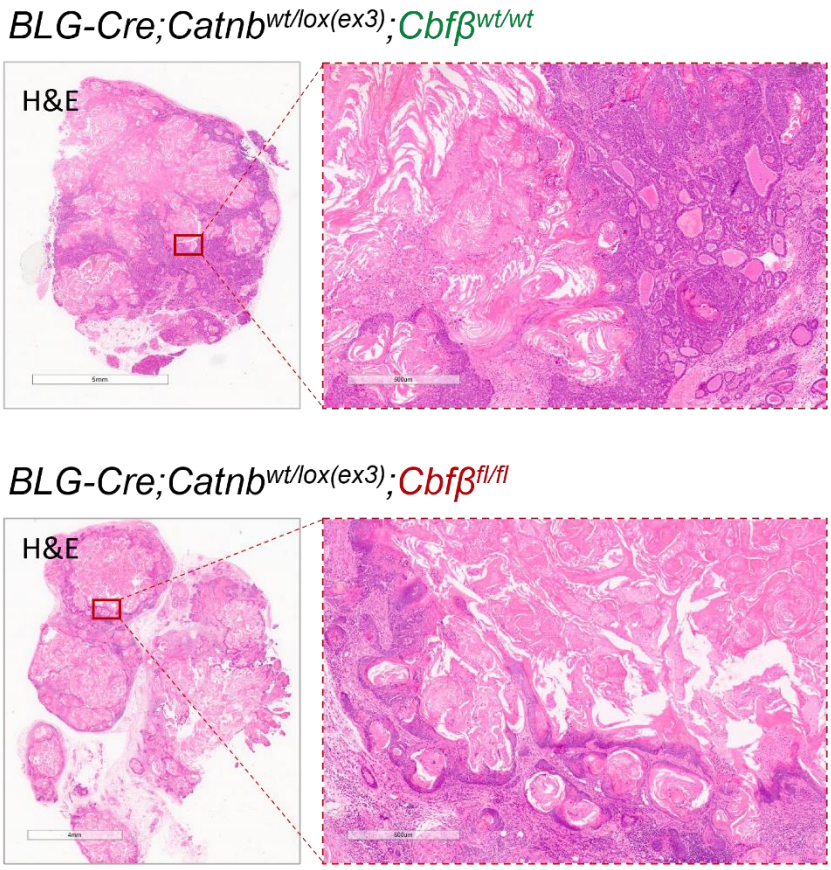

Figure 4.6: Representative H&E images of Wnt/β-catenin driven mammary tumours. Tumours derived at clinical endpoint from *BLG-Cre;Catnb*$^{wt/lox(ex3)}$*;Cbfβ*$^{wt/wt}$ and *BLG-Cre;Catnb*$^{wt/lox(ex3)}$*;Cbfβ*$^{fl/fl}$ mice. Left panel scale bar: 5mm. Right panel scale bar: 600μm.

Through IHC of these tissue sections, epithelial cells within the tumours showed positive staining for ER while highly proliferative tumour cells, as indicated by positive ki67 staining, seemed to reside near the edges of these lesions (Figure 4.7). However, given the diffuse pattern of ER staining, further confirmation is required to determine the ER status of these *BLG-Cre;Catnb*$^{wt/lox(ex3)}$ end-stage mammary status.

Additional IHC analysis of these areas stained for luminal (CK18), and basal (CK14) markers revealed an interesting pattern (Figure 4.7). In both cohorts of *BLG-Cre;Catnb*$^{wt/lox(ex3)}$ mice, the external edges of the keratinous cores or distended mammary ducts consisted of CK18 positive cells surrounded by CK14 positive basal epithelial cells. However, tumours from *BLG-Cre;Catnb*$^{wt/lox(ex3)}$*;Cbfβ*$^{fl/fl}$ seemed to contain thicker layers of basal epithelia compared to those from *BLG-Cre;Catnb*$^{wt/lox(ex3)}$*;Cbfβ*$^{wt/wt}$ mice. Additionally, the former samples appeared to contain fewer proportions of CK18 positive luminal cells throughout the tumour landscape compared to samples from the latter cohort. These results indicated

that loss of *Cbfβ* in a Wnt/β-catenin activated mammary environment might be preferentially inducing the expansion of basal cells. However, further quantification and investigation into this qualitative correlation is required to confirm this observation.

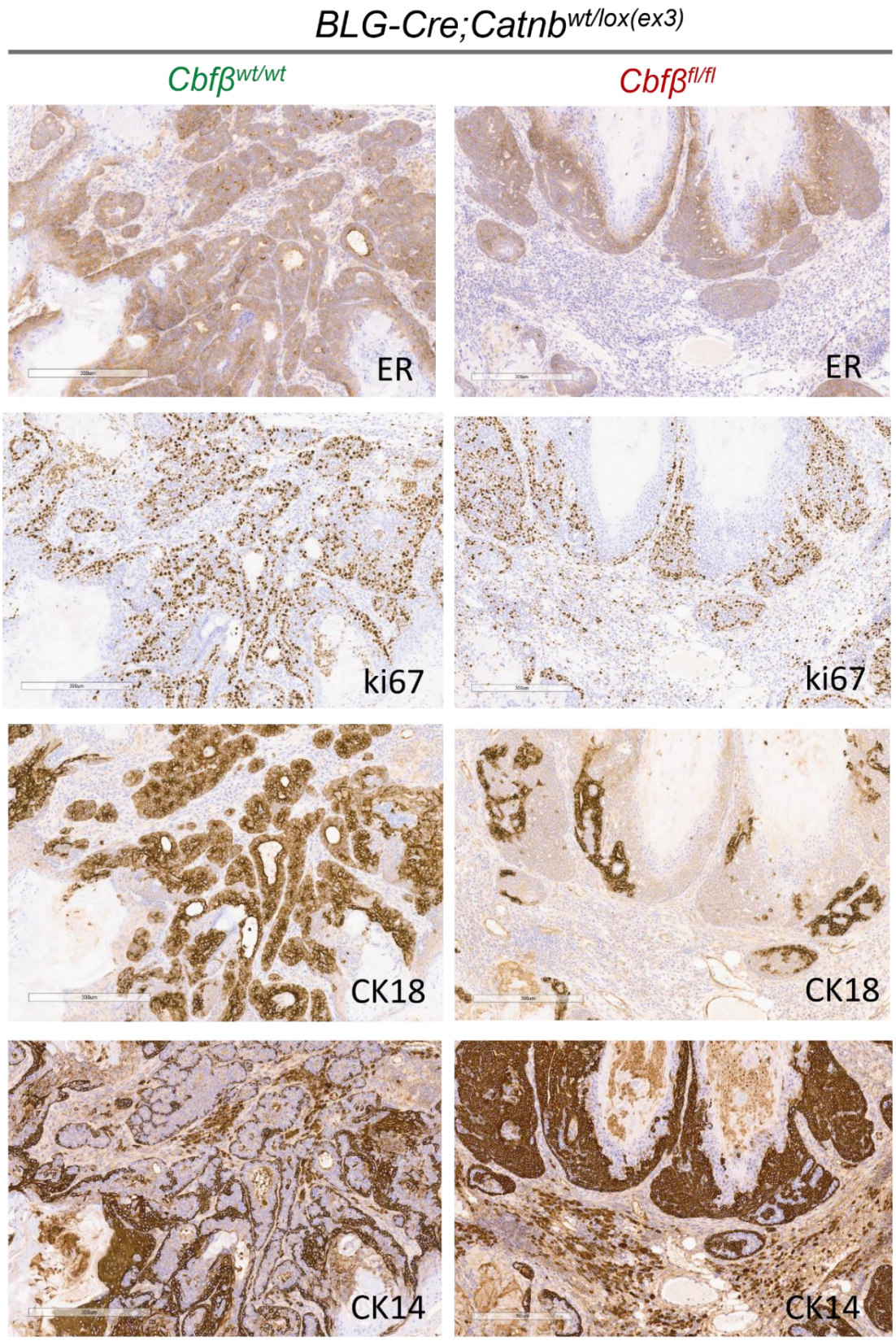

Figure 4.7: Histopathological analysis of *BLG-Cre;Catnb*$^{wt/lox(ex3)}$ tumours with and without *Cbfβ*.

Tumours were harvested at clinical endpoint and stained for ER, ki67, luminal epithelial cell marker: CK18 and basal epithelial cell marker: CK14. Images are representative of N=4 glands from induvial mice per cohort. Scale bare: 300μm.

4.2.5. Loss of *Cbfβ* does not induce mammary tumorigenesis in the absence of Wnt/β-catenin activation *in vivo*

In consideration of the potent oncogenic effect exerted upon loss of *Cbfβ* in the context of activation Wnt/β-catenin signalling, it was questioned whether deletion of this tumour suppressor would affect normal mammary development or induce mammary transformation in the absence of Wnt/β-catenin activation. As such, pubertal (9-week-old) and aged (1 year) cohorts of $Cbf\beta^{wt/wt}$ and $Cbf\beta^{fl/fl}$ mice wildtype for Wnt/β-catenin were analysed for any signs of impaired mammary development or existence of neoplastic lesions within the mammary epithelium.

Consequently, body weight and the cumulative mammary gland weight did not seem to differ significantly in pubertal mice with and without *Cbfβ (*Figure 4.8A). Likewise, in mice aged to 1 year, *Cbfβ* loss did not seem to affect these parameters (Figure 4.8A). Analysis of mammary gland wholemounts using the inguinal gland from 9-week-old mice displayed healthy morphology in $Cbf\beta^{fl/fl}$ mice (Figure 4.8B). Similarly, at 1 year of age, mammary infrastructure in both $Cbf\beta^{wt/wt}$ and $Cbf\beta^{fl/fl}$ mice remained comparable (Figure 4.8B). Additionally, the absence of any overt hyperplasia in the mammary wholemounts suggested that loss of *Cbfβ* alone was perhaps not enough to induce mammary transformation *in vivo*. These findings were validated by histological analysis of formalin fixed mammary glands from both cohorts in pubertal (Figure 4.9) and aged mice (Figure 4.10). No signs of pre-neoplastic lesions were observed in any of the samples examined. Furthermore, ki67 expression indicative of actively proliferating cells remained comparable in mice with and without *Cbfβ*. Tissue sections stained for luminal (CK18) and basal (CK14) markers also indicated towards normal development of murine mammary glands in both $Cbf\beta^{wt/wt}$ and $Cbf\beta^{fl/fl}$ regardless of their age. Both cohorts also displayed ER positive ducts – with evident nuclear staining although mammary glands from $Cbf\beta^{wt/wt}$ mice seemed to exhibit slightly stronger ER staining compared to $Cbf\beta^{fl/fl}$ mice (Figure 4.11).

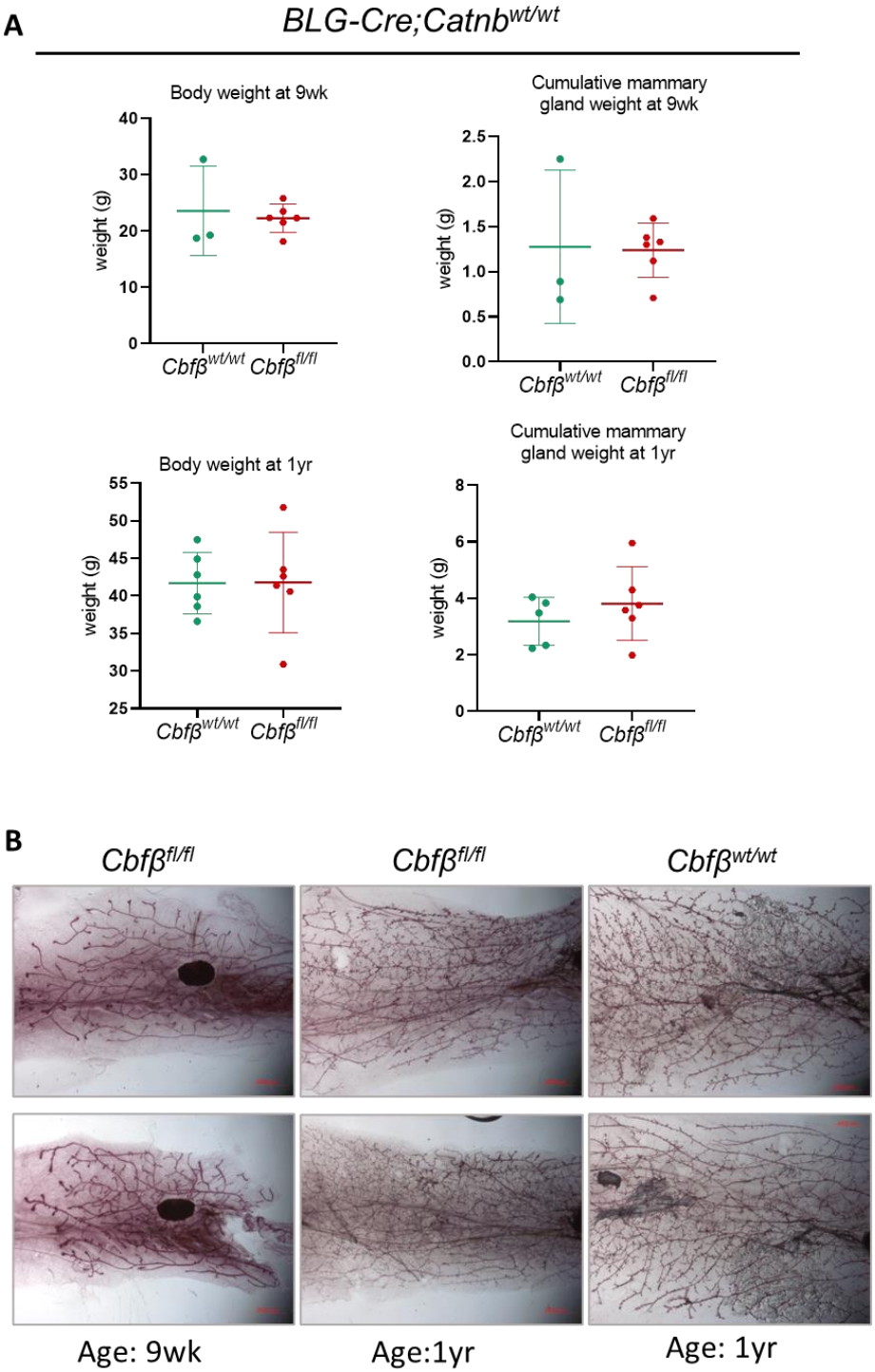

Figure 4.8: Loss of *Cbfβ* does not impact mammary development in the absence of Wnt/β-catenin activation.

(A) Dot plots showing body weights and cumulative mammary gland weights at 9 weeks (top panel) and 1 year of age (bottom panel) from *BLG-Cre;Catnb*$^{wt/wt}$ mice with *Cbfβ*$^{wt/wt}$ or *Cbfβ*$^{fl/fl}$. (B) Representative images of mammary gland wholemounts from *Cbfβ*$^{wt/wt}$ and *Cbfβ*$^{fl/fl}$ mice at 9 weeks and 1 year of age. Error bars represent standard deviation of the mean weights. Data points represent individual mice. For 9-week cohorts *Cbfβ*$^{wt/wt}$ (N=3) and *Cbfβ*$^{fl/fl}$ (N=6). For 1-year aged cohorts *Cbfβ*$^{wt/wt}$ (N=5) and *Cbfβ*$^{fl/fl}$ (N=6). Wholemount images are representative of N=3 glands from 3 separate mice per cohort. Scale bar: 2000μm. Statistical analysis: Student's unpaired t-test.

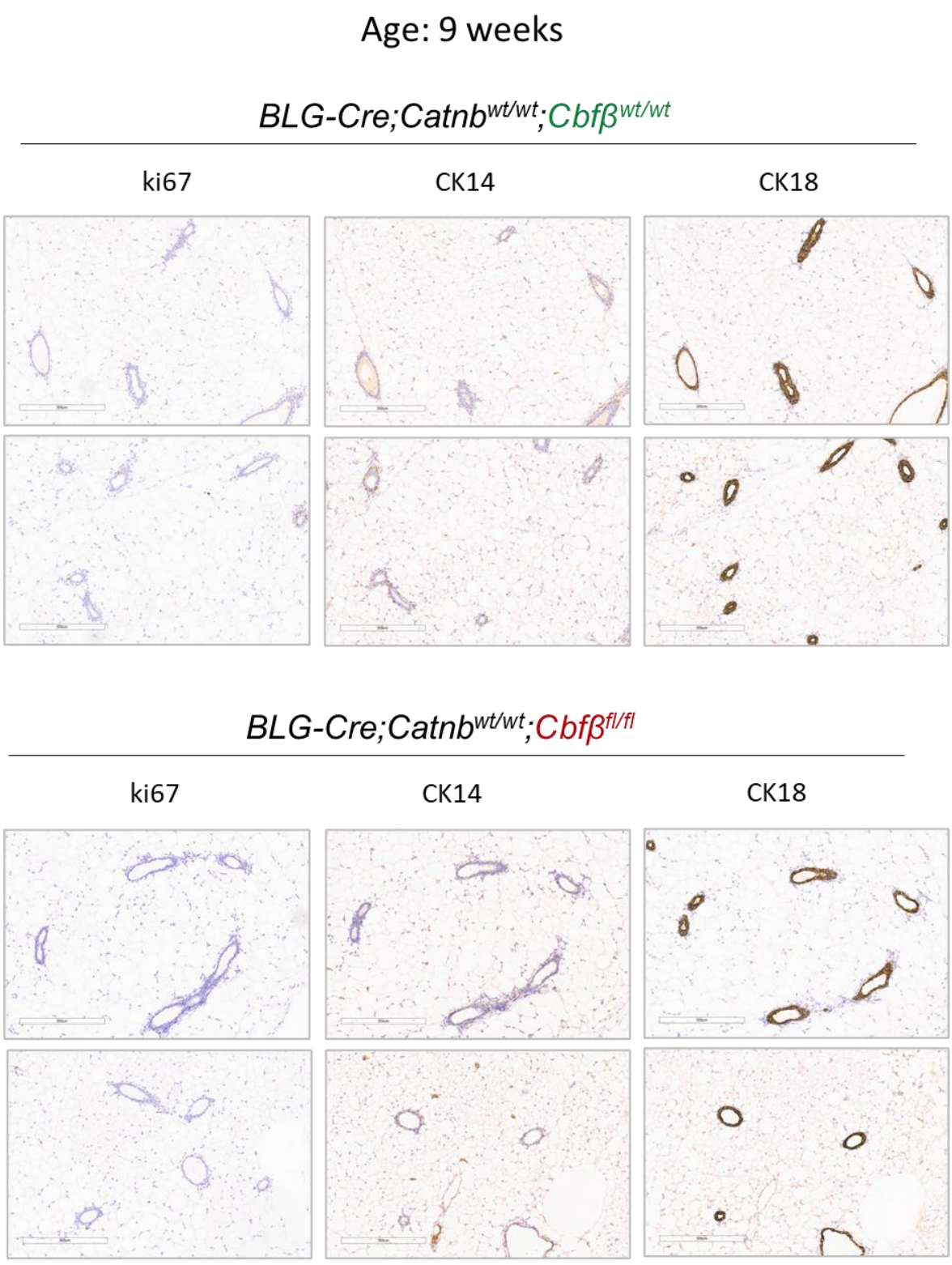

Figure 4.9: Histological analysis of 9 week old mouse mammary glands of *BLG-Cre;Catnb*$^{wt/wt}$ mice with and without *Cbfβ*.

Each panel consists of tissue sections from the inguinal mammary gland from two individual mice. Images are representative of N=4 glands from 4 separate mice per cohort. IHC staining for ki67, CK14 and CK18 from the inguinal mammary gland. Scale bar: 200μm.

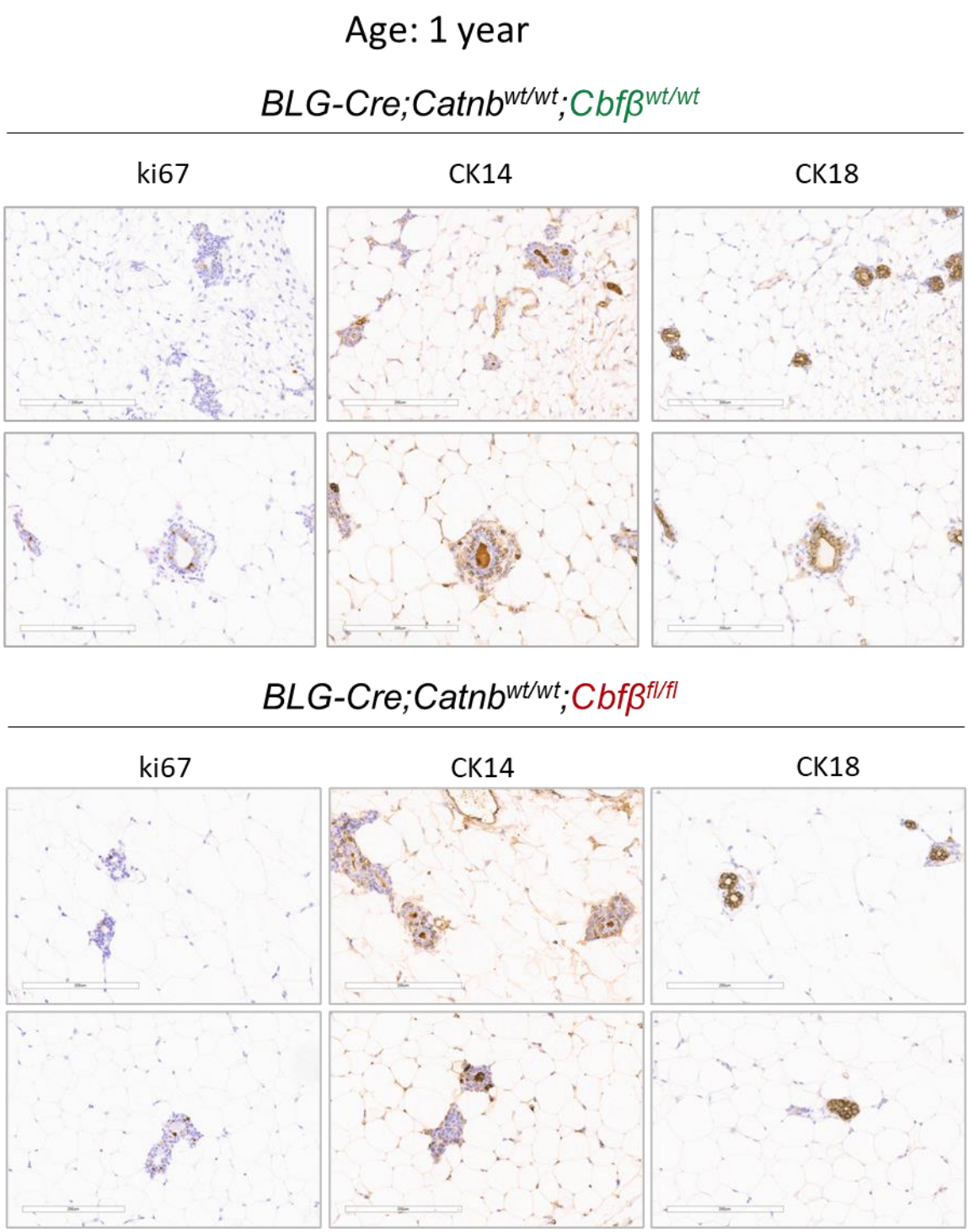

Figure 4.10: Histological analysis of 1 year old mouse mammary glands of *BLG-Cre;Catnb*$^{wt/wt}$ mice with and without *Cbfβ*.

Each panel consists of tissue sections from the inguinal mammary gland from two individual mice. Images are representative of N=4 glands from 4 separate mice per cohort. IHC staining for ki67, CK14 and CK18 from the inguinal mammary gland. Scale bar: 200µm.

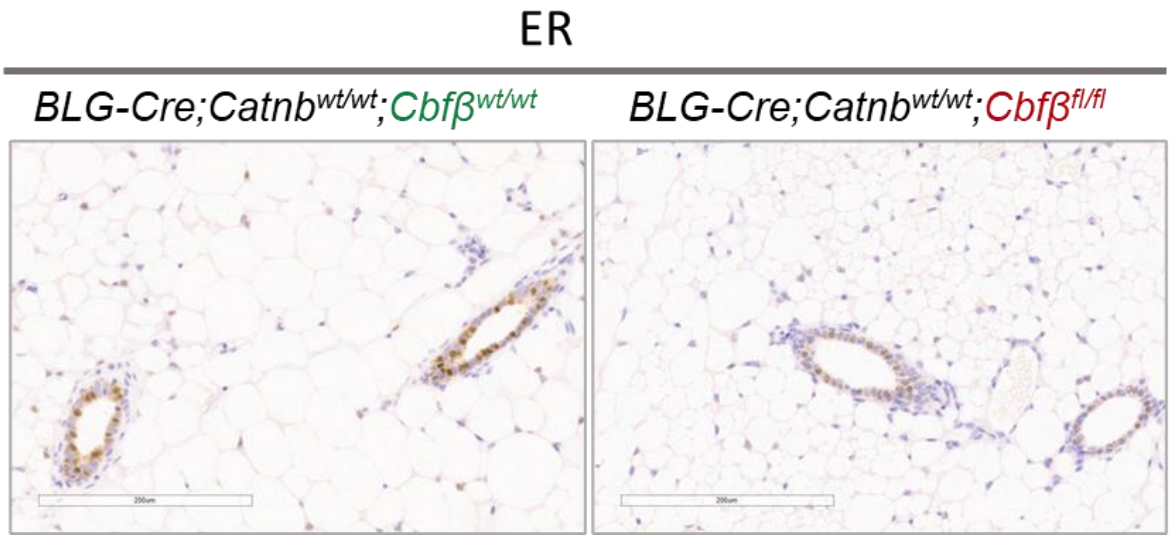

Figure 4.11: Representative IHC images of normal glands from 9 week old *BLG-Cre;Catnb*$^{wt/wt}$ mice with positive ER staining.

Images are representative of N=4 mice per cohort. Scale bar: 200μm.

4.2.6. Combined deletion of *Runx1* and *Runx2* further accelerates tumorigenesis compared to *Cbfβ* loss in the Wnt/β-catenin driven breast cancer setting

Originally, the *BLG-Cre;Catnb*$^{wt/lox(ex3)}$*;Runx1*$^{fl/fl}$*;Runx2*$^{fl/fl}$ model was maintained on a mixed background strain of mice. Therefore, for a strain matched comparison with the current *Blg-Cre;Catnb*$^{wt/lox(ex3)}$*;Cbfβ*$^{fl/fl}$ model, the same line was generated on a pure FVB background. As CBFβ is known to function in close collaboration with RUNX proteins, it was important to directly compare its loss to the combined loss of *Runx1* and *Runx2* in the Wnt/β-Catenin driven breast cancer setting. In this regard, it was hypothesised that loss of the transcription co-factor would phenocopy loss of its RUNX counterparts. Therefore, tumour growth and progression in the two cohorts of *BLG-Cre;Catnb*$^{wt/lox(ex3)}$ mice with either *Runx1*$^{fl/fl}$ or *Runx1*$^{fl/fl}$*;Runx2*$^{fl/fl}$ alleles were compared to cohorts with *Cbfβ*$^{fl/fl}$ and *Cbfβ*$^{wt/fl}$ alleles (as shown in Figure 4.3). *BLG-Cre;Catnb*$^{wt/lox(ex3)}$ mice possessing wildtype copies of *Cbfβ* (*Cbfβ*$^{wt/wt}$), which were also wildtype for *Runx1* and *Runx2* (*Runx1*$^{wt/wt}$*;Runx2*$^{wt/wt}$) were used as controls.

Compared to the *Cbfβ*$^{wt/wt}$*;Runx1*$^{wt/wt}$*;Runx2*$^{wt/wt}$ control cohort (hereafter WT), and in keeping with previous results (A Riggio PhD) (Riggio, 2017) loss either *Runx1* alone or *Runx1* and *Runx2* simultaneously (Runx1-Runx2) resulted in significantly reduced overall survival indicating acceleration of disease (Figure 4.12A). These

results, once superimposed with survival data of *Cbfβ*$^{fl/fl}$ and *Cbfβ*$^{wt/fl}$ mice from Figure 4.3D revealed valuable information regarding the relationship between RUNX and CBFβ and their tumour suppressive functions in this disease setting. For instance, *Runx1* loss appeared to phenocopy heterozygous loss of *Cbfβ* in reducing overall survival of *BLG-Cre;Catnb*$^{wt/lox(ex3)}$ mice as depicted by the overlapping Kaplan Meier curves showing median survival of 226 days and 222 days respectively (Figure 4.12A). This highlighted the importance of *Cbfβ* in the regulation and support of RUNX1 function as losing just one copy of the former was enough to mimic homozygous loss of the latter in Wnt/β-catenin driven mammary tumorigenesis. The more striking result, however, was how compared to *Cbfβ*$^{fl/fl}$ mice, *Runx1-Runx2* double knockout mice had significantly reduced overall survival (Figure 4.12A). This indicated that while both cohorts followed the same pattern in reducing overall survival in mice, deleting *Cbfβ* did not exactly phenocopy the combined loss of *Runx1* and *Runx2*. Noting the multifaceted role of CBFβ in not only transcription but also translation (Malik et al., 2019), it could be that loss of this protein potentially activates other compensatory mechanisms within the mammary cells that would otherwise not be triggered from the loss of RUNX1 and RUNX2.

Dissecting these results further, looking at clinical onset (Figure 4.12B), a similar pattern was noted with *Runx1*$^{fl/fl}$*;Runx2*$^{fl/fl}$ mice experiencing significant acceleration of disease onset compared to wildtype controls, *Cbfβ*$^{wt/fl}$ and *Runx1*$^{fl/fl}$ mice (Figure 4.12C). Compared to *Cbfβ*$^{fl/fl}$ mice which developed tumous within 95 days on averge, loss of *Runx1-Runx2* displayed reduction in the time to tumour onset (79 days), although not significant in this instance. Clinical onset of mammary tumours in response to loss of *Runx1* alone, as in the case of overall survival, was significantly reduced compared to control cohorts but again remained similar to the effects observed in mice expressing *Cbfβ*$^{wt/fl}$. Thus, in tumour initiation, the impact of *Runx1* loss appears comparable to the heterozygous loss of *Cbfβ*.

During tumour progression, however, this outcome was slightly altered (Figure 4.12D). In this case, taking out *Runx1* did not seem to mimic heterozygous loss of *Cbfβ*. While *Runx1*$^{fl/fl}$ mice did not show any significant differences in the time to disease progression compared to the control cohort, in comparison to mice in the *Cbfβ*$^{wt/fl}$ cohort (as well as *Cbfβ*$^{fl/fl}$ and *Runx1*$^{fl/fl}$*;Runx2*$^{fl/fl}$ mice) taking out *Runx1*

seemed to have an almost decelerating effect on tumour progression. This suggested that during the later stages of oncogenesis, loss of *Runx1* may be somewhat disadvantageous to tumour growth. Similar to $Cbf\beta^{fl/fl}$ mice, taking out both *Runx1* and *Runx2* led to dramatic acceleration in tumour progression compared to control mice. Albeit not significant, *Runx1-Runx2* loss displayed a slightly greater impact in accelerating tumour progression (21 days on average) compared to homozygous *Cbfβ* loss (31 days).

Thus, although the differences between $Cbf\beta^{fl/fl}$ and $Runx1^{fl/fl}$;$Runx2^{fl/fl}$ cohorts in clinical onset and tumour progression were slim, the combined loss of *Runx1* and *Runx2* consistently lead to further acceleration of tumorigenesis– which ultimately resulted in a significant reduction in the overall survival of mice compared to $Cbf\beta^{fl/fl}$ mice (Figure 4.12A).

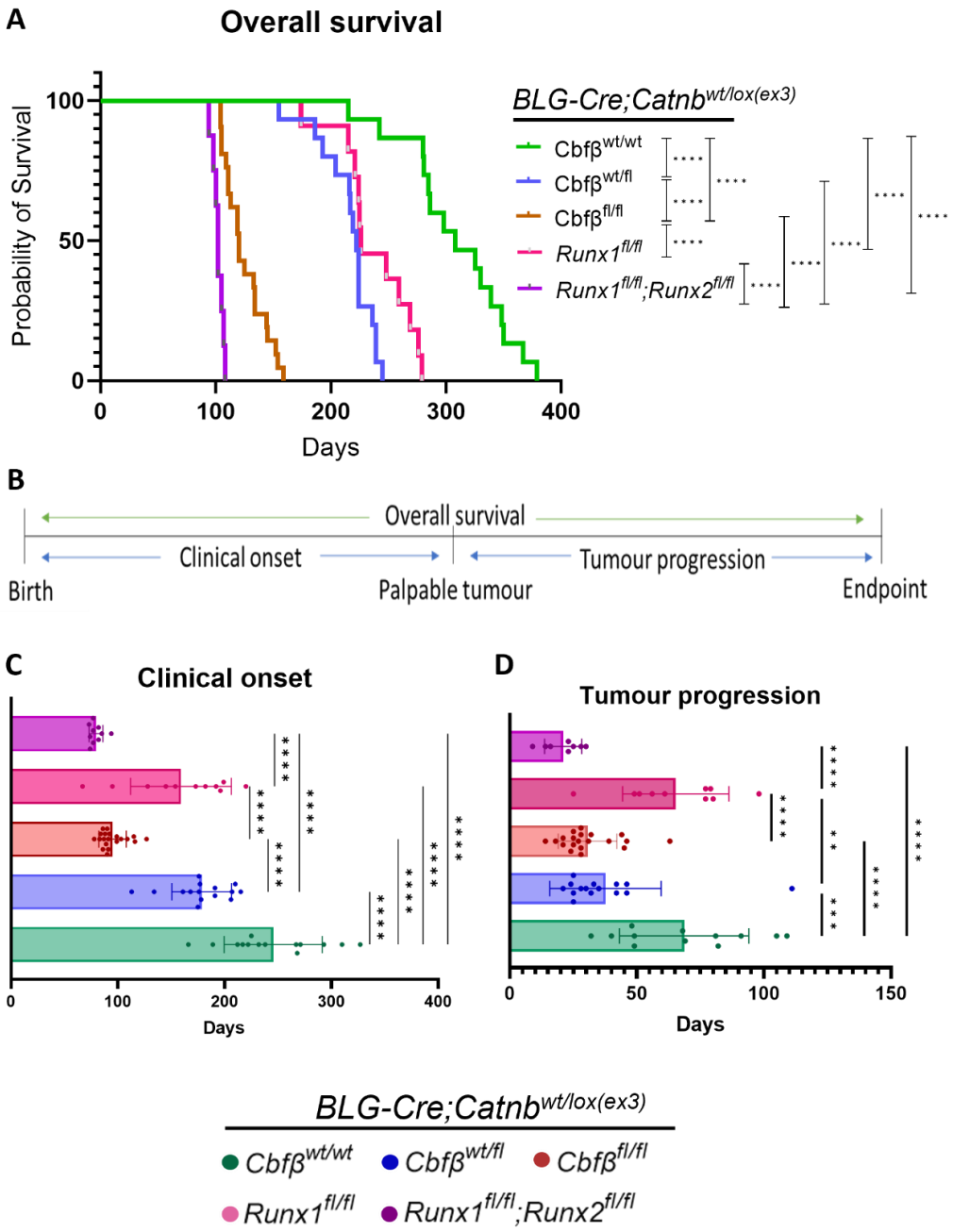

Figure 4.12: Combined loss of *Runx1* and *Runx2* leads to acceleration of Wnt/β-catenin driven tumorigenesis.

(A) Kaplan Meier curves comparing overall survival in *BLG-Cre;Catnb*$^{wt/lox(ex3)}$*;Runx1*$^{fl/fl}$ (N=11) and *BLG-Cre;Catnb*$^{wt/lox(ex3)}$*;Runx1*$^{fl/fl}$*;Runx2*$^{fl/fl}$ (N=8) mice superimposed to those from Figure 4.3D. The *Cbfβ*$^{wt/wt}$ cohort (N=15) includes *BLG-Cre;Catnb*$^{wt/lox(ex3)}$*;Runx1*$^{wt/wt}$*;Runx2*$^{wt/wt}$ mice. (B) Schematic representation of the three parameters used to determine the impact of the chosen genetic alterations on mammary tumorigenesis. (C) Time to clinical onset of *BLG-Cre;Catnb*$^{wt/lox(ex3)}$*;Runx1*$^{fl/fl}$ (N=11) and *BLG-Cre;Catnb*$^{wt/lox(ex3)}$*;Runx1*$^{fl/fl}$*;Runx2*$^{fl/fl}$ (N=10) mice and D) tumour progression of *BLG-Cre;Catnb*$^{wt/lox(ex3)}$*;Runx1*$^{fl/fl}$ (N=11) and *BLG-Cre;Catnb*$^{wt/lox(ex3)}$*;Runx1*$^{fl/fl}$*;Runx2*$^{fl/fl}$ (N=9) mice compared to *Cbfβ*$^{wt/wt}$ *Cbfβ*$^{wt/fl}$ and *Cbfβ*$^{fl/fl}$ cohorts. Graphs have been superimposed to data from Figure 4.3A-B. Data points represent individual animals. Statistical tests: Log-Rank (Mantel-Cox) test for survival analysis, Tukey's multiple comparisons test for bar charts. **p<0.01, ***p<0.001, ****p<0.0001.

These results confirmed that while loss of *Cbfβ* and the combined loss of *Runx1* and *Runx2* had similar growth promoting effects on Wnt/β-catenin driven tumorigenesis, the latter produced a slightly more aggressive disease phenotype. To investigate whether this translated into any changes on the oncogenic burden across the different cohorts, tumour burden was calculated using the total body weight and mammary gland weight recorded at clinical endpoint. Loss of *Runx1* increased tumour burden significantly compared to the control, $Cbf\beta^{wt/fl}$ and $Cbf\beta^{fl/fl}$ cohorts (Figure 4.13A). *Runx2* loss, on top of *Runx1* deletion did not seem to increase tumour burden any further, however, compared to $Cbf\beta^{fl/fl}$ cohorts these mice displayed a significant increase in tumour burden. This relationship was also evident when the number of tumour or neoplasm-burdened mammary glands at endpoint were compared across the cohorts (Figure 4.13B). The gross pathology observed in these cohorts are represented in Figure 4.13C. Strikingly, mice in both $Runx1^{fl/fl}$ and $Runx1^{fl/fl}$;$Runx2^{fl/fl}$ cohorts displayed overt multifocal tumours in all 10 mammary glands at clinical endpoint. This suggested that even though loss of *Runx1* alone is enough to drive Wnt/β-catenin mediated transformation in a similar number of mammary epithelial cells, the rate of tumorigenesis is restricted until *Runx2* is also lost. This would explain the difference in tumour onset and progression between $Runx1^{fl/fl}$ and $Runx1^{fl/fl}$;$Runx2^{fl/fl}$ cohorts. On the other hand, while homozygous *Cbfβ* loss and the co-deletion of *Runx1 and Runx2* had similar effects on the rate of Wnt/β-catenin mediated mammary tumorigenesis, the latter seemed to have a greater increase in the number of mammary epithelial cells that could undergo this oncogenic transformation.

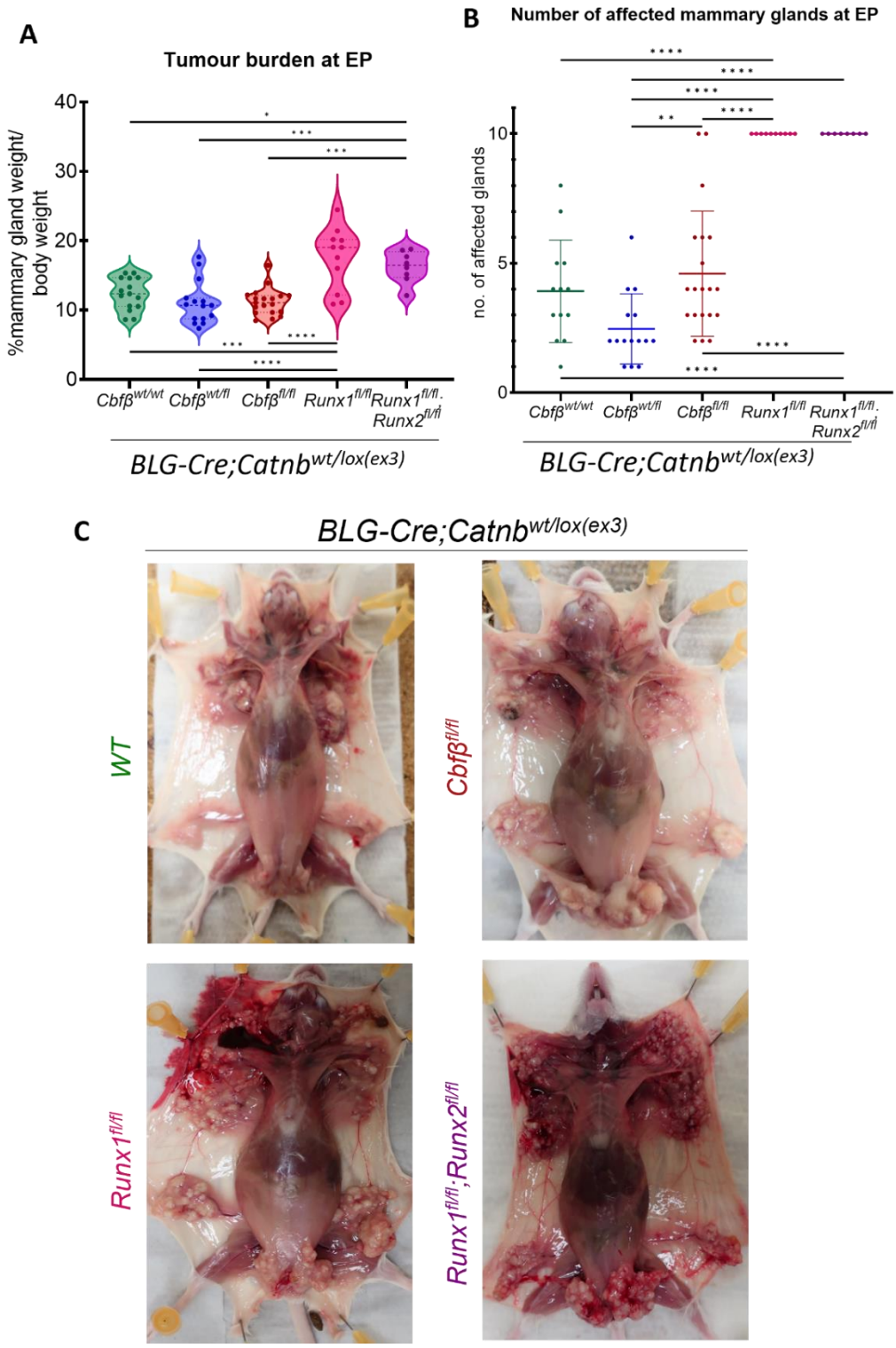

Figure 4.13: Gross pathology of *BLG-Cre;Catnb*$^{wt/lox(ex3)}$ mice exacerbated upon combined loss of Runx1 and Runx2.

(A) Tumour burden and (B) number of affected mammary glands with gross lesions at clinical endpoint (EP) compared among experimental cohorts. *Cbfβ*$^{wt/wt}$ (N=14), *Cbfβ*$^{wt/fl}$ (N=15), *Cbfβ*$^{fl/fl}$ (N=20), *Runx1*$^{fl/fl}$ (N=10) and *Runx1*$^{fl/fl}$;*Runx2*$^{fl/fl}$ (N=8). Data superimposed to those from Figure 4.4C and Figure 4.4D respectively. (C) Representative images of gross mammary pathology induced upon loss of *Cbfβ*, *Runx1 or Runx1-Runx2* in *BLG-Cre;Catnb*$^{wt/lox(ex3)}$ mice compared to the *WT* cohort Data points represent individual animals. Statistical tests: ANOVA and Tukey's multiple comparisons test. *p<0.05, **p<0.01, ***p<0.001, ****p<0.0001.

Together these results demonstrated the striking additive effects of losing either *Cbfβ* or *Runx1-Runx2* in Wnt driven breast cancer and proved that while RUNX and CBFβ work as a complex, their independent roles in mammary epithelial cells may have slightly different effects on tumorigenesis.

4.2.7. Transcriptomic analysis reveals loss of *Cbfβ* synergistically activates Wnt/β-catenin signalling

The dramatic acceleration of Wnt/β-catenin driven mammary carcinogenesis induced upon deletion of *Cbfβ* strongly hinted towards an inverse correlation between normal *Cbfβ* regulation and Wnt activation. Thus, in pursuit of understanding the relationship between *Cbfβ* and Wnt driven mammary tumorigenesis, RNAseq analysis was performed using RNA extracts from end-stage tumours of *BLG-Cre;Catnb*$^{wt/lox(ex3)}$*;Cbfβ*$^{wt/wt}$ (termed as WT) and *BLG-Cre; Catnb*$^{wt/lox(ex3)}$*;Cbfβ*$^{fl/fl}$ (referred to as CBFB_HOM) mice. Additionally, to compare and contrast this data with the transcriptomic changes brought about by the co-deletion of *Runx1* and *Runx2*, tumour derived RNA extracts from mice with *BLG-Cre;Catnb*$^{wt/lox(ex3)}$*;Runx1*$^{fl/fl}$*;Runx2*$^{fl/fl}$ (R1R2_HOM) was included in the RNAseq analysis. Figure 4.14 represents a schematic of this experimental plan.

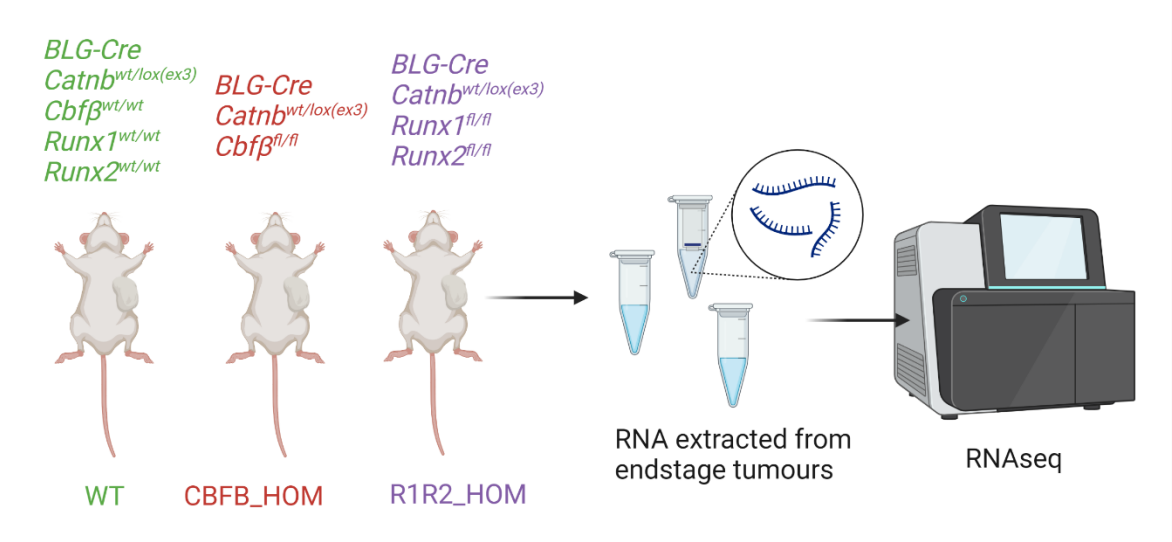

Figure 4.14: Schematic of the RNA sequencing experimental plan.
RNA was extracted from one end-stage tumour per mouse from *BLG-Cre;Catnb*$^{wt/lox(ex3)}$ mice with wildtype *Cbfβ*, *Runx1* and *Runx2* (WT, N=6) versus those with homozygous deletion of *Cbfβ* (*Cbfβ*$^{fl/fl}$) (CBFB _HOM, N=6) or *Runx1* and *Runx2* (*Runx1*$^{fl/fl}$;*Runx2*$^{fl/fl}$) (R1R2_HOM, N=6). RNA sequencing was conducted by CRUK Beatson Molecular technologies. Processing of raw RNAseq data, differential gene expression analysis and pathway analysis was assisted by Robin Shaw. Figure created using BioRender.com.

In the first instance, sequencing data from *BLG-Cre;Catnb*$^{wt/lox(ex3)}$;*Cbfβ*$^{fl/fl}$ and *BLG-Cre;Catnb*$^{wt/lox(ex3)}$;*Cbfβ*$^{wt/wt}$ tumours was compared to gain insight into the role of *Cbfβ* as a tumour suppressor in Wnt/β-catenin driven mammary cancer. As depicted by the volcano plot in Figure 4.15A, over 2500 genes were found to be differentially expressed in CBFB_HOM samples compared to WT. Pathway analysis using these genes revealed that the Wnt signalling network was the topmost relevant network altered in CBFB_HOM samples compared to WT (Figure 4.15B) Interestingly, immune regulatory pathways, and ionotropic receptor signalling pathways were also highlighted in this process. Considering the close association between Wnt signalling and modulation of cancer immune and metabolic processes, it is possible that upregulation of Wnt/β-catenin activity due to loss of *Cbfβ* resulted in alterations in these processes (El-Sahli et al., 2019). Gene set enrichment analysis further supported the results as gene sets involved in Wnt protein binding and Wnt activated receptor activity was found to be among the top 25 gene sets enriched in CBFB_HOM tumours (Figure 4.16A and B). While the differences between CBFB_HOM and WT samples did not reach significance, the trend suggested that loss of *Cbfβ* may be directly impacting the Wnt signalling cascade. Other gene sets that were found enriched in CBFB_HOM tumours included those involved in embryonic pattern specification, anterior and posterior axis

specification, bone growth, cartilage development and regulation of osteoblast differentiation. All of these processes are known to be under varying degrees of Wnt regulation and to some extent *Runx*/*Cbfβ* regulation (Yoshida et al., 2002; Logan and Nusse, 2004; Hikasa and Sokol, 2013; Sweeney, Cameron and Blyth, 2020).

A

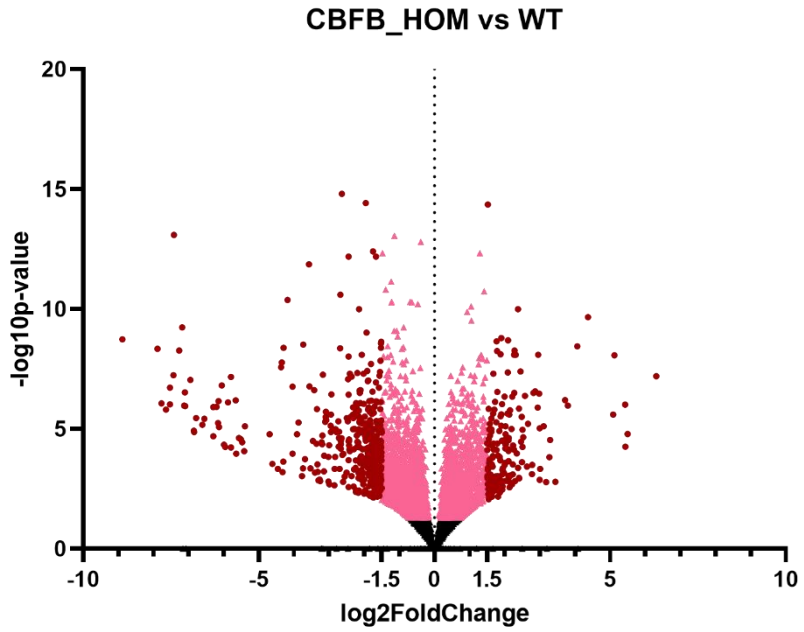

B

No	Network name	Processes	Size	Target	Pathways	p-Value	zScore	gScore
1	Tcf(Lef), Axin, Frizzled, WNT, Collagen II	canonical Wnt signaling pathway (40.0%), tissue development (82.0%), regulation of Wnt signaling pathway (52.0%), tube development (68.0%), epithelium development (72.0%)	50	16	87	3.02e-22	25.79	134.54
2	RBP4, NEBL, MTMR11, Syntrophin B1, ZNF804A	glutamate receptor signaling pathway (12.5%), ionotropic glutamate receptor signaling pathway (10.4%), synaptic transmission, glutamatergic (10.4%), peptide hormone processing (8.3%), signaling receptor ligand precursor processing (8.3%)	50	39	0	2.06e-73	63.73	63.73
3	GATA-2, MPEG1, GIPC3, SPINK8, GRAP	B cell affinity maturation (12.5%), peripheral B cell selection (12.5%), B cell selection (12.5%), positive regulation of antigen processing and presentation (12.5%), positive regulation of T-helper 1 type immune response (12.5%)	50	34	0	4.09e-61	56.06	56.06

Figure 4.15: Loss of *Cbfβ* in Wnt/β-catenin driven mammary cancer alters expression of 2500 genes and stimulates the Wnt pathway.

(A) Volcano plot showing significantly altered genes in CBFB_HOM tumours compared to WT tumours. Significantly altered genes with a fold change greater than 1.5 and padj <0.05 (red), significantly altered genes with padj <0.05 but fold change below 1.5 threshold (pink) and non-significant gene expression (black) are displayed. Data points represent individual genes. (B) Network analysis from MetaCore displaying the top 3 altered networks in CBFB_HOM samples compared to WT samples. Wnt signalling network highlighted in the red box.

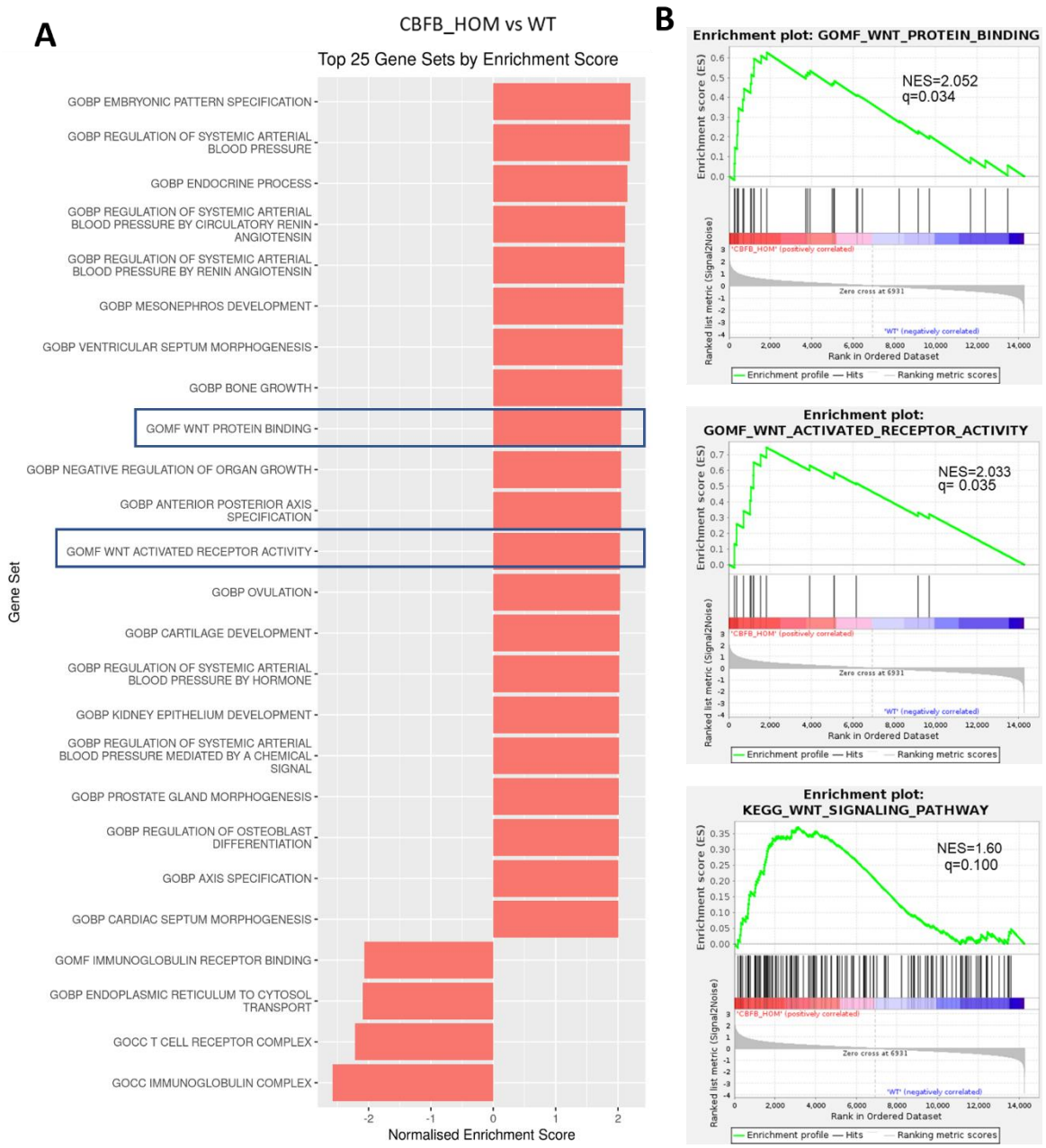

Figure 4.16: Gene set enrichment analysis shows loss of *Cbfβ* activates Wnt signalling.
(A) Overall Gene Ontology results. Wnt pathway gene sets highlighted in blue box. (B) Enrichment plots of Wnt activated receptor activity (top), Wnt protein binding (middle) and Wnt signalling pathway (bottom).

To further assess the impact of *Cbfβ* loss on Wnt signalling, expression patterns of manually curated Wnt pathway genes in CBFB_HOM samples were compared to those in WT samples. Among these, 22 genes involved in the regulation of canonical Wnt/β-catenin signalling, with functional roles both upstream and downstream of β-catenin, were found to be significantly altered in CBFB_HOM tumour samples (Figure 4.17A-B). Separating these genes into those encoding positive regulators of Wnt activation and negative regulators or inhibitors of the

signalling cascade, revealed a remarkable relationship between *Cbfβ* loss and Wnt pathway activation. 19 out of the 22 genes were those encoding proteins associated to activated Wnt signalling and expression of all these genes were significantly upregulated in CBFB_HOM tumours compared to WT tumours (Figure 4.18). Upregulation of multiple Frizzled receptors (*Fzd3, Fzd6, Fsd7, Fzd10os, Fzd10*), *Wnt3*, *Lgr6*, *Kremen2 (*a Wnt-Frizzled co-receptor involved in Wnt activation) indicated direct Wnt driven activation of the canonical signalling pathway in this cohort. Similarly, elevated levels of genes encoding various members of the TCF/LEF family such as *Tcf7, Tcfl5, Tcf4, Lef1* as well as Wnt/β-catenin target genes *Mycn* and C*cnd1* further suggested that loss of *Cbfβ* facilitated in propelling Wnt/β-catenin mediated transcriptional regulation in mammary tumour cells. Expression of *Ror2*, an alternative receptor of Wnt ligands in the non-canonical pathway was also increased in CBFB_HOM tumours. This protein is known to be upregulated in response to hyperactivation of Wnt/β-catenin signalling and has been implicated in facilitating breast tumour progression (Roarty et al., 2017). In further support of these results, *Cela1*, *Sfrp5* and *Dkk* genes involved in the downregulation or inhibition of the Wnt pathway were significantly downregulated in the CBFB_HOM tumour samples compared to WT Figure 4.18. Therefore, it appears that not only does loss of *Cbfβ* expedite the advancement of Wnt/β-catenin signalling, but it also removes some of the "brakes" in the system to favour its unrestricted progression.

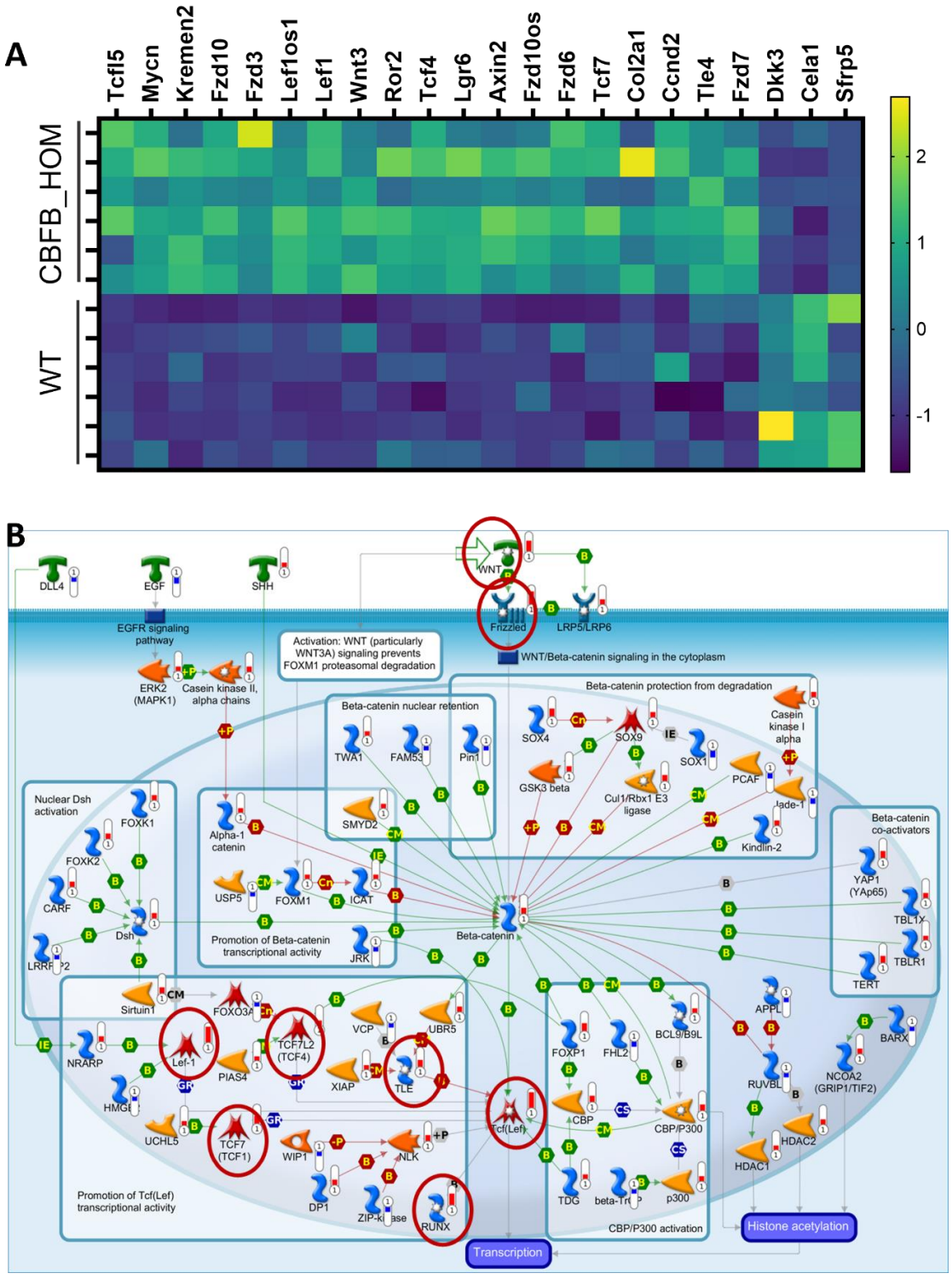

Figure 4.17: Wnt pathway genes altered upon *Cbfβ* deletion in *BLG-Cre;Catnb*$^{wt/lox(ex3)}$ tumours. (A) Heatmap shows expression pattern of the top 22 significantly altered genes (from a manually compiled list of 100 Wnt pathway genes) in CBFB_HOM tumours versus WT tumours. Heatmap generated using z-scores of gene expression values acquired from RNA sequencing of end-stage tumours. (B) Pathway map shows location of the altered Wnt pathway genes relative to β-catenin. Proteins encoded by the significantly altered genes highlighted in the heatmap are circled in red. Pathway map acquired from MetaCore. P-value threshold = 0.01. Absolute fold change threshold: 1.5 for CBFB _HOM samples (N=6) compared to WT samples (N=6).

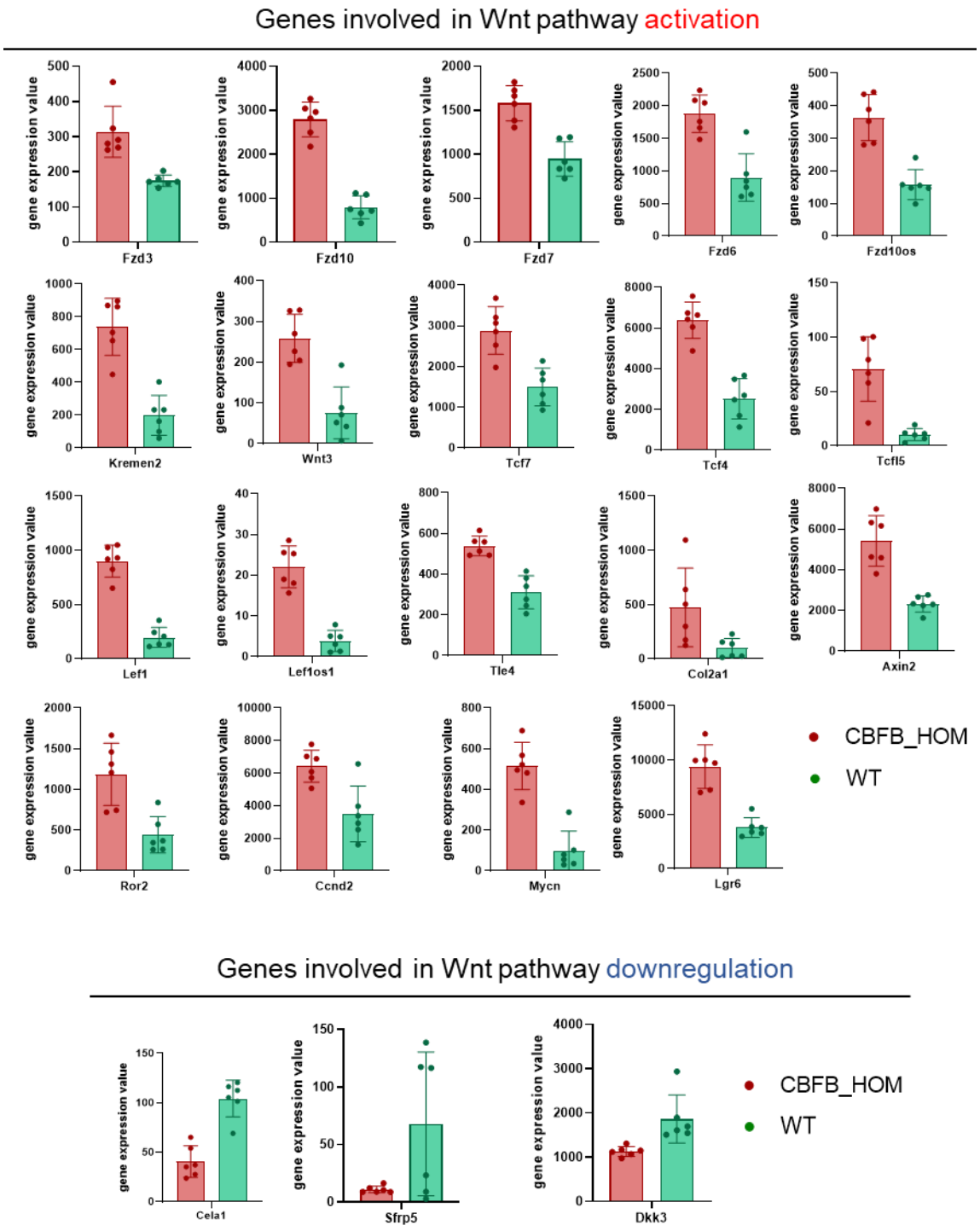

Figure 4.18: *Cbfβ* deletion in *BLG-Cre;Catnb*$^{wt/lox(ex3)}$ tumours upregulates Wnt pathway activating genes and downregulates Wnt pathway inhibitors.

Graphs generated from gene expression data acquired through RNA sequencing. Genes displayed were significantly altered in CBFB_HOM compared to WT with a padj<0.05 and an absolute fold change threshold of 1.5. Data points represent gene expression data from individual tumours from N=6 separate mice per cohort. Error bars represent standard deviation of the mean.

In addition to exploring the impact of *Cbfβ* loss on the direct regulators of canonical Wnt signalling, indirect influencers of this system such as the Notch signalling cascade were also investigated. Considering the intimate association

between Notch and Wnt signalling in the carcinogenic transformation of mammary epithelial cells (Ayyanan et al., 2006; Braune, Seshire and Lendahl, 2018), it was not surprising to find several genes encoding members of Notch pathway upregulated in CBFB_HOM tumours (Figure 4.19A). Notably gene expression of *Notch1*, *Jag1*, and *Maml2* and were significantly upregulated beyond a p-adjusted value of 0.05 and a fold-change threshold of 1.5 in CBFB_HOM tumours compared to WT samples. Albeit not significant, elevated levels of two additional Notch receptors: *Notch2* and *Notch3* and the Notch ligand *Jag2* were also noted in these cohorts. Additionally, expression of *Deltex1* (*Dxt1*), known to inhibit Notch signalling (X. Liu et al., 2021), was significantly downregulated in CBFB_HOM samples. These results suggested that alongside Wnt signalling, *Cbfβ* loss also activated the Notch signalling cascade. Notch mediated regulation of Wnt signalling has already been implicated in the induction of human mammary epithelial cells transformation (Ayyanan et al., 2006). It could be possible that through activating Notch signalling, *Cbfβ* loss adds an indirect stimulus in supplementing activation of Wnt signalling pathways (Figure 4.19B). The culmination of these effects, with this form of multi-layered approach to activating the Wnt/β-catenin network, could be leading to a hyper-accelerated tumorigenic process in the mammary epithelium as observed in *BLG-Cre;Catnb*$^{wt/lox(ex3)}$*;Cbfβ*$^{fl/fl}$ mice.

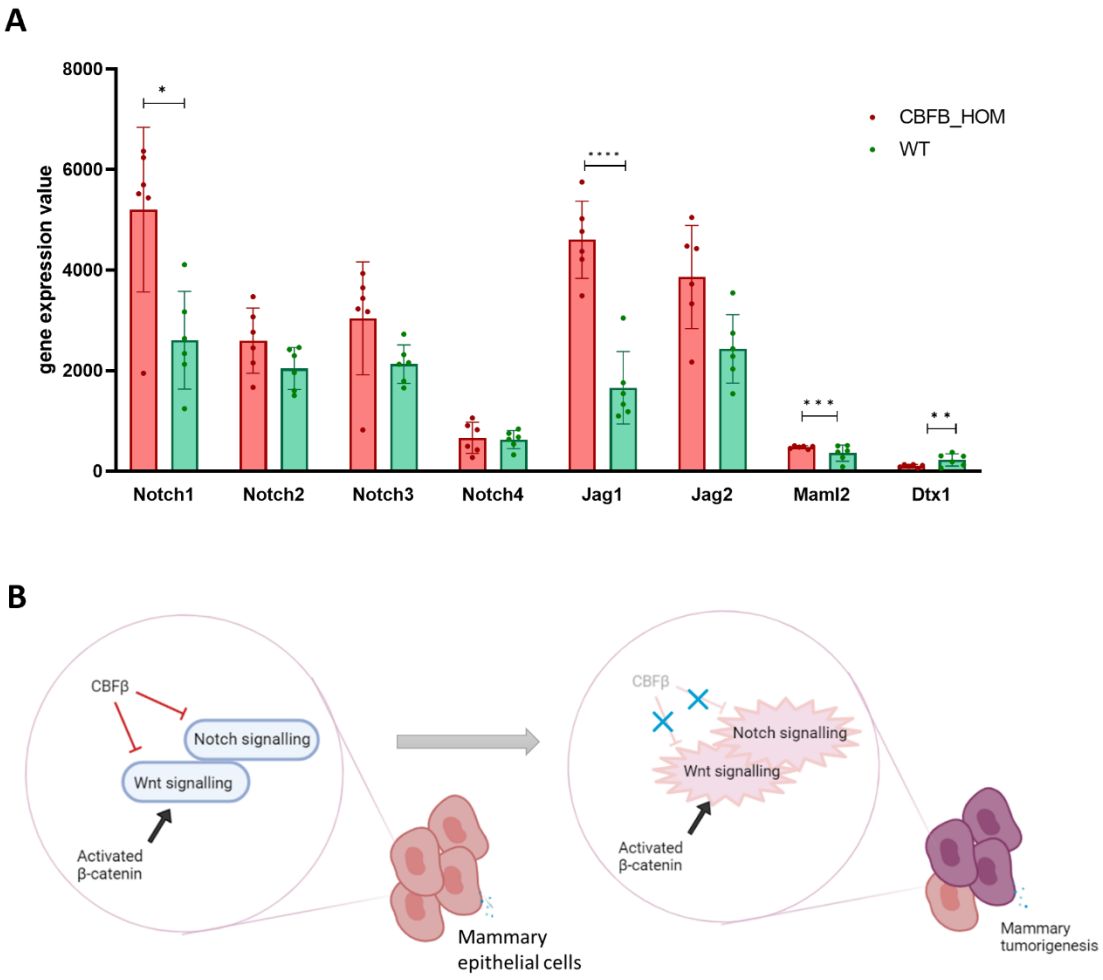

Figure 4.19: Notch pathway activated upon loss of *Cbfβ* in *BLG-Cre;Catnb*$^{wt/lox(ex3)}$ tumours. (A) Gene expression data from RNAseq analysis of mammary tumours. (B) Schematic of the proposed hypothesis where *Cbfβ* loss synergises with both Wnt and Notch pathway activation to drive mammary tumorigenesis in *BLG-Cre;Catnb*$^{wt/lox(ex3)}$ mice. Figure created through BioRender.com. Data points represent individual tumours from N=6 separate mice per cohort. Error bars represent standard deviation of the mean. *p<0.05, **p<0.01, ***p<0.001, ****p<0.0001.

4.2.8. Comparing the transcriptomic changes induced by *Runx1* and *Runx2* loss to deletion of *Cbfβ* in Wnt/β-catenin driven mammary cancer.

In addressing the effects of *Runx1-Runx2* deletion on Wnt/β-catenin driven mammary pathology, transcriptomic analysis of the R1R2_HOM tumours compared to WT samples revealed approximately 1500 differentially expressed genes (Figure 4.20A). Wnt regulatory pathways, in this instance, ranked second among the top 3 relevant networks altered in this cohort according to pathway analysis with immune regulatory pathways ranking number 1 (Figure 4.20B). Gene set enrichment analysis also revealed upregulation of genes involved in the

complement and coagulation cascade alongside gene sets enriched in Wnt signalling or Wnt signalling associated processes such as the basal cell carcinoma (Figure 4.20C). Thus, on top of the association with Wnt signalling, an interesting relationship between loss of the two RUNX proteins and the immune system was suggested – a topic explored further in the Chapter 5.

A

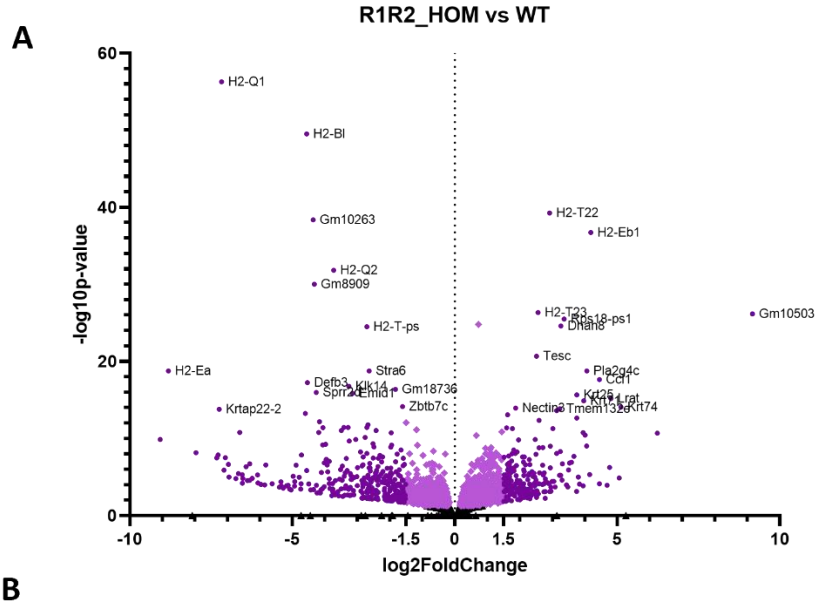

B

Top 3 most relevant networks

No	Network name	Processes	Size	Target	Pathways	p-Value	zScore	gScore
1	HSP70, MMP-13, IL17BR, Bone sialoprotein, TRAF6	response to cytokine (84.0%), cellular response to interleukin-1 (56.0%), response to interleukin-1 (58.0%), cellular response to cytokine stimulus (80.0%), cytokine-mediated signalling pathway (70.0%)	50	4	2289	6.27e-05	8.26	2869.51
2	WNT, Frizzled, NRCAM, p14ARF, Claudin-1	canonical Wnt signalling pathway (46.0%), cell surface receptor signalling pathway involved in cell-cell signalling (58.0%), regulation of Wnt signalling pathway (52.0%), regulation of canonical Wnt signalling pathway (48.0%), cell-cell signalling by Wnt (50.0%)	50	14	171	4.43e-22	30.06	243.81
3	C1s, CHODL, C4B protein, SEZ6L2, CFA54	phosphatidylglycerol acyl-chain remodelling (12.2%), phosphatidylserine acyl-chain remodelling (12.2%), phosphatidylethanolamine acyl-chain remodelling (12.2%), phosphatidylcholine acyl-chain remodelling (12.2%), phosphatidylserine metabolic process (12.2%)	50	27	0	2.81e-51	59.00	59.00

C

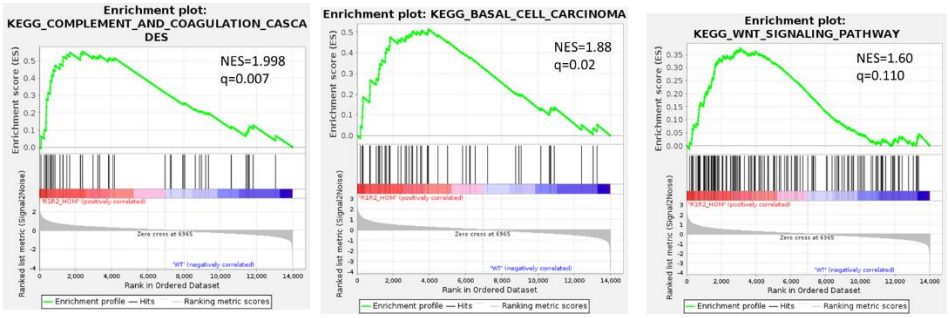

Figure 4.20: Transcriptomic changes induced upon combined loss of *Runx1* and *Runx2* in Wnt/β-catenin driven breast cancer.

(A) Volcano plot shows differentially altered genes in R1R2_HOM tumour samples (N=6) compared to WT tumour samples (N=6). Significantly altered genes (p value threshold=0.01) with a fold change greater than 1.5 (purple), significantly altered genes below the fold change threshold (lavender) and non-significant gene expression (black) are displayed. Data points represent individual genes. (B) Network analysis from MetaCore displaying the top 3 altered networks in R1R2_HOM samples compared to WT samples. (C) Enrichment plots from gene set enrichment analysis for KEGG complement and coagulation cascades (left), basal cell carcinoma (middle) and Wnt signalling pathway (right). NES=Normalised enrichment score. q=FDR value.

Focussing on the interplay between *Runx1*, *Runx2* and Wnt/β-catenin signalling, data from the transcriptomic analysis surprisingly revealed that despite yielding a more aggressive form of mammary pathology, the combined loss of *Runx1 and Runx2* seemed to have more subtle influences on the WNT signalling cascade. Gene expression of only 3 of the 22 significantly altered Wnt pathway regulators noted in the CBFB_HOM tumour samples (Figure 4.18), were significantly altered in R1R2_HOM tumour samples (Figure 4.21). As activators of Wnt signalling, *Kremen2*, *Tcfl5* and *Mycn* upregulation in R1R2_HOM tumours indicated that the combined loss of these two proteins also assisted Wnt signalling progression, albeit not to the same degree as that exerted by *Cbfβ* loss. Two further activators of the canonical pathway, *Wnt2* and *Prkaa2* (involved in the phosphorylation mediated stabilisation of β-catenin) were additionally significantly upregulated in R1R2_HOM tumours compared to CBFB_HOM and WT samples. While these results indicated towards a positive correlation between the cumulative loss of *Runx1* and *Runx2* and escalation of Wnt signalling, upregulation of the Wnt antagonist *Sfrp4,* indicative of negative regulation of canonical signalling (Ayyanan et al., 2006) was also noted in these samples. This could be a compensatory attempt of dampening down aberrant Wnt signalling. Overall, these results suggest that a more enigmatic relationship exists between the RUNX proteins and Wnt/β-catenin signalling in mammary tumorigenesis.

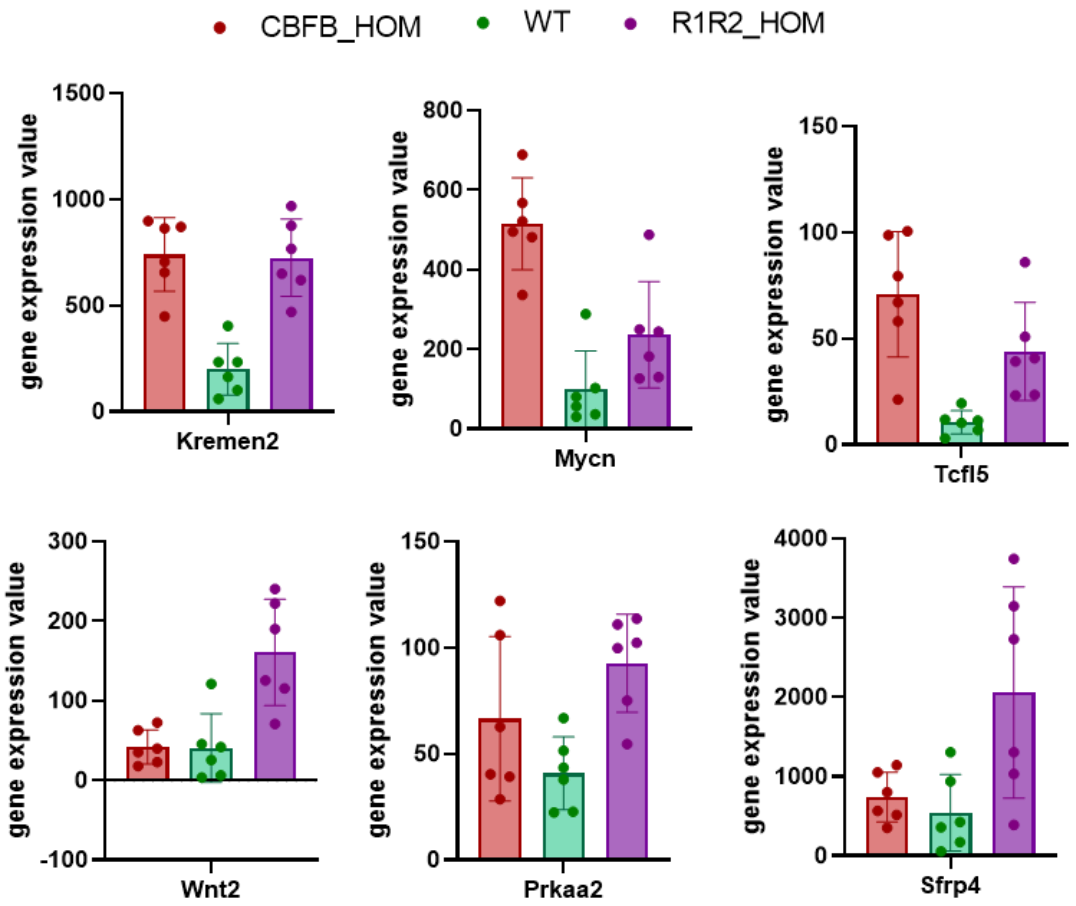

Figure 4.21: Comparing the impact of *Runx1-Runx2* loss to wildtype controls on Wnt pathway activation. Gene expression data from RNA sequencing.

Data points represent individual tumours from N=6 separate mice per cohort. Data from the *Cbfβ*$^{fl/fl}$ tumours (as shown in Figure 4.18) given to compare against the R1R2_HOM samples. Error bars represent standard deviation of the mean. Selected genes are significantly altered in R1R2_HOM samples with a padj<0.05 and an absolute fold change threshold of 1.5 compared to WT samples.

Together, these results highlighted that despite working as a complex, and in spite of the fact that RUNX1-RUNX2 and CBFβ, adopt a tumour suppressor role in Wnt/β-catenin driven mammary tumorigenesis, the underlying mechanism for each of their roles may be considerably different.

Intriguingly, of the 2524 genes altered by loss of *Cbfβ* and the 1456 genes differentially expressed upon deletion of *Runx1* and *Runx2*, 594 genes overlapped in both cohorts (Figure 4.22). Since loss of either CBF counterpart (*Cbfβ* or *Runx1* and *Runx2)* results in the marked acceleration of disease, it is possible that genetic alterations common to both cohorts might be responsible for the phenotypic consequence. Preliminary gene ontology analysis suggested that the majority of

the gene products appeared to reside in extracellular compartments while some were associated with intermediate and keratin filaments. This could be due to the highly keratinous nature of *BLG-Cre;Catnb*$^{wt/lox(ex3)}$ driven mammary tumorigenesis. Additionally, a significant proportion of the genetic changes also seemed to be associated with activation of various immune processes. This resembles the results from pathway analysis which also highlighted alteration of various immune regulatory pathways in both cohorts. Perhaps, loss of either *Cbfβ* or *Runx1* and *Runx2* triggers mammary tumorigenesis not only via intrinsic supplementation of Wnt signalling but also through the induction of extrinsic pro-tumorigenic factors such as the tumour immune microenvironment. As such it would be important to investigate the impact of deleting *Cbfβ* or *Runx1* and *Runx2* on the immune-microenvironment of *BLG-Cre;Catnb*$^{wt/lox(ex3)}$ mammary tumours. Additionally, determining how many of the 594 genes directly associate with the core binding factor complex and how they are regulated by CBFβ or the two RUNX proteins would be imperative in understanding the mechanism of Wnt augmentation upon loss of *Cbfβ* or *Runx1* and *Runx2*.

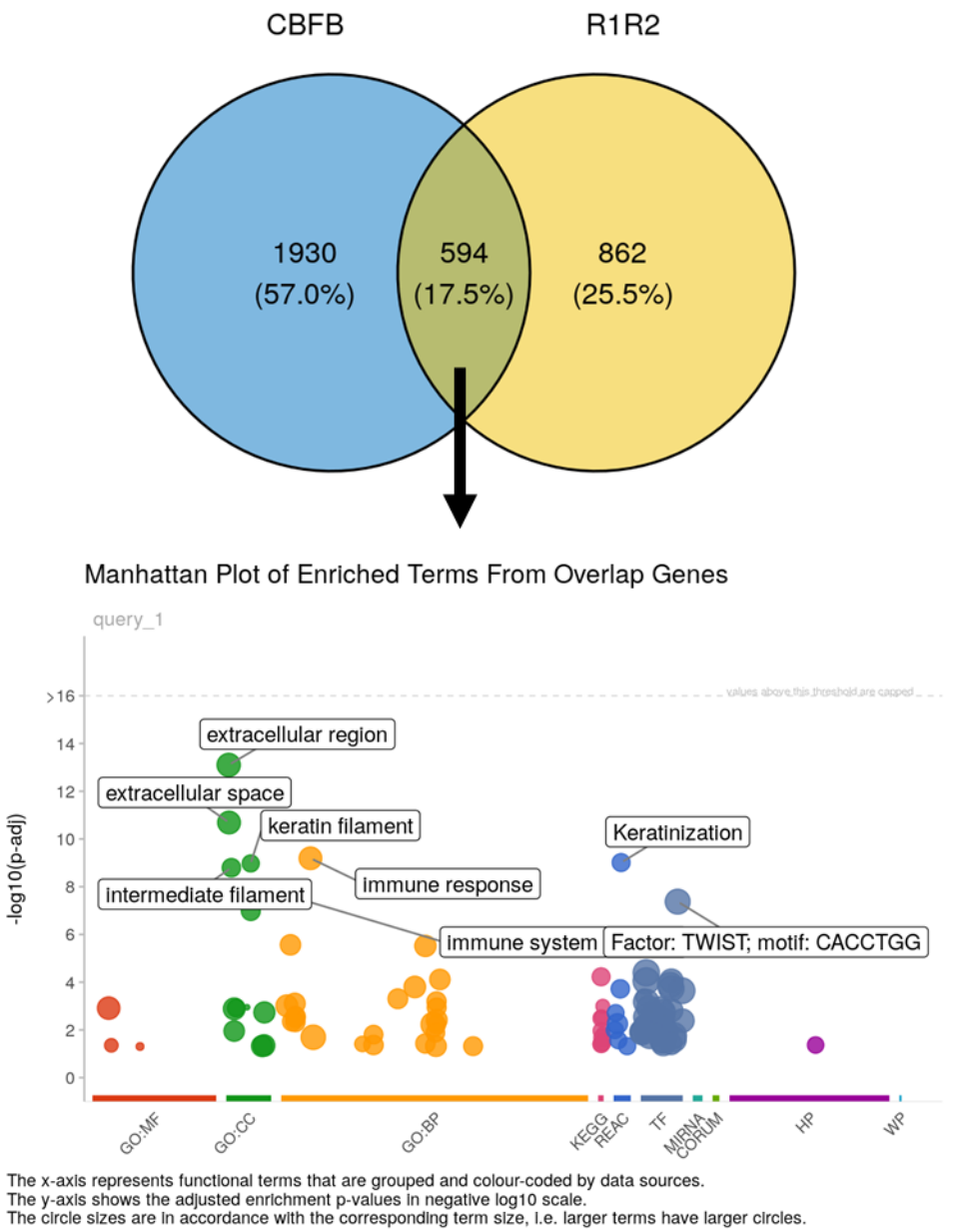

Figure 4.22: Overlapping genetic alterations noted upon deletion of either *Cbfβ* or *Runx1* and *Runx2*.

Venn diagram comparing gene expression changes between CBFB_HOM and R1R2_HOM tumour samples both compared to WT samples, all groups N=6, clinical endpoint tumours. Manhattan plot shows gene ontology reports on the overlapping genetic changes induced by both *Cbfβ* and *Runx1-Runx2* loss.

4.3. Discussion

The evolutionarily conserved Wnt signalling cascade is one of the indispensable molecular signalling pathways involved in the regulation of cell fate throughout the lifespan of an animal. Beginning from early embryonic development where Wnt/β-catenin signalling mediates tissue segmentation, body axis formation and

development of organs, to its contributions in cell survival, regeneration, tissue differentiation and homeostasis in adults, the pleotropic roles adopted by this signalling system is crucial for normal functioning of metazoans (Sanson, 2001; Petersen and Reddien, 2009; Niehrs, 2010; Dickinson, Nelson and Weis, 2011; Trompouki et al., 2011). As one of the key effector molecules in canonical Wnt signalling, β-catenin is responsible for transducing Wnt driven signals into the transactivation or repression of Wnt-target gene transcription through which Wnt signalling functions are ultimately exerted. Naturally, tight regulation of this signalling cascade is a key priority and thus several modulators of β-catenin activity starting from Wnt ligands and their cognate receptors to proteins involved in the inactivation and destruction of β-catenin are put in place to ensure homeostatic balance of this signalling cascade. Understandably, deregulation or an imbalance in any of these components, especially those leading to β-catenin hyperactivation, contribute to the development of various forms of disease. Indeed, accumulation of β-catenin and aberrant Wnt pathway activation has been noted in numerous cases of human cancers including prostate, ovarian, glioma, neuroblastoma as well as breast cancers (Wang et al., 2015). Approximately 50% of breast cancer cases display activated Wnt signalling which is correlated to poor prognosis and reduced patient survival (Lin et al., 2000). Genetic and epigenetic alterations as well as post-transcriptional and post-translational modifications of integral members of Wnt signalling have been repeatedly implicated in breast tumorigenic processes (Lin et al., 2000; Xu et al., 2020). Mounting evidence from primary tumour samples associate activation of Wnt signalling by means of either upregulated expression or activating mutations of its drivers – Wnt ligands, Frizzled receptors, LRP5/6, Disheveled and Myc – or downregulation/inactivation of its inhibitors such as sFRPs, DKK, SOX1, APC and AXIN to name a few, to breast oncogenesis (Incassati et al., 2010). Activated Wnt signalling by means of mutations in the human *CTNNB1* and *APC* genes has been correlated to metaplastic breast cancers while nuclear accumulation of β-catenin has been implicated in basal like breast cancers and TN breast cancers (Incassati et al., 2010). EMT induction of mammary cells due to overexpression of ROR1 in breast cancer has been linked to tumour metastasis and increased patient mortality (Cui et al., 2013). Studies using an *MMTV-Wnt1* driven model of breast cancer, where mammary tumours consisted of both basal and luminal cells, indicated that Wnt signalling plays a critical role in modulating the phenotype of molecular and

histological subtypes of breast cancer (Teissedre et al., 2009). In another model where β-catenin expression was placed under the MMTV promoter, β-catenin mediated Wnt signalling progression was reported in ductal lumina resembling alveolar progenitor cells. Additionally, luminal deregulation of β-catenin was shown to produce tumours of varying lineages – similar to human cases where TN basal type tumours are considered to arise from epithelial cells of the luminal progeny (Michaelson and Leder, 2001; Li et al., 2003; Liu et al., 2003, 2004; Zhang et al., 2009). In almost all these cases of mammary cell malignancy, tumorigenesis seems to be a consequence of β-catenin stabilisation, accumulation and its translocation into the nucleus.

With this characteristic in mind, several mouse models have employed a constitutively activated β-catenin protein in the study of breast transformation and tumorigenesis. For example, MMTV mediated expression of ΔN89-β-catenin or ΔN90-β-catenin, a stabilising mutant version of normal β-catenin, induced luminal adenocarcinoma in mice (Imbert et al., 2001; Michaelson and Leder, 2001; Teissedre et al., 2009). Expression of *Catnb*$^{wt/lox(ex3)}$ under the influence of MMTV or Wap-Cre on the other hand, generated squamous metaplastic tumours whereas, the K5-ΔN57-β-catenin model displayed an invasive mammary tumour phenotype resembling basal carcinoma (Miyoshi et al., 2002; Gu et al., 2009). These GEMMs, albeit not directly recapitulating deregulations of Wnt signalling in human breast cancer, provided invaluable information regarding Wnt mediated mammary pathology. The hormonally regulated BLG-Cre;Catnb$^{wt/lox(ex3)}$ model where BLG-Cre expression is relatively low in virgin mammary glands, provides an added benefit in limiting expression of β-catenin and its potent transforming effect on a few select mammary epithelial cells (Selbert et al., 1998). This translates into an extended tumour latency period as noted in the control BLG-Cre;Catnb$^{wt/lox(ex3)}$ mice described in this chapter – a feature ideal for the investigation of putative tumour suppressors, whose loss would synergise with aberrant Wnt/β-catenin activation. Considering the association between RUNX proteins and Wnt signalling in mammary stemness and tumorigenesis (Sweeney, Cameron and Blyth, 2020), it was hypothesised that loss of CBFβ, similar to loss of its RUNX binding partners would expedite Wnt/β-catenin activated transformation of the mammary epithelium.

In this regard, the tumour suppressive role of *Cbfβ* in the context of Wnt/β-catenin driven mammary cancer was proven when loss of just one copy of *Cbfβ* in *BLG-Cre;Catnb*$^{wt/lox(ex3)}$ mice was enough to significantly reduce overall survival of mice. Homozygous loss of *Cbfβ* resulted in a dramatic reduction of their lifespan and a significant acceleration of tumour initiation. While tumour progression time ranged from 31, 38 and 68 days respectively in *BLG-Cre;Catnb*$^{wt/lox(ex3)}$*;Cbfβ*$^{fl/fl}$, *BLG-Cre;Catnb*$^{wt/lox(ex3)}$*;Cbfβ*$^{wt/fl}$ and *BLG-Cre;Catnb*$^{wt/lox(ex3)}$*;Cbfβ*$^{wt/wt}$ mice, the difference between clinical onset in *BLG-Cre;Catnb*$^{wt/lox(ex3)}$*;Cbfβ*$^{fl/fl}$ and *BLG-Cre;Catnb*$^{wt/lox(ex3)}$*;Cbfβ*$^{wt/wt}$ mice was almost 155 days. Thus, the reduction in overall survival of *Cbfβ*$^{fl/fl}$ mice could be attributed primarily to the significantly accelerated clinical onset rather than tumour progression. These results indicated for the first time *in vivo*, that CBFβ plays an important tumour suppressive role in the initiation of Wnt driven tumorigenesis.

Additionally, histopathological analysis of end-stage tumours from *Cbfβ*$^{fl/fl}$ and *Cbfβ*$^{wt/wt}$ cohorts revealed the characteristic of Wnt/β-catenin driven mammary tumour phenotype with the mammary epithelium transformed into highly keratinous, adenoma-like squamous lesions. Curiously, a higher proportion of basal epithelial cells -as marked by CK14 staining on IHC, was noted in the tumours from *Cbfβ*$^{fl/fl}$ compared to *Cbfβ*$^{wt/wt}$ cohorts. The latter consisted of more luminal CK18 positive cells surrounding the keratinous tumour cores. It is possible that loss of *Cbfβ* in the mammary luminal cells induces a switch from luminal to more basal like CK14 expressing phenotype – similar to what is noted in BRCA1 breast cancers which have been shown to originate from epithelial cells of luminal progeny (Molyneux et al., 2010). However, it should be noted that while CK14 is known to be a marker for basal epithelial cells, certain subpopulations of luminal cells in human luminal breast cancers and mouse models often express CK14 (Smith, Mehrel and Roop, 1990; Gusterson et al., 2005). Thus, further characterisation of these tumours with markers that are more accurate in discriminating between these two lineages such as CD271 and p63 (Álvarez-Viejo, Menéndez-Menéndez and Otero-Hernández, 2015; Steurer et al., 2021), should be used before presuming any associations.

With respect to characterisation of tumour gross pathology, almost all glands bearing neoplastic lesions at disease endpoint in *Cbfβ*$^{fl/fl}$ mice and not in *Cbfβ*$^{wt/wt}$ tumours, seemed to display an increase in the frequency of Wnt/β-catenin driven mammary epithelial cell transformation upon *Cbfβ* loss. Both *Runx1* and *Runx2*

have been associated to the regulation of mammary epithelial stemness (Ferrari et al., 2015; Riggio, 2017; Fritz et al., 2020). Given the close relationship between these two proteins and CBFβ, and their collaborative approach in the regulation of various cell developmental processes, it is possible CBFβ also influences the mammary stem/progenitor cells under Wnt regulation in a similar manner to the RUNX proteins. In fact, RNAseq data displayed significantly upregulated expression of *Snai2* – a key regulator of EMT associated to an aggressive, mesenchymal phenotype in breast cancer cells (Alves et al., 2018) – in *Cbfβ* deficient tumour samples compared to WT samples. Thus, future experiments to characterise any transcriptomic changes in the expression of other stem-cell markers along with the use of biological assays, such as mammospheres or tumoursphere assays, could help investigate the impact of *Cbfβ* loss on mammary tumour cell stemness.

Interestingly, *Cbfβ* loss in mammary glands of mice with wildtype Wnt/β-catenin did not seem to induce transformation of mammary epithelial cells. This contradicts *in vitro* data from Malik et al demonstrating loss of *CBFβ* inducing transformation of normal mammary epithelial cells using the MCF10A cell line (Malik et al., 2019). Perhaps the selective pressures against tumour growth *in vivo* exerted by the mammary microenvironment or the immune system for instance, overpower any oncogenic effects of *Cbfβ* loss in the absence of Wnt/β-catenin activation.

In an effort to further investigate the relationship between *Cbfβ* and Wnt/β-catenin signalling in mammary tumorigenesis, transcriptomic analysis of end-stage tumours from *BLG-Cre;Catnb*$^{wt/lox(ex3)}$*;Cbfβ*$^{fl/fl}$ and *BLG-Cre;Catnb*$^{wt/lox(ex3)}$*;Cbfβ*$^{wt/wt}$mice was conducted. Remarkably, RNA sequencing results revealed significantly upregulated expression of various genes encoding activators of the Wnt pathway and downregulation of certain inhibitors and antagonists of the system in *Cbfβ*$^{fl/fl}$ tumours compared to those from *Cbfβ*$^{wt/wt}$ mice. This validated our hypothesis of *Cbfβ* loss potentiating Wnt/β-catenin activation to bring about dramatic acceleration of the tumorigenic phenotype.

In addition to this, the impact of *Cbfβ* loss on Notch signalling was also interrogated. The Notch signalling cascade, as an evolutionarily conserved pathway is known to be intimately linked with Wnt signalling in both normal development and disease (Edwards and Brennan, 2021). Both Notch and Wnt pathways share target genes such as *Ccnd1* and *c-Myc* – two key perpetrators known to induce proliferation of breast tumour cells (Klinakis et al., 2006; Cohen

et al., 2010). Indeed, a positive correlation was noted between expression of the Notch ligand JAG1 and CCND1 in the basal subtype of breast cancer (Cohen et al., 2010). On the other hand, ablation of the proto-oncogene *c-Myc* was shown to prevent formation of mammary tumours in MMTV-NICD1 mice (Klinakis et al., 2006). In fact, inhibition of one of the receptors of this pathway – NOTCH1 – in both ER positive and ER negative breast cancer cell lines (MCF7 and MDA-MB-231) resulted in significant reduction in tumour cell proliferation, migratory and invasive properties. Upon further examination into the molecular alterations brought about by Notch inhibition, significant decrease in β-catenin expression and its nuclear levels were noted, indicating concomitant repression of canonical Wnt signalling brought about by the suppression of Notch (Lai et al., 2018). Notch and Wnt signalling have also been implicated in the epithelial to mesenchymal transition of breast tumour cells with inactivation of β-catenin associated to inhibition of NOTCH4 and suppression of breast tumour growth and metastasis in an *in vivo* xenograft model (Leong et al., 2007).

With these discoveries in mind, upregulation of Notch signalling as a result of *Cbfβ* loss and the subsequent augmentation of the Wnt/β-catenin pathway was expected in *BLG-Cre;Catnb*$^{wt/lox(ex3)}$*;Cbfβ*$^{fl/fl}$ tumours. Predictably, expression of various members of Notch signalling including Notch receptors and ligands were found elevated in tumours lacking *Cbfβ*. Coincidentally, in support of this finding, a recent paper by Malik et al. showed that CBFβ complexes with RUNX1 in the nucleus and acts as a tumour suppressor by repressing NOTCH3 transcription (Malik et al., 2019). RNAseq of *CBFβ*$^{-/-}$ MCF10A cells in this study also correlated loss of *Cbfβ* to Wnt pathway alteration.

Therefore, it is possible that loss of *Cbfβ* in the Wnt/β-catenin driven breast cancer model could be stimulating activation of the Wnt pathway in a multi-hit manner: direct upregulation of Wnt activators, repression of Wnt inhibitors and upregulation of pathways that further potentiate Wnt signalling such as the Notch signalling pathway. The resulting hyperactivation of Wnt signalling would explain why loss of *Cbfβ* yields such a potent oncogenic effect on Wnt/β-catenin driven mammary transformation.

In the comparison of *Runx1* and *Runx2* deletion with that of their binding partner, *Cbfβ,* the former led to further reduction in the overall survival of cohort mice with significantly increased tumour burden. Additionally, while Wnt signalling was also stimulated upon the loss of *Runx1* and *Runx2*, *Cbfβ* loss in comparison

appeared to impose a much stronger effect. While at least 22 genes involved in the Wnt pathway were significantly altered upon loss of *Cbfβ*, only 6 such genes investigated were differentially expressed in the R1R2_HOM tumour samples. Conversely, pathway analysis of these samples hinted towards an association between immune regulatory pathways and the two RUNX proteins. These results indicated that despite functioning as a unit in the CBF complex and generating overtly similar phenotypic consequences, the underlying molecular mechanisms behind this phenotype might be significantly different in *Cbfβ* and *Runx1-Runx2* deficient tumours.

It was interesting to see that a distinguishing factor between *Cbfβ* and *Runx1-Runx2* null tumours was the differential involvement of immune regulatory pathways. There is an increasing appreciation for the complex role played by the tumour microenvironment in tumour development. Therefore, the relationship between loss of *Cbfβ* or *Runx1-Runx2* and the immune niche of Wnt/β-catenin driven breast tumours was investigated subsequently in the next chapter.

Chapter 5. Impact of epithelial *Cbfβ/Runx* loss on the immune landscape of Wnt/β-catenin driven mammary cancer

Analysis of *BLG-Cre;Catnb*$^{wt/lox(ex3)}$ mice revealed a coo-operative relationship between loss of *Cbfβ* or *Runx1-Runx2* and Wnt/β-catenin signalling activation in mammary tumorigenesis. Interestingly, transcriptomic analysis indicated that alongside Wnt signalling, immune regulatory pathways were also significantly altered upon *Cbfβ* deletion and to a greater extent, combined loss of *Runx1* and *Runx2* in *BLG-Cre;Catnb*$^{wt/lox(ex3)}$ mice. Therefore, the impact of RUNX/CBFβ on the breast tumour micro-environment was interrogated.

5.1. Introduction

5.1.1. The mammary immune microenvironment and its role in tumour promotion

Emerging evidence from prospective studies as well as retrospective investigations have highlighted the importance of the mammary immune microenvironment in breast tumour development and disease progression (Adams et al., 2014; Dieci et al., 2015; Carbognin et al., 2016). As discussed in chapter 1, the natural anti-tumorigenic cast of immune cells of the mammary gland help protect it being invaded by transformed cells. In fact, a high lymphocyte infiltrate in breast tumours, particularly anti-tumorigenic cytotoxic CD8+ T cells, have been associated with favourable prognosis of patients (Adams et al., 2014; Dieci et al., 2015; Carbognin et al., 2016). These T cells, once activated, interact with target pre-neoplastic mammary cells to induce cell lysis and apoptosis through perforin and granzyme B. Additionally, DCs and macrophages along with NK cells that present tumour neoantigens, can release IL12 and IFNγ to activate CD4+ T helper type 1 (Th1) cells (Xu et al., 2020). These in turn, secrete IL2, IFNγ and TNFα to assist CD8+ T cells in elimination of tumour cells. This process is further aided by NK T cells. IL12 from DCs along with CD1d (MHC I-like molecules) which are also found on tumour cells surfaces also activate NK T cells which release more IFNγ to attract killer NK cells (Xu et al., 2020).

On the other hand, tumour cells that evade the initial clearance round by the mammary immune system, promote a pro-tumorigenic immune response (concept introduced in chapter 1). Elevated levels of TAMs and FoxP3+ Tregs are frequently correlated to poor prognosis of breast cancer patients (DeNardo et al., 2011; Liu et al., 2012). Both cell types inhibit cytotoxic CD8+ T cells as well as CD4+ Th1 and Th2 cells through secretion of immunosuppressive factors such as IL10, TGFβ, IL35. IL10 and TGFβ expression also promotes activation of TAMs and Tregs in a positive feedback loop (Xu et al., 2020). Additionally, TAMs are able to directly interact with T cells through expression of PDL1, PDL2, CD80 and CD86 and inhibit activity of T cells (Cassetta and Pollard, 2018; Wagner et al., 2019). IL1β secretion from TAMs can also stimulate γδT cells to produce IL17 which induces polarisation and expansion of neutrophils mediated by G-CSF (Xu et al., 2020). This results in a systemic inflammatory response where neutrophils are able to suppress CD8+ T cells and facilitate breast cancer metastasis. Tregs, through consumption of the APC-activating cytokine IL2, can suppress the anti-tumorigenic immune population and promote tumour metastasis through ECM-degrading MMPs and angiogenesis promoting VEGFs (Xu et al., 2020). Thus, on top of genetic deregulations that induce mammary cell transformation, the mammary tumour immune system plays a key role in the progression of cancerous lesions.

5.1.2. Immune microenvironment in Wnt driven mammary cancer

Involvement of the immune system in breast cancers with altered Wnt/β-catenin signalling has been explored in various studies (Shulewitz et al., 2006; Betancur et al., 2017; Barkal et al., 2019; Castagnoli et al., 2019; Feng et al., 2019). Breast tumours with high expression of β-catenin also displayed high infiltration of lymphocytes (Ma et al., 2018). Activation of Wnt/β-catenin signalling in malignant breast cancer cells has been shown to repress the natural anti-tumour response and promote various immune evasion strategies. For instance, CD24, expressed on tumour cells in response to Wnt activation and CD47 whose production is mediated by Wnt directed expression of SNAI1 and ZEB1, can inhibit macrophage induced phagocytosis of cancer cells (Shulewitz et al., 2006; Noman et al., 2018; Barkal et al., 2019). Myc – a known target of Wnt canonical signalling, is known to regulate CD47 and PDL1 used in blocking cytotoxic function of CD8+ T cells (Casey et al., 2016). Furthermore, secretion of Wnt ligands such as Wnt1, Wnt6 and Wnt7a from metastatic breast cancer cells, promotes crosstalk between tumour cells and TAMs

which help induce the neutrophil and γδT cell mediated systemic pro-tumorigenic inflammatory response favourable for tumour growth and metastasis (Wellenstein et al., 2019). Additionally, invasive breast cancer cells have been shown to secrete various MMPs and angiogenic factors such as VEGFs all of which are expressed through activation of Wnt/β-catenin signalling (Schmalhofer, Brabletz and Brabletz, 2009). Therefore, Wnt/β-catenin activation in mammary tumours helps modulate the tumour-immune microenvironment in various ways to ensure an immunosuppressive niche to favour tumour development and metastasis.

5.1.3. Relationship between RUNX/CBFβ and the mammary tumour-immune microenvironment

While activation of a pro-tumorigenic immune response and alterations in RUNX/CBFβ have been implicated separately in various cases of breast cancer, the relationship between these two arms involved in mammary tumorigenesis has been interrogated in only a handful of studies (Gao and Zhou, 2021; Fu et al., 2022). Recently, bioinformatic analysis of patient tumour data available through online datasets and databases has provided insight into alterations in the mammary tumour microenvironment in relation to RUNX expression in breast tumours (Gao and Zhou, 2021; Fu et al., 2022). Mutations and copy number alterations in *RUNX1* were positively correlated to infiltration of CD8+, CD4+ T cells, B cells and macrophages in luminal breast tumours. Alterations in *RUNX2* was positively associated to an increased infiltration of CD8 and CD4 T cells, macrophages and neutrophils in basal and luminal subtypes (Gao and Zhou, 2021; Fu et al., 2022). Additionally, an association between TGFβ signalling – a critical member in mediating immunosuppression in tumour microenvironments, and methylation of *RUNX* genes was also suggested (Gao and Zhou, 2021). Similar analysis associating CBFβ to breast cancer immune microenvironment is yet to be conducted. However, considering the close relationship between RUNX proteins and CBFβ it is possible that alterations in the latter has similar influences on breast cancer immunity. While *in silico* data is useful in identifying previously uncharacterised associations, mechanistic information underlying such associations are not adequately addressed. Thus, further research to understand whether RUNX/CBFβ status in breast tumours directly or indirectly, helps shape the immune microenvironment is imperative.

5.1.4. Hypothesis and Aims

Wnt/β-catenin activation has been shown to influence the recruitment and maintenance of an immunosuppressive, pro-tumorigenic microenvironment in breast cancer. Interestingly, upon deletion of either *Cbfβ* or *Runx1* and *Runx2* in *BLG-Cre;Catnb*$^{wt/lox(ex3)}$ tumours, immune regulatory pathways appeared significantly altered at clinical endpoint according to pathway analysis data introduced in Chapter 4. This suggested, loss of *Cbfβ* or *Runx1* and *Runx2,* on top of augmenting tumour intrinsic Wnt/β-catenin signalling, may also be stimulating tumour extrinsic changes on the immune microenvironment – potentially through augmentation of Wnt signalling – of malignant glands to ultimately exacerbate disease phenotype. Additionally, with regards to the differences noted in transcriptomic data (Chapter 4) between *Runx1*$^{fl/fl}$*;Runx2*$^{fl/fl}$ and *Cbfβ*$^{fl/fl}$ cohorts, it was hypothesised that while *Cbfβ* loss has a more direct impact on Wnt/β-catenin activation, the combined loss of *Runx1* and *Runx2* impinges more on the tumour immune microenvironment to exacerbate Wnt/β-catenin driven mammary tumorigenesis.

Thus, to explore these notions further, the mammary tumour immune microenvironment in *BLG-Cre;Catnb*$^{wt/lox(ex3)}$*;Cbfβ*$^{fl/fl}$ and *BLG-Cre;Catnb*$^{wt/lox(ex3)}$*;Runx1*$^{fl/fl}$*;Runx2*$^{fl/fl}$ cohorts were investigated and compared to that in *BLG-Cre;Catnb*$^{wt/lox(ex3)}$ mice wildtype for *Cbfβ*, *Runx1* and *Runx2*.

5.2. Results

5.2.1. Transcriptomic analysis indicates alteration of immune pathways upon loss of *Cbfβ* or *Runx1-Runx2* in Wnt/β-catenin driven breast cancer

Following on from the transcriptomic results hinting towards an altered immune landscape in end-stage tumours from *Blg-Cre;Catnb*$^{wt/lox(ex3)}$ mice lacking either *Cbfβ* (CBFB_HOM) or *Runx1* and *Runx2 (R1R2_HOM)* (Chapter 4), further interrogation into this area was conducted. Pathway analysis on the 2524 genes altered in CBFB_HOM tumours compared to WT (*BLG-Cre;Catnb*$^{wt/lox(ex3)}$*)* samples revealed multiple nodes of immune regulatory pathways significantly altered (Figure 5.1A). Pathway maps involving chemokines, regulation of granulocyte

development, signalling associated with neutrophils, immune responses related to antigen presentation by MHC Class I and T cell signalling were all altered significantly in CBFB_HOM samples compared to WT. Similarly, pathway analysis of the 1456 genes altered in R1R2_HOM tumours also highlighted multiple pathway maps related to immune system regulation altered in the end-stage *Blg-Cre;Catnb*$^{wt/lox(ex3)}$ tumours lacking *Runx1* and *Runx2* compared to WT samples (Figure 5.1B). These results suggested that loss of either *Cbfβ* or *Runx1* and *Runx2* impacted the immune microenvironment of Wnt/β-catenin activated mammary tumours in *Blg-Cre;Catnb*$^{wt/lox(ex3)}$ mice.

Whether genetic alterations unique to each cohort or the ones common between CBFB_HOM and R1R2_HOM tumours were responsible for the changes in immune pathways were also questioned. In view of this, pathway analysis was subsequently conducted separately on three groups of genes: (1) Genes altered exclusively in CBFB_HOM samples (Figure 4.22, blue area) compared to WT samples, (2) genes altered specifically in R1R2_HOM samples (Figure 4.22, yellow area) and (3) Overlapping genes that were altered in both CBFB_HOM and R1R2_HOM samples relative to WT controls (Figure 4.22, intersection). Immune regulatory pathway maps appeared to be altered in all three groups (data not shown) in a similar pattern suggesting that while genes altered only in response to *Cbfβ* loss or those altered specifically by deletion of *Runx1* and Runx2 impinged on the immune microenvironment of mammary tumours, various genes commonly regulated by both sets may also serve similar functions. This was not surprising, considering the cooperative roles between CBFβ and RUNX proteins and the various redundancies in their functions set in place to maintain the critical regulatory pathways mediated by either counterpart under normal circumstances.

In support of the pathway analysis results, GSEA indicated that various gene sets involved in the response to inflammatory cytokines such as IFNγ and IFNα and a general inflammatory response were significantly enriched in CBFB_HOM (Figure 5.1C) and R1R2_HOM tumours (Figure 5.1D) in comparison to WT. In WT tumours a slight downregulation was noted in the expression of genes involved in the hallmark inflammatory response gene-set but expression of genes involved in the two other gene sets mentioned remained unaltered. Additionally, considering the cytokine/chemokine related pathways that appeared significantly altered in both CBFB_HOM and R1R2_HOM samples, expression of significantly altered cytokines were analysed. A distinct pattern of cytokine expression distinguished R1R2_HOM

samples from the CBFB_HOM and WT samples (Figure 5.2A). While gene expression of cytokines and cytokine receptors were significantly downregulated in CBFB_HOM samples compared to those in WT (Figure 5.2B), gene expression of various pro-tumorigenic cytokines such as *Ccl1, Ccl2, Ccl7, Ccl8 and Ccl11* were significantly upregulated in R1R2_HOM tumours (Figure 5.2C). This suggested that albeit altering the immune phenotype under Wnt/β-catenin activation, *Runx1-Runx2* loss may have different mechanisms of inducing the tumour-immune microenvironment compared to loss of *Cbfβ*.

Despite these differences, overall, the marked upregulation of immune regulatory gene-sets noted in tumours lacking either *Cbfβ* or *Runx1* and *Runx2* suggested, that on top of any influences of Wnt/β-catenin activation, *Cbfβ*/*Runx* loss has further implications on stimulating the mammary tumour microenvironment.

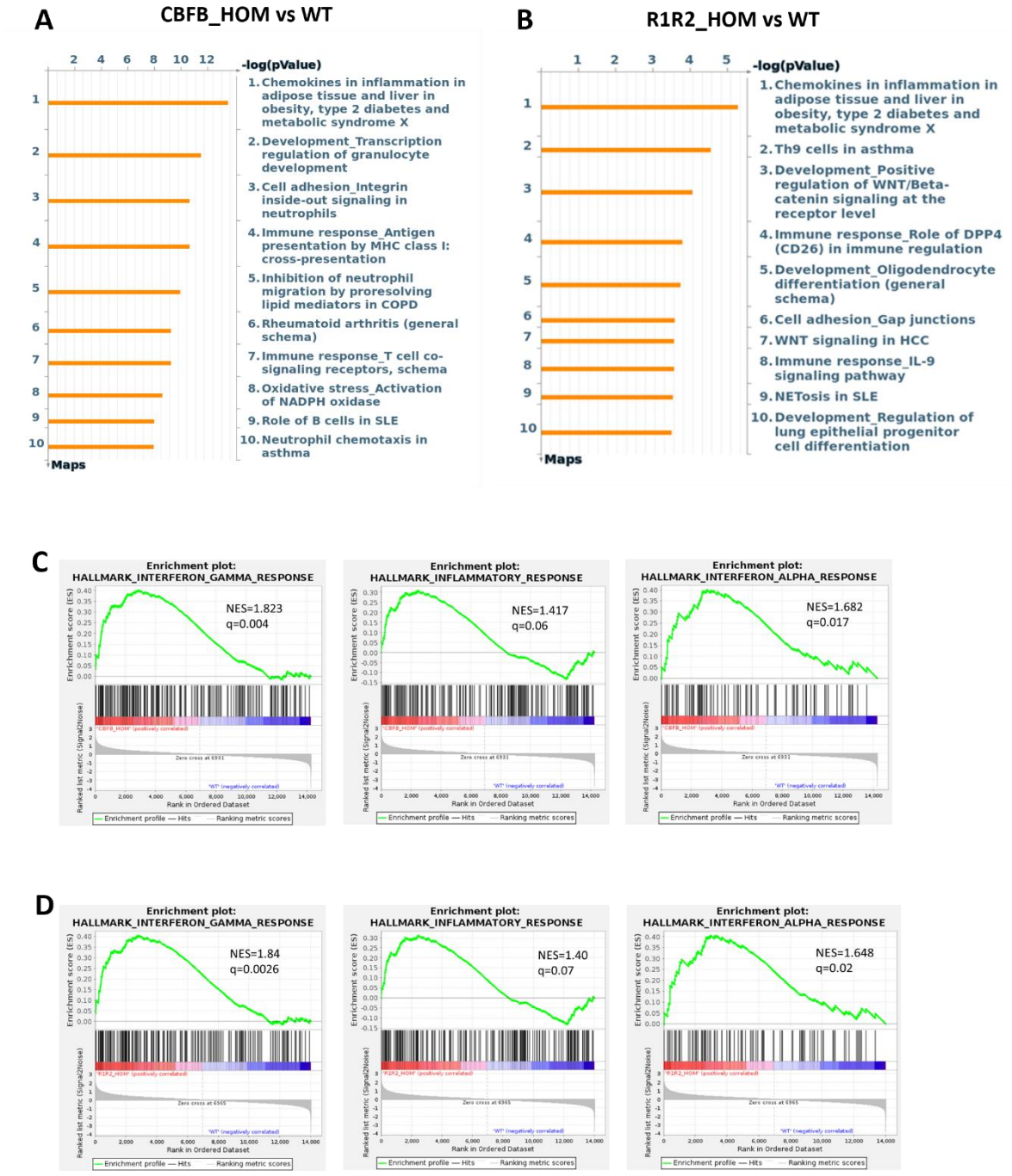

Figure 5.1: Transcriptomic analysis highlighting the impact of *Cbfβ* or *Runx1* and *Runx2* loss on immune regulatory pathways in Wnt/β-catenin activated mammary tumours.

Graphs show the top 10 significantly altered pathways maps in CBFB_HOM (A) and R1R2_HOM (B) WNT-activated mammary tumour samples compared to CBFβ/RUNX WT tumour samples. p.adj<0.05; fold-change threshold=1.5. Enrichment plots showing gene set enrichment in (C) CBFB_HOM (N=6) tumours, and (D) R1R2_HOM (N=6) samples compared to WT (N=6) for the following gene sets: Hallmark Interferon Gamma Response, Hallmark Inflammatory Response and Hallmark Interferon Alpha Response. Normalised enrichment scores (NES) and FDR-q values displayed on the graphs. RNA sequencing done by Billy Clark (Beatson Molecular Technologies). Pathway analysis and GSEA conducted by Robin Shaw.

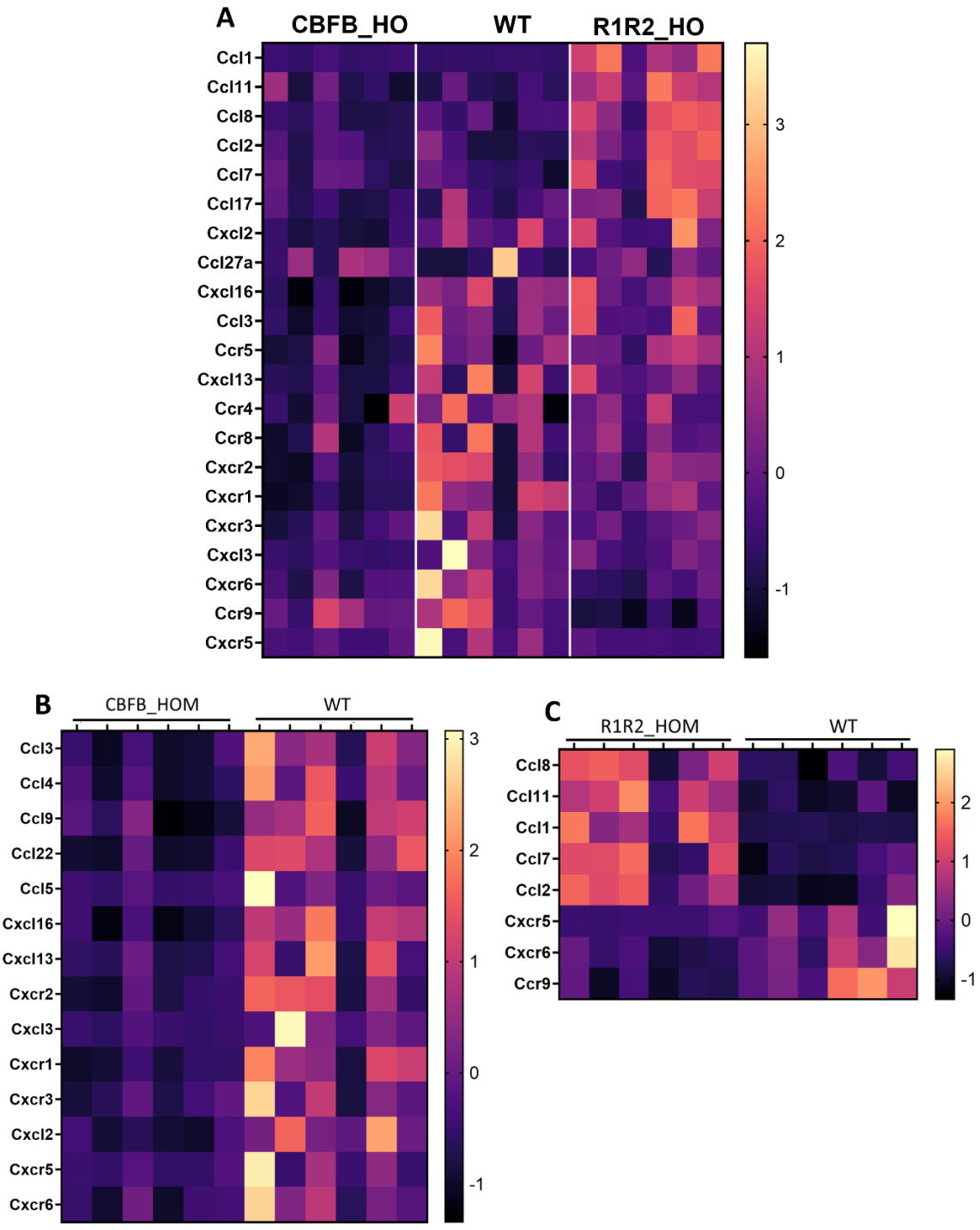

Figure 5.2: Gene expression patterns of significantly altered cytokines and cytokine receptors in CBFB_HOM, WT and R1R2_HOM samples from *BLG-Cre;Catnb$^{wt/lox(ex3)}$* mice.

Expression data acquired through RNA sequencing. (A) Heatmap showing gene expression patterns in all three groups of samples. List of genes contains significantly altered genes in either CBFB_HOM (N=6) or R1R2_HOM (N=6) samples compared to WT (N=6). (B) Heatmap shows expression of genes significantly altered in CBFB_HOM compared to WT samples. (C) Heatmap shows expression of genes significantly altered in R1R2 _HOM compared to WT samples. Data presented in B and C are a subset of data shown in A. Significant genes chosen according p.adj<0.05 and absolute fold-change threshold=1.5. Heatmap generated in Graphpad prism using z-scores of gene expression values from differentially expressed gene analysis (DEGA).

5.2.2. Immunohistochemical analysis of *Cbfβ* or *Runx1* and *Runx2* deficient Wnt/β-catenin driven tumours at clinical endpoint

To determine phenotypic changes in the *BLG-Cre;Catnb*$^{wt/lox(ex3)}$ mammary tumour-immune microenvironment induced by *Runx*/*Cbfβ* loss, tumours at clinical endpoint were extracted. Following formalin fixation and embedding in paraffin, tumour sections were stained by IHC for CD8, CD4, F4/80 and Ly6G to visualise the presence of CD8+ and CD4+ T cells, macrophages and neutrophils respectively within the tumour infrastructure.

Immunohistochemical analysis of end-stage tumours from *BLG-Cre;Catnb*$^{wt/lox(ex3)}$ mice wildtype for *Cbfβ* and *Runx* genes (WT) demonstrated a significant presence of tumour infiltrating lymphocytes (CD8 and CD4), macrophages and neutrophils (Figure 5.3A). This was in line with the phenotype observed in established literature on Wnt/β-catenin mammary tumours, which are characterised by a relatively immune active tumour microenvironment (Ma et al., 2018). Compared to tumours from WT mice, the populations of immune cells in *Cbfβ*$^{fl/fl}$ and *Runx1*$^{fl/fl}$*;Runx2*$^{fl/fl}$ cohorts did not seem to differ significantly. This is observable in the representative IHC images provided in Figure 5.3A and the corresponding quantifications for each marker presented in Figure 5.3B-E. Interestingly a significant population of F4/80+ macrophages were noted in tumours from all three cohorts indicating an association between macrophage infiltration, perhaps TAMs, and Wnt/β-catenin activated mammary tumorigenesis. In contrast, Ly6G staining displayed a significantly low level of tumour infiltrating neutrophils in *Runx1*$^{fl/fl}$*;Runx2*$^{fl/fl}$ mice compared to *Cbfβ* deficient tumours but not the control cohort.

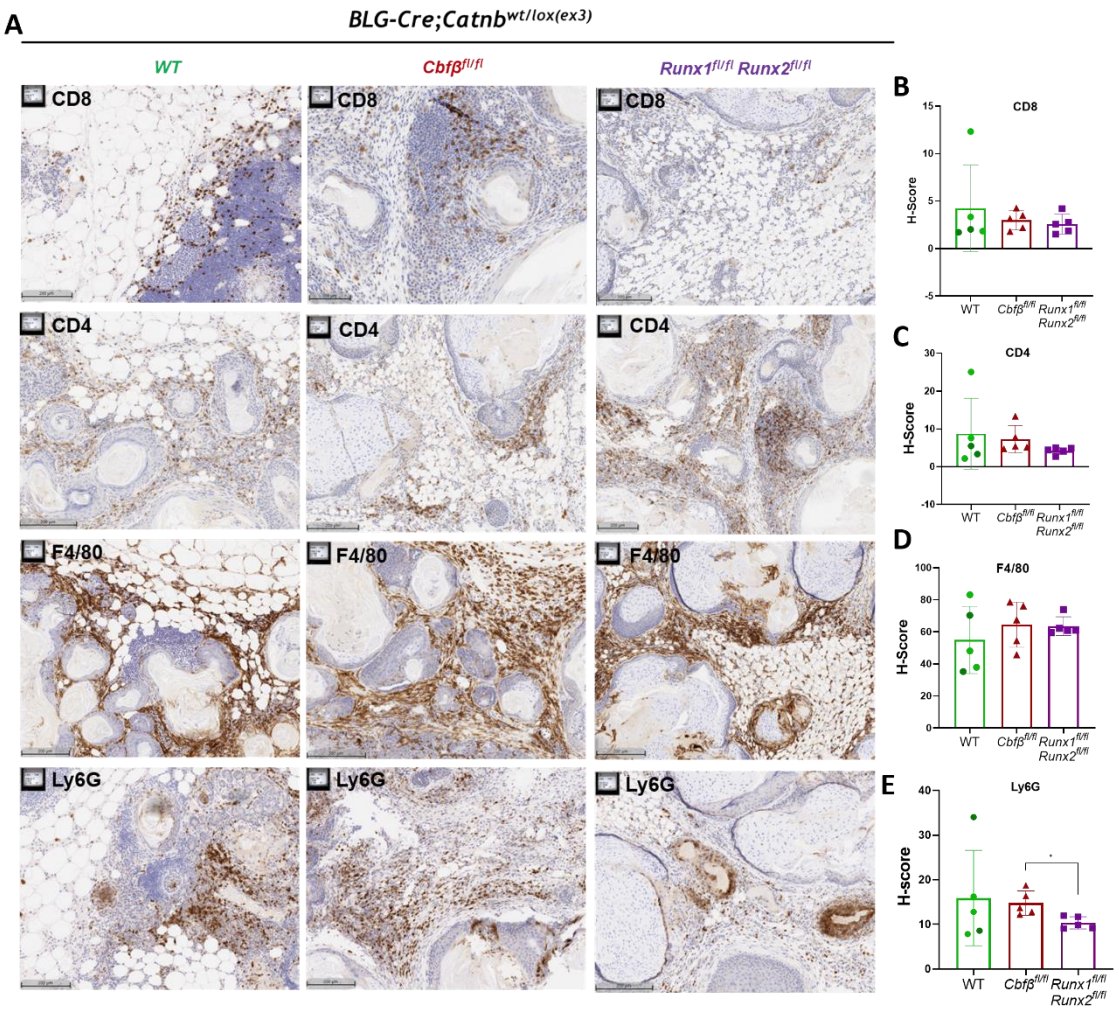

Figure 5.3: Immunohistochemical analysis of end-stage mammary tumours depicting infiltration of immune cells.

(A) Representative IHC images of end-stage tumours from *BLG-Cre;Catnb*$^{wt/lox(ex3)}$ mice with wildtype *Cbfβ*, *Runx1* and *Runx2* (WT) (N=5), *Cbfβ*$^{fl/fl}$ (N=5) and *Runx1*$^{fl/fl}$;*Runx2*$^{fl/fl}$ (N=5) alleles. IHC was conducted for CD8+ T cells, CD4+ T cells, macrophages (F4/80) and neutrophils (Ly6G). (B-E) Quantification of positively stained immune cells within bulk tumour tissue. IHCs performed on tissues from the same tumour samples that were used for RNAseq. Data points represent one tumour from an individual mouse. *p<0.05. Scale bar=300μm.

Chemokines were also analysed as they are known to play a role in attracting and recruiting immune cells to the tumour microenvironment (Palacios-Arreola et al., 2014). CXCL1, CXCL2 and CXCL5 for instance, are known to induce chemotaxis of a variety of immune cells and play an important role in angiogenesis, metastasis and tumour progression (E. Chen et al., 2018). Serial sections of tumour samples analysed for the immune cell populations discussed above were stained for the above-mentioned chemokines using RNAScope (Figure 5.4A). In contrast to the lymphocyte infiltrates, chemokine expression across all three cohorts appeared considerably low. The total RNA copies as well as the percentage of positively

stained area within each tumour section were quantified (Figure 5.4B-C). Similar to the results noted from analysing the immune cell populations, no significant differences were noted in the levels of CXCL1, CXCL2 and CXCL5 between the three cohorts. (Figure 5.4B-C).

These results indicated that at disease endpoint, the tumour immune microenvironment in *Cbfβ* or *Runx1-Runx2* deficient mice might remain comparable to their wildtype counterparts. While this is contradictory to the transcriptomic data, it is possible that due to the immune enriched nature of all *BLG-Cre;Catnb*$^{wt/lox(ex3)}$ tumours at clinical endpoint, subtle differences between the cohorts may be difficult to detect. Additionally, the genetic changes involving immune regulatory pathways identified in CBFB_HOM and R1R2_HOM tumours could have been induced at a much earlier stage of disease. For instance, changes to the immune landscape may have been induced during the tumour initiation stage in response to loss of *Cbfβ* or *Runx1* and *Runx2*. Therefore, at endpoint the results from pathway analysis and GSEA do not seem to reflect the tumour-immune phenotype.

These results were interesting especially in light of work carried out by a previous PhD student in the lab who was particularly focussed on the early stages of disease progression in *Runx1* and *Runx2* deficient murine mammary glands in the *BLG-Cre;Catnb*$^{wt/lox(ex3)}$ model. RNA sequencing carried out using extracts from 9-week-old murine pre-neoplastic mammary glands, revealed a significantly strong immune signature compared with WT, which was substantiated by IHC and quantification of immune cell populations from circulating blood. In view of this, changes in the immune cell population of *Cbfβ* deficient preneoplastic glands were further interrogated.

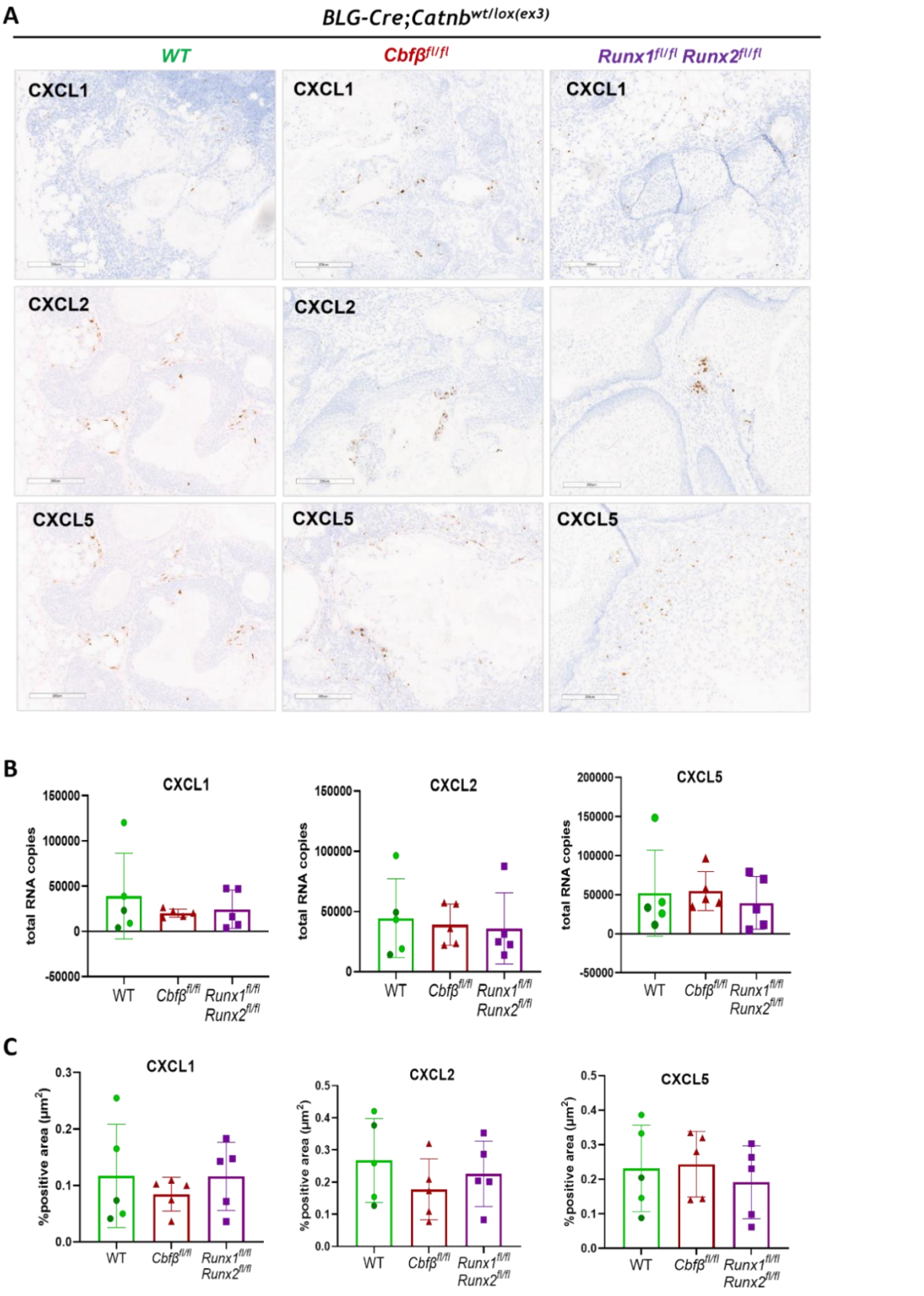

Figure 5.4: RNAscope analysis of end-stage mammary tumours depicting presence of chemokines.

(A) Representative RNAscope images of end-stage tumours from *BLG-Cre;Catnb*$^{wt/lox(ex3)}$ mice with wildtype *Cbfβ*, *Runx1* and *Runx2* (WT) (N=5), *Cbfβ*$^{fl/fl}$ (N=5) and *Runx1*$^{fl/fl}$;*Runx2*$^{fl/fl}$ (N=5) alleles. RNAscope was conducted for CXCL1, CXCL2 and CXCL5. Quantification of total RNA copies (B) and percentage of positive area (C) within bulk tumour tissue. Data points represent tumours from an individual mouse. Scale bar=200µm.

5.2.3. Characterising the impact of *Cbfβ* loss on the immune infiltrate of pre-neoplastic mammary glands

Data acquired previously by RNAseq and IHC in the lab, highlighted an increase in inflammatory cytokines and immune infiltrate in 9-week-old *BLG-Cre;Catnb*$^{wt/lox(ex3)}$*;Runx1*$^{fl/fl}$*;Runx2*$^{fl/fl}$ murine mammary glands. Tumours from mice lacking both *Runx1* and *Runx2* showed upregulated expression of *Il1β*, *Il17β* and *Ccl2* while analysis of total blood cell counts indicated a significant increase in the number of circulating neutrophils and elevated levels of monocytes (A. Riggio, unpublished). In view of this, to determine whether loss of *Cbfβ* induced similar effects on the immune infiltrate at an early stage of disease, mammary glands from 9-week-old *BLG-Cre;Catnb*$^{wt/lox(ex3)}$*;Cbfβ*$^{fl/fl}$ and *BLG-Cre;Catnb*$^{wt/lox(ex3)}$*;Cbfβ*$^{wt/wt}$ mice were extracted and used for IHC staining of CD8, CD4 and NIMP (antibody against neutrophils) markers after formalin fixation and paraffin embedding. The aim was to determine any changes in the population of CD8+ T cells, CD4+ T cells, and neutrophils respectively in the mammary microenvironment across the two cohorts. H&E of mammary glands from *Cbfβ*$^{fl/fl}$ mice displayed presence of multiple pre-neoplastic lesions throughout the gland (Figure 5.5). In *Cbfβ*$^{wt/wt}$ mice, the frequency and size of such lesions were smaller in comparison. Interestingly, microscopic analysis of these glands stained with immune markers clearly displayed a higher level of positive staining in *Cbfβ*$^{fl/fl}$ glands for CD8, CD4 and NIMP compared to glands from *Cbfβ*$^{wt/wt}$ mice (Figure 5.5). Particularly, around bigger lesions in glands from *Cbfβ*$^{fl/fl}$ animals, a higher density of positively stained cells were noted. Representative H&E and IHC scans from 9-week-old wildtype FVB mice are presented in Figure 5.6 to demonstrate the absence of an immune infiltrate in normal glands at 9 weeks of age. These results suggested that loss of *Cbfβ* in *BLG-Cre;Catnb*$^{wt/lox(ex3)}$ mammary glands may be inducing an influx of immune infiltrates, particularly CD4+ T cells alongside CD8+ T cells and neutrophils. The observed association between an increased immune population with size of neoplastic lesions could be a result of an inflammatory response induced by actively growing neoplasms within the mammary gland. Consequently, the immune infiltrate could be potentiating growth of mammary lesions to allow progression and proliferation of tumours.

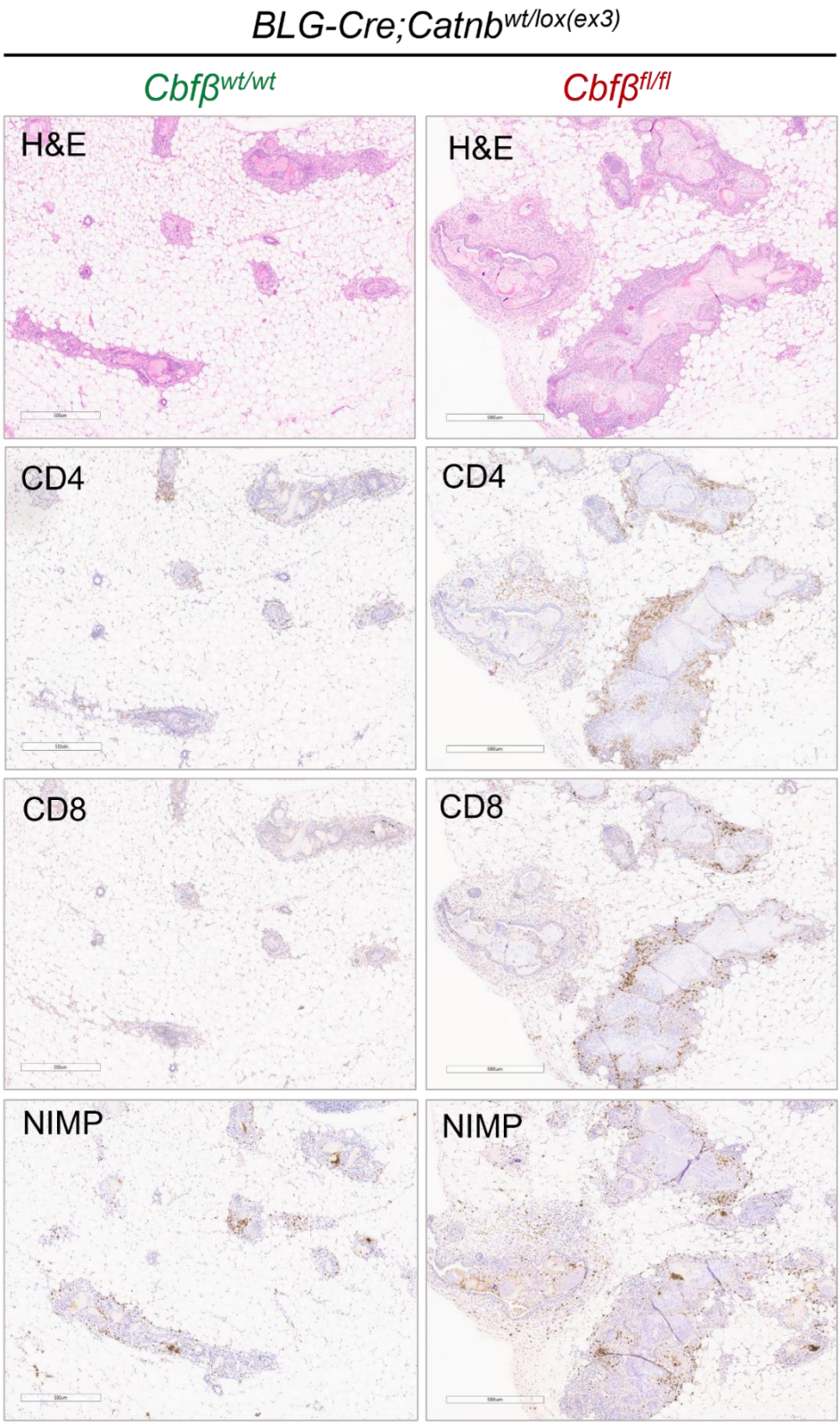

Figure 5.5: Immunohistochemical analysis of pre-neoplastic mammary glands from 9-week-old mice depicting infiltration of immune cells.

Representative H&E and IHC images of pre-neoplastic mammary glands of *BLG-Cre;Catnb*$^{wt/lox(ex3)}$ mice with wildtype *Cbfβ* (N=3), and *Cbfβ*$^{fl/fl}$ (N=3) alleles. Right inguinal gland from each mouse was used for analysis. IHC was conducted to stain for CD8+ T cells, CD4+ T cells, and neutrophils (NIMP). Scale bar=500μm.

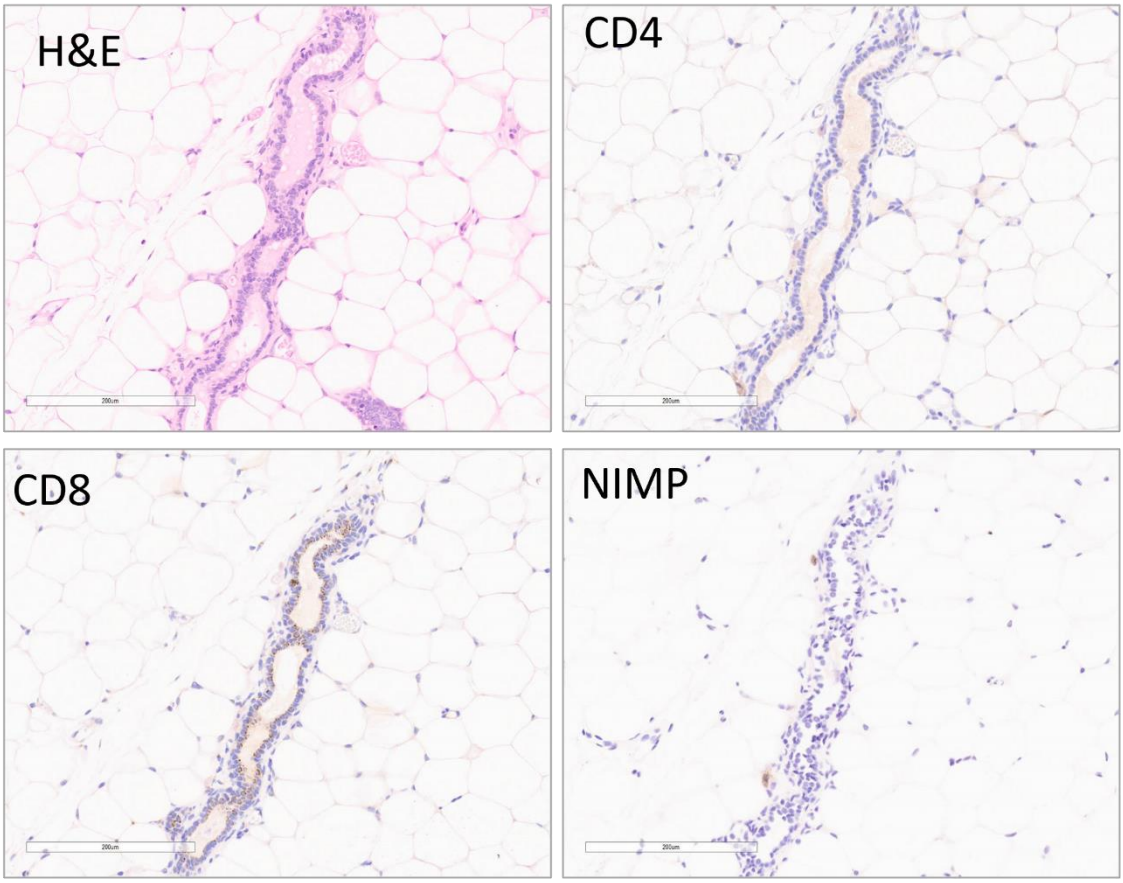

Figure 5.6: Immunohistochemical analysis of normal mammary glands from 9-week-old mice. Representative H&E and IHC images of normal mammary glands of wildtype FVB mice (N=3). Right inguinal gland from each 9-week-old mouse was used for analysis to match that of GEM glands shown in Figure 1.5. IHC was conducted to stain for CD8+ T cells, CD4+ T cells, and neutrophils (NIMP). Scale bar=300μm.

5.2.4. Flow cytometric analysis of the immune infiltrate in *Cbfβ* deficient pre-neoplastic glands.

In pursuit of validating the IHC results and characterising the immune populations observed to infiltrate into the *Cbfβ* deficient, Wnt/β-catenin activated mammary microenvironment, flow cytometric analysis was conducted. Mammary glands from 9 week old *BLG-Cre;Catnb*$^{wt/lox(ex3)}$ mice carrying either *Cbfβ*$^{fl/fl}$ or *Cbfβ*$^{wt/wt}$ alleles were harvested. After removal of lymph nodes, glands were subjected to manual and chemical dissociation to acquire single cell suspensions. Subsequently, erythrocytes were removed, and live cells counted using the trypan blue exclusion method. Two separate flow cytometry antibody panels, kindly provided by the Coffelt Lab, were used to identify populations of T cells and myeloid cells within the mammary single cell suspension. Mammary immune cells stained with

fluorescent antibodies were then analysed by flow cytometry and the data analysed using Flowjo software.

5.2.4.1. T cell populations in mammary glands from *BLG-Cre;Catnb$^{wt/lox(ex3)}$* mice

For investigation of T cell populations within the mammary pre-neoplastic niche, bulk populations of CD3 T cells along with CD4, CD8, γδ T and NK cells were analysed. CD44 and CD69 makers were used to identify activated T cells, whereas CD27 status was used to distinguish between pro- and anti-tumorigenic γδ T subsets (Ribot et al., 2009; Rei et al., 2014; Coffelt et al., 2015). IFNγ, Granzyme B and IL17 production was revealed through intracellular staining. Mature NK cells were identified as positive for CD27 and negative CD11b markers. The gating strategy for T cell analysis is represented in Figure 5.7.

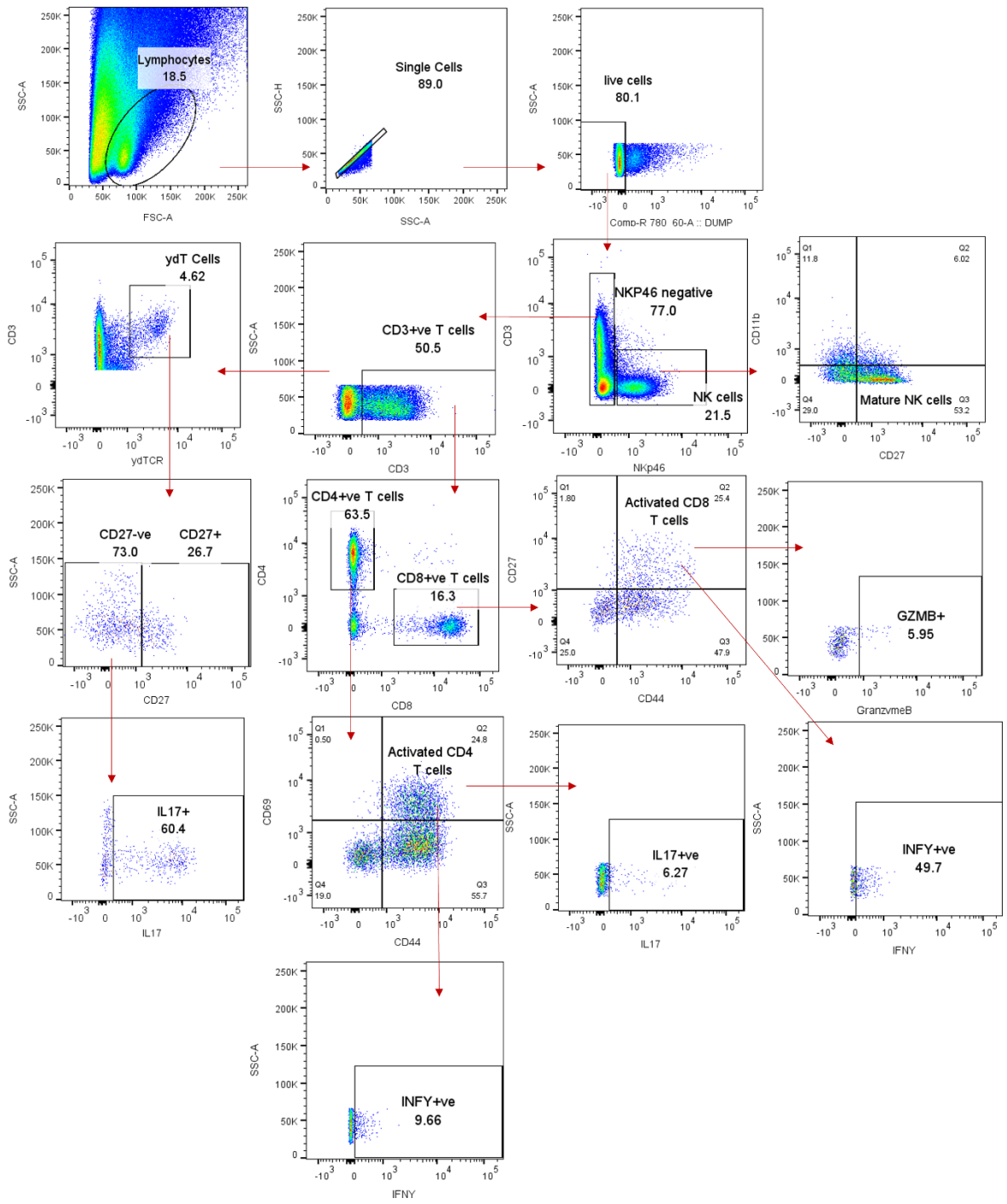

Figure 5.7: Gating strategy for T cell panel implemented to identify CD3+ T cells, CD4+ T cells, CD8+ T cells and NK (NKp46+) cells.

Activated CD4+ and CD8+ T cells were identified to be CD44+ CD69+ and production of IFNγ and IL17 cytokines by CD4+, and IFNγ and Granzyme B by CD8+ T cells was analysed. Mature NK cells were identified as NKp46+ CD11b+ CD27− and differentiated into two groups producing either IFNγ or Granzyme B. γδ T cells were identified as NKp46-ve, CD3+ γδ TCR+. CD27- γδ T cells were considered pro-tumorigenic and IL17 producing while CD27+ γδ T cells were considered anti-tumorigenic. Representative plots were obtained from mammary glands of a 9-week-old FVB mouse.

Preliminary analysis using glands from two *Cbfβ*$^{wt/wt}$ and two *Cbfβ*$^{fl/fl}$ 9-week-old mice suggested slightly elevated levels of bulk CD3+ T cells in the *Cbfβ*$^{fl/fl}$ cohort, however, levels of CD4+ and CD8+ T cells seemed comparable across the two cohorts (Figure 5.8A-C). Interestingly, when the focus was placed on only activated CD44+ CD69+ CD4 T cells (Figure 5.8D), and particularly IL17 producing CD4 T cells (Figure 5.8E), a considerably lower percentage was observed in *Cbfβ*$^{fl/fl}$ glands compared to those in *Cbfβ*$^{wt/wt}$ mice. IFNγ producing CD4 T cells remained comparable across both cohorts (Figure 5.8F). Conversely, no difference was apparent in activated CD44+ CD69+ populations of CD8+ T cells in any of the samples analysed (Figure 5.8G). Granzyme B producing CD8+ T cells were slightly elevated in glands from *Cbfβ*$^{fl/fl}$ mice, but a marked increase was noted in the proportions of IFNγ producing activated CD8+ T cells in this cohort compared to glands from *Cbfβ*$^{wt/wt}$ mice (Figure 5.8H-I). Interestingly, proportions of bulk γδ T cells (Figure 5.8J) and a subpopulation of these, CD27– pro-tumorigenic γδ T cells (Figure 5.8K), appeared slightly elevated in *Cbfβ*$^{fl/fl}$ glands compared to *Cbfβ*$^{wt/wt}$, although the sample size was too small to test for significance. Of these pro-tumorigenic γδ T cells, around 70% were IL17 producing in the *Cbfβ*$^{fl/fl}$ cohort. In the *Cbfβ*$^{wt/wt}$ cohort approximately 84% of the CD27- γδ T cells were positive for IL17 (Figure 5.8L). Additionally, glands from *Cbfβ*$^{fl/fl}$ mice consisted reduced levels of anti-tumorigenic CD27+ γδ T cells in comparison to *Cbfβ*$^{wt/wt}$ cohorts (Figure 5.8M).

Bulk NK cell fractions including those that were considered mature (CD27+ CD11b-) did not seem altered upon loss of *Cbfβ (*Figure 5.8N-O). On the other hand, a reciprocal relationship between Granzyme B producing and IFNγ producing mature NK cells were noted in glands from *Cbfβ*$^{fl/fl}$ mice (Figure 5.8P-Q). Compared to glands from *Cbfβ*$^{wt/wt}$ mice, GZMB+ mature NK cells were considerably lower, but those positive for IFNγ were substantially higher.

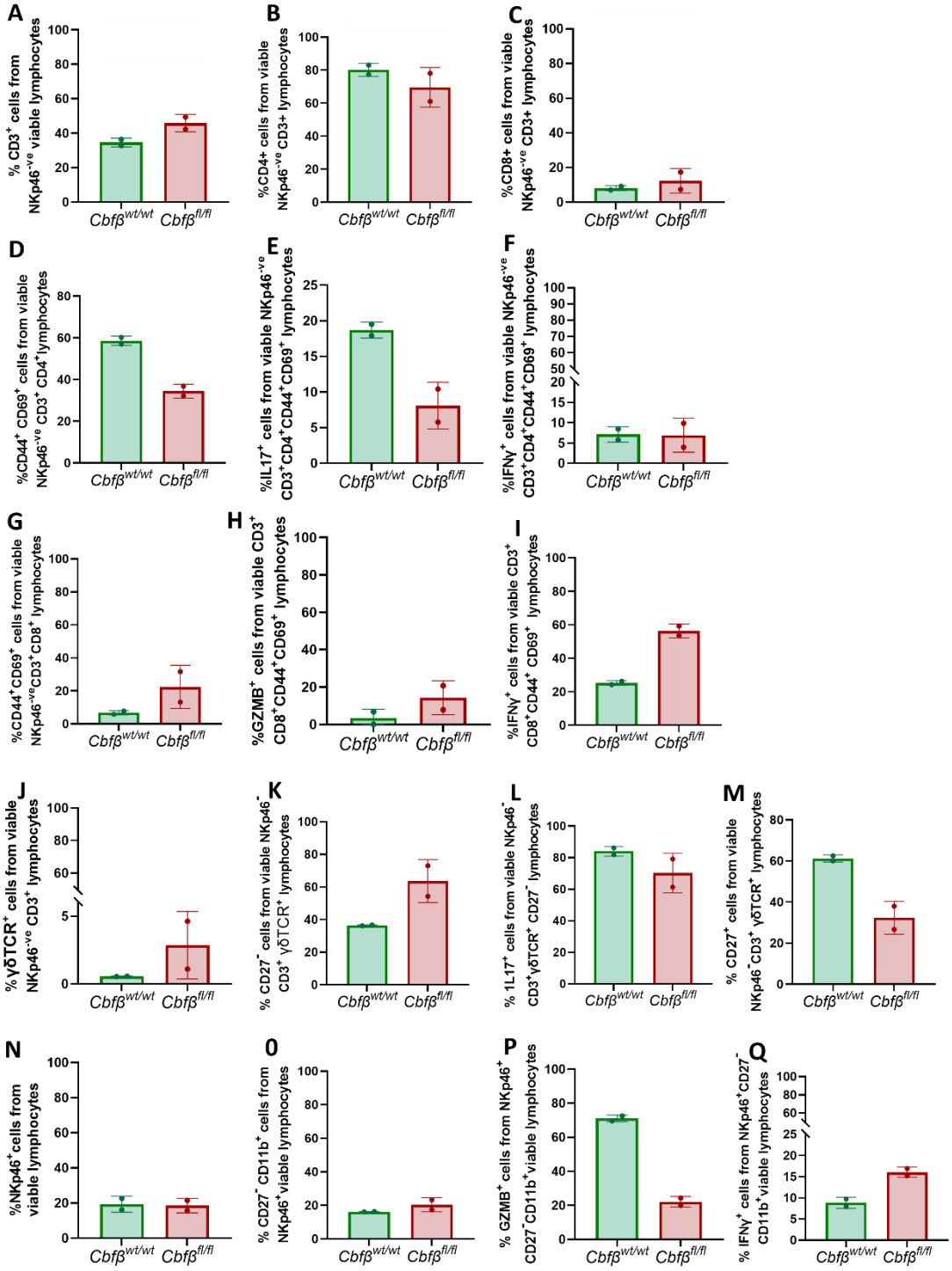

Figure 5.8: Flow cytometric analysis of T cell subpopulations, activation states and cytokine production in preneoplastic mammary glands from 9 week old *BLG-Cre;Catnb$^{wt/lox(ex3)}$* mice.

All 5 pairs of mammary glands from each cohort mouse carrying *Cbfβ$^{fl/fl}$* (N=2) or *Cbfβ$^{wt/wt}$* (N=2) alleles were used. (A-C) Bulk proportions of CD3+, CD4+ and CD8+ T cells were analysed. (D) Activated CD4+ T cells (CD44+ 69+), producing IL17 (E) and IFNγ (F); activated CD8+ T cells (CD44+ 69+) (G), producing Granzyme B (H) and IFNγ (I); γδ T cells (CD3+ γδ TCR+) (J), delineated into (K) pro-tumorigenic (CD27-) producing IL17 (L) and (M) anti-tumorigenic (CD27+) subpopulations are represented. (N) Bulk NK cells (NKp46+) and mature NK cells (O) producing Granzyme B (P) and IFNγ (Q) are displayed. Data points represent individual mice.

5.2.4.2. Myeloid cell populations in mammary glands from *BLG-Cre;Catnb$^{wt/lox(ex3)}$* mice.

Next, the distribution of myeloid cells within the pre-neoplastic mammary environment was assessed. Single cell suspensions of mammary gland single cell suspensions were stained with antibodies from the myeloid panel for flow cytometry to distinguish between populations of neutrophils, macrophages and dendritic cells. The gating strategy adapted from (Ruffell et al., 2014), has been represented in Figure 5.9. Within the mammary environment, the percentage of total myeloid cells, dendritic cells and monocytes seemed slightly elevated in *Cbfβ$^{fl/fl}$* mice compared to the *Cbfβ$^{wt/wt}$* cohort (Figure 5.10A-C). Neutrophil levels, and proportions of tumour associated macrophages including MHCII^{hi} and MHCII^{lo} populations remained comparable between the two sample groups (Figure 5.10D-F). It should be noted, due to insufficient *Cbfβ$^{wt/wt}$* controls it is difficult to determine the impact of *Cbfβ* loss on the myeloid population of Wnt/β-catenin activated preneoplastic mammary glands. Further analysis with a greater number of samples is therefore required before any conclusions can be drawn. However, these results highlight that, murine mammary glands with activated Wnt/β-catenin have a significant infiltrate of immune cells, suggesting a potential avenue for therapy through manipulation of this characteristic.

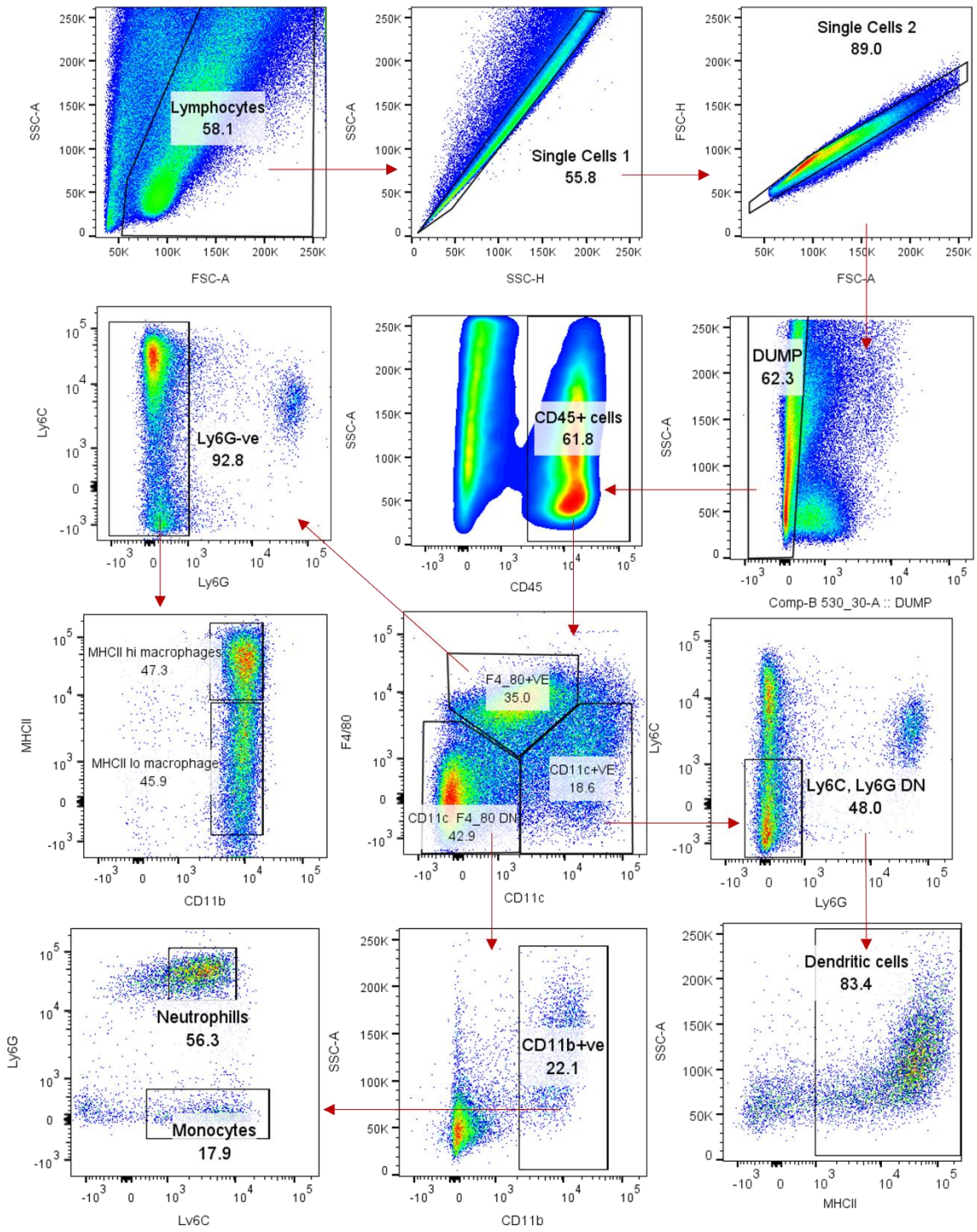

Figure 5.9: Gating strategy for myeloid cell panel implemented to identify macrophages, dendritic cells, monocytes and neutrophils.

Myeloid cells were distinguished from B cells and T cells through CD3- CD19- (DUMP gating) and CD45+ staining. Macrophages were considered F4/80+ Ly6C+ Ly6G- and separated into CD11b+ $MHCII^{hi}$ and $MHCII^{lo}$ groups. Dendritic cells were identified as CD11c+ F4/80- Ly6G- Ly6C- while Neutrophils were identified as F4/80- CD11c- CD11b+ Ly6G+ Ly6C+. Monocytes were identified as F4/80- CD11c- CD11b+ Ly6G- Ly6C+. Representative plots were obtained from FVB mammary glands.

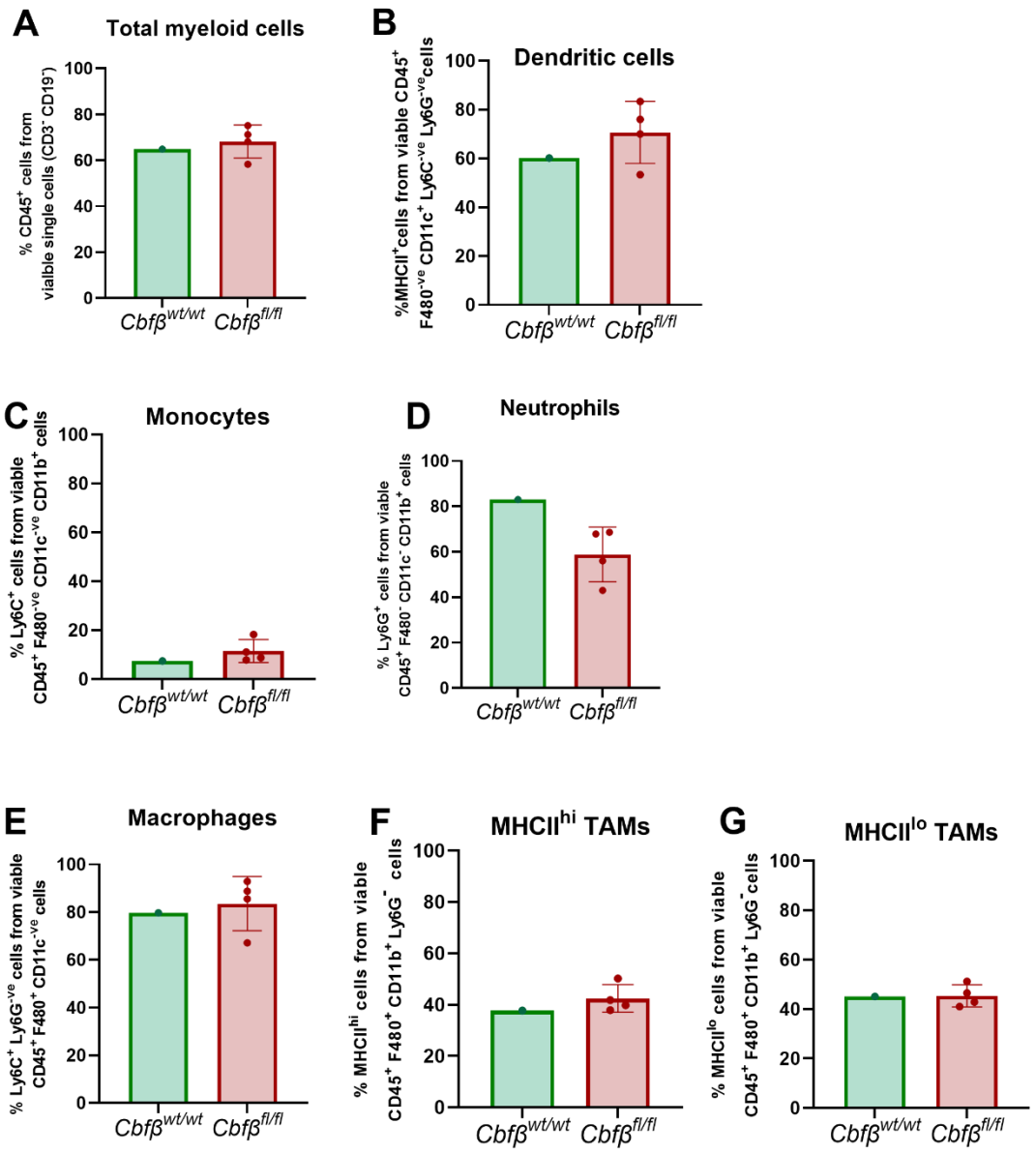

Figure 5.10: Flow cytometric analysis of myeloid cell subpopulations and cytokine production in preneoplastic mammary glands from 9 week old *BLG-Cre;Catnb*$^{wt/lox(ex3)}$ mice.

All 5 pairs of mammary glands from each cohort of mice carrying *Cbfβ*$^{fl/fl}$ (N=4) or *Cbfβ*$^{wt/wt}$ (N=1) were used. (A) Bulk proportions of CD45+ myeloid cells, (B) Dendritic cells, (C) Monocytes, (D) Neutrophils, (E) Tumour infiltrating macrophages subdivided into (F) MHCII^{hi} and (G) MHCII^{lo} are represented. Data points represent individual mice.

5.3. Discussion

Development of breast tumours, driven primarily through accumulated mutational changes are often supplemented by microenvironmental elements such as immune cells, fibroblasts, growth factors and cytokines (Degnim et al., 2014; Zumwalde et al., 2016; Azizi et al., 2018). From maintenance of normal and healthy breast tissue to progression through carcinogenic stages in breast cancer, the mammary

immune cell population undergoes varying degrees of qualitative and quantitative changes (Cichon et al., 2010; Degnim et al., 2014; Tower, Ruppert and Britt, 2019). In breast tumours the immune infiltrate consists of a diverse collection of immune cell subtypes including CD4+, CD8+ and γδTCR+ T cells, NK cells, neutrophils, monocytes/macrophages and dendritic cells. This allows the mammary immune compartment to influence growth, progression, and metastasis of breast tumours either through direct cytotoxic effects of anti-tumorigenic cells or via indirect immunostimulatory or immunosuppressive effects mediated through secretion of cytokines, cytolytic agents and growth factors (Hussein and Hassan, 2006; Ruffell et al., 2012; Korbecki et al., 2020). A cooperative effort mediated via crosstalk between tumour intrinsic factors that induce tumorigenesis and the supporting elements of the tumour microenvironment such as immune cells is key in ensuring unrestricted advancement of malignant breast cells. In this regard, multiple reports have associated activation of Wnt/β-catenin signalling in breast cells to suppression of anti-tumorigenic immune responses (Shulewitz et al., 2006; Betancur et al., 2017; Barkal et al., 2019; Castagnoli et al., 2019; Feng et al., 2019). Breast cancer cells with deregulated activation of Wnt/β-catenin adopt various avenues of immune evasion and immune suppression to induce an immune infiltrate that would be advantageous for tumour growth (Xu et al., 2020). Additionally, mutations in the RUNX family in breast tumour cells have also been suggested to influence prognosis through interaction with the mammary immune cell infiltrate (Gao and Zhou, 2021; Fu et al., 2022). In line with established literature, transcriptomic analysis of Wnt/β-catenin activated mammary tumours deficient of either *Cbfβ* or *Runx1* and *Runx2* revealed significant alteration of various immune regulatory pathways. Following sequencing of RNA extracts from end-stage tumours, pathway analysis and GSEA results indicated alterations in cytokine related pathways and elevated expression of genes involved in interferon signalling and inflammatory immune responses. Particularly in tumours lacking *Runx1* and *Runx2*, expression of multiple pro-tumorigenic cytokines such as Ccl1, Ccl2, Ccl7, Ccl8, Ccl11 and Ccl17 among others was significantly upregulated in comparison to tumours proficient for RUNX proteins. High expression of these cytokines has been associated to an increased infiltration of FoxP3+ Tregs and TAMs, and an overall poor prognosis of human breast cancer in multiple studies (Farmaki et al., 2016; Sun et al., 2017; Kuehnemuth et al., 2018; Korbecki et al., 2020; Wang and Huang, 2020). Ccl2, Ccl8 and Ccl17 have been shown to increase

proliferation, EMT induction, invasion and stemness of cancer cells (Farmaki et al., 2016; Sun et al., 2017; Korbecki et al., 2020). Ccl2 additionally has been shown to interfere with anti-tumour T cell and DC function and induce resistance to apoptosis and drug treatment in breast cancer cells through induction of the PI3K/mTOR pathway (Korbecki et al., 2020). Therefore, RNAseq results focussing on alteration of the breast immune system, suggested that acceleration of mammary tumorigenesis in response to loss of *Runx1* and *Runx2* under Wnt/β-catenin activated state may be partly attributable to the induction of a pro-inflammatory, pro-tumorigenic immune infiltrate. In the same context, the cytokine expression profile in *Cbfβ* deficient tumours at clinical endpoint resembled those in *Cbfβ* proficient tumours. This highlighted a difference between *Cbfβ* loss and *Runx1-Runx2* deletion in altering the Wnt/β-catenin activated mammary immune niche. In order to investigate the phenotypic impact of *Cbfβ* or *Runx1-Runx2* deletion in this disease setting, tumour samples fixed at clinical endpoint were used for immunohistochemical analysis to determine the distribution of CD4 and CD8 T cells, macrophages and neutrophils. Surprisingly, qualitative, and quantitative IHC analysis indicated that, while tumours across the three cohorts displayed extensive immune cell infiltration at clinical endpoint, the proportions of all immune cells analysed remained comparable. However, the activation status of these cells and their cytokine expression profiles need to be evaluated. It should also be noted, that throughout the tumour developmental process, immune regulatory signals may be constantly modulated by the cumulative impact of Wnt/β-catenin activation, loss of *Cbfβ* or *Runx1-Runx2* as well as any other genetic/epigenetic alterations acquired during tumour progression. Culmination of all these effects may result in the induction of a systemic tumour-induced inflammatory response to generate an immune microenvironment that would ultimately favour progression of the mammary tumours to clinical endpoint. Therefore, at this stage it is likely that differences in the tumour-immune niche across the different cohorts would be difficult to differentiate, hence justifying the IHC results.

Consequently, and in consideration of how loss of *Cbfβ* was seen to cause dramatic acceleration of tumorigenesis particularly during tumour initiation (Figure 4.3), it was hypothesised that perhaps modulation of the immune microenvironment in response to *Cbfβ* loss occurs in earlier phases of disease. As data from pre-

neoplastic Runx*1*$^{-/-}$;*Runx2*$^{-/-}$ murine mammary glands had previously revealed a strong inflammatory immune signature, IHC of mammary glands from 9-week-old *BLG-Cre;Catnb*$^{wt/lox(ex3)}$;*Cbfβ*$^{fl/fl}$ mice were analysed for the presence of tumour-infiltrating T cells and neutrophils. In support of the hypothesis, qualitative analysis displayed a marked increase in the number of CD4+ and CD8+ T cells as well as neutrophils around pre-neoplastic lesions in mammary glands lacking *Cbfβ*. Based on the larger size and more advance phenotype of malignant lesions observed in glands from *Cbfβ*$^{fl/fl}$ mice versus *Cbfβ*$^{wt/wt}$ mice at 9 weeks of age, it seemed likely that the immune cell infiltrates may be supporting tumorigenesis. Thus, to further characterise the mammary immune population in these cohorts, flow cytometric analysis was conducted.

Intriguingly, while levels of bulk CD4+ and CD8+ T cells remained comparable in mammary glands from *Cbfβ*$^{wt/wt}$ and *Cbfβ*$^{fl/fl}$ mice, activated CD4+ T cells (CD44+, CD69+) appeared lower and the CD4+/CD8+ ratio seemed reversed in the latter cohort. This phenotype has been associated with accelerated tumour growth and metastasis in cervical cancer which may also translate to breast cancer in this instance (Sheu et al., 1999). IL17 producing CD4+ T cells were reduced in the *Cbfβ*$^{fl/fl}$ cohort. Similarly, levels of IL17 producing pro-tumorigenic γδ T cells (CD27-) were also reduced, although not significantly, in tumours from this cohort compared to *Cbfβ*$^{wt/wt}$ mice. Contrastingly, IFNγ producing CD8+ T and NK cells were elevated. Expression of IL17 in CD4+ and γδ T cells is associated with immunosuppressive characteristics and is known to play critical roles in various pathologies including cancer (Crawford et al., 2020). IFNγ on the other hand is released in copious amounts by a multitude of immune cells including macrophages, activated CD8+ T cells, CD4+ Th1 cells and mature NK cells (Bhat et al., 2017). IFNγ is primarily famous for acting as a chemoattractant in the recruitment of T cells and neutrophils, and for inducing T cell mediated cytotoxicity (Bhat et al., 2017). However, in some cases it has been shown to reduce proliferation and increase apoptosis of T cells (Cone et al., 2007). In fact, mounting evidence regarding tumour promoting roles of IFNγ have highlighted that IFNγ can facilitate initiation and growth of tumours and promote immune evasion (Mojic, Takeda and Hayakawa, 2018). Gene expression in tumour cells altered in response to IFNγ are involved in expression of immune suppressive markers that help to inhibit function of effector T cells and NK cells (Mojic, Takeda and

Hayakawa, 2018). Therefore, with a higher proportion of IFNγ producing CD8+ T cells noted in glands from *Cbfβ*$^{fl/fl}$ mice, it is possible that these may be aiding the tumorigenic process. Alternatively, reduced population of the immunosuppressive IL17 secreting T cells and increased IFNγ producing CD8+ T and NK cells in glands from *Cbfβ*$^{fl/fl}$ mice could be representing an anti-tumorigenic response initiated against the growth of lesions. Considering how tumour initiation is accelerated in these mice, one explanation behind this could be that the anti-tumorigenic response noted at the initial stages select for aggressive, immune resistant malignant cells. Once these cells escape immune surveillance, they could be priming the immune system to induce a systemic pro-tumorigenic response which finally allows for accelerated tumorigenesis. For analysis of the myeloid population in the Wnt/β-catenin activated mammary gland, loss of *Cbfβ* did not seem to exert any overt impacts in the proportions of macrophages, monocytes, neutrophils or dendritic cells.

It should be noted however, that results from this part of the study analysing the lymphoid and myeloid cell populations by flow cytometry, are still very preliminary and a bigger sample size, with appropriate controls are required for robust analysis. Therefore, flow cytometry analysis results discussed above are simply notable observations that require further investigation in order to draw any conclusions. Additionally, RNA sequencing of pre-neoplastic glands is currently underway. Evaluation of flow cytometric data paired with transcriptomic data will provide valuable insight into the mechanistic changes occurring in the mammary microenvironment of *BLG-Cre;Catnb*$^{wt/lox(ex3)}$ in response to altered levels of *Cbfβ* or *Runx1* and *Runx2*.

Chapter 6. Future work and conclusions

A significant proportion of breast cancer patients harbour genetic alterations in *CBFβ* with most of these mutations associated to loss of function of the protein (Pereira et al., 2016; Griffith et al., 2018; Pegg et al., 2019). Despite being frequently mutated in breast cancers, limited information about the functional role of CBFβ in this disease setting is known. Results from published literature, as well as data collected so far in the Blyth lab, suggested that the RUNX/CBFβ transcriptional complex adopts pro-tumorigenic and anti-tumorigenic roles depending on the disease stage or subtype (Mendoza-Villanueva et al., 2010; Mendoza-Villanueva, Zeef and Shore, 2011; Banerji et al., 2012; Nik-Zainal et al., 2016; Pereira et al., 2016; Riggio, 2017; Rooney et al., 2017; Griffith et al., 2018; Malik et al., 2019, 2021). CBFβ is crucial for the normal functioning of RUNX proteins as it increases their DNA binding affinity and protects RUNX proteins from proteasomal degradation (Gu et al., 2000; Bravo et al., 2001; Huang et al., 2001; Yan et al., 2004). As a key regulator in both development and disease, CBFβ holds multifaceted attributes which need to be unravelled further to understand the mechanisms behind their circumstantial impact on breast cancer. One way to do this is through the use of GEMMs that allow precise investigation of a gene's function in developmental and disease processes in a physiologically relevant context. As whole-body deletion of *Cbfβ* is known to result in embryonic lethality (Qing Wang et al., 1996), *g*enetically engineered conditional knockout mouse models were used in this project to determine whether CBFβ acts as a tumour suppressor, an oncogene or has a dualistic context dependent effect – similar to the RUNX proteins (Blyth, Ewan R Cameron and Neil, 2005; Chimge and Frenkel, 2013; Rooney et al., 2017) – within the natural mammary microenvironment. Additionally, it was particularly interesting to interrogate whether deletion of *Runx* genes were functionally modelling loss of their co-factor CBFβ.

In this regard, the effect of *Cbfβ* loss in mammary tumorigenesis was studied in the *MMTV-PyMT;MMTV-Cre* mouse model. However, the stochastic nature of MMTV promoter expression resulted in producing *MMTV-Cre* negative "escapee tumours". In such tumour cells, while the PyMT oncogene was successfully expressed, Cre-recombinase expression was very low to almost absent resulting in no significant deletion of the conditional *Cbfβ* alleles. This was validated through

tdRFP reporter based tracking of Cre activity in *MMTV-PyMT;MMTV-Cre;tdRFP* mice shown in Chapter 3. Owing to this issue, deletion of *Cbfβ* remained inconsistent within the mammary gland and thus no overt effect on tumorigenesis was noted. To circumvent this issue, the *MMTV-PyMT;ROSA-CreER*^{T2} model was generated with a view of having the ability of conditionally deleting *Cbfβ* upon induction through tamoxifen or 4OHT. Using this system, the impact of *in vivo* deletion of *Cbfβ* could be investigated both temporally (thereby allowing investigation of the role of CBFβ in different stages of mammary tumorigenesis), and spatially through intraductal delivery of tamoxifen for instance. However, due to the COVID-19 pandemic and the restrictions imposed on laboratory work, use of this model for *in vivo* investigation of *Cbfβ* loss in mammary cancer was interrupted. Therefore, in accordance with the principle of 3Rs, tumours from these 'Cbfβ-wild type' mice were utilised in *ex vivo* generation of primary tumour derived cell lines. *Cbfβ* was conditionally deleted *in vitro* through 4OHT mediated activation of ROSA-CreER^{T2} and the impact on tumour cell viability, growth and colony forming ability was assessed. Results from these experiments indicated towards an oncogenic role of *Cbfβ* in established MMTV-PyMT mammary tumour cells. Reduction in cell viability, proliferation and clonogenicity noted in *Cbfβ* deficient cells seemed to disprove our original hypothesis of *Cbfβ* acting as a tumour suppressor in a model which transcriptionally aligns with luminal B breast cancer (Pfefferle et al., 2013). These results were further validated by work of a master's student (Nimrit Kaur) who showed reduced proliferation and clonogenicity of *MMTV-PyMT;Cbfβ*$^{fl/fl}$ cells with Adeno-virus mediated expression of Cre and deletion of *Cbfβ*. Interestingly, these results align with evidence from ER negative MDA-MB-231 breast cancer cells which showed that CBFβ acts as an oncogene and is critical for the maintenance of an invasive, metastatic phenotype (Mendoza-Villanueva et al., 2010; Ran et al., 2020). Expression of various genes involved in the induction of EMT, and breast cancer metastasis was reduced upon knockdown of CBFβ (Mendoza-Villanueva et al., 2010; Mendoza-Villanueva, Zeef and Shore, 2011; Ran et al., 2020). It is possible that a similar mechanism underpins the reduction in tumour cell proliferation and clonogenicity noted in the *Cbfβ* deficient PyMT cell lines discussed above. In view of this, analysing the genetic and molecular changes induced in these cell lines in response to *Cbfβ* deletion would reveal relationships between CBFβ, and pathways involved in

mammary tumorigenesis, thereby, shedding light on the functional role of CBFβ in this context.

It should be noted that Cre-recombinase mediated excision of *Cbfβ*$^{fl/fl}$ alleles induces DNA double strand breaks for subsequent homologous recombination (Wagner et al., 1997). This could potentially trigger DNA-damage responses resulting in reduced cell viability and proliferation. Therefore, alternative methods of disrupting CBFβ function, instead of direct modification of the gene, can be employed to validate these *in vitro* results. In this regard, *Cbfβ* shRNAs have been used in the lab to successfully reduce CBFβ protein expression in HC11 cells. Generation of *Cbfβ* deficient cells lines through CRISPR/Cas9 mediated deletion of the gene would also allow analysis of the long-term effects of *Cbfβ* loss on mammary tumour cells. Alternatively, the small molecule inhibitor of the RUNX/CBFβ complex can be used (Illendula et al., 2016). The inhibitor disrupts the CBF complex, thereby preventing translocation of CBFβ/RUNX complex into the nucleus (Illendula et al., 2016). In an *in vitro* 3D model of basal-like breast cancer, use of the RUNX/CBFβ inhibitor was shown to reduce cell viability (Illendula et al., 2016). In mammary epithelial MCF10A cells, disruption of the CBF complex using the inhibitor was shown to induce a mesenchymal phenotype (Rose et al., 2020), similar to the changes in cell morphology noted in *Cbfβ* deficient PyMT tumour cells (Chapter 3). It would be interesting to see whether limiting transcriptional modulation mediated by CBFβ and therefore RUNX, in this manner results in the same growth reducing effect on *MMTV-PyMT* tumour cells or whether oncogenic impacts of CBFβ are mediated through its roles in translational regulation of mRNAs (Malik et al., 2019). If administration of the inhibitor on established mammary cancer cells induces a negative impact on cell growth and clonogenicity, it would endorse disruption of the CBF complex in human patients where oncogenic roles *Cbfβ* are presented such as in ER negative breast cancer.

In vitro results of course would need to be validated through *in vivo* approaches to confirm the biological relevance of results. In the first instance, orthotopic transplantation experiments using *MMTV-PyMT;ROSA-CreER*^{T2}*;LSL-tdRFP;Cbfβ*$^{fl/fl}$ tumour cell lines and syngeneic hosts, can be used to determine oncogenicity of tumours in the absence of *Cbfβ* within a physiological environment. The added benefit of this model is in the temporal control of genetic manipulation. Moreover, this model would allow deletion of *Cbfβ* specifically in the transplanted tumour cells, thereby enabling investigation of tumour cell intrinsic effects of *Cbfβ* loss

in an otherwise *Cbfβ* proficient micro-environment. This allograft model would additionally allow investigation of the metastatic potential of *Cbfβ* deficient *MMTV-PyMT* tumour cells and the impact of acute deletion of this gene on the mammary tumour immune microenvironment. Subsequently, *MMTV-PyMT;ROSA-CreER^{T2};LSL-tdRFP;Cbfβ$^{fl/fl}$* mouse mammary epithelial cells (MMECs) could be generated and subjected to a similar experimental plan to investigate the impact of *Cbfβ* loss in the initial stages of mammary tumorigenesis.

In breast cancer patients, *CBFβ* alterations have been shown to co-occur with other oncogenic drivers of this disease such as *PIK3CA* and *GATA3* (Pereira et al., 2016). Mammary epithelial cells containing an inducible Cre recombinase can be used to control expression of *Cbfβ* temporally and spatially and study its role in mammary tumorigenesis induced by such drivers of breast cancer. *In vitro* interrogation of the role of *Cbfβ* under the context of different oncogenes would be an important first step which can be followed up by *in vivo* investigation through mouse models where mammary cancer is driven by transgenic expression of various oncogenes (Hennighausen, 2000).

Addressing the caveats of the *MMTV-PyMT;MMTV-Cre* model, a more sophisticated *in vivo* system such as the tetO-MIC (tetO-PyMT-IRES-Cre) mouse model would be useful in studying the impact of *Cbfβ* loss on mammary tumorigenesis (Rao et al., 2014). In this system, expression of a doxycycline inducible PyMT oncogene is coupled to expression of Cre recombinase through an internal ribosome entry sequence (IRES) (Rao et al., 2014). Additionally, in this model, the histopathology of mammary tumours and their propensity for metastasising to lungs resemble those noted in *MMTV-PyMT* and human breast cancers (Rao et al., 2014). Genetic crossing of this line onto the *Cbfβ$^{fl/fl}$* line would therefore enable deletion of the gene in Cre proficient, PyMT oncogene driven mammary tumour cells. This would allow *in vivo* determination of the role of *Cbfβ* in PyMT driven spontaneous mammary tumorigenesis. Together these approaches would provide further insight into understanding the importance of *Cbfβ* in both early and late stages of breast cancer. Notably, it would be crucial to characterise all *in vitro* and *in vivo* models with respect to hormone receptor status, EMT phenotype, luminal vs basal properties in all instances to relate oncogenic or tumour suppressive roles of *Cbfβ* to the appropriate human breast cancer subtype.

6.1. First *in vivo* evidence of CBFβ as a tumour suppressor in a Wnt/β-catenin driven breast cancer model

Accumulation of activated β-Catenin due to mutations in the *CTNNB1* gene or uncontrolled Wnt/β-catenin signalling has been strongly implicated in tumour promotion in breast cancer patients and in inducing mammary tumours in mice (Hatsell et al., 2003; Wang et al., 2015). Alterations in CBFβ/RUNX proteins have been found to coincide with alterations in multiple Wnt/β-catenin pathway regulators in various patients according to gene expression data acquired from tumour samples (Cerami et al., 2012; Gao et al., 2013; Pereira et al., 2016). The *BLG-Cre;Catnb*$^{wt/lox(ex3)}$ genetic mouse model used in Chapters 4-5, excitingly confirmed a tumour suppressive role of CBFβ in mammary tumorigenesis, particularly in tumour initiation (Chapter 4). Transcriptomic analysis of established tumours in this model suggested that this tumour suppressive role may be asserted through negative regulation of Wnt/β-catenin signalling and potentially Notch signalling. There is much more interrogation to be done regarding the influence of CBFβ on other oncogenic pathways involved in breast cancer. Preliminary analysis of GSEA results from *Cbfβ* deficient *BLG-Cre;Catnb*$^{wt/lox(ex3)}$ end-stage tumours revealed enrichment of several genes sets associated to upregulation of ERBB2, RAF/MEK, EGFR,TGFβ and VEGF (data not shown). Further investigation would be important to understand underpinning mechanisms behind these alterations and determine whether CBFβ associated changes in these pathways are specific to the context of activated Wnt/β-catenin signalling.

Regarding the oncogenic effect induced upon deletion of *Cbfβ* in Wnt/β-catenin driven breast cancer, a series of future experiments have been planned to build on the results discussed in this thesis. Firstly, since *Cbfβ* loss seems to be augmenting Wnt signalling, a key experiment would be to determine whether inhibition of this pathway in *Cbfβ* deficient *BLG-Cre;Catnb*$^{wt/lox(ex3)}$ tumour cells, and subsequently in mice, delays the tumorigenic process to a level similar to that noted in *Cbfβ* proficient mice. Various therapeutics aimed at inhibiting the Wnt signalling pathway are already underway with several of these being tested in phase I/II clinical trials as elaborated in a review by Pai *et al* (Pai et al., 2017). Wnt947 for instance, an inhibitor of PORCN – the enzyme involved in the

palmitoylisation mediated activation of Wnt proteins – has been shown to induce cell cycle arrest in ovarian cancer cells and reduce tumour growth and metastasis of head and neck carcinomas *in vivo*. Vantictumab (OMP-18R5) a monoclonal antibody that antagonises Wnt signalling through blocking Frizzled receptor 8 has already been tested in Phase1b clinical trial of HER2 negative breast cancer patients (Diamond et al., 2020). If inhibition of Wnt signalling in *Cbfβ* deficient tumours delays tumour initiation, tumour progression or rescues the tumorigenic phenotype, this could be used as an alternative therapeutic option in patients with loss of function mutations in *Cbfβ*. As an additional validation step, CBFβ could be re-introduced into *Cbfβ* deficient *BLG-Cre;Catnb*$^{wt/lox(ex3)}$ tumour derived cells, as described in a recent paper by Hsu *et al*. (Hsu et al., 2022), to determine whether the ectopic expression of this tumour suppressor can reverse the impact on Wnt signalling and mammary cell tumorigenic properties.

To analyse the role of CBFβ primarily on tumour initiation, RNAseq of pre-neoplastic glands would provide useful information regarding the transcriptomic changes occurring during early phases of disease. In this regard, RNA extracts from mammary glands of 9 week old *BLG-Cre;Catnb*$^{wt/lox(ex3)}$*;Cbfβ*$^{fl/fl}$ and *BLG-Cre;Catnb*$^{wt/lox(ex3)}$*;Cbfβ*$^{wt/wt}$ mice will be interrogated. Analysis of bulk mammary gland tissues would also provide information regarding the tumour-immune niche at this disease stage. This would also help supplement findings from the IHC and flow cytometry analysis of the immune population in pre-neoplastic glands discussed in Chapter 5. Additionally, it would be important to determine the impact of CBFβ loss on nascent tumour cells, often considered as the tumour cell of origin (Visvader, 2009). Depending on the mammary cell population first exhibiting loss of key tumour suppressors, different subtypes of mammary tumours could be generated. For instance, loss of the tumour suppressor gene BRCA1 in the luminal progenitor population perturbs differentiation and maturation of these cells and triggers their transformation (Lim *et al.*, 2009; Visvader, 2009). Gene expression patterns of such luminal progenitors have been significantly correlated to aggressive subtypes of breast cancer (Lim *et al.*, 2009; Visvader, 2009). Similarly, in pre-neoplastic glands from *BLG-Cre;Catnb*$^{wt/lox(ex3)}$*Cbfβ*$^{fl/fl}$ mice, genetic loss of *CBFβ* could be triggering transformation of luminal progenitors, as directed by BLG-Cre, and initiating a highly aggressive and accelerated form of mammary cancer. Further immunohistochemical

characterisation of pre-neoplastic glands from cohort mice along with flow cytometric analysis to determine any changes in the population densities of luminal and basal mammary epithelial cells could provide important clues. Additional interrogation could be carried out through lineage tracing and clonality studies as described in an elegant paper by (Lim *et al.*, 2009) and single-cell profiling with respect to early timepoints in tumorigenesis (Bach *et al.*, 2021). These could reveal how epithelial progenitors and their differentiation patterns are impacted upon loss of *Cbfβ* under WNT activated carcinogenesis. Multiple *in vitro* studies have already indicated how CBFβ plays context dependent roles in mammary tumorigenesis (Mendoza-Villanueva *et al.*, 2010; Mendoza-Villanueva, Zeef and Shore, 2011; Malik *et al.*, 2019, 2021; Pegg *et al.*, 2019; Ran *et al.*, 2020) and a potential explanation for this conundrum may lie in the epithelial subtype or maturation state of the cell of tumour origin. It would be interesting to observe the transcriptomic changes induced by genetic deletion of *Cbfβ* in different cell populations in the mammary epithelial hierarchy and determine whether these could be correlated to generation of different breast tumour phenotypes.

Furthermore, to unravel the relationship between *Cbfβ, Runx1-Runx2* and the Wnt signalling pathway, it would be interesting to determine whether altered members of this pathway are directly regulated by CBFβ. (Malik et al., 2019) showed how loss of *Cbfβ* transforms MCF10A cells (immortalised normal mammary epithelial cells), a phenotype which can subsequently be rescued by re-introduction of the protein. The study suggests that CBFβ complexes with RUNX1 in the nucleus and acts as a tumour suppressor by repressing NOTCH3 transcription (Malik et al., 2019). Interestingly, this paper also showed that CBFβ plays a critical role in initiating translation of hundreds of mRNA transcripts including a collection of Wnt pathway members (Malik et al., 2019). It is possible that CBFβ could be exerting its tumour suppressive function through regulating translation of various Wnt/β-catenin signalling members. However, RNAseq results from *Runx1-Runx2* deficient *BLG-Cre;Catnb*$^{wt/lox(ex3)}$ tumours displayed normal expression of *Cbfβ* (data not shown). Considering the accelerated tumorigenesis noted in this cohort and the fact that CBFβ is not able to translocate into the nucleus without RUNX proteins, this indicates that the role of CBFβ in translational regulation may not be enough to repress the Wnt pathway. In this case, it is likely that CBFβ may be exerting its tumour suppressor function through transcription regulation, perhaps in conjunction with RUNX proteins. Indeed, there is mounting evidence regarding a

reciprocal regulation of transcription between the RUNX/CBFβ complex and various Wnt pathway members (Sweeney, Cameron and Blyth, 2020). Therefore, using a CBFβ/RUNX inhibitor to inhibit interaction with RUNX and thereby, translocation of CBFβ into the nucleus could help discern whether CBFβ interferes with transcription of Wnt/β-catenin regulators. Determining whether CBFβ is directly involved in the translation or transcriptional repression of genes encoding Wnt/β-catenin activators would provide valuable insight into the mechanism behind tumorigenesis associated to *Cbfβ* loss. Additionally, this would also provide insight into the relationship between Runx1, Runx2 and the Wnt signalling pathway in mammary tumorigenesis. Furthermore, immunoprecipitation experiments and chromatin immunoprecipitation sequencing (CHIP-Seq) would provide valuable information regarding protein-protein and protein-DNA interactions involving CBFβ. The unavailability of effective CBFβ antibodies suitable for these purposes have hindered progress in this aspect thus far.

It is worth mentioning that while RUNX3 as a member of the RUNX/CBFβ complex was not investigated in this project, it should not be dismissed. *Runx3* expression was downregulated in end-stage tumours in both *Cbfβ* deficient and *Runx1-Runx2* deficient *BLG-Cre;Catnb*$^{wt/lox(ex3)}$ mice according to RNAseq data (not shown). However, the expression of *Runx3* in epithelial cells have been questioned by various studies. For instance, while some studies showed expression of *Runx3* in whole murine glands (Blyth et al., 2010) and indicated a putative tumour suppressor function for RUNX3 in ER positive breast cancer (Huang et al., 2012); this was contradicted by evidence from sorted mammary epithelial cells and normal human MCF10A cells showing undetectable levels of *Runx3* (Wang, Brugge and Janes, 2011; McDonald et al., 2014). These results indicated that perhaps the expression of *Runx3* detected in whole glands were attributable to the mammary stromal compartment rather than epithelial cells. Furthermore, a thorough analysis of *Runx3* expression in gastrointestinal epithelial cells validated a lack of expression of this gene in epithelial cells (Levanon et al., 2011). Therefore, it is possible that the expression of *Runx3* noted in bulk tumour samples from *BLG-Cre;Catnb*$^{wt/lox(ex3)}$ mice reflect *Runx3* levels within the stromal compartment of the gland. Alternatively, alteration of the Wnt/β-catenin pathway could trigger upregulation of this RUNX protein as a compensatory protective mechanism against tumorigenesis. This feature may be lost upon deletion of *Cbfβ* or the two

other *Runx* members. For determination of either scenario, one option would be to use fluorescent activated cell sorting to differentiate mammary tumour cells from the stromal compartment. Investigation based on such a pure population of tumour cells would allow more accurate transcriptomic or proteomic characterisation without confounding data from surrounding cells. Additionally single cell sequencing and profiling of these tumours would allow further dissection of the precise cellular components that make up the mammary microenvironment and identify the genetic changes induced in specific subsets of cells (Bach et al., 2021).

6.2. RUNX/CBFβ complex and its role in mammary immune micro-environmental signalling

Alteration of various immune regulatory pathways in *Cbfβ* deficient end-stage tumours suggested towards a role of *Cbfβ* in modulation of the tumour-immune micro-environment. While, IHC analysis of end-stage *BLG-Cre;Catnb*$^{wt/lox(ex3)}$ tumours indicated a considerable infiltration of immune cells, the impact of *Cbfβ* loss on the immune niche at this disease stage was not noticeable. Conversely, pre-neoplastic *Cbfβ* deficient mammary glands displayed a marked increase in mammary immune infiltrate compared to *Cbfβ* proficient *BLG-Cre;Catnb*$^{wt/lox(ex3)}$ mice. It is worth highlighting that, for the latter case, presence of more advanced lesions was noted in *Cbfβ* deficient mammary glands compared to those expressing wildtype *Cbfβ* in mice of the same age group (9 weeks old). Therefore, whether the increase in mammary immune infiltrate was a direct result of *Cbfβ* loss or whether it was a consequence of disease advancement requires further evaluation. In this regard, staining of *BLG-Cre;Cbfβ*$^{fl/fl}$ mammary glands, (where Wnt/β-catenin has not been genetically perturbed and we see no evidence of neoplasia) for similar immune markers has been planned. Due to insufficient sample numbers in flow cytometric analysis, it has been difficult to assess any significant differences in the immune cell populations infiltrating pre-neoplastic glands from *Cbfβ*$^{fl/fl}$ or *Cbfβ*$^{wt/wt}$ mice. So far preliminary data supports an impact of *Cbfβ* deletion on the immune microenvironment. It is tempting to speculate this could have a prognostic outlook for patients as has been shown for RUNX1 (Tian et al., 2020; Fu et al., 2022). Of course, whether the *CBFβ* mutations found

in the patients would be the same as *Cbfβ* deletion in the mouse model warrants caution in its interpretation.

To determine the connection between *Cbfβ* or *Runx1-Runx2* loss and the immune microenvironment of the Wnt/β-catenin activated mammary epithelium, the crosstalk between tumour cells and the surrounding immune niche must be characterised. Whilst IHC staining of end-stage *BLG-Cre;Catnb*$^{wt/lox(ex3)}$*;Cbfβ*$^{fl/fl}$ tumours suggested that the immune infiltrate in this cohort remains similar to that from *Cbfβ*$^{wt/wt}$ and *Runx1*$^{fl/fl}$*;Runx2*$^{fl/fl}$ cohorts, flow cytometric analysis of these tumours might allow further characterisation of the immune population. Particularly the activation states of immune cells and their cytokine profiles, which modulate their anti- and pro-tumorigenic immune responses, are better captured through flow cytometric analysis as shown in Chapter 5. Therefore, while the IHC results indicate similar immune profiles across the three cohorts, flow cytometric analysis could reveal potential differences in terms of immune cell polarisation. The characterisation of the immune infiltrate in pre-neoplastic glands should also be prioritised as loss of *Cbfβ* was shown to impact clinical onset to a greater degree compared to tumour progression. It would be important to study the functional crosstalk between the immune population and mammary tumour cells from *Cbfβ*$^{fl/fl}$ and *Cbfβ*$^{wt/wt}$ cohorts using following flow cytometric analysis with greater number of samples. The increased immune infiltrate, in pre-neoplastic glands from the *Cbfβ*$^{fl/fl}$ cohort (Chapter 5), could be a result of accelerated Wnt signalling in these glands (Schmalhofer, Brabletz and Brabletz, 2009; Ma et al., 2018; Wellenstein et al., 2019). Augmentation of Wnt/β-catenin signalling and potentially Notch signalling induced upon loss of *Cbfβ* could be secreting endogenous Wnt ligands and cytokines from tumour cells. Such signals from tumour cells have been shown to stimulate immune cells such as neutrophils, TAMs and pro-tumorigenic T cells such as γδ T cells (Coffelt, Wellenstein and de Visser, 2016; Wellenstein et al., 2019). This in turn could trigger a pro-tumorigenic inflammasome response (Wissman et al., 2003; Coffelt, Hughes and Lewis, 2009; Coffelt et al., 2015; Shen et al., 2017). The resulting recruitment of monocytes and macrophages would give rise to a vicious self-perpetuating cycle (Coffelt, Hughes and Lewis, 2009; Coffelt and de Visser, 2016). Indeed, genomic data submitted to the Gene Expression Omnibus (GEO) by (Malik et al., 2019), was used to conduct gene expression analysis (data not shown). This revealed an

interesting result supporting the above hypothesis: In *Cbfβ* knockout MCF10A cells, expression of multiple immune regulatory genes including *IL1β* and *CCND2*, was upregulated significantly. Additionally, data acquired previously by RNAseq and IHC in the lab, showed how pre-neoplastic glands in mice lacking both *Runx1 and Runx2* expressed elevated levels of *Il1β*, *1l17β* and *Ccl2*. It is possible that loss of *Cbfβ* in early disease stages may also be influencing the tumour-immune microenvironment in a similar fashion. A schematic of this speculative hypothesis is presented in Figure 6.1

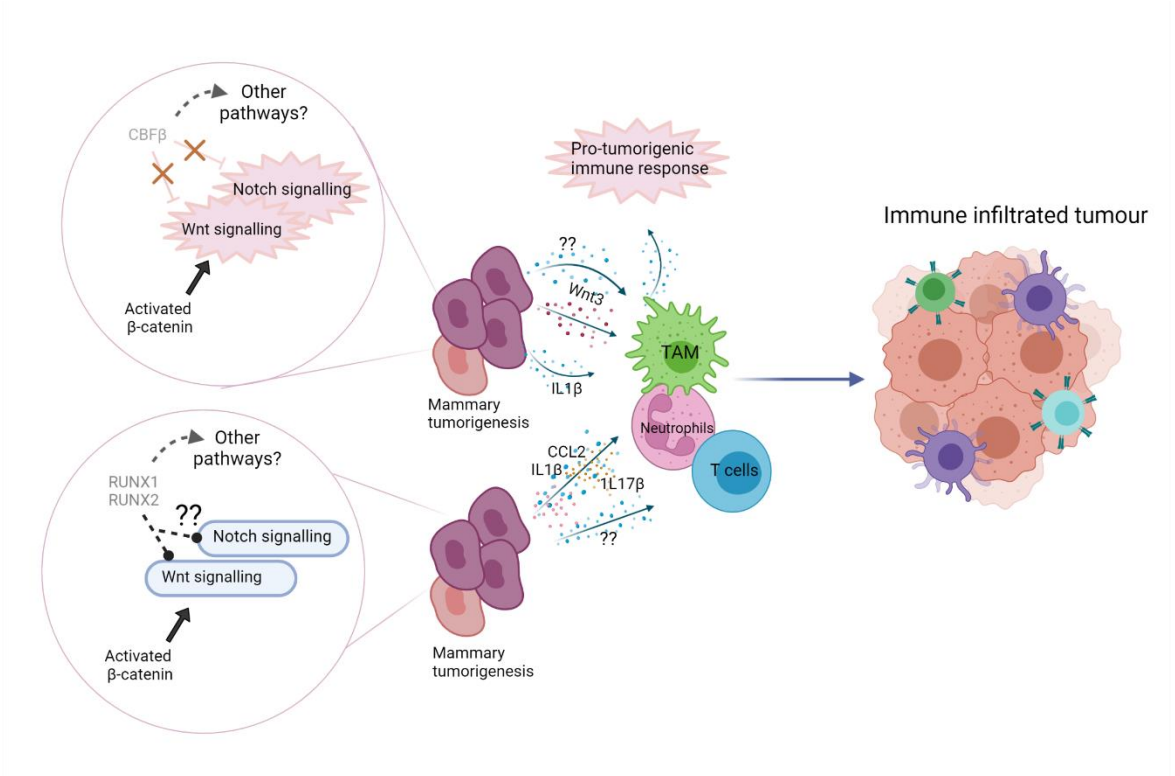

Figure 6.1: Schematic representation of a speculative mechanism outlining mammary tumour-immune crosstalk in response to loss of *Cbfβ* or *Runx1-Runx2*.

Augmentation of the Wnt and Notch pathways upon loss of *Cbfβ* may be driving transformation of mammary epithelial cells. Alternatively, and/or in addition, *Cbfβ* loss could be triggering changes in other oncogenic pathways to drive tumorigenesis. Cytokine and Wnt mediated signals from tumour cells could be inducing and attracting a pro-tumorigenic immune response which leads to advancement of disease. A similar scenario may be ensuing the combined loss of *Runx1* and *Runx2* in mammary epithelial cells, although the relationship between RUNX proteins and the signalling pathways involved in carcinogenesis require further evaluation. As loss of *Runx1-Runx2* has been shown to upregulate expression of *Il17β*, *Ilβ* and *Ccl2 (*A. Riggio, unpublished) these factors in combination with other cytokines and interleukins may be involved in mediating the cross talk between *Runx1-Runx2* deficient tumours cells and the mammary immune infiltrate. Figure created using Biorender.com

Therefore, investigating the tumour immune secretome might provide important insight into this crosstalk. It would be interesting to perform cytokine arrays to identify the chemokines being released from tumour cells and involved in the crosstalk with the mammary immune microenvironment. Co-culture experiments with tumour cells proficient or deficient of *Cbfβ* and immune cells such as T cells or macrophages would additionally help determine whether signals from tumour cells induce activation of certain populations of immune cells or their polarisation into either pro- or anti-tumour phenotypes (Carron et al., 2017). These together

with *ex vivo/in vitro* experiments involving media swapping between tumour cells and immune cells followed by transcriptomic and proteomic analysis of cells and their secretome would unveil signals exchanged between tumours cells and their immune neighbours. For further validation, antibodies blocking specific signalling components could help reveal key factors involved in this crosstalk. These could subsequently be tested *in vivo* using pharmacologically or genetically immune depleted hosts. An elegant paper employed similar approaches in depleting NK cells and CD8+ T cells to determine their roles in leukaemia (Tirado-Gonzalez et al., 2021). This would be crucial in understanding the differences observed in *Cbfβ* deficient and *Runx1-Runx2* deficient *BLG-Cre;Catnb*$^{wt/lox(ex3)}$ tumours where a greater alteration of the tumour immune profile was noted in the latter group through RNAseq analysis. If loss of *Runx1-Runx2* increases the co-stimulatory signals between mammary tumour cells and immune cells, then an immune depleted microenvironment should be disadvantageous to tumour growth. The same phenomenon can be tested in *Cbfβ* null mice and results from the two cohorts compared to assess their mechanistic differences. Additionally, an inducible Cre/lox system could be used to switch on and off expression of *Cbfβ* or *Runx1-Runx2* in mammary epithelial cells at different stages of tumorigenesis. Shen et al utilised a similar approach in revealing tumour-immune crosstalk mediated through Notch signalling (Shen et al., 2017). Subsequent changes in the immunological environment can then be tracked to understand acute impacts of *Cbfβ* or *Runx1-Runx2* loss on the tumour-immune profile. Further, it would be important to distinguish *Cbfβ* specific effects from the intrinsic impacts of constitutive Wnt/β-catenin activation on the mammary immune microenvironment. To this end *Cbfβ*$^{fl/fl}$ MMECs containing an inducible Cre can be orthotopically transplanted into syngeneic mice and changes in the immune microenvironment monitored through IHC analysis of glands, flow cytometry and characterisation of the circulating blood immune population. These experiments would start to unpick the cause versus consequence relationship between *Cbfβ* deletion, immune infiltration, and mammary tumorigenesis.

6.3. Concluding remarks

A tumour suppressive role of CBFβ in Wnt/β-catenin activated mammary cancer has been proven for the first time *in vivo* through the work conducted in this

project. Through interrogation of the transcriptomic and immune profiles of *Cbfβ* deficient Wnt/β-catenin activated mammary tumours, the underlying mechanism behind the accelerated tumour onset in *BLG-Cre;Catnb*$^{wt/lox(ex3)}$;*Cbfβ*$^{fl/fl}$ mice is thought to be two-pronged where: (1) Loss of *Cbfβ* imposes an additive effect on Wnt signalling activation in an already Wnt/β-catenin activated setting and (2) augmented Wnt signalling and other related signalling pathways in response to *Cbfβ* loss induces expression of pro-inflammatory factors such as Wnt ligands and cytokines which could induce an extrinsic pro-tumorigenic immune response further priming the mammary microenvironment for growth of tumours. Noting the influence of CBFβ on Wnt signalling in the context of the mammary gland, Wnt inhibitors may serve as a useful therapeutic option in patients with loss of function mutations or deletions of *Cbfβ*. This opens up new avenues of therapy in patients involving personalised medicine based on the vulnerabilities of signalling pathways. Of course, it would be essential to characterise patient tumours and use Wnt inhibitors to treat tumours where *Cbfβ* loss coincides with deregulated Wnt signalling. Further, mammary tumours with loss of *Cbfβ* or *Runx1-Runx2* in the Wnt/β-catenin mouse model displayed a strong immune presence, with marked increase in lymphocytes and neutrophils at the pre-neoplastic stage of disease. Breast tumours have been traditionally considered immunogenically "cold"; however, emerging evidence has started to highlight the importance of tumour infiltrating immune cells in both progression and suppression of different breast cancer subsets (Nathan and Schmid, 2018). If the immune profile of these tumours become immunogenically active in patients with loss of CBFβ and/or RUNX1-RUNX2, the mutation status of these genes could potentially serve as a biomarker. Such patients may benefit from cancer immunotherapy alongside standard chemotherapy/targeted therapy (Nathan and Schmid, 2018). Thus, understanding how RUNX/CBFβ status influences the intrinsic tumour cell properties as well as the extrinsic crosstalk between tumour cells and the immune system would help personalise therapeutics to the individual patients' genetic makeup.

References

A, K. *et al*. (2017) 'Primary and secondary prevention of breast cancer', *Annals of agricultural and environmental medicine : AAEM*, 24 (4). Available at: https://doi.org/10.26444/AAEM/75943.

A. Longo, P. *et al*. (2013) 'Generating Mammalian Stable Cell Lines by Electroporation', *Methods in enzymology*, 529, p. 209. Available at: https://doi.org/10.1016/B978-0-12-418687-3.00017-3.

Abd El-Rehim, D.M. *et al*. (2004) 'Expression of luminal and basal cytokeratins in human breast carcinoma', *Journal of Pathology*, 203 (2), pp. 661–671. Available at: https://doi.org/10.1002/path.1559.

Adams, S. *et al*. (2014) 'Prognostic value of tumor-infiltrating lymphocytes in triple-negative breast cancers from two phase III randomized adjuvant breast cancer trials: ECOG 2197 and ECOG 1199', *Journal of Clinical Oncology*, 32 (27), pp. 2959–2966. Available at: https://doi.org/10.1200/JCO.2013.55.0491.

Affolter, M. *et al*. (2003) 'Tube or Not Tube: Remodeling Epithelial Tissues by Branching Morphogenesis', *Developmental Cell*, 4 (1), pp. 11–18. Available at: https://doi.org/10.1016/S1534-5807 (02)00410-0.

Ajkay, N. *et al*. (2015) 'A Comparison of Complication Rates in Early-Stage Breast Cancer Patients Treated with Brachytherapy Versus Whole-Breast Irradiation', *Annals of Surgical Oncology*, 22 (4), pp. 1140–1145. Available at: https://doi.org/10.1245/s10434-014-4131-6.

Akram, M. *et al*. (2017) 'Awareness and current knowledge of breast cancer', *Biological Research*, 50 (1), p. 33. Available at: https://doi.org/10.1186/s40659-017-0140-9.

Álvarez-Viejo, M., Menéndez-Menéndez, Y. and Otero-Hernández, J. (2015) 'CD271 as a marker to identify mesenchymal stem cells from diverse sources before culture', *World Journal of Stem Cells*, 7 (2), p. 470. Available at: https://doi.org/10.4252/WJSC.V7.I2.470.

Alves, C.L. *et al*. (2018) 'SNAI2 upregulation is associated with an aggressive phenotype in fulvestrant-resistant breast cancer cells and is an indicator of poor response to endocrine therapy in estrogen receptor-positive metastatic breast cancer', *Breast Cancer Research*, 20 (1), p. 60. Available at: https://doi.org/10.1186/s13058-018-0988-9.

Amann, A. *et al*. (2017) 'Development of a 3D angiogenesis model to study tumour – endothelial cell interactions and the effects of anti-angiogenic drugs', *Scientific Reports*, 7 (1). Available at: https://doi.org/10.1038/S41598-017-03010-6.

American cancer society (2019) *Chemotherapy for Breast Cancer*. Available at: https://www.cancer.org/cancer/breast-cancer/treatment/chemotherapy-for-breast-cancer.html (Accessed: 25 July 2020).

Amir, E. *et al*. (2011) 'Toxicity of Adjuvant Endocrine Therapy in Postmenopausal Breast Cancer Patients: A Systematic Review and Meta-analysis', *JNCI: Journal of the National Cancer Institute*, 103 (17), pp. 1299–1309. Available at: https://doi.org/10.1093/JNCI/DJR242.

Andersen, C.L. *et al*. (2009) 'Dysregulation of the transcription factors SOX4, CBFB and SMARCC1 correlates with outcome of colorectal cancer', *British Journal of Cancer*, 100 (3), pp. 511–523. Available at: https://doi.org/10.1038/sj.bjc.6604884.

Andrechek, E.R. *et al*. (2000) 'Amplification of the neu/erbB-2 oncogene in a mouse model of mammary tumorigenesis', *Proceedings of the National Academy of Sciences of the United States of America*, 97 (7), p. 3444. Available at: https://doi.org/10.1073/PNAS.050408497.

Anfray, C. *et al*. (2019) 'Current Strategies to Target Tumor-Associated-Macrophages to Improve Anti-Tumor Immune Responses', *Cells 2020, Vol. 9, Page 46*, 9 (1), p. 46. Available at: https://doi.org/10.3390/CELLS9010046.

Anstine, L.J. and Keri, R. (2019) 'A new view of the mammary epithelial hierarchy and its implications for breast cancer initiation and metastasis', *Journal of cancer metastasis and treatment*, 5. Available at: https://doi.org/10.20517/2394-4722.2019.24.

Anurag, M., Ellis, M.J. and Haricharan, S. (2018) 'DNA damage repair defects as a new class of endocrine treatment resistance driver', *Oncotarget*, 9 (91), p. 36252. Available at: https://doi.org/10.18632/ONCOTARGET.26363.

Attalla, S. *et al*. (2020) 'Insights from transgenic mouse models of PyMT-induced breast cancer: recapitulating human breast cancer progression in vivo', *Oncogene 2020 40:3*, 40 (3), pp. 475–491. Available at: https://doi.org/10.1038/s41388-020-01560-0.

Avagliano, A. *et al*. (2020) 'Influence of Fibroblasts on Mammary Gland Development, Breast Cancer Microenvironment Remodeling, and Cancer Cell Dissemination',

Cancers, 12 (6), pp. 1–35. Available at: https://doi.org/10.3390/CANCERS12061697.

Awan, A. and Esfahani, K. (2018) 'Endocrine therapy for breast cancer in the primary care setting', *Current Oncology*, 25 (4), p. 285. Available at: https://doi.org/10.3747/CO.25.4139.

Ayyanan, A. *et al*. (2006) 'Increased Wnt signaling triggers oncogenic conversion of human breast epithelial cells by a Notch-dependent mechanism', *Proceedings of the National Academy of Sciences of the United States of America*, 103 (10), pp. 3799–3804. Available at: https://doi.org/10.1073/PNAS.0600065103/SUPPL_FILE/00065FIG7.PDF.

Azizi, E. *et al*. (2018) 'Single-cell Map of Diverse Immune Phenotypes in the Breast Tumor Microenvironment', *Cell*, 174 (5), p. 1293. Available at: https://doi.org/10.1016/J.CELL.2018.05.060.

Bach, K. *et al*. (2017) 'Differentiation dynamics of mammary epithelial cells revealed by single-cell RNA sequencing', *Nature Communications*, 8 (1), p. 2128. Available at: https://doi.org/10.1038/s41467-017-02001-5.

Bach, K. *et al*. (2021) 'Time-resolved single-cell analysis of Brca1 associated mammary tumourigenesis reveals aberrant differentiation of luminal progenitors', *Nature Communications*, 12 (1), p. 1502. Available at: https://doi.org/10.1038/s41467-021-21783-3.

Badowska-Kozakiewicz, A.M. and Budzik, M.P. (2016) 'Immunohistochemical characteristics of basal-like breast cancer', *Współczesna Onkologia*, 6 (6), pp. 436–443. Available at: https://doi.org/10.5114/wo.2016.56938.

Bahcecioglu, G. *et al*. (2020) 'Breast cancer models: Engineering the tumor microenvironment', *Acta Biomaterialia*, 106, pp. 1–21. Available at: https://doi.org/10.1016/J.ACTBIO.2020.02.006.

Banerji, S. *et al*. (2012) 'Sequence analysis of mutations and translocations across breast cancer subtypes', *Nature*, 486 (7403), pp. 405–409. Available at: https://doi.org/10.1038/nature11154.

Bardia, A. *et al*. (2019) 'Sacituzumab Govitecan-hziy in Refractory Metastatic Triple-Negative Breast Cancer', *New England Journal of Medicine*, 380 (8), pp. 741–751. Available at: https://doi.org/10.1056/NEJMoa1814213.

Barkal, A.A. *et al*. (2019) 'CD24 signalling through macrophage Siglec-10 is a target for cancer immunotherapy', *Nature 2019 572:7769*, 572 (7769), pp. 392–396. Available at: https://doi.org/10.1038/s41586-019-1456-0.

Bense, R.D. *et al.* (2016) 'Relevance of Tumor-Infiltrating Immune Cell Composition and Functionality for Disease Outcome in Breast Cancer', *Journal of the National Cancer Institute*, 109 (1). Available at: https://doi.org/10.1093/jnci/djw192.

Betancur, P.A. *et al.* (2017) 'A CD47-associated super-enhancer links pro-inflammatory signalling to CD47 upregulation in breast cancer', *Nature Communications 2017 8:1*, 8 (1), pp. 1–14. Available at: https://doi.org/10.1038/ncomms14802.

Bhargava, R. *et al.* (2010) 'Immunohistochemical surrogate markers of breast cancer molecular classes predicts response to neoadjuvant chemotherapy', *Cancer*, 116 (6), pp. 1431–1439. Available at: https://doi.org/10.1002/cncr.24876.

Bhat, P. *et al.* (2017) 'Interferon-γ derived from cytotoxic lymphocytes directly enhances their motility and cytotoxicity', *Cell Death & Disease 2017 8:6*, 8 (6), pp. e2836–e2836. Available at: https://doi.org/10.1038/cddis.2017.67.

Binnewies, M. *et al.* (2018) 'Understanding the tumor immune microenvironment (TIME) for effective therapy', *Nature Medicine*, 24 (5), pp. 541–550. Available at: https://doi.org/10.1038/s41591-018-0014-x.

Biswas, S.K. *et al.* (2022) 'The Mammary Gland: Basic Structure and Molecular Signaling during Development', *International Journal of Molecular Sciences*, 23 (7), p. 3883. Available at: https://doi.org/10.3390/IJMS23073883.

Bittner, J.J. (1936) 'Some possible effects of nursing on the mammary gland tumor incidence in mice.', *Science*, 84 (2172), pp. 162–162. Available at: https://doi.org/10.1126/science.84.2172.162.

Bloom, H.J.G. and Richardson, W.W. (no date) *HISTOLOGICAL GRADING AND PROGNOSIS IN BREAST CANCER A STUDY OF 1409 CASES OF WHICH 359 HAVE BEEN FOLLOWED FOR 15 YEARS*.

Blyth, K. *et al.* (2010) 'Runx2 in normal tissues and cancer cells: A developing story', *Blood Cells, Molecules, and Diseases*, 45 (2), pp. 117–123. Available at: https://doi.org/10.1016/j.bcmd.2010.05.007.

Blyth, K., Cameron, Ewan R and Neil, J.C. (2005) 'The RUNX genes: gain or loss of function in cancer.', *Nature reviews. Cancer*, 5 (5), pp. 376–87. Available at: https://doi.org/10.1038/nrc1607.

Bonewald, L.F. and Johnson, M.L. (2008) 'Osteocytes, mechanosensing and Wnt signaling', *Bone*, 42 (4), pp. 606–615. Available at: https://doi.org/10.1016/J.BONE.2007.12.224.

Borowsky, A.D. (2011) 'Choosing a Mouse Model: Experimental Biology in Context—The Utility and Limitations of Mouse Models of Breast Cancer', *Cold Spring Harbor*

Perspectives in Biology, 3 (9), p. a009670. Available at: https://doi.org/10.1101/CSHPERSPECT.A009670.

Bosma, M.J. and Carroll, A.M. (2003) 'The SCID Mouse Mutant: Definition, Characterization, and Potential Uses', *http://dx.doi.org/10.1146/annurev.iy.09.040191.001543*, 9, pp. 323–350. Available at: https://doi.org/10.1146/ANNUREV.IY.09.040191.001543.

Bowles, E.J.A. *et al.* (2012) 'Patient-reported discontinuation of endocrine therapy and related adverse effects among women with early-stage breast cancer', *Journal of Oncology Practice*, 8 (6). Available at: https://doi.org/10.1200/JOP.2012.000543.

Brandt, R. *et al.* (2000) 'Mammary gland specific hEGF receptor transgene expression induces neoplasia and inhibits differentiation', *Oncogene 2000 19:17*, 19 (17), pp. 2129–2137. Available at: https://doi.org/10.1038/sj.onc.1203520.

Braune, E.B., Seshire, A. and Lendahl, U. (2018) 'Notch and Wnt Dysregulation and Its Relevance for Breast Cancer and Tumor Initiation', *Biomedicines*, 6 (4). Available at: https://doi.org/10.3390/BIOMEDICINES6040101.

Bravo, J. *et al.* (2001) 'The leukemia-associated AML1 (Runx1)-CBFβ complex functions as a DNA-induced molecular clamp', *Nature Structural Biology*, 8, pp. 371–378. Available at: https://doi.org/https://doi.org/10.1038/86264.

Brenton, J.D. *et al.* (2005) 'Molecular classification and molecular forecasting of breast cancer: ready for clinical application?', *Journal of clinical oncology : official journal of the American Society of Clinical Oncology*, 23 (29), pp. 7350–60. Available at: https://doi.org/10.1200/JCO.2005.03.3845.

Breslin, S. *et al.* (2016) 'The relevance of using 3D cell cultures, in addition to 2D monolayer cultures, when evaluating breast cancer drug sensitivity and resistance', *Oncotarget*, 7 (29), pp. 45745–45756. Available at: https://doi.org/10.18632/ONCOTARGET.9935.

Briand, P. and Lykkesfeldt, A.E. (2001) 'An in vitro Model of Human Breast Carcinogenesis: Epigenetic Aspects', *Breast Cancer Research and Treatment 2001 65:2*, 65 (2), pp. 179–187. Available at: https://doi.org/10.1023/A:1006434503061.

Bruchard, M. and Ghiringhelli, F. (2019) 'Deciphering the roles of innate lymphoid cells in cancer', *Frontiers in Immunology*, 10 (APR), p. 656. Available at: https://doi.org/10.3389/FIMMU.2019.00656/BIBTEX.

Bruna, A. *et al*. (2016) 'A Biobank of Breast Cancer Explants with Preserved Intra-tumor Heterogeneity to Screen Anticancer Compounds', *Cell*, 167 (1), pp. 260-274.e22. Available at: https://doi.org/10.1016/J.CELL.2016.08.041.

Buffet, N.C. *et al*. (1998) 'Regulation of the Human Menstrual Cycle', *Frontiers in Neuroendocrinology*, 19 (3), pp. 151–186. Available at: https://doi.org/10.1006/FRNE.1998.0167.

Burstein, H.J. *et al*. (2019) 'Adjuvant endocrine therapy for women with hormone receptor–positive breast cancer: ASCO clinical practice guideline focused update', *Journal of Clinical Oncology*, 37 (5), pp. 423–438. Available at: https://doi.org/10.1200/JCO.18.01160.

Bushweller, J.H. *et al*. (1999) 'Solution structure of core binding factor ß and map of the CBFα binding site', *Nature Structural Biology*, 6 (7), pp. 624–627. Available at: https://doi.org/10.1038/10670.

Byers, S.L. *et al*. (2012) 'Mouse Estrous Cycle Identification Tool and Images', *PLOS ONE*, 7 (4), p. e35538. Available at: https://doi.org/10.1371/JOURNAL.PONE.0035538.

Cairns, J. (1975) 'Mutation selection and the natural history of cancer', *Nature 1975 255:5505*, 255 (5505), pp. 197–200. Available at: https://doi.org/10.1038/255197a0.

Caley, A. and Jones, R. (2012) 'The principles of cancer treatment by chemotherapy', *Surgery (Oxford)*, 30 (4), pp. 186–190. Available at: https://doi.org/10.1016/j.mpsur.2012.01.004.

Cancer (2022) *World Health Organisation*. Available at: https://www.who.int/news-room/fact-sheets/detail/cancer (Accessed: 2 August 2022).

Cancer Research UK (2016) *Breast cancer statistics*. Available at: https://www.cancerresearchuk.org/health-professional/cancer-statistics/statistics-by-cancer-type/breast-cancer#heading-Two (Accessed: 2 August 2022).

Cao, W. *et al*. (1998) 'The core binding factor (CBF) α interaction domain and the smooth muscle myosin heavy chain (SMMHC) segment of CBFß-SMMHC are both required to slow cell proliferation', *Journal of Biological Chemistry*, 273 (47), pp. 31534–31540. Available at: https://doi.org/10.1074/jbc.273.47.31534.

Carbognin, L. *et al*. (2016) 'Predictive and Prognostic Role of Tumor-Infiltrating Lymphocytes for Early Breast Cancer According to Disease Subtypes: Sensitivity Analysis of Randomized Trials in Adjuvant and Neoadjuvant Setting', *The*

Oncologist, 21 (3), pp. 283–291. Available at: https://doi.org/10.1634/THEONCOLOGIST.2015-0307.

Cardiff, R.D. and Wellings, S.R. (1999) *The Comparative Pathology of Human and Mouse Mammary Glands*, *Journal of Mammary Gland Biology and Neoplasia*.

Carey, L.A. *et al*. (2007) 'The triple negative paradox: Primary tumor chemosensitivity of breast cancer subtypes', *Clinical Cancer Research*, 13 (8), pp. 2329–2334. Available at: https://doi.org/10.1158/1078-0432.CCR-06-1109.

Carlton, A.L. *et al*. (2018) 'Small molecule inhibition of the CBFβ/RUNX interaction decreases ovarian cancer growth and migration through alterations in genes related to epithelial-to-mesenchymal transition', *Gynecologic Oncology*, 149 (2), pp. 350–360. Available at: https://doi.org/10.1016/J.YGYNO.2018.03.005.

Carron, E.C. *et al*. (2017) 'Macrophages promote the progression of premalignant mammary lesions to invasive cancer', *Oncotarget*, 8 (31), pp. 50731–50746. Available at: https://doi.org/10.18632/oncotarget.14913.

Casey, S.C. *et al*. (2016) 'MYC regulates the antitumor immune response through CD47 and PD-L1', *Science*, 352 (6282), pp. 227–231. Available at: https://doi.org/10.1126/SCIENCE.AAC9935/SUPPL_FILE/PAPV2.PDF.

Cassetta, L. and Pollard, J.W. (2018) 'Targeting macrophages: therapeutic approaches in cancer', *Nature Reviews Drug Discovery 2018 17:12*, 17 (12), pp. 887–904. Available at: https://doi.org/10.1038/nrd.2018.169.

Castagnoli, L. *et al*. (2019) 'WNT signaling modulates PD-L1 expression in the stem cell compartment of triple-negative breast cancer', *Oncogene 2019 38:21*, 38 (21), pp. 4047–4060. Available at: https://doi.org/10.1038/s41388-019-0700-2.

Castilla, L.H. *et al*. (1996) 'Failure of embryonic hematopoiesis and lethal hemorrhages in mouse embryos heterozygous for a knocked-in leukemia gene CBFB-MYH11', *Cell*, 87 (4), pp. 687–696. Available at: https://doi.org/10.1016/S0092-8674(00)81388-4.

Castilla, L.H. *et al*. (2004) 'Identification of genes that synergize with Cbfb-MYH11 in the pathogenesis of acute myeloid leukemia', *Proceedings of the National Academy of Sciences of the United States of America*, 101 (14), pp. 4924–4929. Available at: https://doi.org/10.1073/PNAS.0400930101/SUPPL_FILE/00930TABLE3.HTML.

Cerami, E. *et al*. (2012) 'The cBio Cancer Genomics Portal: An Open Platform for Exploring Multidimensional Cancer Genomics Data', *Cancer Discovery*, 2 (5), pp. 401–404. Available at: https://doi.org/10.1158/2159-8290.CD-12-0095.

Cerliani, J.P. *et al*. (2011) 'Interaction between FGFR-2, STAT5, and progesterone receptors in breast cancer', *Cancer Research*, 71 (10), pp. 3720–3731. Available at: https://doi.org/10.1158/0008-5472.CAN-10-3074/649549/AM/INTERACTION-BETWEEN-FGFR-2-STAT5-AND-PROGESTERONE.

Ceruti, S. *et al*. (2003) 'A Key Role for Caspase-2 and Caspase-3 in the Apoptosis Induced by 2-Chloro-2′-deoxy-adenosine (Cladribine) and 2-Chloro-adenosine in Human Astrocytoma Cells', *Molecular Pharmacology*, 63 (6), pp. 1437–1447. Available at: https://doi.org/10.1124/mol.63.6.1437.

Chanmee, T. *et al*. (2014) 'Tumor-Associated Macrophages as Major Players in the Tumor Microenvironment', *Cancers 2014, Vol. 6, Pages 1670-1690*, 6 (3), pp. 1670–1690. Available at: https://doi.org/10.3390/CANCERS6031670.

Cheang, M.C.U. *et al*. (2009) 'Ki67 Index, HER2 Status, and Prognosis of Patients With Luminal B Breast Cancer', *Articles | JNCI*, 101, p. 736. Available at: https://doi.org/10.1093/jnci/djp082.

Chen, E. *et al*. (2018) 'Identification of Potential Therapeutic Targets among CXC Chemokines in Breast Tumor Microenvironment Using Integrative Bioinformatics Analysis', *Cellular Physiology and Biochemistry*, 45 (5), pp. 1731–1746. Available at: https://doi.org/10.1159/000487782.

Chen, L.-F. (2012) 'Tumor suppressor function of RUNX3 in breast cancer.', *Journal of cellular biochemistry*, 113 (5), pp. 1470–7. Available at: https://doi.org/10.1002/jcb.24074.

Chen, X. *et al*. (2018) 'Long noncoding RNA LINC01234 functions as a competing endogenous RNA to regulate CBFB expression by sponging miR-204-5p in gastric cancer', *Clinical Cancer Research*, 24 (8), pp. 2002–2014. Available at: https://doi.org/10.1158/1078-0432.CCR-17-2376.

Chimge, N.O. *et al*. (2016) 'RUNX1 prevents oestrogen-mediated AXIN1 suppression and β-catenin activation in ER-positive breast cancer', *Nature Communications*, 7 (1), pp. 1–12. Available at: https://doi.org/10.1038/ncomms10751.

Chimge, N.-O. and Frenkel, B. (2013) 'The RUNX family in breast cancer: relationships with estrogen signaling', *Oncogene*, 32 (17), pp. 2121–2130. Available at: https://doi.org/10.1038/onc.2012.328.

Chua, A.C.L. *et al*. (2010) 'Dual roles for macrophages in ovarian cycle-associated development and remodelling of the mammary gland epithelium', *Development*, 137 (24), pp. 4229–4238. Available at: https://doi.org/10.1242/DEV.059261.

Chuang, L.S.H., Ito, K. and Ito, Y. (2013) 'RUNX family: Regulation and diversification of roles through interacting proteins', *International Journal of Cancer*, 132 (6), pp. 1260–1271. Available at: https://doi.org/10.1002/IJC.27964.

Cichon, M.A. *et al.* (2010) 'Microenvironmental influences that drive progression from benign breast disease to invasive breast cancer', *Journal of Mammary Gland Biology and Neoplasia*, 15 (4), pp. 389–397. Available at: https://doi.org/10.1007/S10911-010-9195-8/FIGURES/3.

Ciriello, G. *et al.* (2015) 'Comprehensive Molecular Portraits of Invasive Lobular Breast Cancer', *Cell*, 163 (2), pp. 506–519. Available at: https://doi.org/10.1016/J.CELL.2015.09.033.

Cochrane, D.R. *et al.* (2014) 'Role of the androgen receptor in breast cancer and preclinical analysis of enzalutamide', *Breast Cancer Research*, 16 (1), pp. 1–19. Available at: https://doi.org/10.1186/BCR3599/FIGURES/6.

Coffelt, S.B. *et al.* (2015) 'IL-17-producing γδ T cells and neutrophils conspire to promote breast cancer metastasis', *Nature*, 522 (7556), pp. 345–348. Available at: https://doi.org/10.1038/nature14282.

Coffelt, S.B., Hughes, R. and Lewis, C.E. (2009) 'Tumor-associated macrophages: Effectors of angiogenesis and tumor progression', *Biochimica et Biophysica Acta (BBA) - Reviews on Cancer*, 1796 (1), pp. 11–18. Available at: https://doi.org/10.1016/J.BBCAN.2009.02.004.

Coffelt, S.B. and de Visser, K.E. (2016) 'Systemic inflammation: Cancer's long-distance reach to maximize metastasis', *OncoImmunology*, 5 (2). Available at: https://doi.org/10.1080/2162402X.2015.1075694.

Coffelt, S.B., Wellenstein, M.D. and de Visser, K.E. (2016) 'Neutrophils in cancer: neutral no more', *Nature Reviews Cancer*, 16 (7), pp. 431–446. Available at: https://doi.org/10.1038/nrc.2016.52.

Cohen, B. *et al.* (2010) 'Cyclin D1 is a direct target of JAG1-mediated Notch signaling in breast cancer', *Breast Cancer Research and Treatment*, 123 (1), pp. 113–124. Available at: https://doi.org/10.1007/S10549-009-0621-9/FIGURES/6.

Comsa, S., Cimpean, A.M. and Raica, M. (2015) 'The Story of MCF-7 Breast Cancer Cell Line: 40 years of Experience in Research', *Anticancer Research*, 35 (6), pp. 3147–3154. Available at: https://ar.iiarjournals.org/content/35/6/3147 (Accessed: 31 July 2022).

Cone, R.E. *et al*. (2007) 'The suppression of delayed-type hypersensitivity by CD8+ regulatory T cells requires interferon-γ', *Immunology*, 120 (1), pp. 112–119. Available at: https://doi.org/10.1111/J.1365-2567.2006.02486.X.

Cope, L.M. *et al*. (2014) 'Do Breast Cancer Cell Lines Provide a Relevant Model of the Patient Tumor Methylome?', *PLoS ONE*. Edited by P. Rameshwar, 9 (8), p. e105545. Available at: https://doi.org/10.1371/journal.pone.0105545.

Correa Geyer, F. and Reis-Filho, J.S. (2009) 'Microarray-based gene expression profiling as a clinical tool for breast cancer management: are we there yet?', *International journal of surgical pathology*, 17 (4), pp. 285–302. Available at: https://doi.org/10.1177/1066896908328577.

Crawford, M.P. *et al*. (2020) 'CD4 T cell-intrinsic role for the T helper 17 signature cytokine IL-17: Effector resistance to immune suppression', *Proceedings of the National Academy of Sciences of the United States of America*, 117 (32), pp. 19408–19414. Available at: https://doi.org/10.1073/PNAS.2005010117/SUPPL_FILE/PNAS.2005010117.SAPP.PDF.

Cruse, J.M., Lewis, R.E. and Wang, H. (eds) (2004) 'Molecules, Cells, and Tissues of Immunity', in *Immunology Guidebook*. Academic Press, pp. 1–15. Available at: https://doi.org/10.1016/B978-012198382-6/50025-X.

Cui, B. *et al*. (2013) 'Targeting ROR1 Inhibits Epithelial-Mesenchymal Transition and Metastasis', *Cancer research*, 73 (12), pp. 3649–3660. Available at: https://doi.org/10.1158/0008-5472.CAN-12-3832.

Cynthia X Ma, M. and PhDJoseph A Sparano, M. (2020) *Treatment approach to metastatic hormone receptor-positive, HER2-negative breast cancer: Endocrine therapy and targeted agents - UpToDate*. Available at: https://www.uptodate.com/contents/treatment-approach-to-metastatic-hormone-receptor-positive-her2-negative-breast-cancer-endocrine-therapy-and-targeted-agents (Accessed: 25 July 2020).

Dadi, S. *et al*. (2016a) 'Cancer Immunosurveillance by Tissue-Resident Innate Lymphoid Cells and Innate-like T Cells', *Cell*, 164 (3), pp. 365–377. Available at: https://doi.org/10.1016/J.CELL.2016.01.002.

Dadi, S. *et al*. (2016b) 'Cancer Immunosurveillance by Tissue-Resident Innate Lymphoid Cells and Innate-like T Cells', *Cell*, 164 (3), pp. 365–377. Available at: https://doi.org/10.1016/J.CELL.2016.01.002.

Dai, X. *et al.* (2017) 'Breast Cancer Cell Line Classification and Its Relevance with Breast Tumor Subtyping', *Journal of Cancer*, 8 (16), p. 3131. Available at: https://doi.org/10.7150/JCA.18457.

van Dalen, F.J. *et al.* (2018) 'Molecular Repolarisation of Tumour-Associated Macrophages', *Molecules 2019, Vol. 24, Page 9*, 24 (1), p. 9. Available at: https://doi.org/10.3390/MOLECULES24010009.

Daniel, C.W. *et al.* (1968) 'The in vivo life span of normal and preneoplastic mouse mammary glands: a serial transplantation study.', *Proceedings of the National Academy of Sciences of the United States of America*, 61 (1), pp. 53–60. Available at: https://doi.org/10.1073/pnas.61.1.53.

Daniel, V.C. *et al.* (2009) 'A primary xenograft model of small-cell lung cancer reveals irreversible changes in gene expression imposed by culture in vitro', *Cancer Research*, 69 (8), pp. 3364–3373. Available at: https://doi.org/10.1158/0008-5472.CAN-08-4210/654954/P/A-PRIMARY-XENOGRAFT-MODEL-OF-SMALL-CELL-LUNG.

Daniels, D.L. and Weis, W.I. (2002) 'ICAT Inhibits ß-Catenin Binding to Tcf/Lef-Family Transcription Factors and the General Coactivator p300 Using Independent Structural Modules', *Molecular Cell*, 10 (3), pp. 573–584. Available at: https://doi.org/10.1016/S1097-2765 (02)00631-7.

Darby, S. *et al.* (2011) 'Effect of radiotherapy after breast-conserving surgery on 10-year recurrence and 15-year breast cancer death: Meta-analysis of individual patient data for 10 801 women in 17 randomised trials', *The Lancet*, 378 (9804), pp. 1707–1716. Available at: https://doi.org/10.1016/S0140-6736 (11)61629-2.

Davie, S.A. *et al.* (2007) 'Effects of FVB/NJ and C57Bl/6J strain backgrounds on mammary tumor phenotype in inducible nitric oxide synthase deficient mice', *Transgenic Research*, 16 (2), pp. 193–201. Available at: https://doi.org/10.1007/s11248-006-9056-9.

Davies, C. *et al.* (2013) 'Long-term effects of continuing adjuvant tamoxifen to 10 years versus stopping at 5 years after diagnosis of oestrogen receptor-positive breast cancer: ATLAS, a randomised trial', *The Lancet*, 381 (9869), pp. 805–816. Available at: https://doi.org/10.1016/S0140-6736 (12)61963-1.

Davis, J.N. *et al.* (2010) 'Association of core-binding factor ß with the malignant phenotype of prostate and ovarian cancer cells', *Journal of Cellular Physiology*, 225 (3), pp. 875–887. Available at: https://doi.org/10.1002/jcp.22298.

Degnim, A.C. *et al.* (2014) 'Immune cell quantitation in normal breast tissue lobules with and without lobulitis', *Breast Cancer Research and Treatment*, 144 (3), p. 539. Available at: https://doi.org/10.1007/S10549-014-2896-8.

Degnim, A.C. *et al.* (2017) 'Alterations in the immune cell composition in premalignant breast tissue that precede breast cancer development', *Clinical Cancer Research*, 23 (14), pp. 3945–3952. Available at: https://doi.org/10.1158/1078-0432.CCR-16-2026/72479/AM/ALTERATIONS-IN-THE-IMMUNE-CELL-COMPOSITION-IN.

DeNardo, D.G. *et al.* (2011) 'Leukocyte complexity predicts breast cancer survival and functionally regulates response to chemotherapy', *Cancer Discovery*, 1 (1), pp. 54–67. Available at: https://doi.org/10.1158/2159-8274.CD-10-0028/42904/P/LEUKOCYTE-COMPLEXITY-PREDICTS-BREAST-CANCER.

Denton, A.E., Roberts, E.W. and Fearon, D.T. (2018) 'Stromal cells in the tumor microenvironment', *Advances in Experimental Medicine and Biology*, 1060, pp. 99–114. Available at: https://doi.org/10.1007/978-3-319-78127-3_6/COVER.

Derose, Y.S. *et al.* (2011) 'Tumor grafts derived from women with breast cancer authentically reflect tumor pathology, growth, metastasis and disease outcomes', *Nature Medicine 2011 17:11*, 17 (11), pp. 1514–1520. Available at: https://doi.org/10.1038/nm.2454.

DeRose, Y.S. *et al.* (2013) 'Patient-Derived Models of Human Breast Cancer: Protocols for In Vitro and In Vivo Applications in Tumor Biology and Translational Medicine', *Current Protocols in Pharmacology*, 60 (1), pp. 14.23.1-14.23.43. Available at: https://doi.org/10.1002/0471141755.PH1423S60.

Diamond, J.R. *et al.* (2020) 'Phase Ib clinical trial of the anti-frizzled antibody vantictumab (OMP-18R5) plus paclitaxel in patients with locally advanced or metastatic HER2-negative breast cancer', *Breast Cancer Research and Treatment*, 184 (1), pp. 53–62. Available at: https://doi.org/10.1007/s10549-020-05817-w.

Dickinson, D.J., Nelson, W.J. and Weis, W.I. (2011) 'A Polarized Epithelium Organized by β- and α-Catenin Predates Cadherin and Metazoan Origins', *Science (New York, N.Y.)*, 331 (6022), p. 1336. Available at: https://doi.org/10.1126/SCIENCE.1199633.

Dieci, M. v. *et al.* (2015) 'Prognostic and predictive value of tumor-infiltrating lymphocytes in two phase III randomized adjuvant breast cancer trials', *Annals of Oncology*, 26 (8), pp. 1698–1704. Available at: https://doi.org/10.1093/ANNONC/MDV239.

Donehower, L.A. *et al.* (1992) 'Mice deficient for p53 are developmentally normal but susceptible to spontaneous tumours', *Nature*, 356 (6366), pp. 215–221. Available at: https://doi.org/10.1038/356215a0.

Dontu, G. *et al.* (2003) 'In vitro propagation and transcriptional profiling of human mammary stem/progenitor cells', *Genes and Development*, 17 (10), pp. 1253–1270. Available at: https://doi.org/10.1101/gad.1061803.

Dontu, G. and Ince, T.A. (2015) 'Of Mice and Women: A Comparative Tissue Biology Perspective of Breast Stem Cells and Differentiation', *Journal of Mammary Gland Biology and Neoplasia*, 20 (1–2), p. 51. Available at: https://doi.org/10.1007/S10911-015-9341-4.

Ducy, P. *et al.* (1997) 'Osf2/Cbfa1: A Transcriptional Activator of Osteoblast Differentiation', *Cell*, 89 (5), pp. 747–754. Available at: https://doi.org/10.1016/S0092-8674 (00)80257-3.

Dudley, J.P. (2008) 'Mouse Mammary Tumor Virus', *Encyclopedia of Virology*, pp. 334–341. Available at: https://doi.org/10.1016/B978-012374410-4.00445-3.

Durand, R.E. and Raleigh, J.A. (1998) 'Identification of nonproliferating but viable hypoxic tumor cells in vivo', *Cancer Research*, 58 (16), pp. 3547–3550. Available at: https://pubmed.ncbi.nlm.nih.gov/9721858/ (Accessed: 31 July 2022).

Duval, K. *et al.* (2017) 'Modeling Physiological Events in 2D vs. 3D Cell Culture', *Physiology*, 32 (4), p. 266. Available at: https://doi.org/10.1152/PHYSIOL.00036.2016.

Edmondson, R. *et al.* (2014) 'Three-Dimensional Cell Culture Systems and Their Applications in Drug Discovery and Cell-Based Biosensors', *Assay and Drug Development Technologies*, 12 (4), p. 207. Available at: https://doi.org/10.1089/ADT.2014.573.

Edwards, A. and Brennan, K. (2021) 'Notch Signalling in Breast Development and Cancer', *Frontiers in Cell and Developmental Biology*, 9, p. 1709. Available at: https://doi.org/10.3389/FCELL.2021.692173/XML/NLM.

Ellison, G. *et al.* (2002) 'Further evidence to support the melanocytic origin of MDA-MB-435', *Molecular Pathology*, 55 (5), pp. 294–299. Available at: https://doi.org/10.1136/MP.55.5.294.

El-Sahli, S. *et al.* (2019) 'Wnt Signaling in Cancer Metabolism and Immunity', *Cancers*, 11 (7). Available at: https://doi.org/10.3390/CANCERS11070904.

Elston, C.W. *et al*. (1982) 'The cancer research campaign (King's/Cambridge trial for early breast cancer: Clinico-pathological aspects', *British Journal of Cancer*, 45 (5), pp. 655–669. Available at: https://doi.org/10.1038/bjc.1982.106.

Elston, C.W. and Ellis, I.O. (1991) 'pathological prognostic factors in breast cancer. I. The value of histological grade in breast cancer: experience from a large study with long-term follow-up', *Histopathology*, 19 (5), pp. 403–410. Available at: https://doi.org/10.1111/j.1365-2559.1991.tb00229.x.

Emens, L.A. (2018) 'Breast Cancer Immunotherapy: Facts and Hopes', *Clinical Cancer Research*, 24 (3), pp. 511–520. Available at: https://doi.org/10.1158/1078-0432.CCR-16-3001.

Esserman, L.J. *et al*. (2009) 'Breast cancer molecular profiles and tumor response of neoadjuvant doxorubicin and paclitaxel: The I-SPY TRIAL (CALGB 150007/150012, ACRIN 6657)', *Journal of Clinical Oncology*, 27 (18_suppl), pp. LBA515–LBA515. Available at: https://doi.org/10.1200/jco.2009.27.18_suppl.lba515.

Estrada, M.F. *et al*. (2016) 'Modelling the tumour microenvironment in long-term microencapsulated 3D co-cultures recapitulates phenotypic features of disease progression', *Biomaterials*, 78, pp. 50–61. Available at: https://doi.org/10.1016/J.BIOMATERIALS.2015.11.030.

Fantozzi, A. and Christofori, G. (2006) 'Mouse models of breast cancer metastasis', *Breast Cancer Research*, 8 (4), p. 212. Available at: https://doi.org/10.1186/BCR1530.

Farley, F.W. *et al*. (2000) 'Widespread Recombinase Expression Using FLPeR (Flipper) Mice'. Available at: https://doi.org/10.1002/1526-968X.

Farmaki, E. *et al*. (2016) 'A CCL8 gradient drives breast cancer cell dissemination', *Oncogene*, 35 (49), p. 6309. Available at: https://doi.org/10.1038/ONC.2016.161.

Fata, J.E., Chaudhary, V. and Khokha, R. (2001) 'Cellular Turnover in the Mammary Gland Is Correlated with Systemic Levels of Progesterone and Not 17β-Estradiol During the Estrous Cycle', *Biology of Reproduction*, 65 (3), pp. 680–688. Available at: https://doi.org/10.1095/BIOLREPROD65.3.680.

FDA grants regular approval to sacituzumab govitecan for triple-negative breast cancer (no date) *FDA*. Available at: https://www.fda.gov/drugs/resources-information-approved-drugs/fda-grants-regular-approval-sacituzumab-govitecan-triple-negative-breast-cancer (Accessed: 3 August 2022).

Fehérvari, Z. and Sakaguchi, S. (2004) 'CD4+ Tregs and immune control', *Journal of Clinical Investigation*, 114 (9), p. 1209. Available at: https://doi.org/10.1172/JCI23395.

Feng, M. *et al*. (2019) 'Pharmacological inhibition of ß-catenin/BCL9 interaction overcomes resistance to immune checkpoint blockades by modulating Treg cells', *Science Advances*, 5 (5). Available at: https://doi.org/10.1126/SCIADV.AAU5240.

Ferrari, N. *et al*. (2013) 'RUNX2 in mammary gland development and breast cancer', *Journal of Cellular Physiology*, 228 (6), pp. 1137–1142. Available at: https://doi.org/10.1002/jcp.24285.

Ferrari, N. *et al*. (2015) 'Runx2 contributes to the regenerative potential of the mammary epithelium', *Scientific Reports 2015 5:1*, 5 (1), pp. 1–16. Available at: https://doi.org/10.1038/srep15658.

Figueroa-Magalhães, M.C. *et al*. (2014) 'Treatment of HER2-positive breast cancer', *The Breast*, 23 (2), pp. 128–136. Available at: https://doi.org/10.1016/j.breast.2013.11.011.

Flanagan, S.P. (1966) '"Nude", a new hairless gene with pleiotropic effects in the mouse', *Genetics Research*, 8 (3), pp. 295–309. Available at: https://doi.org/10.1017/S0016672300010168.

Franken, N.A.P. *et al*. (2006) 'Clonogenic assay of cells in vitro', *Nature Protocols 2006 1:5*, 1 (5), pp. 2315–2319. Available at: https://doi.org/10.1038/nprot.2006.339.

Freedman, O.C. *et al*. (2015) 'Adjuvant endocrine therapy for early breast cancer: A systematic review of the evidence for the 2014 cancer care Ontario systemic therapy guideline', *Current Oncology*, 22 (Suppl 1), pp. S95–S113. Available at: https://doi.org/10.3747/co.22.2326.

Fritz, A.J. *et al*. (2020) 'RUNX transcription factor mediated control of breast cancer stem cells', *Journal of cellular physiology*, 235 (10), p. 7261. Available at: https://doi.org/10.1002/JCP.29625.

Fu, J. *et al*. (2022) 'RUNX regulated immune-associated genes predicts prognosis in breast cancer', *Frontiers in Genetics*, 0, p. 2204. Available at: https://doi.org/10.3389/FGENE.2022.960489.

Fulford, L.G. *et al*. (2006) 'Specific morphological features predictive for the basal phenotype in grade 3 invasive ductal carcinoma of breast', *Histopathology*, 49 (1), pp. 22–34. Available at: https://doi.org/10.1111/j.1365-2559.2006.02453.x.

Fulghieri, P., Stivala, L.A. and Sottile, V. (2021) 'Modulating cell differentiation in cancer models', *Biochemical Society Transactions*, 49 (4), pp. 1803–1816. Available at: https://doi.org/10.1042/BST20210230.

Gao, H. *et al*. (2015) 'High-throughput screening using patient-derived tumor xenografts to predict clinical trial drug response', *Nature Medicine 2015 21:11*, 21 (11), pp. 1318–1325. Available at: https://doi.org/10.1038/nm.3954.

Gao, J. *et al*. (2013) 'Integrative Analysis of Complex Cancer Genomics and Clinical Profiles Using the cBioPortal', *Science Signaling*, 6 (269), p. pl1. Available at: https://doi.org/10.1126/scisignal.2004088.

Gao, L. and Zhou, F. (2021) 'Comprehensive Analysis of RUNX and TGF-β Mediated Regulation of Immune Cell Infiltration in Breast Cancer', *Frontiers in Cell and Developmental Biology*, 9, p. 730380. Available at: https://doi.org/10.3389/FCELL.2021.730380/FULL.

Gao, X.L. *et al*. (2019) 'NR2F1 contributes to cancer cell dormancy, invasion and metastasis of salivary adenoid cystic carcinoma by activating CXCL12/CXCR4 pathway', *BMC Cancer*, 19 (1). Available at: https://doi.org/10.1186/S12885-019-5925-5.

Gatti-Mays, M.E. *et al*. (2019) 'If we build it they will come: targeting the immune response to breast cancer', *npj Breast Cancer 2019 5:1*, 5 (1), pp. 1–13. Available at: https://doi.org/10.1038/s41523-019-0133-7.

Gerlinger, M. *et al*. (2012) 'Intratumor Heterogeneity and Branched Evolution Revealed by Multiregion Sequencing', *New England Journal of Medicine*, 366 (10), pp. 883–892. Available at: https://doi.org/10.1056/NEJMOA1113205/SUPPL_FILE/NEJMOA1113205_DISCLOSURES.PDF.

Gest, C. *et al*. (2013) 'Rac3 induces a molecular pathway triggering breast cancer cell aggressiveness: differences in MDA-MB-231 and MCF-7 breast cancer cell lines', *BMC Cancer*, 13, p. 63. Available at: https://doi.org/10.1186/1471-2407-13-63.

Geyer, C.E. *et al*. (2006) *Lapatinib plus Capecitabine for HER2-Positive Advanced Breast Cancer A bs t r ac t*.

Giraddi, R.R. *et al*. (2018) 'Single-Cell Transcriptomes Distinguish Stem Cell State Changes and Lineage Specification Programs in Early Mammary Gland Development', *Cell Reports*, 24 (6), pp. 1653-1666.e7. Available at: https://doi.org/10.1016/j.celrep.2018.07.025.

Goff, S.L. and Danforth, D.N. (2021) 'The Role of Immune Cells in Breast Tissue and Immunotherapy for the Treatment of Breast Cancer', *Clinical Breast Cancer*, 21 (1), pp. e63–e73. Available at: https://doi.org/10.1016/j.clbc.2020.06.011.

Goldman, A.S.M. (1993) 'The immune system of human milk: antimicrobial, antiinflammatory and immunomodulating properties', *The Pediatric Infectious Disease Journal*, 12 (8), pp. 664–672. Available at: https://journals.lww.com/pidj/Citation/1993/08000/The_immune_system_of_human_milk__antimicrobial,.8.aspx (Accessed: 2 August 2022).

Gomes Do Nascimento, R. and Otoni, K.M. (2020) 'Histological and molecular classification of breast cancer: what do we know?', *Mastology*, 30. Available at: https://doi.org/10.29289/25945394202020200024.

Gordon, J.W. *et al.* (1980) 'Genetic transformation of mouse embryos by microinjection of purified DNA.', *Proceedings of the National Academy of Sciences*, 77 (12), pp. 7380–7384. Available at: https://doi.org/10.1073/PNAS.77.12.7380.

Goss, P.E. and Strasser, K. (2001) 'Aromatase inhibitors in the treatment and prevention of breast cancer.', *Journal of clinical oncology : official journal of the American Society of Clinical Oncology*, 19 (3), pp. 881–94. Available at: https://doi.org/10.1200/JCO.2001.19.3.881.

Gradishar, W.J. (2012) 'Taxanes for the Treatment of Metastatic Breast Cancer', *Breast Cancer: Basic and Clinical Research*, 6 (1), p. BCBCR.S8205. Available at: https://doi.org/10.4137/BCBCR.S8205.

Greenough, R. (1925) 'Varying degrees of malignancy in cancer of the breast', *J Cancer Res*, 9, pp. 452–463.

Greshock, J. *et al.* (2007) 'Cancer Cell Lines as Genetic Models of Their Parent Histology: Analyses Based on Array Comparative Genomic Hybridization', *Cancer Research*, 67 (8), pp. 3594–3600. Available at: https://doi.org/10.1158/0008-5472.CAN-06-3674.

Griffith, O.L. *et al.* (2018) 'The prognostic effects of somatic mutations in ER-positive breast cancer', *Nature Communications*, 9 (1), p. 3476. Available at: https://doi.org/10.1038/s41467-018-05914-x.

Grimshaw, M.J. *et al.* (2008) 'Mammosphere culture of metastatic breast cancer cells enriches for tumorigenic breast cancer cells', *Breast Cancer Research*, 10 (3), pp. 1–10. Available at: https://doi.org/10.1186/BCR2106/FIGURES/5.

Groot, J.S. de *et al.* (2017) 'Intraductal cisplatin treatment in a BRCA -associated breast cancer mouse model attenuates tumor development but leads to systemic tumors

in aged female mice', *Oncotarget*, 8 (37), pp. 60750–60763. Available at: https://doi.org/10.18632/ONCOTARGET.18490.

Growney, J.D. *et al.* (2005) 'Loss of Runx1 perturbs adult hematopoiesis and is associated with a myeloproliferative phenotype', *Blood*, 106 (2), pp. 494–504. Available at: https://doi.org/10.1182/BLOOD-2004-08-3280.

Gu, B. *et al.* (2009) 'Pygo2 expands mammary progenitor cells by facilitating histone H3 K4 methylation', *Journal of Cell Biology*, 185 (5), pp. 811–826. Available at: https://doi.org/10.1083/JCB.200810133.

Gu, T.L. *et al.* (2000) 'Auto-inhibition and partner proteins, core-binding factor beta (CBFbeta) and Ets-1, modulate DNA binding by CBFalpha2 (AML1).', *Molecular and cellular biology*, 20 (1), pp. 91–103. Available at: https://doi.org/10.1128/MCB.20.1.91-103.2000.

Gusterson, B.A. *et al.* (2005) 'Basal cytokeratins and their relationship to the cellular origin and functional classification of breast cancer', *Breast Cancer Research*, 7 (4), pp. 143–148. Available at: https://doi.org/10.1186/BCR1041/FIGURES/1.

Guy, C.T., Cardiff, R.D. and Muller, W.J. (1992) 'Induction of mammary tumors by expression of polyomavirus middle T oncogene: a transgenic mouse model for metastatic disease.', *Molecular and Cellular Biology*, 12 (3), pp. 954–961. Available at: https://doi.org/10.1128/MCB.12.3.954.

Hachim, M.Y. *et al.* (2020) 'M1 Polarization Markers Are Upregulated in Basal-Like Breast Cancer Molecular Subtype and Associated With Favorable Patient Outcome', *Frontiers in Immunology*, 11, p. 1. Available at: https://doi.org/10.3389/FIMMU.2020.560074/FULL.

Hajra, A. and Collins, F.S. (1995) 'Structure of the leukemia-associated human CBFB gene', *Genomics*, 26 (3), pp. 571–579. Available at: https://doi.org/10.1016/0888-7543 (95)80177-N.

Hall, B., Limaye, A. and Kulkarni, A.B. (2009) 'Overview: Generation of Gene Knockout Mice', in *Current protocols in cell biology / editorial board, Juan S. Bonifacino ... [et al.]*. NIH Public Access. Available at: https://doi.org/10.1002/0471143030.CB1912S44.

Hameyer, D. *et al.* (2007) 'Toxicity of ligand-dependent Cre recombinases and generation of a conditional Cre deleter mouse allowing mosaic recombination in peripheral tissues', *Physiological Genomics*, 31 (1), pp. 32–41. Available at: https://doi.org/10.1152/physiolgenomics.00019.2007.

Hanahan, D. and Weinberg, R.A. (2000) 'The Hallmarks of Cancer', *Cell*, 100 (1), pp. 57–70. Available at: https://doi.org/10.1016/S0092-8674 (00)81683-9.

Hanahan, D. and Weinberg, R.A. (2011) 'Hallmarks of Cancer: The Next Generation', *Cell*, 144 (5), pp. 646–674. Available at: https://doi.org/10.1016/J.CELL.2011.02.013.

Harada, N. *et al*. (1999) 'Intestinal polyposis in mice with a dominant stable mutation of the ß-catenin gene', *The EMBO Journal*, 18 (21), pp. 5931–5942. Available at: https://doi.org/10.1093/EMBOJ/18.21.5931.

Harrington, L.E. *et al*. (2005) 'Interleukin 17–producing CD4+ effector T cells develop via a lineage distinct from the T helper type 1 and 2 lineages', *Nature Immunology 2005 6:11*, 6 (11), pp. 1123–1132. Available at: https://doi.org/10.1038/ni1254.

Haruyama, N., Cho, A. and Kulkarni, A.B. (2009) 'Overview: Engineering transgenic constructs and mice', in *Current protocols in cell biology* . NIH Public Access. Available at: https://doi.org/10.1002/0471143030.CB1910S42.

Hatsell, S. *et al*. (2003) *ß-Catenin and Tcfs in Mammary Development and Cancer*, *Journal of Mammary Gland Biology and Neoplasia*.

Hayes, M.J. *et al*. (2008) 'Genetic Changes of Wnt Pathway Genes Are Common Events in Metaplastic Carcinomas of the Breast', *Clinical Cancer Research*, 14 (13), pp. 4038–4044. Available at: https://doi.org/10.1158/1078-0432.CCR-07-4379.

He, Z. *et al*. (2019) 'Stratification of Breast Cancer by Integrating Gene Expression Data and Clinical Variables', *Molecules*, 24 (3), pp. 631–647. Available at: https://doi.org/10.3390/molecules24030631.

Heape, W. (1900) 'The "sexual season" of mammals and the relation of the "pro-oestrum" to menstruation ', *The Qarterly Journal of Microscopial Science*, pp. 1855–1929. Available at: https://wellcomecollection.org/works/p97unrys (Accessed: 2 August 2022).

Hennighausen, L. (2000) 'Mouse models for breast cancer', *Breast Cancer Research*, 2 (1), p. 2. Available at: https://doi.org/10.1186/BCR20.

Hikasa, H. and Sokol, S.Y. (2013) 'Wnt Signaling in Vertebrate Axis Specification', *Cold Spring Harbor Perspectives in Biology*, 5 (1). Available at: https://doi.org/10.1101/CSHPERSPECT.A007955.

Hoffman, R.M. (1999) 'Orthotopic Metastatic Mouse Models for Anticancer Drug Discovery and Evaluation: a Bridge to the Clinic', *Investigational New Drugs 1999 17:4*, 17 (4), pp. 343–360. Available at: https://doi.org/10.1023/A:1006326203858.

Holen, I. *et al*. (2017a) 'In vivo models in breast cancer research: Progress, challenges and future directions', *DMM Disease Models and Mechanisms*. Company of Biologists Ltd, pp. 359–371. Available at: https://doi.org/10.1242/dmm.028274.

Holen, I. *et al*. (2017b) 'In vivo models in breast cancer research: progress, challenges and future directions', *Disease Models & Mechanisms*, 10 (4), p. 359. Available at: https://doi.org/10.1242/DMM.028274.

Hollern, D.P. and Andrechek, E.R. (2014) 'A genomic analysis of mouse models of breast cancer reveals molecular features ofmouse models and relationships to human breast cancer', *Breast Cancer Research*, 16 (3), p. R59. Available at: https://doi.org/10.1186/bcr3672.

Hollestelle, A. *et al*. (2010) 'Distinct gene mutation profiles among luminal-type and basal-type breast cancer cell lines', *Breast Cancer Research and Treatment*, 121 (1), pp. 53–64. Available at: https://doi.org/10.1007/S10549-009-0460-8/FIGURES/3.

Holtmeier, W. and Kabelitz, D. (2005) 'γδ T Cells Link Innate and Adaptive Immune Responses', *Mechanisms of Epithelial Defense*, 86, pp. 151–183. Available at: https://doi.org/10.1159/000086659.

Honvo-Houéto, E. and Truchet, S. (2015) 'Indirect Immunofluorescence on Frozen Sections of Mouse Mammary Gland', *Journal of Visualized Experiments : JoVE*, 2015 (106). Available at: https://doi.org/10.3791/53179.

Hovey, R.C., Trott, J.F. and Vonderhaar, B.K. (2002) 'Establishing a Framework for the Functional Mammary Gland: From Endocrinology to Morphology', *Journal of Mammary Gland Biology and Neoplasia 2002 7:1*, 7 (1), pp. 17–38. Available at: https://doi.org/10.1023/A:1015766322258.

Hsu, C.-H. *et al*. (2022) 'Cancer-Associated Exosomal CBFB Facilitates the Aggressive Phenotype, Evasion of Oxidative Stress, and Preferential Predisposition to Bone Prometastatic Factor of Breast Cancer Progression.', *Disease markers*, 2022, p. 8446629. Available at: https://doi.org/10.1155/2022/8446629.

Hu, Z. *et al*. (2006) 'The molecular portraits of breast tumors are conserved across microarray platforms', *BMC Genomics*, 7, p. 96. Available at: https://doi.org/10.1186/1471-2164-7-96.

Huang, B. *et al*. (2012) 'RUNX3 acts as a tumor suppressor in breast cancer by targeting estrogen receptor α', *Oncogene*, 31 (4), pp. 527–534. Available at: https://doi.org/10.1038/onc.2011.252.

Huang, G. *et al.* (2001) 'Dimerization with PEBP2beta protects RUNX1/AML1 from ubiquitin-proteasome-mediated degradation.', *The EMBO journal*, 20 (4), pp. 723–33. Available at: https://doi.org/10.1093/emboj/20.4.723.

Hulkower, K.I. and Herber, R.L. (2011) 'Cell Migration and Invasion Assays as Tools for Drug Discovery', *Pharmaceutics 2011, Vol. 3, Pages 107-124*, 3 (1), pp. 107–124. Available at: https://doi.org/10.3390/PHARMACEUTICS3010107.

Hülsken, J., Birchmeier, W. and Behrens, J. (1994) 'E-cadherin and APC compete for the interaction with beta-catenin and the cytoskeleton.', *Journal of Cell Biology*, 127 (6), pp. 2061–2069. Available at: https://doi.org/10.1083/JCB.127.6.2061.

Hussein, M.R. and Hassan, H.I. (2006) 'Analysis of the mononuclear inflammatory cell infiltrate in the normal breast, benign proliferative breast disease, in situ and infiltrating ductal breast carcinomas: preliminary observations', *Journal of Clinical Pathology*, 59 (9), p. 972. Available at: https://doi.org/10.1136/JCP.2005.031252.

Ignatiadis, M. *et al.* (2009) 'A Meta-Analysis of Gene Expression Profiling Studies Identifies Clinically Relevant Oncogenic Pathways in Basal-Like Breast Cancer.', in *Cancer Research*. American Association for Cancer Research (AACR), pp. 106–106. Available at: https://doi.org/10.1158/0008-5472.sabcs-09-106.

Illendula, A. *et al.* (2016) 'Small Molecule Inhibitor of CBFß-RUNX Binding for RUNX Transcription Factor Driven Cancers', *EBioMedicine*, 8, pp. 117–131. Available at: https://doi.org/10.1016/j.ebiom.2016.04.032.

Imamura, Y. *et al.* (2015) 'Comparison of 2D- and 3D-culture models as drug-testing platforms in breast cancer', *Oncology Reports*, 33 (4), pp. 1837–1843. Available at: https://doi.org/10.3892/OR.2015.3767/HTML.

Imbert, A. *et al.* (2001) 'Δn89ß-Catenin Induces Precocious Development, Differentiation, and Neoplasia in Mammary Gland', *Journal of Cell Biology*, 153 (3), pp. 555–568. Available at: https://doi.org/10.1083/JCB.153.3.555.

Incassati, A. *et al.* (2010) 'Key signaling nodes in mammary gland development and cancer: ß-catenin', *Breast Cancer Research : BCR*, 12 (6), p. 213. Available at: https://doi.org/10.1186/BCR2723.

Indra, A.K. *et al.* (1999) 'Temporally-controlled site-specific mutagenesis in the basal layer of the epidermis: comparison of the recombinase activity of the tamoxifen-inducible Cre-ERT and Cre-ERT2 recombinases', *Nucleic Acids Research*, 27 (22), pp. 4324–4327. Available at: https://doi.org/10.1093/NAR/27.22.4324.

Infanger, D.W. *et al*. (2013) 'Glioblastoma stem cells are regulated by interleukin-8 signaling in a tumoral perivascular niche', *Cancer Research*, 73 (23), pp. 7079–7089. Available at: https://doi.org/10.1158/0008-5472.CAN-13-1355/651233/AM/GLIOBLASTOMA-STEM-CELLS-ARE-REGULATED-BY.

Inman, J.L. *et al*. (2015) 'Mammary gland development: cell fate specification, stem cells and the microenvironment', *Development*, 142 (6), pp. 1028–1042. Available at: https://doi.org/10.1242/dev.087643.

Inoue, K. *et al*. (2002) 'Runx3 controls the axonal projection of proprioceptive dorsal root ganglion neurons', *Nature Neuroscience*, 5 (10), pp. 946–954. Available at: https://doi.org/10.1038/nn925.

Inoue, M. *et al*. (2017) 'Specific sites of metastases in invasive lobular carcinoma: a retrospective cohort study of metastatic breast cancer', *Breast Cancer*, 24 (5), pp. 667–672. Available at: https://doi.org/10.1007/s12282-017-0753-4.

Irshad, S. *et al*. (2017) 'RORγt+ innate lymphoid cells promote lymph node metastasis of breast cancers', *Cancer Research*, 77 (5), pp. 1083–1096. Available at: https://doi.org/10.1158/0008-5472.CAN-16-0598/652574/AM/ROR-T-INNATE-LYMPHOID-CELLS-PROMOTE-LYMPH-NODE.

Ishii, K., Morii, N. and Yamashiro, H. (2019) 'Pertuzumab in the treatment of HER2-positive breast cancer: an evidence-based review of its safety, efficacy, and place in therapy', *Core Evidence*, Volume 14, pp. 51–70. Available at: https://doi.org/10.2147/ce.s217848.

Ivshina, A. V. *et al*. (2006) 'Genetic reclassification of histologic grade delineates new clinical subtypes of breast cancer', *Cancer Research*, 66 (21), pp. 10292–10301. Available at: https://doi.org/10.1158/0008-5472.CAN-05-4414.

Jacks, T. *et al*. (1994) 'Tumor spectrum analysis in p53-mutant mice', *Current Biology*, 4 (1), pp. 1–7. Available at: https://doi.org/10.1016/S0960-9822 (00)00002-6.

Janeway, C.A. *et al*. (2001) 'The components of the immune system ', in *Immunobiology: The Immune System in Health and Disease*. 5th edn. Garland Science. Available at: https://www.ncbi.nlm.nih.gov/books/NBK27092/ (Accessed: 1 August 2022).

Jayasingam, S.D. *et al*. (2020) 'Evaluating the Polarization of Tumor-Associated Macrophages Into M1 and M2 Phenotypes in Human Cancer Tissue: Technicalities and Challenges in Routine Clinical Practice', *Frontiers in Oncology*, 9, p. 1512. Available at: https://doi.org/10.3389/FONC.2019.01512/BIBTEX.

Jeanne, P.S.M. (2008) 'Management of Mastitis in Breastfeeding Women', *American Family Publication*, 78 (6), pp. 727–731. Available at:

https://www.aafp.org/pubs/afp/issues/2008/0915/p727.html (Accessed: 2 August 2022).

Jin, Y.H. *et al.* (2004) 'Transforming Growth Factor-ß Stimulates p300-dependent RUNX3 Acetylation, Which Inhibits Ubiquitination-mediated Degradation', *Journal of Biological Chemistry*, 279 (28), pp. 29409–29417. Available at: https://doi.org/10.1074/JBC.M313120200.

Jo, D. *et al.* (2001) 'Epigenetic regulation of gene structure and function with a cell-permeable Cre recombinase', *Nature Biotechnology 2001 19:10*, 19 (10), pp. 929–933. Available at: https://doi.org/10.1038/nbt1001-929.

Johnstone, T.C., Park, G.Y. and Lippard, S.J. (2014) 'Understanding and improving platinum anticancer drugs - Phenanthriplatin', in *Anticancer Research*. International Institute of Anticancer Research, pp. 471–476.

Jordan, V.C. (1993) 'A current view of tamoxifen for the treatment and prevention of breast cancer', *British Journal of Pharmacology*, 110 (2), pp. 507–517. Available at: https://doi.org/10.1111/J.1476-5381.1993.TB13840.X.

Jovanovic, I.P. *et al.* (2014) 'Interleukin-33/ST2 axis promotes breast cancer growth and metastases by facilitating intratumoral accumulation of immunosuppressive and innate lymphoid cells', *International Journal of Cancer*, 134 (7), pp. 1669–1682. Available at: https://doi.org/10.1002/IJC.28481.

Kagoshima, H. *et al.* (1993) 'The runt domain identifies a new family of heterometric transcriptional regulators', *Trends in Genetics*, 9 (10), pp. 338–341. Available at: https://doi.org/10.1016/0168-9525 (93)90026-E.

Kang, Y. *et al.* (2003) 'A multigenic program mediating breast cancer metastasis to bone', *Cancer Cell*, 3 (6), pp. 537–549. Available at: https://doi.org/10.1016/S1535-6108 (03)00132-6.

Kanno, Y. *et al.* (1998) 'Cytoplasmic Sequestration of the Polyomavirus Enhancer Binding Protein 2 (PEBP2)/Core Binding Factor α (CBFα) Subunit by the Leukemia-Related PEBP2/CBFß-SMMHC Fusion Protein Inhibits PEBP2/CBF-Mediated Transactivation', *Molecular and Cellular Biology*, 18 (7), pp. 4252–4261. Available at: https://doi.org/10.1128/MCB.18.7.4252/ASSET/672D7EE8-1053-4ABA-B37C-65C26789860A/ASSETS/GRAPHIC/MB078030707D.JPEG.

Kao, J. *et al.* (2009) 'Molecular Profiling of Breast Cancer Cell Lines Defines Relevant Tumor Models and Provides a Resource for Cancer Gene Discovery', *PLoS ONE*, 4 (7). Available at: https://doi.org/10.1371/JOURNAL.PONE.0006146.

Katt, M.E. *et al.* (2016) 'In Vitro Tumor Models: Advantages, Disadvantages, Variables, and Selecting the Right Platform', *Frontiers in Bioengineering and Biotechnology*, 4 (FEB). Available at: https://doi.org/10.3389/FBIOE.2016.00012.

Kent, W.J. *et al.* (2002) 'The Human Genome Browser at UCSC', *Genome Research*, 12 (6), pp. 996–1006. Available at: https://doi.org/10.1101/GR.229102.

Kersten, K. *et al.* (2017) 'Genetically engineered mouse models in oncology research and cancer medicine', *EMBO Molecular Medicine*, 9 (2), p. 137. Available at: https://doi.org/10.15252/EMMM.201606857.

van Keymeulen, A. *et al.* (2017) 'Lineage-Restricted Mammary Stem Cells Sustain the Development, Homeostasis, and Regeneration of the Estrogen Receptor Positive Lineage.', *Cell reports*, 20 (7), pp. 1525–1532. Available at: https://doi.org/10.1016/j.celrep.2017.07.066.

Kim, H. *et al.* (2018) 'Mouse Cre-LoxP system: general principles to determine tissue-specific roles of target genes', *Laboratory Animal Research*, 34 (4), p. 147. Available at: https://doi.org/10.5625/LAR.2018.34.4.147.

Kim, I.S. and Baek, S.H. (2010) 'Mouse models for breast cancer metastasis', *Biochemical and Biophysical Research Communications*, 394 (3), pp. 443–447. Available at: https://doi.org/10.1016/J.BBRC.2010.03.070.

Kim, J. *et al.* (2019) 'Clinical significance of lymph-node ratio in determining supraclavicular lymph-node radiation therapy in pn1 breast cancer patients who received breast-conserving treatment (KROG 14-18): A multicenter study', *Cancers*, 11 (5), p. 680. Available at: https://doi.org/10.3390/cancers11050680.

Kim, J.B., O'Hare, M.J. and Stein, R. (2004) 'Models of breast cancer: Is merging human and animal models the future?', *Breast Cancer Research*, 6 (1), pp. 22–30. Available at: https://doi.org/10.1186/BCR645/TABLES/1.

Kim, W.Y. *et al.* (1999) 'Mutual activation of Ets-1 and AML1 DNA binding by direct interaction of their autoinhibitory domains', *The EMBO Journal*, 18 (6), pp. 1609–1620. Available at: https://doi.org/10.1093/EMBOJ/18.6.1609.

Klinakis, A. *et al.* (2006) 'Myc is a Notch1 transcriptional target and a requisite for Notch1-induced mammary tumorigenesis in mice', *Proceedings of the National Academy of Sciences of the United States of America*, 103 (24), pp. 9262–9267. Available at: https://doi.org/10.1073/PNAS.0603371103/SUPPL_FILE/03371SUPPTEXT.PDF.

Komori, T. *et al*. (1997) 'Targeted Disruption of Cbfa1Results in a Complete Lack of Bone Formation owing to Maturational Arrest of Osteoblasts', *Cell*, 89 (5), pp. 755–764. Available at: https://doi.org/10.1016/S0092-8674 (00)80258-5.

Kopetz, S., Lemos, R. and Powis, G. (2012) 'The promise of patient-derived xenografts: The best laid plans of mice and men', *Clinical Cancer Research*, 18 (19), pp. 5160–5162. Available at: https://doi.org/10.1158/1078-0432.CCR-12-2408/85283/AM/THE-PROMISE-OF-PATIENT-DERIVED-XENOGRAFTS-THE-BEST.

Korbecki, J. *et al*. (2020) 'CC Chemokines in a Tumor: A Review of Pro-Cancer and Anti-Cancer Properties of the Ligands of Receptors CCR1, CCR2, CCR3, and CCR4', *International Journal of Molecular Sciences 2020, Vol. 21, Page 8412*, 21 (21), p. 8412. Available at: https://doi.org/10.3390/IJMS21218412.

Kuehnemuth, B. *et al*. (2018) 'CCL1 is a major regulatory T cell attracting factor in human breast cancer', *BMC Cancer*, 18 (1). Available at: https://doi.org/10.1186/S12885-018-5117-8.

Kühn, R. *et al*. (1995) 'Inducible Gene Targeting in Mice', *Science*, 269 (5229), pp. 1427–1429. Available at: https://doi.org/10.1126/SCIENCE.7660125.

van der Kuip, H. *et al*. (2006) 'Short term culture of breast cancer tissues to study the activity of the anticancer drug taxol in an intact tumor environment', *BMC Cancer*, 6 (1), pp. 1–11. Available at: https://doi.org/10.1186/1471-2407-6-86/FIGURES/5.

Kundu, M., Javed, A., *et al*. (2002) 'Cbfß interacts with Runx2 and has a critical role in bone development', *Nature Genetics*, 32 (4), pp. 639–644. Available at: https://doi.org/10.1038/ng1050.

Kundu, M., Chen, A., *et al*. (2002) 'Role of Cbfb in hematopoiesis and perturbations resulting from expression of the leukemogenic fusion gene Cbfb-MYH11', *Blood*, 100 (7), pp. 2449–2456. Available at: https://doi.org/10.1182/blood-2002-04-1064.

Kundu, M. and Liu, P.P. (2001) 'Function of the inv (16) fusion gene CBFB-MYH11', *Current Opinion in Hematology*, 8 (4), pp. 201–205. Available at: https://doi.org/10.1097/00062752-200107000-00004.

Lacroix, M. *et al*. (2004) 'Gene regulation by phorbol 12-myristate 13-acetate in MCF-7 and MDA-MB-231, two breast cancer cell lines exhibiting highly different phenotypes', *Oncology reports*, 12 (4), pp. 701–707. Available at: https://doi.org/10.3892/OR.12.4.701.

Lai, X.X. *et al*. (2018) 'Interference of Notch 1 inhibits the proliferation and invasion of breast cancer cells: Involvement of the β-catenin signaling pathway', *Molecular Medicine Reports*, 17 (2), pp. 2472–2478. Available at: https://doi.org/10.3892/MMR.2017.8161/HTML.

Lakso, M. *et al*. (1992) 'Targeted oncogene activation by site-specific recombination in transgenic mice.', *Proceedings of the National Academy of Sciences of the United States of America*, 89 (14), p. 6232. Available at: https://doi.org/10.1073/PNAS.89.14.6232.

Lallemend, F. *et al*. (2012) 'Positional differences of axon growth rates between sensory neurons encoded by runx3', *The EMBO Journal*, 31 (18), pp. 3718–3729. Available at: https://doi.org/10.1038/EMBOJ.2012.228.

Lasfargues, E.Y. and Ozzello, L. (1958) 'Cultivation of Human Breast Carcinomas', *JNCI: Journal of the National Cancer Institute* [Preprint]. Available at: https://doi.org/10.1093/jnci/21.6.1131.

Lei, J.T. *et al*. (2019) 'Endocrine therapy resistance: new insights', *Breast (Edinburgh, Scotland)*, 48 (Suppl 1), p. S26. Available at: https://doi.org/10.1016/S0960-9776(19)31118-X.

Leong, K.G. *et al*. (2007) 'Jagged1-mediated Notch activation induces epithelial-to-mesenchymal transition through Slug-induced repression of E-cadherin', *Journal of Experimental Medicine*, 204 (12), pp. 2935–2948. Available at: https://doi.org/10.1084/JEM.20071082.

Lester, S.C. *et al*. (2009) 'Protocol for the Examination of Specimens From Patients With Invasive Carcinoma of the Breast', *Archives of Pathology & Laboratory Medicine*, 133 (10), pp. 1515–1538. Available at: https://doi.org/10.5858/133.10.1515.

Levanon, D. *et al*. (2011) 'Absence of Runx3 expression in normal gastrointestinal epithelium calls into question its tumour suppressor function', *EMBO Molecular Medicine*, 3 (10), pp. 593–604. Available at: https://doi.org/10.1002/emmm.201100168.

Li, Q. *et al*. (2022) 'INK4 tumor suppressor proteins mediate resistance to CDK4/6 kinase inhibitors', *Cancer discovery*, 12 (2), p. 356. Available at: https://doi.org/10.1158/2159-8290.CD-20-1726.

Li, S. *et al*. (2018) 'Overview of the reporter genes and reporter mouse models', *Animal Models and Experimental Medicine*, 1 (1), p. 29. Available at: https://doi.org/10.1002/AME2.12008.

Li, Y. *et al.* (2003) 'Evidence that transgenes encoding components of the Wnt signaling pathway preferentially induce mammary cancers from progenitor cells', *Proceedings of the National Academy of Sciences of the United States of America*, 100 (26), pp. 15853–15858. Available at: https://doi.org/10.1073/PNAS.2136825100/SUPPL_FILE/6825FIG8.JPG.

Lim, E. *et al.* (2009) 'Aberrant luminal progenitors as the candidate target population for basal tumor development in BRCA1 mutation carriers', *Nature Medicine*, 15 (8), pp. 907–913. Available at: https://doi.org/10.1038/nm.2000.

Lim, E. *et al.* (2010) 'Transcriptome analyses of mouse and human mammary cell subpopulations reveal multiple conserved genes and pathways', *Breast Cancer Research*, 12 (2), p. R21. Available at: https://doi.org/10.1186/bcr2560.

Lin, E.Y. *et al.* (2003) 'Progression to Malignancy in the Polyoma Middle T Oncoprotein Mouse Breast Cancer Model Provides a Reliable Model for Human Diseases', *The American Journal of Pathology*, 163 (5), pp. 2113–2126. Available at: https://doi.org/10.1016/S0002-9440 (10)63568-7.

Lin, S.Y. *et al.* (2000) 'ß-catenin, a novel prognostic marker for breast cancer: Its roles in cyclin D1 expression and cancer progression', *Proceedings of the National Academy of Sciences of the United States of America*, 97 (8), pp. 4262–4266. Available at: https://doi.org/10.1073/PNAS.060025397/ASSET/F8EBEB18-8AC2-4B38-8A82-A914770F1FD5/ASSETS/GRAPHIC/PQ0600253003.JPEG.

Liu, B.Y. *et al.* (2003) 'Mammary gland development requires syndecan-1 to create a ß-catenin/TCF-responsive mammary epithelial subpopulation', *Oncogene 2003 22:58*, 22 (58), pp. 9243–9253. Available at: https://doi.org/10.1038/sj.onc.1207217.

Liu, B.Y. *et al.* (2004) 'The transforming activity of Wnt effectors correlates with their ability to induce the accumulation of mammary progenitor cells', *Proceedings of the National Academy of Sciences of the United States of America*, 101 (12), pp. 4158–4163. Available at: https://doi.org/10.1073/PNAS.0400699101/SUPPL_FILE/00699SUPPTEXT.HTML.

Liu, C. *et al.* (2021) 'Advances in Rodent Models for Breast Cancer Formation, Progression, and Therapeutic Testing', *Frontiers in Oncology*, 11, p. 346. Available at: https://doi.org/10.3389/FONC.2021.593337/BIBTEX.

Liu, F. *et al.* (2012) 'Peritumoral FOXP3+ regulatory T cell is sensitive to chemotherapy while intratumoral FOXP3+ regulatory T cell is prognostic predictor of breast

cancer patients', *Breast Cancer Research and Treatment*, 135 (2), pp. 459–467. Available at: https://doi.org/10.1007/S10549-012-2132-3/TABLES/4.

Liu, J. *et al.* (2001) 'Siah-1 Mediates a Novel β-Catenin Degradation Pathway Linking p53 to the Adenomatous Polyposis Coli Protein', *Molecular Cell*, 7 (5), pp. 927–936. Available at: https://doi.org/10.1016/S1097-2765 (01)00241-6.

Liu, X. *et al.* (2021) 'The associations between Deltex1 and clinical characteristics of breast cancer', *Gland Surgery*, 10 (11), pp. 3116–3127. Available at: https://doi.org/10.21037/gs-21-739.

Liu, Y.L. *et al.* (2019) 'Assessing metastatic potential of breast cancer cells based on EGFR dynamics', *Scientific Reports 2019 9:1*, 9 (1), pp. 1–13. Available at: https://doi.org/10.1038/s41598-018-37625-0.

Livasy, C.A. *et al.* (2006) 'Phenotypic evaluation of the basal-like subtype of invasive breast carcinoma', *Modern Pathology*, 19 (2), pp. 264–271. Available at: https://doi.org/10.1038/modpathol.3800528.

llis, P. , Schnitt, S.J. , Sastre-Garau, X. , Bussolati, G. , Tavassoli, F.A. , Eusebi, V. , Peterse, J.L. , Mukai, K. , Tabar, L. , Jacquemier, J. , Cornelisse, C.J. , Sasco, A.J. , Kaaks, R. , Pisani, P. , Goldgar, D.E. , Devilee, P. , Cleton-Jansen, M., A. (2003) *Invasive breast carcinoma. In Tavassoli F.A., Devilee P. (Eds.), WHO Classification of Tumours Pathology and Genetics of Tumours of the Breast and Female Genital Organs. Lyon Press; Lyon:* Available at: https://books.google.co.uk/books?hl=en&lr=&id=gYMlMcE1-bsC&oi=fnd&pg=PA45&ots=naQwmMDOXZ&sig=GvMtwzGKwuAfeRGBCRDIV12bcXg&redir_esc=y#v=onepage&q&f=false (Accessed: 24 July 2020).

Logan, C.Y. and Nusse, R. (2004) 'The Wnt Signalling Pathway in Development and Disease', *Annual Review of Cell and Developmental Biology*, 20, pp. 781–810. Available at: https://doi.org/10.1146/ANNUREV.CELLBIO.20.010403.113126.

Look, A.T. (1997) 'Oncogenic Transcription Factors in the Human Acute Leukemias', *Science*, 278 (5340), pp. 1059–1064. Available at: https://doi.org/10.1126/science.278.5340.1059.

Lorenzo-Sanz, L. and Muñoz, P. (2019) 'Tumor-Infiltrating Immunosuppressive Cells in Cancer-Cell Plasticity, Tumor Progression and Therapy Response', *Cancer Microenvironment 2019 12:2*, 12 (2), pp. 119–132. Available at: https://doi.org/10.1007/S12307-019-00232-2.

Luche, H. *et al.* (2007) 'Faithful activation of an extra-bright red fluorescent protein in "knock-in" Cre-reporter mice ideally suited for lineage tracing studies', *European*

Journal of Immunology, 37 (1), pp. 43–53. Available at: https://doi.org/10.1002/EJI.200636745.

Lutterbach, B. and Hiebert, S.W. (2000) 'Role of the transcription factor AML-1 in acute leukemia and hematopoietic differentiation', *Gene*, 245 (2), pp. 223–235. Available at: https://doi.org/10.1016/S0378-1119 (00)00014-7.

Lwin, K.Y. *et al*. (1985) 'An immunohistological study of leukocyte localization in benign and malignant breast tissue', *International Journal of Cancer*, 36 (4), pp. 433–438. Available at: https://doi.org/10.1002/IJC.2910360404.

Ma, X. *et al*. (2018) 'Tumor-infiltrating lymphocytes are associated with β-catenin overexpression in breast cancer', *Cancer Biomarkers*, 21 (3), pp. 639–650. Available at: https://doi.org/10.3233/CBM-170708.

Maglione, J. *et al*. (2001) 'Transgenic Polyoma middle-T mice model premalignant mammary disease', *Cancer Research*, 61 (22), pp. 8298–8305. Available at: https://pubmed.ncbi.nlm.nih.gov/11719463/ (Accessed: 23 August 2022).

Malhotra, G.K. *et al*. (2010) 'Histological, molecular and functional subtypes of breast cancers', *Cancer Biology and Therapy*. Taylor & Francis, pp. 955–960. Available at: https://doi.org/10.4161/cbt.10.10.13879.

Malik, N. *et al*. (2019) 'The transcription factor CBFB suppresses breast cancer through orchestrating translation and transcription', *Nature Communications*, 10 (1), p. 2071. Available at: https://doi.org/10.1038/s41467-019-10102-6.

Malik, N. *et al*. (2021) 'CBFB cooperates with p53 to maintain TAp73 expression and suppress breast cancer', *PLoS Genetics*, 17 (5 May), p. e1009553. Available at: https://doi.org/10.1371/journal.pgen.1009553.

Mallo, M. *et al*. (2007) 'Gain of multiple copies of the CBFB gene: a new genetic aberration in a case of granulocytic sarcoma', *Cancer Genetics and Cytogenetics*, 179 (1), pp. 62–65. Available at: https://doi.org/10.1016/J.CANCERGENCYTO.2007.07.018.

Manna, S. and Holz, M.K. (2016) 'Tamoxifen Action in ER-Negative Breast Cancer', *Signal Transduction Insights*, 5, pp. 1–7. Available at: https://doi.org/10.4137/STI.S29901.

Manning, H.C., Buck, J.R. and Cook, R.S. (2016) 'Mouse Models of Breast Cancer: Platforms for Discovering Precision Imaging Diagnostics and Future Cancer Medicine', *Journal of Nuclear Medicine*, 57 (Supplement 1), pp. 60S-68S. Available at: https://doi.org/10.2967/JNUMED.115.157917.

Martelotto, L.G. *et al*. (2014) 'Breast cancer intra-tumor heterogeneity', *Breast Cancer Research*, 16 (3), pp. 1–11. Available at: https://doi.org/10.1186/BCR3658/FIGURES/3.

Martincorena, I. and Campbell, P.J. (2015) 'Somatic mutation in cancer and normal cells', *Science*, 349 (6255), pp. 1483–1489. Available at: https://doi.org/10.1126/SCIENCE.AAB4082/ASSET/63C4918F-DDB9-4495-8177-B8E70A746DD8/ASSETS/GRAPHIC/349_1483_F4.JPEG.

Martinez, L.M. *et al*. (2019) 'Regulatory T cells control the switch from in situ to invasive breast cancer', *Frontiers in Immunology*, 10 (AUG), p. 1942. Available at: https://doi.org/10.3389/FIMMU.2019.01942/BIBTEX.

Matulka, L.A. and Wagner, K.U. (2005) 'Models of breast cancer', *Drug Discovery Today: Disease Models*, 2 (1), pp. 1–6. Available at: https://doi.org/10.1016/J.DDMOD.2005.05.008.

McCann, K.E. and Hurvitz, S.A. (2018) 'Advances in the use of PARP inhibitor therapy for breast cancer', *Drugs in Context*, 7, pp. 1–30. Available at: https://doi.org/10.7573/dic.212540.

McDonald, E.S. *et al*. (2016) 'Clinical diagnosis and management of breast cancer', *Journal of Nuclear Medicine*, 57 (Supplement 1), pp. 9S-16S. Available at: https://doi.org/10.2967/jnumed.115.157834.

McDonald, L. *et al*. (2014) 'RUNX2 correlates with subtype-specific breast cancer in a human tissue microarray, and ectopic expression of Runx2 perturbs differentiation in the mouse mammary gland.', *Disease models & mechanisms*, 7 (5), pp. 525–34. Available at: https://doi.org/10.1242/dmm.015040.

McGowan, J. V. *et al*. (2017) 'Anthracycline Chemotherapy and Cardiotoxicity', *Cardiovascular Drugs and Therapy*, 31 (1), pp. 63–75. Available at: https://doi.org/10.1007/s10557-016-6711-0.

Melaiu, O. *et al*. (2020) 'Influence of the Tumor Microenvironment on NK Cell Function in Solid Tumors', *Frontiers in Immunology*, 10, p. 3038. Available at: https://doi.org/10.3389/FIMMU.2019.03038/BIBTEX.

Mendoza-Villanueva, D. *et al*. (2010) 'The Runx transcriptional co-activator, CBFß, is essential for invasion of breast cancer cells', *Molecular Cancer*, 9 (1), p. 171. Available at: https://doi.org/10.1186/1476-4598-9-171.

Mendoza-Villanueva, D., Zeef, L. and Shore, P. (2011) 'Metastatic breast cancer cells inhibit osteoblast differentiation through the Runx2/CBFß-dependent expression

of the Wnt antagonist, sclerostin.', *Breast cancer research : BCR*, 13 (5), p. R106. Available at: https://doi.org/10.1186/bcr3048.

Merlo, G.R. *et al.* (1996) 'Growth, differentiation and survival of HC11 mammary epithelial cells: diverse effects of receptor tyrosine kinase-activating peptide growth factors', *European Journal of Cell Biology*, 70 (2), pp. 97–105. Available at: https://pubmed.ncbi.nlm.nih.gov/8793381/ (Accessed: 31 July 2022).

Michaelson, J.S. and Leder, P. (2001) 'ß-catenin is a downstream effector of Wnt-mediated tumorigenesis in the mammary gland', *Oncogene 2001 20:37*, 20 (37), pp. 5093–5099. Available at: https://doi.org/10.1038/sj.onc.1204586.

Mikkola, M.L. and Millar, S.E. (2006) 'The mammary bud as a skin appendage: Unique and shared aspects of development', *Journal of Mammary Gland Biology and Neoplasia*, 11 (3–4), pp. 187–203. Available at: https://doi.org/10.1007/S10911-006-9029-X/TABLES/1.

Milanese, T.R. *et al.* (2006) 'Age-Related Lobular Involution and Risk of Breast Cancer', *JNCI: Journal of the National Cancer Institute*, 98 (22), pp. 1600–1607. Available at: https://doi.org/10.1093/JNCI/DJJ439.

von Minckwitz, G. *et al.* (2019) 'Trastuzumab Emtansine for Residual Invasive HER2-Positive Breast Cancer', *New England Journal of Medicine*, 380 (7), pp. 617–628. Available at: https://doi.org/10.1056/NEJMoa1814017.

Miyagawa, K. *et al.* (2006) 'Down-regulation of RUNX1, RUNX3 and CBFß in hepatocellular carcinomas in an early stage of hepatocarcinogenesis', *Anticancer Research*, 26 (5 B), pp. 3633–3643. Available at: https://pdfs.semanticscholar.org/e121/f4130c6b2b3f968549afb38543a8d77aaf79.pdf (Accessed: 18 May 2019).

Miyoshi, H. *et al.* (1991) 't (8;21) breakpoints on chromosome 21 in acute myeloid leukemia are clustered within a limited region of a single gene, AML1.', *Proceedings of the National Academy of Sciences of the United States of America*, 88 (23), p. 10431. Available at: https://doi.org/10.1073/PNAS.88.23.10431.

Miyoshi, K. *et al.* (2002) 'Activation of ß-catenin signaling in differentiated mammary secretory cells induces transdifferentiation into epidermis and squamous metaplasias', *Proceedings of the National Academy of Sciences of the United States of America*, 99 (1), pp. 219–224. Available at: https://doi.org/10.1073/PNAS.012414099/ASSET/BD1E199C-F760-4A14-8E9C-2CF1901DF8A7/ASSETS/GRAPHIC/PQ0124140007.JPEG.

Modi, S. *et al.* (2020) 'Trastuzumab deruxtecan in previously treated HER2-positive breast cancer', *New England Journal of Medicine*, 382 (7), pp. 610–621. Available at: https://doi.org/10.1056/NEJMoa1914510.

Mohammed, A.A. (2021) 'The clinical behavior of different molecular subtypes of breast cancer', *Cancer Treatment and Research Communications*, 29, p. 100475. Available at: https://doi.org/10.1016/J.CTARC.2021.100469.

Mojic, M., Takeda, K. and Hayakawa, Y. (2018) 'The Dark Side of IFN-γ: Its Role in Promoting Cancer Immunoevasion', *International Journal of Molecular Sciences*, 19 (1), p. 89. Available at: https://doi.org/10.3390/IJMS19010089.

Molyneux, G. *et al.* (2010) 'BRCA1 basal-like breast cancers originate from luminal epithelial progenitors and not from basal stem cells', *Cell Stem Cell*, 7 (3), pp. 403–417. Available at: https://doi.org/10.1016/j.stem.2010.07.010.

Morita, K., Noura, M., *et al.* (2017) 'Autonomous feedback loop of RUNX1-p53-CBFB in acute myeloid leukemia cells', *Scientific Reports*, 7 (1), pp. 1–12. Available at: https://doi.org/10.1038/s41598-017-16799-z.

Morita, K., Suzuki, K., *et al.* (2017) 'Genetic regulation of the RUNX transcription factor family has antitumor effects', *Journal of Clinical Investigation*, 127 (7), pp. 2815–2828. Available at: https://doi.org/10.1172/JCI91788.

Morton, C.L. and Houghton, P.J. (2007) 'Establishment of human tumor xenografts in immunodeficient mice', *Nature Protocols 2007 2:2*, 2 (2), pp. 247–250. Available at: https://doi.org/10.1038/nprot.2007.25.

Mowat, A.M.I., Scott, C.L. and Bain, C.C. (2017) 'Barrier-tissue macrophages: functional adaptation to environmental challenges', *Nature Medicine 2017 23:11*, 23 (11), pp. 1258–1270. Available at: https://doi.org/10.1038/nm.4430.

Müller-Quernheim, U.C. *et al.* (2012) 'Tumor-Cell Co-Culture Induced Alternative Activation of Macrophages Is Modulated by Interferons In Vitro', *Journal of Interferon & Cytokine Research*, 32 (4), p. 169. Available at: https://doi.org/10.1089/JIR.2011.0020.

Murata, S. *et al.* (2006) 'Ductal Access for Prevention and Therapy of Mammary Tumors', *Cancer Research*, 66 (2), pp. 638–645. Available at: https://doi.org/10.1158/0008-5472.CAN-05-4329.

Muschler, J. and Streuli, C.H. (2010) 'Cell–Matrix Interactions in Mammary Gland Development and Breast Cancer', *Cold Spring Harbor Perspectives in Biology*, 2 (10), p. a003202. Available at: https://doi.org/10.1101/CSHPERSPECT.A003202.

Nagy, A. (2000) ‘Cre Recombinase: The Universal Reagent for Genome Tailoring’, *Genesis*, 26, pp. 99–109. Available at: https://doi.org/10.1002/ (SICI)1526-968X (200002)26:2.

Nakhlis, F. and Morrow, M. (2003) ‘Ductal carcinoma in situ’, *Surgical Clinics of North America*, 83 (4), pp. 821–839. Available at: https://doi.org/10.1016/S0039-6109 (03)00072-0.

Nanno, M. *et al.* (2007) ‘γδ T cells: firefighters or fire boosters in the front lines of inflammatory responses’, *Immunological Reviews*, 215 (1), pp. 103–113. Available at: https://doi.org/10.1111/J.1600-065X.2006.00474.X.

Naoe, Y. *et al.* (2007) ‘Repression of interleukin-4 in T helper type 1 cells by Runx/Cbfß binding to the Il4 silencer’, *Journal of Experimental Medicine*, 204 (8), pp. 1749–1755. Available at: https://doi.org/10.1084/jem.20062456.

le Naour, A. *et al.* (2020) ‘EO771, the first luminal B mammary cancer cell line from C57BL/6 mice’, *Cancer Cell International*, 20 (1), pp. 1–13. Available at: https://doi.org/10.1186/S12935-020-01418-1/FIGURES/5.

Nath, S. and Devi, G.R. (2016) ‘Three-dimensional culture systems in cancer research: Focus on tumor spheroid model’, *Pharmacology & Therapeutics*, 163, pp. 94–108. Available at: https://doi.org/10.1016/J.PHARMTHERA.2016.03.013.

Nathan, M.R. and Schmid, P. (2018) ‘The emerging world of breast cancer immunotherapy’, *The Breast*, 37, pp. 200–206. Available at: https://doi.org/10.1016/j.breast.2017.05.013.

Neve, R.M. *et al.* (2006) ‘A collection of breast cancer cell lines for the study of functionally distinct cancer subtypes’, *Cancer Cell*, 10 (6), pp. 515–527. Available at: https://doi.org/10.1016/J.CCR.2006.10.008.

Nguyen, Q.H. *et al.* (2018) ‘Profiling human breast epithelial cells using single cell RNA sequencing identifies cell diversity’, *Nature Communications*, 9 (1), p. 2028. Available at: https://doi.org/10.1038/s41467-018-04334-1.

Niehrs, C. (2010) ‘On growth and form: a Cartesian coordinate system of Wnt and BMP signaling specifies bilaterian body axes’, *Development*, 137 (6), pp. 845–857. Available at: https://doi.org/10.1242/DEV.039651.

Niini, T. *et al.* (2000) ‘AML1 gene amplification: a novel finding in childhood acute lymphoblastic leukemia.’, *Haematologica*, 85 (4), pp. 362–6. Available at: http://www.ncbi.nlm.nih.gov/pubmed/10756360 (Accessed: 18 May 2019).

Nik-Zainal, S. *et al.* (2016) 'Landscape of somatic mutations in 560 breast cancer whole-genome sequences', *Nature*, 534 (7605), pp. 47–54. Available at: https://doi.org/10.1038/nature17676.

Noman, M.Z. *et al.* (2018) 'CD47 is a direct target of SNAI1 and ZEB1 and its blockade activates the phagocytosis of breast cancer cells undergoing EMT', *OncoImmunology*, 7 (4). Available at: https://doi.org/10.1080/2162402X.2017.1345415/SUPPL_FILE/KONI_A_1345415_SM7384.DOCX.

Nowell, P.C. (1976) 'The Clonal Evolution of Tumor Cell Populations', *Science*, 194 (4260), pp. 23–28. Available at: https://doi.org/10.1126/SCIENCE.959840.

Nusse, R. *et al.* (1991) 'A new nomenclature for int-1 and related genes: The Wnt gene family', *Cell*, 64 (2), p. 231. Available at: https://doi.org/10.1016/0092-8674(91)90633-A.

Nusse, R. and Varmus, H.E. (1982) 'Many tumors induced by the mouse mammary tumor virus contain a provirus integrated in the same region of the host genome', *Cell*, 31 (1), pp. 99–109. Available at: https://doi.org/10.1016/0092-8674(82)90409-3.

Nusslein-Volhard, C. and Wieschaus, E. (1980) 'Mutations affecting segment number and polarity in Drosophila', *Nature*, 287 (2), pp. 787–790. Available at: https://doi.org/10.1038/287795a0.

O'Brien, J. *et al.* (2012) 'Macrophages are crucial for epithelial cell death and adipocyte repopulation during mammary gland involution', *Development*, 139 (2), pp. 269–275. Available at: https://doi.org/10.1242/DEV.071696.

Oftedal, O.T. (2002) 'The Mammary Gland and Its Origin During Synapsid Evolution', *Journal of Mammary Gland Biology and Neoplasia 2002 7:3*, 7 (3), pp. 225–252. Available at: https://doi.org/10.1023/A:1022896515287.

Ogawa, E. *et al.* (1993) 'Molecular Cloning and Characterization of PEBP2β, the Heterodimeric Partner of a Novel Drosophila runt-Related DNA Binding Protein PEBP2α', *Virology*, 194 (1), pp. 314–331. Available at: https://doi.org/10.1006/viro.1993.1262.

Okuda, T. *et al.* (1996) 'AML1, the target of multiple chromosomal translocations in human leukemia, is essential for normal fetal liver hematopoiesis.', *Cell*, 84 (2), pp. 321–30. Available at: https://doi.org/10.1016/S0092-8674(00)80986-1.

Okugawa, H. *et al.* (2005) 'Effect of perductal paclitaxel exposure on the development of MNU-induced mammary carcinoma in female S-D rats', *Breast Cancer Research*

and Treatment 2005 91:1, 91 (1), pp. 29–34. Available at: https://doi.org/10.1007/S10549-004-6455-6.

van Ooyen, A. and Nusse, R. (1984) 'Structure and nucleotide sequence of the putative mammary oncogene int-1; proviral insertions leave the protein-encoding domain intact', *Cell*, 39 (1), pp. 233–240. Available at: https://doi.org/10.1016/0092-8674 (84)90209-5.

Orban, P.C., Chui, D. and Marth, J.D. (1992) 'Tissue- and site-specific DNA recombination in transgenic mice.', *Proceedings of the National Academy of Sciences of the United States of America*, 89 (15), p. 6861. Available at: https://doi.org/10.1073/PNAS.89.15.6861.

Orford, K., Orford, C.C. and Byers, S.W. (1999) 'Exogenous Expression of ß-Catenin Regulates Contact Inhibition, Anchorage-Independent Growth, Anoikis, and Radiation-Induced Cell Cycle Arrest', *The Journal of Cell Biology*, 146 (4), p. 855. Available at: https://doi.org/10.1083/JCB.146.4.855.

Otto, F. *et al.* (1997) 'Cbfa1, a Candidate Gene for Cleidocranial Dysplasia Syndrome, Is Essential for Osteoblast Differentiation and Bone Development', *Cell*, 89 (5), pp. 765–771. Available at: https://doi.org/10.1016/S0092-8674 (00)80259-7.

Otto, F., Lübbert, M. and Stock, M. (2003) 'Upstream and downstream targets of RUNX proteins', *Journal of Cellular Biochemistry*, 89 (1), pp. 9–18. Available at: https://doi.org/10.1002/jcb.10491.

Pai, S.G. *et al.* (2017) 'Wnt/beta-catenin pathway: modulating anticancer immune response', *Journal of Hematology & Oncology*, 10 (1), p. 101. Available at: https://doi.org/10.1186/s13045-017-0471-6.

Paine, I. *et al.* (2016) 'A Geometrically-Constrained Mathematical Model of Mammary Gland Ductal Elongation Reveals Novel Cellular Dynamics within the Terminal End Bud', *PLOS Computational Biology*. Edited by A. v Morozov, 12 (4), p. e1004839. Available at: https://doi.org/10.1371/journal.pcbi.1004839.

Paine, I.S. and Lewis, M.T. (2017) 'The Terminal End Bud: the Little Engine that Could', *Journal of Mammary Gland Biology and Neoplasia*, 22 (2), pp. 93–108. Available at: https://doi.org/10.1007/s10911-017-9372-0.

Palacios-Arreola, M.I. *et al.* (2014) 'The role of chemokines in breast cancer pathology and its possible use as therapeutic targets', *Journal of Immunology Research*. Hindawi Publishing Corporation. Available at: https://doi.org/10.1155/2014/849720.

Paluskievicz, C.M. *et al.* (2019) 'T regulatory cells and priming the suppressive tumor microenvironment', *Frontiers in Immunology*, 10 (OCT), p. 2453. Available at: https://doi.org/10.3389/FIMMU.2019.02453/BIBTEX.

Pampaloni, F., Reynaud, E.G. and Stelzer, E.H.K. (2007) 'The third dimension bridges the gap between cell culture and live tissue', *Nature Reviews Molecular Cell Biology 2007 8:10*, 8 (10), pp. 839–845. Available at: https://doi.org/10.1038/nrm2236.

Panda, S.K. and Colonna, M. (2019) 'Innate Lymphoid Cells in Mucosal Immunity', *Frontiers in Immunology*, 10 (MAY), p. 861. Available at: https://doi.org/10.3389/FIMMU.2019.00861.

Patey, D.H. and Scarff, R.W. (1928) 'The Position of Histology in the Prognosis of Carcinoma of the Breast.', *Lancet*, pp. 801–4.

Pathology Outlines - WHO classification. Available at: https://www.pathologyoutlines.com/topic/breastmalignantwhoclassification.html (Accessed: 24 July 2020).

Patienten, S. and Therapie, N. (2020) 'PAKT Inhibitor May Promote Better Responses to Abiraterone in mCRPC', *onclive*, 7 (Suppl 10), pp. 1–7. Available at: https://doi.org/10.1093/annonc.

Peaker, M. (2002) 'The Mammary Gland in Mammalian Evolution: A Brief Commentary on Some of the Concepts', *Journal of Mammary Gland Biology and Neoplasia 2002 7:3*, 7 (3), pp. 347–353. Available at: https://doi.org/10.1023/A:1022860902083.

Pegg, H.J. *et al.* (2019) 'The RUNX Transcriptional Coregulator, CBFβ, Suppresses Migration of ER+ Breast Cancer Cells by Repressing ERα-Mediated Expression of the Migratory Factor TFF1', *Molecular Cancer Research*, 17 (5), pp. 1015–1023. Available at: https://doi.org/10.1158/1541-7786.MCR-18-1039.

Pellacani, D. *et al.* (2019) 'Transcriptional regulation of normal human mammary cell heterogeneity and its perturbation in breast cancer', *The EMBO Journal*, 38 (14), p. e100330. Available at: https://doi.org/10.15252/EMBJ.2018100330.

Peng, G.L. *et al.* (2019) 'CD8+ cytotoxic and FoxP3+ regulatory T lymphocytes serve as prognostic factors in breast cancer', *American Journal of Translational Research*, 11 (8), p. 5039. Available at: /pmc/articles/PMC6731430/ (Accessed: 1 August 2022).

Peppercorn, J., Perou, C.M. and Carey, L.A. (2008) 'Molecular Subtypes in Breast Cancer Evaluation and Management: Divide and Conquer', *Cancer Investigation*, 26 (1), pp. 1–10. Available at: https://doi.org/10.1080/07357900701784238.

Pereira, B. *et al.* (2016) 'The somatic mutation profiles of 2,433 breast cancers refine their genomic and transcriptomic landscapes', *Nature Communications*, 7 (1), p. 11479. Available at: https://doi.org/10.1038/ncomms11479.

Perou, C.M. *et al.* (2000) 'Molecular portraits of human breast tumours', *Nature*, 406 (6797), pp. 747–752. Available at: https://doi.org/10.1038/35021093.

Petersen, C.P. and Reddien, P.W. (2009) 'Wnt Signaling and the Polarity of the Primary Body Axis', *Cell*, 139 (6), pp. 1056–1068. Available at: https://doi.org/10.1016/J.CELL.2009.11.035.

Petrovick, M.S. *et al.* (1998) 'Multiple Functional Domains of AML1: PU.1 and C/EBPα Synergize with Different Regions of AML1', *Molecular and Cellular Biology*, 18 (7), pp. 3915–3925. Available at: https://doi.org/10.1128/MCB.18.7.3915/ASSET/06DAAC3F-53F1-497A-B997-D32FE4D494B6/ASSETS/GRAPHIC/MB0780188007.JPEG.

Pfefferle, A.D. *et al.* (2013) 'Transcriptomic classification of genetically engineered mouse models of breast cancer identifies human subtype counterparts', *Genome Biology*, 14 (11), pp. 1–16. Available at: https://doi.org/10.1186/GB-2013-14-11-R125/FIGURES/5.

Pillai, S.G. *et al.* (2018) 'Identifying biomarkers of breast cancer micrometastatic disease in bone marrow using a patient-derived xenograft mouse model', *Breast Cancer Research*, 20 (1), pp. 1–12. Available at: https://doi.org/10.1186/S13058-017-0927-1/TABLES/4.

Pinto, C., Estrada, M.F. and Brito, C. (2020) 'In Vitro and Ex Vivo Models – The Tumor Microenvironment in a Flask', *Advances in Experimental Medicine and Biology*, 1219, pp. 431–443. Available at: https://doi.org/10.1007/978-3-030-34025-4_23/FIGURES/1.

Polyak, K. and Kalluri, R. (2010) 'The Role of the Microenvironment in Mammary Gland Development and Cancer', *Cold Spring Harbor Perspectives in Biology*, 2 (11), p. a003244. Available at: https://doi.org/10.1101/CSHPERSPECT.A003244.

Ponti, D. *et al.* (2005) 'Isolation and In vitro Propagation of Tumorigenic Breast Cancer Cells with Stem/Progenitor Cell Properties', *Cancer Research*, 65 (13), pp. 5506–5511. Available at: https://doi.org/10.1158/0008-5472.CAN-05-0626.

Prabhakaran, P. *et al.* (2013) 'Cisplatin induces differentiation of breast cancer cells', *Frontiers in Oncology*, 3 JUN, p. 134. Available at: https://doi.org/10.3389/FONC.2013.00134/BIBTEX.

Prinz, J.C. *et al.* (1979) *Fusion Between Transcription Factor CBFP/PEBP2I3 and a Myosin Heavy Chain in Acute Myeloid Leukemia*, *Proc. Natl. Acad. Sci. U.S.A.*

Pruneri, G., Vingiani, A. and Denkert, C. (2018) 'Tumor infiltrating lymphocytes in early breast cancer', *The Breast*, 37, pp. 207–214. Available at: https://doi.org/10.1016/J.BREAST.2017.03.010.

Puleo, J. and Polyak, K. (2021) 'The MCF10 Model of Breast Tumor Progression', *Cancer Research*, 81 (16), pp. 4183–4185. Available at: https://doi.org/10.1158/0008-5472.CAN-21-1939.

Pulido, C. *et al.* (2017) 'Bone metastasis risk factors in breast cancer', *ecancermedicalscience*, 11, p. 715. Available at: https://doi.org/10.3332/ecancer.2017.715.

Pusztai, L. *et al.* (2006) 'Molecular Classification of Breast Cancer: Limitations and Potential', *The Oncologist*, 11 (8), pp. 868–877. Available at: https://doi.org/10.1634/theoncologist.11-8-868.

Rajendran, B.K. and Deng, C.X. (2017) 'Characterization of potential driver mutations involved in human breast cancer by computational approaches', *Oncotarget*, 8 (30), p. 50252. Available at: https://doi.org/10.18632/ONCOTARGET.17225.

Ramirez, R.A. *et al.* (2012) 'Alterations in mast cell frequency and relationship to angiogenesis in the rat mammary gland during windows of physiologic tissue remodeling', *Developmental Dynamics*, 241 (5), pp. 890–900. Available at: https://doi.org/10.1002/DVDY.23778.

Ran, R. *et al.* (2020) 'A role for CBFβ in maintaining the metastatic phenotype of breast cancer cells', *Oncogene*, 39 (12), pp. 2624–2637. Available at: https://doi.org/10.1038/s41388-020-1170-2.

Rao, T. *et al.* (2014) 'Inducible and coupled expression of the polyomavirus middle T antigen and Cre recombinase in transgenic mice: an in vivo model for synthetic viability in mammary tumour progression', *Breast Cancer Research*, 16 (1), p. R11. Available at: https://doi.org/10.1186/bcr3603.

Rebbeck, T.R. *et al.* (2004) 'Bilateral prophylactic mastectomy reduces breast cancer risk in BRCA1 and BRCA2 mutation carriers: the PROSE Study Group.', *Journal of clinical oncology : official journal of the American Society of Clinical Oncology*, 22 (6), pp. 1055–62. Available at: https://doi.org/10.1200/JCO.2004.04.188.

Recouvreux, M.S. *et al.* (2016) 'RUNX1 and FOXP3 interplay regulates expression of breast cancer related genes', *Oncotarget*, 7 (6), p. 6552. Available at: https://doi.org/10.18632/ONCOTARGET.6771.

Rei, M. *et al*. (2014) 'Murine CD27− Vγ6+ γδ T cells producing IL-17A promote ovarian cancer growth via mobilization of pro-tumor small peritoneal macrophages', *Proceedings of the National Academy of Sciences*, 111 (34), pp. E3562–E3570. Available at: https://doi.org/10.1073/pnas.1403424111.

Ribot, J.C. *et al*. (2009) 'CD27 is a thymic determinant of the balance between interferon-γ- and interleukin 17–producing γδ T cell subsets', *Nature Immunology*, 10 (4), pp. 427–436. Available at: https://doi.org/10.1038/ni.1717.

Richert, M.M. *et al*. (2000) 'An Atlas of Mouse Mammary Gland Development', *Journal of Mammary Gland Biology and Neoplasia 2000 5:2*, 5 (2), pp. 227–241. Available at: https://doi.org/10.1023/A:1026499523505.

Riggio, A.I. (2017) *The role of Runx1 in genetic models of breast cancer - Enlighten: Theses*. Available at: http://theses.gla.ac.uk/9103/ (Accessed: 20 May 2020).

Riggio, A.I. and Blyth, K. (2017) 'The enigmatic role of RUNX1 in female-related cancers - current knowledge & future perspectives', *The FEBS Journal*, 284 (15), pp. 2345–2362. Available at: https://doi.org/10.1111/febs.14059.

Van de Rijn, M. *et al*. (2002) 'Expression of cytokeratins 17 and 5 identifies a group of breast carcinomas with poor clinical outcome', *American Journal of Pathology*, 161 (6), pp. 1991–1996. Available at: https://doi.org/10.1016/S0002-9440(10)64476-8.

Rijsewijk, F. *et al*. (1987) 'The Drosophila homology of the mouse mammary oncogene int-1 is identical to the segment polarity gene wingless', *Cell*, 50 (4), pp. 649–657. Available at: https://doi.org/10.1016/0092-8674(87)90038-9.

Ring, A. and Dowsett, M. (2004) 'Mechanisms of tamoxifen resistance', *Endocrine-Related Cancer*, 11 (4), pp. 643–658. Available at: https://erc.bioscientifica.com/view/journals/erc/11/4/0110643.xml (Accessed: 1 May 2020).

Riss, T.L. *et al*. (2016) 'Cell Viability Assays', *Assay Guidance Manual* [Preprint]. Available at: https://www.ncbi.nlm.nih.gov/books/NBK144065/ (Accessed: 20 August 2022).

Roarty, K. *et al*. (2017) 'Ror2-mediated alternative Wnt signaling regulates cell fate and adhesion during mammary tumor progression', *Oncogene*, 36 (43), p. 5958. Available at: https://doi.org/10.1038/ONC.2017.206.

Rodriguez-Viciana, P., Collins, C. and Fried, M. (2006) 'Polyoma and SV40 proteins differentially regulate PP2A to activate distinct cellular signaling pathways involved in growth control', *Proceedings of the National Academy of Sciences of*

the United States of America, 103 (51), pp. 19290–19295. Available at: https://doi.org/10.1073/PNAS.0609343103/ASSET/A1D41765-0ABA-41E3-9E45-94518B0F38D4/ASSETS/GRAPHIC/ZPQ0500644530006.JPEG.

De Ronde, J.J. *et al.* (2010) 'Concordance of clinical and molecular breast cancer subtyping in the context of preoperative chemotherapy response', *Breast Cancer Research and Treatment*, 119 (1), pp. 119–126. Available at: https://doi.org/10.1007/s10549-009-0499-6.

Rooney, N. *et al.* (2017) 'Runx genes in breast cancer and the mammary lineage', in *Advances in Experimental Medicine and Biology*. Springer, Singapore, pp. 353–368. Available at: https://doi.org/10.1007/978-981-10-3233-2_22.

Rooney, N. *et al.* (2020) 'Rooney et al, RUNX1 and renal cell carcinoma RUNX1 is a driver of renal cell carcinoma correlating with clinical outcome'. Available at: https://doi.org/10.1158/0008-5472.CAN-19-3870.

Rose, J.T. *et al.* (2020) 'Inhibition of the RUNX1-CBFβ transcription factor complex compromises mammary epithelial cell identity: A phenotype potentially stabilized by mitotic gene bookmarking', *Oncotarget*, 11 (26), pp. 2512–2530. Available at: https://doi.org/10.18632/oncotarget.27637.

Rouzier, R. *et al.* (2005) 'Breast cancer molecular subtypes respond differently to preoperative chemotherapy', *Clinical Cancer Research*, 11 (16), pp. 5678–5685. Available at: https://doi.org/10.1158/1078-0432.CCR-04-2421.

Roy, D. and Liehr, J.G. (1999) 'Estrogen, DNA damage and mutations', *Mutation Research/Fundamental and Molecular Mechanisms of Mutagenesis*, 424 (1–2), pp. 107–115. Available at: https://doi.org/10.1016/S0027-5107 (99)00012-3.

Royce, M.E. and Osman, D. (2015) 'Everolimus in the treatment of metastatic breast cancer', *Breast Cancer: Basic and Clinical Research*, 9, pp. 73–79. Available at: https://doi.org/10.4137/BCBCR.S29268.

Ruffell, B. *et al.* (2012) 'Leukocyte composition of human breast cancer', *Proceedings of the National Academy of Sciences of the United States of America*, 109 (8), pp. 2796–2801. Available at: https://doi.org/10.1073/PNAS.1104303108/SUPPL_FILE/PNAS.201104303SI.PDF.

Ruffell, B. *et al.* (2014) 'Macrophage IL-10 Blocks CD8+ T Cell-Dependent Responses to Chemotherapy by Suppressing IL-12 Expression in Intratumoral Dendritic Cells', *Cancer Cell*, 26 (5), pp. 623–637. Available at: https://doi.org/10.1016/j.ccell.2014.09.006.

Rutkovskiy, A., Stensløkken, K.-O. and Vaage, I.J. (2016) 'Osteoblast Differentiation at a Glance.', *Medical science monitor basic research*, 22, pp. 95–106. Available at: https://doi.org/10.12659/MSMBR.901142.

Rygaard, J. and Povlsen, C.O. (1969) 'Heterotransplantation of a human malignant tumour to "Nude" mice.', *Acta Pathologica Microbiologica Scandinavica*, 77 (4), pp. 758–760. Available at: https://doi.org/10.1111/J.1699-0463.1969.TB04520.X.

Sakakura, C. *et al.* (2005) 'Frequent downregulation of the runt domain transcription factors RUNX1,RUNX3 and their cofactor CBFB in gastric cancer', *International Journal of Cancer*, 113 (2), pp. 221–228. Available at: https://doi.org/10.1002/ijc.20551.

Sakamoto, K., Schmidt, J.W. and Wagner, K.-U. (2015) 'Mouse models of breast cancer.', *Methods in molecular biology (Clifton, N.J.)*, 1267, pp. 47–71. Available at: https://doi.org/10.1007/978-1-4939-2297-0_3.

Salem, A. *et al.* (2017) 'Myeloid neoplasms with concurrent BCR-ABL1 and CBFB rearrangements: A series of 10 cases of a clinically aggressive neoplasm', *American Journal of Hematology*, 92 (6), pp. 520–528. Available at: https://doi.org/10.1002/ajh.24710.

Salemme, V. *et al.* (2021) 'The Crosstalk Between Tumor Cells and the Immune Microenvironment in Breast Cancer: Implications for Immunotherapy', *Frontiers in Oncology*, 11, p. 289. Available at: https://doi.org/10.3389/FONC.2021.610303/BIBTEX.

Salimi, M. *et al.* (2018) 'Activated innate lymphoid cell populations accumulate in human tumour tissues', *BMC Cancer*, 18 (1), pp. 1–10. Available at: https://doi.org/10.1186/S12885-018-4262-4/FIGURES/4.

Sanson, B. (2001) 'Generating patterns from fields of cells: Examples from Drosophila segmentation', *EMBO Reports*, 2 (12), p. 1088. Available at: https://doi.org/10.1093/EMBO-REPORTS/KVE255.

Sauer, B. and Du, E.I. (1987) 'Functional expression of the cre-lox site-specific recombination system in the yeast Saccharomyces cerevisiae.', *Molecular and Cellular Biology*, 7 (6), p. 2087. Available at: https://doi.org/10.1128/MCB.7.6.2087.

Savage, K. *et al.* (2007) 'Caveolin 1 is overexpressed and amplified in a subset of basal-like and metaplastic breast carcinomas: A morphologic, ultrastructural, immunohistochemical, and in situ hybridization analysis', *Clinical Cancer*

Research, 13 (1), pp. 90–101. Available at: https://doi.org/10.1158/1078-0432.CCR-06-1371.

Savage, K. *et al.* (2008) 'Distribution and significance of caveolin 2 expression in normal breast and invasive breast cancer: An immunofluorescence and immunohistochemical analysis', *Breast Cancer Research and Treatment*, 110 (2), pp. 245–256. Available at: https://doi.org/10.1007/s10549-007-9718-1.

Scherer, W.F., Syverton, J.T. and Gey, G.O. (1953) 'Studies on the propagation in vitro of poliomyelitis viruses. IV. Viral multiplication in a stable strain of human malignant epithelial cells (strain HeLa) derived from an epidermoid carcinoma of the cervix', *The Journal of Experimental Medicine*, 97 (5), p. 695. Available at: https://doi.org/10.1084/JEM.97.5.695.

Schmalhofer, O., Brabletz, S. and Brabletz, T. (2009) 'E-cadherin, ß-catenin, and ZEB1 in malignant progression of cancer', *Cancer and Metastasis Reviews*, 28 (1–2), pp. 151–166. Available at: https://doi.org/10.1007/S10555-008-9179-Y/FIGURES/4.

Schmid, P. *et al.* (2018) 'Atezolizumab and Nab-Paclitaxel in Advanced Triple-Negative Breast Cancer', *New England Journal of Medicine*, 379 (22), pp. 2108–2121. Available at: https://doi.org/10.1056/NEJMoa1809615.

Selbert, S. *et al.* (1998) 'Efficient BLG-Cre mediated gene deletion in the mammary gland', *Transgenic Research*, 7 (5), pp. 387–398. Available at: https://doi.org/10.1023/A:1008848304391.

Shah, M., Nunes, M.R. and Stearns, V. (2018) 'CDK4/6 Inhibitors: Game Changers in the Management of Hormone Receptor–Positive Advanced Breast Cancer?', *Oncology (Williston Park, N.Y.)*, 32 (5), pp. 216–22. Available at: http://www.ncbi.nlm.nih.gov/pubmed/29847850 (Accessed: 22 September 2022).

Sharpe, M. and Mount, N. (2015) 'Genetically modified T cells in cancer therapy: opportunities and challenges', *Disease Models & Mechanisms*, 8 (4), pp. 337–350. Available at: https://doi.org/10.1242/DMM.018036.

Shen, Q. *et al.* (2017) 'Notch Shapes the Innate Immunophenotype in Breast Cancer', *Cancer Discovery*, 7 (11), pp. 1320–1335. Available at: https://doi.org/10.1158/2159-8290.CD-17-0037.

Sheu, B.-C. *et al.* (1999) 'Reversed CD4/CD8 Ratios of Tumor-Infiltrating Lymphocytes Are Correlated with the Progression of Human Cervical Carcinoma', *American Cancer Society*, 86 (8), pp. 1537–1543. Available at: https://doi.org/10.1002/(SICI)1097-0142(19991015)86:8.

Shi, X., Chakraborty, P. and Chaudhuri, A. (2018) 'Unmasking tumor heterogeneity and clonal evolution by single-cell analysis', *Journal of Cancer Metastasis and Treatment*, 4 (8), p. 47. Available at: https://doi.org/10.20517/2394-4722.2018.32.

Shimizu, K. and Ohki, M. (1991) 't (8 ; 21) breakpoints on chromosome 21 in acute myeloid leukemia are clustered within a limited region of a single gene , AMLJ', 88 (December), pp. 10431–10434. Available at: https://www.pnas.org/content/pnas/88/23/10431.full.pdf (Accessed: 18 May 2019).

Shirazi, Farshad Hosseini *et al*. (2011) 'Remarks in Successful Cellular Investigations for Fighting Breast Cancer Using Novel Synthetic Compounds Protective effect of Cydonia oblonga Mill. fruit on carbon tetrachloride-induced hepatotoxicity View project Identification and Spectroscopic Detection of Non-cycling Cancer Cells View project 5 Remarks in Successful Cellular Investigations for Fighting Breast Cancer Using Novel Synthetic Compounds', *InTech Open Access Publisher* [Preprint]. Available at: https://doi.org/10.5772/23005.

Shologu, N. *et al*. (2016) 'Recreating complex pathophysiologies in vitro with extracellular matrix surrogates for anticancer therapeutics screening', *Drug Discovery Today*, 21 (9), pp. 1521–1531. Available at: https://doi.org/10.1016/J.DRUDIS.2016.06.001.

Shulewitz, M. *et al*. (2006) 'Repressor roles for TCF-4 and Sfrp1 in Wnt signaling in breast cancer', *Oncogene 2006 25:31*, 25 (31), pp. 4361–4369. Available at: https://doi.org/10.1038/sj.onc.1209470.

Siegel, R.L. *et al*. (2022) 'Cancer statistics, 2022', *CA: A Cancer Journal for Clinicians*, 72 (1), pp. 7–33. Available at: https://doi.org/10.3322/CAAC.21708.

Sinn, E. *et al*. (1987) 'Coexpression of MMTV/v-Ha-ras and MMTV/c-myc genes in transgenic mice: Synergistic action of oncogenes in vivo', *Cell*, 49 (4), pp. 465–475. Available at: https://doi.org/10.1016/0092-8674 (87)90449-1.

Slamon, D.J. *et al*. (2001) 'Use of Chemotherapy plus a Monoclonal Antibody against HER2 for Metastatic Breast Cancer That Overexpresses HER2', *New England Journal of Medicine*, 344 (11), pp. 783–792. Available at: https://doi.org/10.1056/NEJM200103153441101.

Smart, C.E. *et al*. (2013) 'In Vitro Analysis of Breast Cancer Cell Line Tumourspheres and Primary Human Breast Epithelia Mammospheres Demonstrates Inter- and

Intrasphere Heterogeneity', *PLoS ONE*, 8 (6), p. 64388. Available at: https://doi.org/10.1371/JOURNAL.PONE.0064388.

Smith, G.H. and Medina, D. (1988) 'A morphologically distinct candidate for an epithelial stem cell in mouse mammary gland', *Journal of Cell Science*, 90 (1), pp. 173–183. Available at: https://doi.org/10.1242/jcs.90.1.173.

Smith, G.H., Mehrel, T. and Roop, D.R. (1990) 'Differential keratin gene expression in developing, differentiating, preneoplastic, and neoplastic mouse mammary epithelium', *Cell Growth and Differentiation*, 1 (4), pp. 161–170. Available at: https://pubmed.ncbi.nlm.nih.gov/1707299/ (Accessed: 9 September 2022).

Sørlie, T. *et al*. (2001) 'Gene expression patterns of breast carcinomas distinguish tumor subclasses with clinical implications', *Proceedings of the National Academy of Sciences of the United States of America*, 98 (19), pp. 10869–10874. Available at: https://doi.org/10.1073/pnas.191367098.

Sørlie, T. *et al*. (2003) 'Repeated observation of breast tumor subtypes in independent gene expression data sets', *Proceedings of the National Academy of Sciences of the United States of America*, 100 (14), pp. 8418–8423. Available at: https://doi.org/10.1073/pnas.0932692100.

Sornapudi, T.R. *et al*. (2018) 'Comprehensive profiling of transcriptional networks specific for lactogenic differentiation of HC11 mammary epithelial stem-like cells', *Scientific Reports 2018 8:1*, 8 (1), pp. 1–15. Available at: https://doi.org/10.1038/s41598-018-30122-4.

Sotiriou, C. and Pusztai, L. (2009) 'Gene-Expression Signatures in Breast Cancer', *New England Journal of Medicine*, 360 (8), pp. 790–800. Available at: https://doi.org/10.1056/NEJMra0801289.

Soule, H.D. *et al*. (1990) 'Isolation and characterization of a spontaneously immortalized human breast epithelial cell line, MCF-10 ', *Cancer Research*, 50 (18), pp. 6075–6086. Available at: https://pubmed.ncbi.nlm.nih.gov/1975513/ (Accessed: 31 July 2022).

Speck, N.A. *et al*. (1999) 'Core-Binding Factor: A Central Player in Hematopoiesis and Leukemia 1', *CANCER RESEARCH (SUPPL.)*, 59, pp. 1789–1793. Available at: http://aacrjournals.org/cancerres/article-pdf/59/7_Supplement/1789s/2862669/crs05907s1789s.pdf (Accessed: 23 June 2022).

Spits, H. and di Santo, J.P. (2010) 'The expanding family of innate lymphoid cells: regulators and effectors of immunity and tissue remodeling', *Nature Immunology 2010 12:1*, 12 (1), pp. 21–27. Available at: https://doi.org/10.1038/ni.1962.

Stearns, V. *et al.* (2011) 'Preclinical and clinical evaluation of intraductally administered agents in early breast cancer.', *Science Translational Medicine*, 3 (106), pp. 106ra108-106ra108. Available at: https://doi.org/10.1126/SCITRANSLMED.3002368.

Sternberg, N. and Hamilton, D. (1981) 'Bacteriophage P1 site-specific recombination: I. Recombination between loxP sites', *Journal of Molecular Biology*, 150 (4), pp. 467–486. Available at: https://doi.org/10.1016/0022-2836 (81)90375-2.

Sternlicht, M.D. (2005) 'Key stages in mammary gland development: The cues that regulate ductal branching morphogenesis', *Breast Cancer Research*, 8 (1), pp. 1–11. Available at: https://doi.org/10.1186/BCR1368/TABLES/1.

Steurer, S. *et al.* (2021) 'p63 expression in human tumors and normal tissues: a tissue microarray study on 10,200 tumors', *Biomarker Research*, 9 (1), pp. 1–14. Available at: https://doi.org/10.1186/S40364-021-00260-5/FIGURES/5.

Stewart, T.A., Pattengale, P.K. and Leder, P. (1984) 'Spontaneous mammary adenocarcinomas in transgenic mice that carry and express MTV/myc fusion genes', *Cell*, 38 (3), pp. 627–637. Available at: https://doi.org/10.1016/0092-8674 (84)90257-5.

Stingl, J. and Caldas, C. (2007) 'Molecular heterogeneity of breast carcinomas and the cancer stem cell hypothesis', *Nature Reviews Cancer*. Nature Publishing Group, pp. 791–799. Available at: https://doi.org/10.1038/nrc2212.

St-Onge, L., Furth, P.A. and Gruss, P. (1996) 'Temporal Control of the Cre Recombinase in Transgenic Mice by a Tetracycline Responsive Promoter', *Nucleic Acids Research*, 24 (19), pp. 3875–3877. Available at: https://doi.org/10.1093/NAR/24.19.3875.

Streuli, C.H. (2003) 'Preface: Cell Adhesion in Mammary Gland Biology and Neoplasia', *Journal of Mammary Gland Biology and Neoplasia 2003 8:4*, 8 (4), pp. 375–381. Available at: https://doi.org/10.1023/B:JOMG.0000017501.34884.70.

Strippoli, P. *et al.* (2002) 'Segmental paralogy in the human genome: a large-scale triplication on 1p, 6p, and 21q', *Mammalian Genome*, 13, pp. 456–462. Available at: https://doi.org/10.1007/s00335-001-2157-0.

Sun, X. *et al.* (2017) 'CCL2-driven inflammation increases mammary gland stromal density and cancer susceptibility in a transgenic mouse model', *Breast Cancer*

Research, 19 (1), pp. 1–15. Available at: https://doi.org/10.1186/S13058-016-0796-Z/FIGURES/7.

Sung, H. *et al*. (2021) 'Global Cancer Statistics 2020: GLOBOCAN Estimates of Incidence and Mortality Worldwide for 36 Cancers in 185 Countries', *CA: A Cancer Journal for Clinicians*, 71 (3), pp. 209–249. Available at: https://doi.org/10.3322/CAAC.21660.

Sweeney, K., Cameron, E.R. and Blyth, K. (2020) 'Complex Interplay between the RUNX Transcription Factors and Wnt/β-Catenin Pathway in Cancer: A Tango in the Night', *Molecules and cells*. NLM (Medline), pp. 188–197. Available at: https://doi.org/10.14348/molcells.2019.0310.

Swoboda, A. and Nanda, R. (2018) 'Immune Checkpoint Blockade for Breast Cancer', in *Cancer treatment and research*. NIH Public Access, pp. 155–165. Available at: https://doi.org/10.1007/978-3-319-70197-4_10.

Tahirov, T.H. *et al*. (2001a) 'Structural analyses of DNA recognition by the AML1/Runx-1 runt domain and its allosteric control by CBFβ', *Cell*, 104 (5), pp. 755–767. Available at: https://doi.org/10.1016/S0092-8674 (01)00271-9.

Tahirov, T.H. *et al*. (2001b) 'Structural Analyses of DNA Recognition by the AML1/Runx-1 Runt Domain and Its Allosteric Control by CBFβ', *Cell*, 104 (5), pp. 755–767. Available at: https://doi.org/10.1016/S0092-8674 (01)00271-9.

Takemaru, K.I. *et al*. (2003) 'Chibby, a nuclear β-catenin-associated antagonist of the Wnt/Wingless pathway', *Nature 2003 422:6934*, 422 (6934), pp. 905–909. Available at: https://doi.org/10.1038/nature01570.

Tallerico, R. *et al*. (2017) 'NK cells control breast cancer and related cancer stem cell hematological spread', *OncoImmunology*, 6 (3). Available at: https://doi.org/10.1080/2162402X.2017.1284718/SUPPL_FILE/KONI_A_1284718_SM4903.ZIP.

Taneja, P. *et al*. (2009) 'MMTV mouse models and the diagnostic values of MMTV-like sequences in human breast cancer', *Expert review of molecular diagnostics*, 9 (5), p. 423. Available at: https://doi.org/10.1586/ERM.09.31.

Tanos, T. *et al*. (2013) 'Progesterone/RANKL is a major regulatory axis in the human breast', *Science Translational Medicine*, 5 (182). Available at: https://doi.org/10.1126/SCITRANSLMED.3005654/SUPPL_FILE/5-182RA55_SM.PDF.

Tao, K. *et al*. (2008) 'Imagable 4T1 model for the study of late stage breast cancer', *BMC Cancer*, 8 (1), pp. 1–19. Available at: https://doi.org/10.1186/1471-2407-8-228/FIGURES/11.

Teissedre, B. *et al*. (2009) 'MMTV-Wnt1 and -ΔN89β-Catenin Induce Canonical Signaling in Distinct Progenitors and Differentially Activate Hedgehog Signaling within Mammary Tumors', *PLoS ONE*, 4 (2). Available at: https://doi.org/10.1371/JOURNAL.PONE.0004537.

Thomas, K.R. and Capecchi, M.R. (1987) 'Site-directed mutagenesis by gene targeting in mouse embryo-derived stem cells', *Cell*, 51 (3), pp. 503–512. Available at: https://doi.org/10.1016/0092-8674 (87)90646-5.

Thompson, E.W. *et al*. (1993) 'The invasive and metastatic properties of hormone-independent but hormone-responsive variants of MCF-7 human breast cancer cells', *Clinical & Experimental Metastasis 1993 11:1*, 11 (1), pp. 15–26. Available at: https://doi.org/10.1007/BF00880062.

Thornton, A.M. and Shevach, E.M. (1998) 'CD4+CD25+ Immunoregulatory T Cells Suppress Polyclonal T Cell Activation In Vitro by Inhibiting Interleukin 2 Production', *The Journal of Experimental Medicine*, 188 (2), p. 287. Available at: https://doi.org/10.1084/JEM.188.2.287.

Tian, Z. *et al*. (2020) 'An immune-related prognostic signature for predicting breast cancer recurrence', *Cancer Medicine* [Preprint]. Available at: https://doi.org/10.1002/cam4.3408.

Tirado-Gonzalez, I. *et al*. (2021) 'AXL Inhibition in Macrophages Stimulates Host-versus-Leukemia Immunity and Eradicates Naïve and Treatment-Resistant Leukemia', *Cancer Discovery*, 11 (11), pp. 2924–2943. Available at: https://doi.org/10.1158/2159-8290.CD-20-1378.

Toft, D.J. and Cryns, V.L. (2011) 'Minireview: Basal-Like Breast Cancer: From Molecular Profiles to Targeted Therapies', *Molecular Endocrinology*, 25 (2), pp. 199–211. Available at: https://doi.org/10.1210/me.2010-0164.

Tower, H., Ruppert, M. and Britt, K. (2019) 'The Immune Microenvironment of Breast Cancer Progression', *Cancers*, 11 (9). Available at: https://doi.org/10.3390/CANCERS11091375.

Trompouki, E. *et al*. (2011) 'Lineage regulators direct BMP and Wnt pathways to cell-specific programs during differentiation and regeneration', *Cell*, 147 (3), p. 577. Available at: https://doi.org/10.1016/J.CELL.2011.09.044.

Turner, N.C. *et al.* (2007) 'BRCA1 dysfunction in sporadic basal-like breast cancer', *Oncogene*, 26 (14), pp. 2126–2132. Available at: https://doi.org/10.1038/sj.onc.1210014.

Valachis, A. *et al.* (2010) 'Partial Breast Irradiation or Whole Breast Radiotherapy for Early Breast Cancer: A Meta-Analysis of Randomized Controlled Trials', *The Breast Journal*, 16 (3), pp. 245–251. Available at: https://doi.org/10.1111/j.1524-4741.2010.00905.x.

Vargo-Gogola, T. and Rosen, J.M. (2007) 'Modelling breast cancer: one size does not fit all', *Nature Reviews Cancer 2007 7:9*, 7 (9), pp. 659–672. Available at: https://doi.org/10.1038/nrc2193.

Varricchi, G. *et al.* (2017) 'Eosinophils: The unsung heroes in cancer?', *https://doi.org/10.1080/2162402X.2017.1393134*, 7 (2). Available at: https://doi.org/10.1080/2162402X.2017.1393134.

Ventura, A. *et al.* (2007) 'Restoration of p53 function leads to tumour regression in vivo', *Nature 2006 445:7128*, 445 (7128), pp. 661–665. Available at: https://doi.org/10.1038/nature05541.

Vergote, I. and Robertson, J.F.R. (2004) 'Fulvestrant is an effective and well-tolerated endocrine therapy for postmenopausal women with advanced breast cancer: Results from clinical trials', *British Journal of Cancer*, 90 (Suppl 1), pp. S11–S14. Available at: https://doi.org/10.1038/sj.bjc.6601631.

Visvader, J.E. (2009) 'Keeping abreast of the mammary epithelial hierarchy and breast tumorigenesis', *Genes & Development*, 23 (22), pp. 2563–2577. Available at: https://doi.org/10.1101/gad.1849509.

Vivier, E. *et al.* (2012) 'Targeting natural killer cells and natural killer T cells in cancer', *Nature Reviews Immunology 2012 12:4*, 12 (4), pp. 239–252. Available at: https://doi.org/10.1038/nri3174.

Voon, D.C.C., Hor, Y.T. and Ito, Y. (2015) 'The RUNX complex: reaching beyond haematopoiesis into immunity', *Immunology*, 146 (4), pp. 523–536. Available at: https://doi.org/10.1111/IMM.12535.

Wagner, J. *et al.* (2019) 'A Single-Cell Atlas of the Tumor and Immune Ecosystem of Human Breast Cancer', *Cell*, 177 (5), pp. 1330-1345.e18. Available at: https://doi.org/10.1016/J.CELL.2019.03.005.

Wagner, K.-U. *et al.* (1997) 'Cre-mediated gene deletion in the mammary gland', *Nucleic Acids Research*, 25 (21), pp. 4323–4330. Available at: https://doi.org/10.1093/nar/25.21.4323.

Wagner, K.U. *et al*. (2001) 'Spatial and temporal expression of the Cre gene under the control of the MMTV-LTR in different lines of transgenic mice', *Transgenic Research 2001 10:6*, 10 (6), pp. 545–553. Available at: https://doi.org/10.1023/A:1013063514007.

Wang, C. *et al*. (2017) 'Lineage-Biased Stem Cells Maintain Estrogen-Receptor-Positive and -Negative Mouse Mammary Luminal Lineages.', *Cell reports*, 18 (12), pp. 2825–2835. Available at: https://doi.org/10.1016/j.celrep.2017.02.071.

Wang, C.Q. *et al*. (2013) 'Runx3 deficiency results in myeloproliferative disorder in aged mice', *Blood*, 122 (4), pp. 562–566. Available at: https://doi.org/10.1182/BLOOD-2012-10-460618.

Wang, L., Brugge, J.S. and Janes, K.A. (2011) 'Intersection of FOXO- and RUNX1-mediated gene expression programs in single breast epithelial cells during morphogenesis and tumor progression', *Proceedings of the National Academy of Sciences*, 108 (40), pp. E803–E812. Available at: https://doi.org/10.1073/pnas.1103423108.

Wang, Q *et al*. (1996) 'Disruption of the Cbfa2 gene causes necrosis and hemorrhaging in the central nervous system and blocks definitive hematopoiesis.', *Proceedings of the National Academy of Sciences*, 93 (8), pp. 3444–3449. Available at: https://doi.org/10.1073/pnas.93.8.3444.

Wang, Qing *et al*. (1996) 'The CBFß Subunit Is Essential for CBFα2 (AML1) Function In Vivo', *Cell*, 87 (4), pp. 697–708. Available at: https://doi.org/10.1016/S0092-8674(00)81389-6.

Wang, R. and Huang, K. (2020) 'CCL11 increases the proportion of CD4+CD25+Foxp3+ Treg cells and the production of IL-2 and TGF-ß by CD4+ T cells via the STAT5 signaling pathway', *Molecular Medicine Reports*, 21 (6), pp. 2522–2532. Available at: https://doi.org/10.3892/MMR.2020.11049/HTML.

Wang, Z. *et al*. (2015) 'Clinical implications of ß-catenin protein expression in breast cancer', *International Journal of Clinical and Experimental Pathology*, 8 (11), pp. 14989–14994. Available at: www.ijcep.com/ (Accessed: 28 June 2021).

Watson, C.J. and Khaled, W.T. (2008) 'Mammary development in the embryo and adult: a journey of morphogenesis and commitment', *Development*, 135 (6), pp. 995–1003. Available at: https://doi.org/10.1242/DEV.005439.

Wculek, S.K. *et al*. (2020) 'Dendritic cells in cancer immunology and immunotherapy', *Nature Reviews Immunology*, 20 (1), pp. 7–24. Available at: https://doi.org/10.1038/s41577-019-0210-z.

Webster, J. *et al*. (1995) 'Tissue-specific, temporally regulated expression mediated by the proximal ovine beta-lactoglobulin promoter in transgenic mice', *Cellular and Molecular Biology Research*, 41 (1), pp. 1–5. Available at: https://pubmed.ncbi.nlm.nih.gov/7550448/ (Accessed: 6 September 2022).

Weigelt, B., Geyer, F.C. and Reis-Filho, J.S. (2010) 'Histological types of breast cancer: How special are they?', *Molecular Oncology*, 4 (3), pp. 192–208. Available at: https://doi.org/10.1016/j.molonc.2010.04.004.

Weiswald, L.B., Bellet, D. and Dangles-Marie, V. (2015) 'Spherical Cancer Models in Tumor Biology', *Neoplasia (New York, N.Y.)*, 17 (1), p. 1. Available at: https://doi.org/10.1016/J.NEO.2014.12.004.

Wellenstein, M.D. *et al*. (2019) 'Loss of p53 triggers WNT-dependent systemic inflammation to drive breast cancer metastasis', *Nature*. Nature Publishing Group, pp. 538–542. Available at: https://doi.org/10.1038/s41586-019-1450-6.

Westendorf, J.J. and Hiebert, S.W. (1999) 'Mammalian Runt-Domain Proteins and Their Roles in Hematopoiesis, Osteogenesis, and Leukemia', *Journal of Cellular Biochemistry Supplements*, 32, pp. 51–58. Available at: https://doi.org/10.1002/(SICI)1097-4644(1999)75:32.

Williams, J.M. and Daniel, C.W. (1983) 'Mammary Ductal Elongation: Differentiation of Myoepithelium and Basal Lamina during Branching Morphogenesis', *DEVELOPMENTAL BIOLOGY*, 97, pp. 274–290.

Willson, M.L. *et al*. (2019) 'Taxanes for adjuvant treatment of early breast cancer', *Cochrane Database of Systematic Reviews*, 9 (9). Available at: https://doi.org/10.1002/14651858.CD004421.pub3.

Wirapati, P. *et al*. (2008) 'Meta-analysis of gene expression profiles in breast cancer: Toward a unified understanding of breast cancer subtyping and prognosis signatures', *Breast Cancer Research*, 10 (4), p. R65. Available at: https://doi.org/10.1186/bcr2124.

Wirtz, D., Konstantopoulos, K. and Searson, P.C. (2011) 'The physics of cancer: the role of physical interactions and mechanical forces in metastasis', *Nature Reviews Cancer 2011 11:7*, 11 (7), pp. 512–522. Available at: https://doi.org/10.1038/nrc3080.

Wishart, G.C. *et al*. (2012) 'PREDICT Plus: Development and validation of a prognostic model for early breast cancer that includes HER2', *British Journal of Cancer*, 107 (5), pp. 800–807. Available at: https://doi.org/10.1038/bjc.2012.338.

Wissman, C. *et al.* (2003) 'WIFI, a component of the Wnt pathway, is down-regulated in prostate, breast, lung, and bladder cancer', *Journal of Pathology*, 201 (2), pp. 204–212. Available at: https://doi.org/10.1002/path.1449.

Wotton, D. *et al.* (1994) 'Cooperative binding of Ets-1 and core binding factor to DNA.', *Molecular and Cellular Biology*, 14 (1), p. 840. Available at: https://doi.org/10.1128/MCB.14.1.840.

Wu, G. *et al.* (2003) 'Structure of a β-TrCP1-Skp1-β-Catenin Complex: Destruction Motif Binding and Lysine Specificity of the SCFβ-TrCP1 Ubiquitin Ligase', *Molecular Cell*, 11 (6), pp. 1445–1456. Available at: https://doi.org/10.1016/S1097-2765(03)00234-X.

Xiao, Q. *et al.* (2022) 'Cross-Talk between p53 and Wnt Signaling in Cancer', *Biomolecules 2022, Vol. 12, Page 453*, 12 (3), p. 453. Available at: https://doi.org/10.3390/BIOM12030453.

Xu, X. *et al.* (1999) 'Conditional mutation of Brca1 in mammary epithelial cells results in blunted ductal morphogenesis and tumour formation', *Nature Genetics 1999 22:1*, 22 (1), pp. 37–43. Available at: https://doi.org/10.1038/8743.

Xu, X. *et al.* (2020) 'Wnt signaling in breast cancer: biological mechanisms, challenges and opportunities', *Molecular Cancer*. BioMed Central Ltd, pp. 1–35. Available at: https://doi.org/10.1186/s12943-020-01276-5.

Yamaguchi, Y. *et al.* (2004) 'AML1 Is Functionally Regulated through p300-mediated Acetylation on Specific Lysine Residues', *Journal of Biological Chemistry*, 279 (15), pp. 15630–15638. Available at: https://doi.org/10.1074/JBC.M400355200.

Yan, J. *et al.* (2004) 'CBFβ allosterically regulates the Runx1 Runt domain via a dynamic conformational equilibrium', *Nature Structural and Molecular Biology*, 11 (9), pp. 901–906. Available at: https://doi.org/10.1038/nsmb819.

Yan, M. *et al.* (2011) 'Recruitment of regulatory T cells is correlated with hypoxia-induced CXCR4 expression, and is associated with poor prognosis in basal-like breast cancers', *Breast Cancer Research*, 13 (2), pp. 1–10. Available at: https://doi.org/10.1186/BCR2869/FIGURES/3.

Yang, J. *et al.* (2016) 'Overexpressed genes associated with hormones in terminal ductal lobular units identified by global transcriptome analysis: An insight into the anatomic origin of breast cancer', *Oncology Reports*, 35 (3), pp. 1689–1695. Available at: https://doi.org/10.3892/OR.2015.4523/HTML.

Yersal, O. and Barutca, S. (2014) 'Biological subtypes of breast cancer: Prognostic and therapeutic implications', *World Journal of Clinical Oncology*. Baishideng

Publishing Group Co., Limited, pp. 412–424. Available at: https://doi.org/10.5306/wjco.v5.i3.412.

Yoshida, C.A. *et al.* (2002) 'Core-binding factor ß interacts with Runx2 and is required for skeletal development', *Nature Genetics*, 32 (4), pp. 633–638. Available at: https://doi.org/10.1038/ng1015.

Zambrowicz, B.P. *et al.* (1997) 'Disruption of overlapping transcripts in the ROSA ßgeo 26 gene trap strain leads to widespread expression of ß-galactosidase in mouse embryos and hematopoietic cells', *Proceedings of the National Academy of Sciences of the United States of America*, 94 (8), p. 3789. Available at: https://doi.org/10.1073/PNAS.94.8.3789.

Zeng, Y.A. and Nusse, R. (2010) 'Wnt Proteins Are Self-Renewal Factors for Mammary Stem Cells and Promote Their Long-Term Expansion in Culture', *Cell Stem Cell*, 6 (6), pp. 568–577. Available at: https://doi.org/10.1016/J.STEM.2010.03.020.

Zhang, J. *et al.* (2009) 'Wnt signaling activation and mammary gland hyperplasia in MMTV–LRP6 transgenic mice: implication for breast cancer tumorigenesis', *Oncogene 2010 29:4*, 29 (4), pp. 539–549. Available at: https://doi.org/10.1038/onc.2009.339.

Zhang, T. *et al.* (2014) 'Antitumor Action of a Novel Histone Deacetylase Inhibitor, YF479, in Breast Cancer', *Neoplasia*, 16 (8), pp. 665–677. Available at: https://doi.org/10.1016/J.NEO.2014.07.009.

Zhang, Y. *et al.* (2018) 'Establishment of a murine breast tumor model by subcutaneous or orthotopic implantation', *Oncology Letters*, 15 (5), pp. 6233–6240. Available at: https://doi.org/10.3892/OL.2018.8113/HTML.

Zumwalde, N.A. *et al.* (2016) 'Analysis of immune cells from human mammary ductal epithelial organoids reveals Vδ2+ T cells that efficiently target breast carcinoma cells in the presence of bisphosphonate', *Cancer Prevention Research*, 9 (4), pp. 305–316. Available at: https://doi.org/10.1158/1940-6207.CAPR-15-0370-T/36196/AM/ANALYSIS-OF-IMMUNE-CELLS-FROM-HUMAN-MAMMARY-DUCTAL.